The Role of the AhR in Melanoma

Oliver Peter Lewis Featherstone

Oriel College

University of Oxford

A thesis submitted for the degree of Doctor of Philosophy

2024

Word Count: 50,000

Acknowledgements

In my experience, a DPhil is a lot like a game of monopoly, I enjoy it most when it's going well and can't think of anything worse when it isn't. It's also like a game of monopoly in many other ways; I got bored, I wanted to quit, it felt like it was going nowhere for long periods of time, I wish I had more resources, and it was enjoyed with friends and family.

Old Kent Road and Whitechapel Road

My first supervisors: Mads and Pedro. I'd like to thank you both for initially taking me on as a DPhil student. I am grateful for your current institutions offering you better positions.

The Angel Islington, Euston Road, and Pentonville Road

My first Postdoc childminder: Yilong. I would like to thank you for being there to show me where things were in the lab and being a friend in a new department. I appreciate I was never your favourite person, but I appreciate your begrudging respect over the quality of my qRT-PCRs, the trick was ignoring you talking to me.

Pall Mall, Whitehall, and Northumberland Avenue

My new lab: Colin, Rom, and Diogo. I'm not confident you guys were fans of me, but you were all always amazing help. I appreciate the time you took to help me get through my days, because I'm pretty sure you really didn't want to.

Bow Street, Marlborough Street, and Wine Street

The '22 Lightweight Blue Boat. You guys gave me a fantastic return to rowing and an amazing journey over the season. You were sometimes the best of friends and the worst of my problems, often at the same time. This boat race campaign will forever be something I am proud of, and something I shall treasure as an integral part of the last few years.

Strand, Fleet Street, and Trafalgar Square

My home friends: James and George. Though we haven't had a chance to see each other often in the last few years, I am so glad to have had you only a phone call away. Seeing you both over Christmas is an amazing annual reset, which I value immensely. I don't think I would've made it through Christmas '21 without our chats to put some perspective on the value of Old Kent Road and Whitechapel Road.

Leicester Square, Coventry Street, and Piccadilly

The lunch Club+: Tom, Felice, Magda, Lucy, Alina, Alina, Michael, Emelie, Matt, Matt, and Fieke. You guys kept me going over the years. Having a sounding board to check

my sanity and encourage my insanity. I have enjoyed the woes of Vitamin D deficiency corner only because of the people in it.

Regent Street, Oxford Street, and Bond Street

My family: Liz, Hannah, Adam. Putting you guys as the dark green colours is not only a reflection of your value to me, but also a parallel of my tactics in monopoly: Never the first choice of properties, but often the ones I forget about and rely on, nonetheless. Thank you, Adam, for relinquishing your title as the most accomplished in the family, you have kept if warm and safe for 8 years, but your time has come.

Park Lane

Agamemnon Elvis Crumpton.

Mayfair

There's no single person who I owe more to for helping me get through this thesis than my partner: Pippa. After all the trials and challenges of the last four years, I have made it through because of your support and I couldn't have asked for someone more understanding and loving to keep me going. I am not sure that I would be where I am without you by my side.

Free Parking

Pakavarin Louphrasitthiphol. You have been an amazing friend and mentor. Having you support me over the last few years has been an absolute windfall, and I hope your major wins come to you soon – I'm sure there are many to come.

Kings Cross Station, Marylebone Station, Fenchurch Street Station, Liverpool Street Station

My colleges and the friends and colleagues therein: Oriel, St. Hugh's, St. John's, and Corpus Christi. Oriel: Phil and Zac. You have both been great supporters of me in both sports and personal life, knowing you both have my back has often been the boost that has made the difference in tough times. St. Hugh's: John Stanley, Clive Wilson, and those who regularly breakfast. I would never have got to where I have with teaching without the initial trust and support from you all. St. John's, Luisa, Kaitlyn, and the ECRs. You have made the process of losing my sanity writing my thesis manageable and at times, pleasant. Corpus Christi, thank you for providing the most expensive meal I can bring a guest to.

Electric Company and Water Works

Naomi Petela and Mark Roberts. You supported me as tutors in my undergrad and as friends in my doctorate. You have both shaped the student I was and the teacher I am. Mark, I hope one day to recover from your feedback in first year.

An honourable mention: The guy who crashed into me during a race, leading to two broken collar bones and a clinical trial where I ended up on antidepressants. Without this, I wouldn't have got stuck into the corrections or realised how happy I could be.

Abstract

For a malignant tumour to develop, progress, and metastasise, cancerous cells, generally, must dedifferentiate to acquire more phenotypic plasticity. Cancer cells must also evade detection by the immune system, which recognises mutated proteins from within and on the surface of oncogenically transforming cells, to not be eliminated. Understanding the mechanisms through which a developing tumour can lose phenotypic identity whilst suppressing recognition and elimination by the immune system is essential to developing more effective cancer therapies. Melanoma is a highly immunogenic cancer type, with a high mutational burden that enhances the antigenicity of the tumour, meaning that it must develop robust immunosuppressive mechanisms to survive. The Aryl Hydrocarbon Receptor (AhR) is a ligand-activated transcription factor that acts as a sensor of endogenous and exogenous molecules known to have a pro-oncogenic role in melanoma in establishing an immunosuppressive tumour microenvironment (TME). The AhR is an unambiguous modulator of immunosuppression in the TME in some cancers, although the mechanism through which it acts is unclear, as current *in vivo* and *in vitro* studies do not align. I demonstrate the unliganded AhR mediates immunosuppression in melanoma through suppression of pro-tumorigenic interferon gamma signalling. Melanomas are tumours derived from melanocytes: neural-crest cell derivatives whose cell lineage is defined through the expression and activity of the microphthalmia-associated transcription factor (MITF). Loss of MITF expression is a known driver of dedifferentiation, invasion, and metastasis in melanoma. The mechanisms underlying loss of MITF expression are both essential to tumour progression and poorly characterised. Herein, I describe the role of the AhR

as antagonistic of MITF-mediated transcription and a facilitator of dedifferentiation and metastasis of melanoma cells. My work demonstrates the AhR potentially mediates immunosuppression in melanoma via oncogenic STAT1 signalling and contributing to phenotypic plasticity through antagonism of MITF activity, together highlighting mechanisms whereby the AhR could be central to tumour survival and growth.

AhR you ready kids?

Table of Contents

List of Abbreviations

AhR	Aryl hydrocarbon receptor
AhRE	Aryl Hydrocarbon receptor Response Element
AIP	Aryl Hydrocarbon Receptor Interacting Protein
AhRR	Aryl hydrocarbon receptor repressor
AID	activation-induced cytidine deaminase
APC	Antigen presenting cell
ARNT	Aryl Hydrocarbon Receptor Nuclear Translocator
ATF4	Activating Transcription Factor 4
BaP	Benzo[a]pyrene
bHLH	Basic helix-loop-helix
BrCa	Breast Cancer
CCLE	Cancer Cell Line Encyclopaedia
CCND1	Cyclin D1
CD	Cluster of Differentiation
CH223191	2-methyl-2H-pyrazole-3-carboxylic acid
ChIP	Chromatin Immunoprecipitation
CTLA-4	Cytotoxic T-Lymphocyte antigen-4
CXCL	Chemokine (C-X-C) motif ligand
CYP1A1	Cytochrome p450 family 1 subfamily A member 1
CYP1B1	Cytochrome p450 family 1 subfamily B member 1
DAPI	4',6'-diamidino-2-phenylindole
DBD	DNA binding domain
DCT	Dopachrome Tautomerase
DDX5	DEAD-box helicase 5
DIA1	Diaphanous related formin 1
DIAPH	Diaphanous related formin 1 encoding gene
Dox	Doxycycline
DRE	Dioxin Response Element
ECM	Extracellular Matrix
EIF2AK2	Eukaryotic initiation factor 2 alpha kinase 2
EMT	Epithelial to Mesenchymal Transition
eNLS	Exogenous Nuclear Localisation sequence
FI	Fold induction
FICZ	Formylindolo(3,2-b)carbazole
GAS	Interferon gamma activated sequence
GBP1	Guanylate Binding Protein 1
GEP	Gene Expression Profile
GF	Growth Factor
GO	Gene Ontology
GOF	Gain of Function
GSEA	Gene Set Enrichment Analysis

GTF	General Transcription Factor
HIF1B	Hypoxia Inducible Factor B
HLA-DRA	HLA class II histocompatibility antigen DR alpha chain
HSP90	Heat Shock Protein 90
IDO1	Indolamine 2,3-dioxygenase 1
IFITM1	Interferon-induced transmembrane protein 1
IFNα	Interferon Alpha
IFNγ	Interferon Gamma
IFNGR	Interferon Gamma Receptor
IκK	Inhibitor of nuclear factor kappa B kinase
IL	Interleukin
IRAK1	Interleukin 1 receptor associated kinase 1
IRF	Interferon regulatory factor
ISRE	Interferon-stimulated response element
JAK	Janus kinase
kb	Kilobase
KEGG	Kyoto Encyclopaedia of Genes and Genomes
KO	Knockout
LDTF	Lineage-Determining Transcription Factors
LGI3	Leucine Rich Glioma inactivated 3
linc00673	Long non-coding RNA 00673
LOF	Loss of Function
MAPK	Mitogen-Activated protein kinase
Mb	Megabase
MGP	Matrix Gla Protein
MHC	Major Histocompatibility Complex
MHCI	MHC Class I
MITF	Microphthalmia-associated transcription factor
MLANA	Melan-A
MMP	Matrix Metalloproteinase
NES	Nuclear Export Sequence
NF-κB	Nuclear Factor kappa B
NF1	Neurofibromin 1
NLS	Nuclear localisation sequence
NQ	Normalised Quantity
NSCLC	Non-small cell lung carcinoma
OAS2	2'-5'-oligoadneylate synthetase 2
OCA2	OCA2 melanosomal Transmembrane Protein
OSCC	Oral Squamous Cell Carcinoma
PAS	Per-ARNT-Sim
PCR	Polymerase Chain Reaction
PD-1	Programmed Death-1
PD-L1	Programmed Death-Ligand 1

PI3K	Phosphoinositide 3-kinase
PKB	Protein Kinase B/Akt
POU6F2	POU class 6 homeobox 2
QPCT	Glutaminyl-peptide cyclotransferase
QRD	Glutamine Rich Domain
qRT-PCR	Quantitative Real-Time Reverse Transcription PCR
RAB38	Ras related protein RAB38
SERPING1	Serpin family G member 1
SERTAD4	SERTA domain containing 4
SHP2	Src homology region 2 domain-containing phosphatase-2
SOD2	Superoxide dismutase 2
SOS	Son of Sevenless
SOX6	SRY-box Transcription factor 6
STAT	Signal transducer and activator of transcription
TAD	Topologically Associated Domain
TCDD	2,3,7,8-tetrachlorodibenzodioxin
TCGA	The Cancer Genome Atlas
TCR	T-cell receptor
TF	Transcription Factor
TFE	Transcription factor E
TFII	Transcription Factor II
TME	Tumour Microenvironment
TNF	Tumour Necrosis factor alpha
TRAF6	Tumour Necrosis Factor associated factor 6
TSS	Transcription Start Site
TWIST	Twist-Related protein 1
TYR	Tyrosinase
TYRP1	Tyrosinase related protein 1
WT	Wild-Type
XRE	Xenobiotic Response Element
ZEB1	Zinc finger E-box binding homeobox 1

1. Introduction

1.1. Cancer

1.1.1. Deregulated proliferation

Cancer is a disease of dysregulation (Curtin, 2012; Pozzi et al., 2023; Vaklavas et al., 2017). The cell-cycle is tightly regulated: cells only divide when there are sufficient signals to do so without damage or stress (Vermeulen et al., 2003). Proteins involved in entering the cell-cycle are often mutated in cancer (Kashyap et al., 2021). These mutations are often gain-of-function (GOF) mutations, where the cell becomes independent of growth factor (GF) signalling and enters the cell-cycle independently of GFs (Croft et al., 2014; Leicht et al., 2007; Pylayeva-Gupta et al., 2011; Zandi et al., 2007). Genes encoding these proteins are *proto-oncogenes*, which, when mutated, are *oncogenes* (*Genetics Glossary, Oncogene*, n.d.). There are also proteins responsible for preventing cell-cycle entry, such that a sufficient threshold of GF signalling must be met for a cell to divide, preventing an over-sensitivity to GFs (Sherr, 2004). These proteins often develop loss-of-function (LOF) mutations in cancer, losing the capacity to prevent improper cell-cycle entry (Sherr, 2004). Genes encoding these proteins are *tumour suppressor genes* (Sherr, 2004). GOF mutations in proto-oncogenes and LOF mutations in tumour suppressor genes aren't sufficient to transform a cell into a malignant rather than a benign tumour (*TUMOR CELL MORPHOLOGY - Comparative Oncology - NCBI Bookshelf*, n.d.).

1.1.2. Unlimited Replicative Potential

Each time a eukaryotic cell divides, there's a shortening of the chromosome at either end (Soudet et al., 2014). This is the consequence of the end-replication problem, wherein semi-discontinuous DNA replication of linear strands of DNA, due to the requirement of an RNA primer upstream of the region of synthesis, fails to replicate one strand of the original template to completion (Soudet et al., 2014). The consequence of incomplete replication is loss of telomeric DNA, after approximately 50 divisions, which triggers cells to become senescent (Hayflick & Moorhead, 1961). This maintains genomic integrity, after this limit there may be protein-coding genes which would be mutated by loss of genetic information in each division due to the end-replication problem failing to replicate the entirety of the gene (Jafri et al., 2016). A transforming cell must acquire mechanisms through which it can surpass this limit, evading senescence, continuing to proliferate and develop to become a cancer (Jafri et al., 2016). This is often acquired through GOF mutations in telomerase, the enzyme responsible for synthesising new telomeric DNA at ends of chromosomes (N. J. Robinson & Schiemann, 2022). This extra characteristic that transforming cells must acquire to become a malignant tumour is one of many characteristics thought to be essential for cancer establishment (Hanahan, 2022).

1.1.3. The Hallmarks of Cancer

A seminal review in oncology was Hanahan and Weinberg's Hallmarks of Cancer (Hanahan & Weinberg, 2000), which sought to define core characteristics of all solid tumours. This paper put forward six hallmarks of cancer: "sustaining proliferative

signalling", "evading growth suppressors", "enabling replicative immortality", "resisting cell death", "inducing angiogenesis", and "activating invasion and metastasis" (Hanahan & Weinberg, 2000). This has since been expanded in two further papers by Hanahan: Hallmarks of cancer: the next generation (Hanahan & Weinberg, 2011) and Hallmarks of Cancer: new dimensions (Hanahan, 2022). Of the expanded 14 hallmarks of cancer, three are of particular importance to this thesis: "Avoiding immune destruction", "Activating invasion and metastasis" and "Unlocking phenotypic plasticity".

1.1.4. Avoiding Immune Destruction

Transforming cells accrue mutations, because of dysregulated surveillance of genomic integrity and increased rate of proliferation (Sarasin, 2003). This is essential to development of most cancers, but also a key factor in how transforming cells are identified by the immune system (Altevogt et al., 1985). All nucleated cells in humans bear major histocompatibility complexes (MHC) I, responsible for presenting fragments of the cell's proteome on the cell's surface for recognition by the immune system (Germain, 1994). Peptide fragments of healthy cells are tolerated by the immune system and do not stimulate an adaptive response; however, cells with mutations in coding regions of genes and infected cells will present peptide fragments that aren't healthy-self peptides and immunogenic (Garcia-Lora et al., 2003). High mutagenicity of tumours, a driver of acquiring new phenotypic properties of cancer cells detailed as a hallmark of cancer, is also responsible for generation of immunogenic peptides, allowing cancer cells to be recognised and eliminated by the immune system (Germain, 1994).

As cancers develop, they accrue mutations which may manifest in the production of non-self-peptide fragments on MHC I and neoantigens: mutated cell surface proteins with unique structures, distinct from their WT counterparts and recognisable by the immune system (N. Xie et al., 2023). Thus, enabling the immune system to eliminate transforming tumours (Altevogt et al., 1985; Garcia-Lora et al., 2003; N. Xie et al., 2023). For a cancer to survive it must avoid immune destruction. This can be achieved through directly suppressing cytotoxic processes of immune cells, including effector T cells, that recognise cancer cells or through establishing an immunosuppressive tumour microenvironment (TME) (Fallarino et al., 2002, 2006; Greenwald et al., 2001; Rudd et al., 2009). Both are discussed in section 1.2.2.

1.1.5. Activating Invasion and Metastasis

Metastasis of cancer cells is the leading cause of death due to cancer, accounting for 90% of cancer-associated deaths (Chaffer & Weinberg, 2011). The process of metastasis occurs in 3 phases: invasion, intravasation, and extravasation (Chaffer & Weinberg, 2011). The process of an epithelial cell transitioning to an invasive mesenchymal phenotype is the epithelial to mesenchymal transition (EMT) (Son & Moon, 2010). Processes analogous to the EMT of epithelial cells occur in other cancer cell types yielding invasive phenotypes (Børretzen et al., 2021; Chaffer et al., 2013; Wels et al., 2011), which generally includes the expression of transcription factors (TFs): Twist-related protein 1 (TWIST), zinc finger E-box binding homeobox 1 (ZEB1), Snail, and slug (Son & Moon, 2010; Y. Wang et al., 2014, 2016). An EMT-like transition in cancer cells is coupled with a decrease in proliferative potential – acquiring a

senescence-like state, thought to enhance their survival in the circulatory systems (Najem et al., 2022). Cancer cell motility is enhanced in response to overexpression of these TFs due to cell adhesion molecule E-cadherin repression (Wels et al., 2011). Invasion is further characterised by expression of enzymes capable of degrading the extracellular matrix, frequently matrix metalloproteinases (MMPs) (Gialeli et al., 2011). These MMPs are catabolic enzymes that degrade protein networks forming the extracellular matrix (ECM) and cell-cell adhesion molecules (Gialeli et al., 2011).

Degradation of cell-cell adhesion molecules as the proteinaceous components of the ECM permits tumour mobility and passage through the basal membrane of tissues (Chang & Chaudhuri, 2019). Once cancer cells breach the basal membrane, they may undertake intravasation, the process of entering vessels, hematogenic or lymphatic (Chiang et al., 2016). Once in circulatory systems, cancer cells can move around the body to distant sites from the primary tumour (Zavyalova et al., 2019). At these distant sites, cells must undergo extravasation and leave circulatory systems. This process requires adhesion of the tumour cell to endothelial cells of circulatory systems through protein-protein interactions, allowing necrotic signalling from tumour cells to kill barrier cells also signalling via specific pathways that lead to weakening of the cell-cell interactions that form the barrier of the vasculature (Strilic & Offermanns, 2017). In new metastatic niches, cancer cells must exit invasive and dormant states to proliferate and establish secondary tumours - governed through ERK1/2 signalling activation (Aguirre-Ghiso et al., 2003).

1.1.6. Unlocking Phenotypic Plasticity

Terminally differentiated cells are committed to a phenotype (Missinato et al., 2023). This phenotype is specialised to function, with expression of specific proteins and enzymes conferring identity and abilities (Missinato et al., 2023). As cells transition from healthy to metastatic, it ceases behaving as the cell type it was derived from (Gabbert et al., 1985). Loss of phenotypic identity and commitment to cell fate is essential to invasion and metastasis, processes that require acquisition of proteins that allow digestion of the extracellular matrix and motility from primary tumour (J. Li & Stanger, 2020).

Phenotypic plasticity may be acquired through LOF mutations in cell fate proteins, or changes in the activity of lineage-defining TFs (LDTFs) (C. M. Bailey et al., 2012; Gabbert et al., 1985). In either instance, this loss of cell fate identity and acquisition of an invasive phenotype are crucial steps in the process of metastasis and spread of cancer cells (J. Li & Stanger, 2020).

1.2. Melanoma

Melanoma is the fifth most common cancer in the UK with ≅17,000 new cases in the UK annually (*Melanoma Skin Cancer Incidence Statistics | Cancer Research UK*, n.d.). Whilst patient prognosis has vastly improved in the last 50 years, with survival rates rising from <50% to >90% (*Melanoma Skin Cancer Survival Statistics | Cancer Research UK*, n.d.), prognosis for patients diagnosed at a late-stage remains low (*Survival | Melanoma Skin Cancer | Cancer Research UK*, n.d.), with limited response to immunotherapeutic approaches which have proven highly efficacious in early-stage disease (Mutz-Rabl et al., 2023).

Melanomas are cancers derived from pigment-producing cells, melanocytes. Classified into four types depending on the organ of origin: Cutaneous (Skin) (Naik, 2021), Uveal (Eyes) (Carvajal et al., 2023), Aural (Ears) (Gowthami et al., 2014), and Mucosal (Mucosal membranes) (Sergi et al., 2023), each with distinct biologies (Rabbie et al., 2019). I will focus on the most common, Cutaneous Melanoma (Ali et al., 2013). Melanocytes are neural-crest derived cells that are responsible for the production of melanin (Mort et al., 2015a), a molecule that is responsible for protecting keratinocytes in the skin from UV damage (Brenner & Hearing, 2008). Melanocytes produce melanin, which accumulates in lysosome-like melanosomes (Le et al., 2021). These are released into keratinocytes through exocytosis, phagocytosis, membrane fusion, or transfer of membrane vesicles (Benito-Martínez et al., 2021). Once taken up by keratinocytes, melanosomes form a protective layer around the nucleus to block mutagenic UV radiation reaching the nucleus (Benito-Martínez et al., 2021).

Cutaneous melanomas is sub-classified further into 4 groups defined by their driver mutations: *BRAF* mutant, *RAS* mutant, *Neurofibromin 1* (*NF1*) mutant, and triple wild-type, *i.e.* no mutations in *BRAF*, *RAS*, or *NF1* (*TCGA Study of Genetic Drivers of Melanoma - NCI*, n.d.). The most common mutation associated with melanoma is $BRAF^{V600E/K}$ (Ascierto et al., 2012), the consequence of this mutation is permanent activation of BRAF. *BRAF* is a proto-oncogene in the mitogen-activated protein kinase (MAPK) pathway which is a signal transducer in multitudes of mitogen-activated pathways, driving cell-cycle entry in response to extracellular signals to divide (Fig. 1.1). Permanent activation of BRAF because of the $BRAF^{V600E/K}$ substitution drives oncogenesis as drives independency of GF signalling (Davies et al., 2002), a key Hallmark of cancer (Hanahan & Weinberg, 2000).

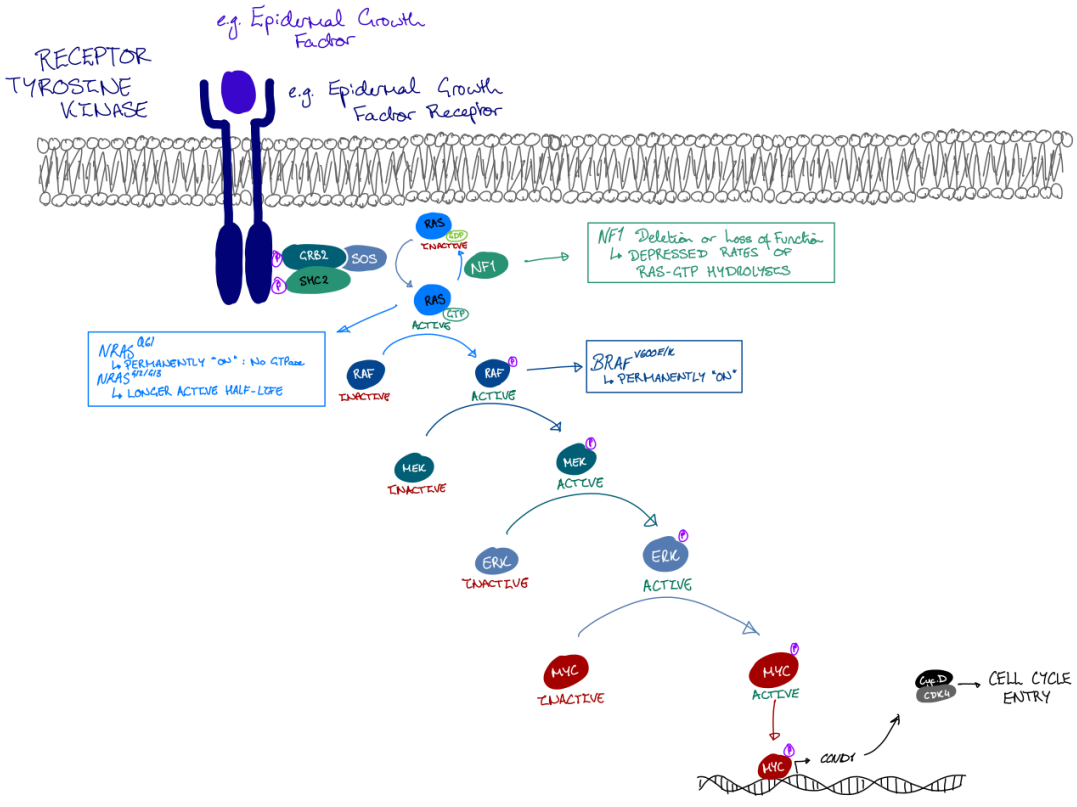

Figure 1.1 Schematic of GF signalling via the Mitogen Activated Protein Kinase Pathway. A representation of the MAPK pathway, highlighting proteins whose mutations are drivers of oncogenesis in melanoma: RAS, RAF, NF1.

RAS and *NF1* mutations drive oncogenesis in melanoma through dysregulating the same GF signalling pathway (Cirenajwis et al., 2017; Muñoz-Couselo et al., 2017). Ras lies upstream of BRAF in the MAPK signalling cascade, activated through Son of Sevenless (SOS) Guanine nucleotide exchange factor, catalysing exchange of GDP for GTP, activating Ras (Boriack-Sjodin et al., 1998). Mutations in *RAS* have two outcomes: reduced GTP hydrolysis and no GTPase functionality, defined by point mutations G61 substitutions and G12/G13 substitutions, respectively (Muñoz-Couselo et al., 2017). Other GTPases may interact with Ras catalysing GTP hydrolysis and inactivation, including NF1 (Cirenajwis et al., 2017). Deletion mutations and LOF mutations in *NF1* are associated with enhanced activity of Ras thereby driving oncogenesis in melanoma (Cirenajwis et al., 2017).

1.2.1. Microphthalmia-associated TF

Melanocyte cell fate is defined by action of microphthalmia-associated TF (MITF) (Hemesath et al., 1994). MITF is a basic-helix-loop-helix-zipper TF binding DNA as a homodimer and a heterodimer with other members of the TF E (TFE) family (TFE3, TFEb, TFEc) to mediate gene expression (Hemesath et al., 1994). MITF-mediated gene expression is stimulated and modulated by post-translational modifications of MITF (Vu et al., 2021). MITF binds to E-box and M-box motifs in the DNA, 5'-*T*CA(C/T)GTG*A*-3', respectively, with the 5'-T and 3'-A flanking the core binding site conferring specificity and enhanced affinity of MITF binding over myc binding (Goding & Arnheiter, 2019). M-box motifs are commonly found in the promoters of genes associated with melanocyte differentiation and pigmentation including Tyrosinase

(TYR) (Bertolotto et al., 1998), Dopachrome Tautomerase (DCT) (Ludwig et al., 2004), and Melan-A (MLANA) (Du et al., 2003). With MITF's central role defining melanocyte cell fate and function, it's unsurprising that aberrant MITF behaviour is associated with melanomagenesis.

MITF suppresses cell-cycle entry by stimulating expression of cyclin-cyclin dependent kinase inhibitors *p21*^{CIP1} and *p16*^{INK4A}, which should define its role as an anti-proliferative tumour suppressor through prevention of cell-cycle entry (Carreira et al., 2005; Loercher et al., 2005). However, interactions of MITF with the Diaphanous related formin 1 (Dia1) encoding gene (*DIAPH*) promoter have demonstrated that MITF drives cell-cycle entry (Carreira et al., 2006). Depressed MITF activity causes concomitant depressed Dia1 expression. Dia1 is responsible for Skp2-mediated ubiquitination and subsequent degradation of $p27^{KIP1}$, resulting in elevated $p27^{KIP1}$ accumulation and G_1 arrest (Carreira et al., 2006; Q. Li et al., 2004). These interactions with Dia1 have an impact on the invasive capacities of these cells, with depressed Dia1 expression resulting in elevated Rho-associated protein kinase-dependent invasiveness (Carreira et al., 2006). MITF protects melanoma cells from becoming senescent by suppression of Checkpoint Kinase 2 activation in response to DNA damage which, in turn, suppresses activation of p53 (Giuliano et al., 2010).

MITF is responsible for suppression of senescence (Giuliano et al., 2010), senescent cells upregulate various signalling pathways, one of which is the nuclear factor kappa B (NF-κB) signalling pathway (Ohanna et al., 2011). NF-κB signalling is oncogenic, its primary function is to drive inflammatory responses but sustained activation of NF-κB pathways in tumours increases reactive oxygen species accumulation (Nakano et

al., 2005), which are responsible for DNA-damage and oxidative stress (Xia et al., 2014). NF-κB-mediated induction of *activation-induced cytidine deaminase* (*AID*) drives tumorigenesis as AID is responsible for enhanced mutagenesis of p53 and myc (Matsumoto et al., 2007).

Although MITF has the capacity to drive cell-cycle entry and enhance invasion via enhanced *DIAPH* expression (Carreira et al., 2006), it may also contribute to tumour suppression via *CIP1* and *INK4A* expression regulation which prevent cell-cycle entry (Carreira et al., 2005; Loercher et al., 2005), it's clear that MITF is central to melanoma albeit in a more complex manner than prototypical oncogenes and tumour suppressors. There's a mutational context dependency of MITF-oncogenicity, wherein MITF activity only drives elevated proliferation in *INK4A* LOF mutation melanocyte backgrounds (Garraway et al., 2005). The role of MITF in melanoma is complicated further given its senescence-dependent role in the mediation of pro-oncogenic inflammatory signalling (Ohanna et al., 2011; Xia et al., 2014).

MITF is a lineage-specific oncogene in melanoma (Garraway et al., 2005), contributing to dysregulated cell-cycle, depression of MITF activity also contributes to invasive and metastatic phenotypes of melanoma cells (Carreira et al., 2006). MITF contributes to cell-cycle entry in melanoma, through stimulating expression of Cyclin-Dependent Kinase (CDK) 2 which enhances rates of cell proliferation in a lineage-dependent manner (Du et al., 2004). Melanoma cell survival is enhanced by MITF, as MITF suppresses transcriptional expression of pro-apoptotic factor BCL2 (McGill et al., 2002). In established tumours, elevated MITF activity drives independency of GF signalling. MITF mediated transcription also confers melanocyte cell identity (Tsoi et

al., 2018). Loss of expression is integral to dedifferentiation of melanomas, which is characteristic of an EMT-like transition in metastatic melanoma (Arozarena & Wellbrock, 2019; C. M. Bailey et al., 2012; Dilshat et al., 2021; Eccles et al., 2013; Tsoi et al., 2018). It's integral to understanding how melanomas undergo metastasis to determine what switches cells from MITF-high proliferative non-motile melanoma cells to MITF-low dedifferentiated and invasive cells. A summary of pro-oncogenic roles of MITF is found in Fig. 1.2.

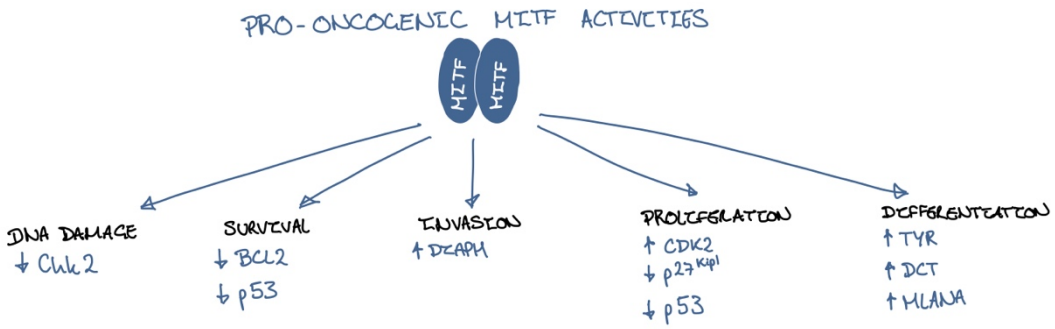

Figure 1.2 A summary of the pro-oncogenic roles of MITF in melanoma.

1.2.2. Melanoma and immunity

Melanoma is one of the most mutated tumour types (Hao et al., 2016; Hodis et al., 2012), due to being a mutagen-driven malignancy (Jardim et al., 2021), with melanomagenesis often occurring because of UV radiation exposure (Sample & He, 2018). Tumours with a higher mutational burden are more likely to generate immunogenic neoantigens which may elicit immune responses, suggesting that one of the key drivers of the immunogenicity in melanoma is its high mutational burden (Passarelli et al., 2017). Regardless of the mechanisms underlying these properties, tumours that are highly immunogenic must develop immunosuppressive properties to not be eliminated (Passarelli et al., 2017; Tie et al., 2022).

Melanoma is one of the most immunogenic types of cancer, meaning that it's highly able to induce adaptive immune responses (Passarelli et al., 2017; Tucci et al., 2019). Immunogenicity of tumours depends upon antigenicity: the presence of tumour-associated antigens on malignant cells recognisable by the immune system, predominantly T-cells, as non-self (Blankenstein et al., 2012). Drivers of high immunogenicity of melanoma are unclear, however, a tumour predisposed to accumulate antigens would consequently be predisposed to greater immunogenicity. In highly mutated cancers, there's heterogeneity between antigens presented across the tumour, driving immune escape (Wolf et al., 2019). This immune escape is not through being unrecognisable to the immune system, but through only sub-populations of cells in tumours presenting the same antigens, immune cells aren't able to eliminate more than subpopulation at once (Wolf et al., 2019). Broadly, tumours may evade the immune system through three mechanisms: limiting MHC class I (MHCI) expression, suppressing cytotoxic T cells, and establishing an immunosuppressive TME. Melanomas engage with all three mechanisms.

MHCI is a protein complex that presents fragments of degraded cytosolic peptides from a cell on its surface (Hewitt, 2003). This is part of healthy functioning of all nucleated cells and doesn't trigger activation of the immune system in healthy cells, except in instances of autoimmune diseases. However, when a cell is accruing mutations and undergoing malignant transformation, the repertoire of peptides within a cell diverges from that of its healthy counterparts. This alternative proteome undergoes typical protein turnover which generates fragments of peptides which may then be displayed on the cell's surface via MHCI complexes (Cornel et al., 2020).

These mutated peptides are recognised as non-healthy self by the immune system, enabling cytotoxic T cells to recognise the cell presenting this antigen as a risk to the host, triggering immune system mediated cell death (Sari & Rock, 2023).

In melanomas, amongst many cancers, there's a selection pressure for mutations that decrease the efficiency of the MHCI pathway (Cornel et al., 2020). The selection pressure driving accumulation of these mutations is clear, cells that fail to present mutated proteins on their surface may evade recognition by the immune system and continue to grow; whilst transforming cells that continue to present peptides via MHCI may be recognised and eliminated by cytotoxic T cells. It's expected that across all cancers, genetic and epigenetic changes that suppress or impair MHCI antigen processing and presentation would be enriched, which is observed (Cornel et al., 2020; Mumphrey et al., 2023). More specifically in melanoma, the frequently occurring $BRAF^{V600E/K}$ mutation drives depressed MHCI retention on the cell's surface via dysregulation of the MAPK pathway (Bradley et al., 2015). Furthermore, across varied cancer type, the EMT is associated with downregulation of MHCI expression and antigen presentation (Terry et al., 2017), suggesting that more dedifferentiated melanoma cells are likely less immunogenic than their melanocytic counterparts (Benboubker et al., 2022). With this reduced MHCI presence on the surface of melanoma cells comes reduced recognition and elimination by the immune system.

For a cell recognised as non-healthy to be eliminated by the immune system, there must not be activation of immune checkpoints in activated immune cells. Immune checkpoints are mechanisms through which cells may interact through cell-surface receptors on both the target and the immune cell which inhibit the cytotoxic activities

of the immune cell. Cytotoxic T-lymphocyte antigen-4 (CTLA-4) and programmed death-1 (PD-1) are amongst the best-studied of these receptors and are often the targets of emerging immunotherapies (Baksh & Weber, 2015).

CTLA-4 is expressed on T-cells and is integral to whether a T-cell, whose T-Cell Receptor (TCR) binds to its cognate MHCI complex presenting a non-healthy or non-self-peptide, commits to action or anergy (Greenwald et al., 2001). On the surface of T-cells are CTLA-4 and Cluster of Differentiation (CD) 28, which are homologs. Both receptors bind to CD80/86 which are present on the surface of antigen-presenting cells (APCs) and tumour cells. Whereas binding of CD28 to CD80/86 produces an activation response in T-cells, CTLA-4 sequesters available CD80/86 to interact with as its affinity for these receptors is greater (Z. Liu et al., 2001; Van Der Merwe et al., 1997). Upon strong TCR binding, there's increased trafficking of intracellular CTLA-4 vesicles to the T-cell's surface (X. B. Wang et al., 2001), this enhances sequestration of CD80/86 preventing co-stimulatory interactions with CD28. Absence of CD28-CD80/86 interactions alongside TCR-MHCI interactions commits the T-cell to anergy, suppressing an immune response. There's evidence of CD80/86-CTLA-4 interactions producing a direct inhibitory response in T-cells beyond competing ligands away from CD28, however, these appear to have a considerably limited effect in comparison to the effects of competing for ligand binding (Masteller et al., 2000; Rudd et al., 2009).

One of these direct inhibitory mechanisms may be through CTLA-4 mediated expression of indolamine 2,3-dioxygenase 1 (IDO1). IDO1 is a tryptophan catabolizing enzyme: converting tryptophan into kynurenine (Badawy, 2017). Tumours, be it malignant or immune cells infiltrating the TME with high IDO1 activity are depleted

of tryptophan. Tryptophan depletion in the TME drives T_{reg} cell fate adoption (Baban et al., 2009) and T_{regs} may suppress the activity of cytotoxic T cells preventing elimination of cancer cells (Sojka et al., 2008).

Targeting CTLA-4 in immunotherapeutic approaches for metastatic melanoma amongst other cancers has proven efficacious (Hodi et al., 2010). Ipilimumab is an anti-CTLA-4 monoclonal antibody used in melanoma treatments, with Phase III trials increasing average survival time from 6.4 to 10.1 months (Hodi et al., 2010; Tawbi et al., 2018; Wolchok et al., 2017). Binding of ipilimumab to CTLA-4 prevents interactions with CD80/86, preventing sequestration of ligands away from CD28, enhancing activation of T-cells committing cells towards cytotoxic fates, preventing anergy (Tarhini et al., 2010).

PD-1 and PD-ligand 1 (PD-L1) interactions drive immune tolerance in cancer through suppression of intracellular signalling pathways downstream of TCR-MHCI and CD28-CD80/86 (Sharpe & Pauken, 2017). T-cells express PD-1 on their surface which, in non-tolerogenic interactions, do not bind to anything on the surface of recognised cancer cells. However, if cancer cells are expressing PD-L1 on their surfaces, PD-1 will bind to it. When PD-1 interacts with PD-L1 it activates Src homology region 2 domain-containing phosphatase-2 (SHP2) on the intracellular face of PD-1 (Patsoukis et al., 2020). SHP2 antagonises activation of RAS, Phosphoinositide 3-kinase (PI3K) (Bai et al., 2017; Patsoukis et al., 2012), and ZAP70 (Sheppard et al., 2004) which are phosphorylated in response to TCR and CD28 signalling. The consequence of this is signals for activation from recognition of MHCI and co-stimulatory CD28 interactions

are no longer efficiently transduced within T cells, suppressing responses that should eliminate detected tumour cells.

Given direct suppressive effects from PD-L1 expression on the surface of tumours, melanomas frequently have elevated PD-L1 expression (Kaunitz et al., 2017). PD-L1 expression is mediated through interferon gamma (IFNγ) signalling via Janus kinase (JAK) and signal transducer and activator of transcription (STAT) mediated pathways (Qian et al., 2018). Epi/genetic changes that elevate activity of IFNγ-signalling pathways enhance immunosuppression in the TME via elevated PD-L1 expression, and those in the promoter of CD274 – the gene encoding the PD-L1 protein (Cha et al., 2019; Fernández-Sánchez et al., 2013).

Like anti-CTLA-4 monoclonal antibodies, anti-PD-1/anti-PD-L1 monoclonal antibodies are immunotherapies that re-sensitise the immune system to immunosuppressive tumours. Standard of care is combination therapies of ipilimumab and anti-PD-1 drugs nivolumab or pembrolizumab for metastatic melanoma patients (Hodi et al., 2016, 2018; Rotte, 2019; Tawbi et al., 2018; Wolchok et al., 2017). Combination of ipilimumab with nivolumab compared to ipilimumab alone increases patient disease-free progression from 13% to 34% (Van der Walde et al., 2023).

1.3. The Aryl Hydrocarbon Receptor

Most proteins influencing tumour development are solely pro- or anti-tumorigenic (Kontomanolis et al., 2020; E. Y. H. P. Lee & Muller, 2010). This is not true of the Aryl Hydrocarbon Receptor (AhR), where tumour cell type provides context in which the AhR may be a driver or suppressor of cancer formation (Elson & Kolluri, 2023; Y. Liu et al., 2017, 2021; Sarić et al., 2020; Tsai et al., 2017; Vogel & Haarmann-Stemmann, 2017; X. Zhang et al., 2021). Given the AhR is a well-studied TF with many known specific inhibitors and agonists (L. Sun, 2021), it's an attractive target for clinical intervention as this would reduce drug development costs compared to *de novo* drug design (*The Process and Costs of Drug Development (2022) | FTLOScience*, n.d.). For these specific inhibitors to be fully explored as clinical interventions (L. Sun, 2021), I must better characterise the AhR's role in context-specific contributions to cancer development.

The AhR is a highly evolutionarily conserved basic Helix-Loop-Helix (bHLH) TF, stimulated to mediate gene expression upon ligand binding (S. Dai et al., 2022; Williams et al., 2014). The AhR is part of the Per-Aryl Hydrocarbon Receptor Nuclear Translocator (ARNT)-Sim (PAS) family of TFs but is the only one dependent on ligand binding for activity (S. Dai et al., 2022; Nebert, 2017), which occurs over its PAS-B domain (Fig. 1.3). The AhR ligand binding domain is plastic, with different ligands binding to slightly different pockets within the PAS-B domain (Corre et al., 2018). Ligands the AhR may bind come from various endogenous and exogenous sources, from 2,3,7,8-Tetrachlorodibenzodioxin (TCDD) in Agent Orange (Baccarelli et al., 2004; S. Li et al., 2014) to Tryptophan photometabolites (Rannug et al., 1987), and their

binding to the AhR induces expression of detoxification enzymes (Jacob et al., 2011; Nebert et al., 2004; Shimada et al., 2002; W. Ye et al., 2019a) which should clear the stressor. In humans, the AhR is expressed in all tissues, with enhanced expression in lung epithelia and intestines (Dolwick et al., 1993).

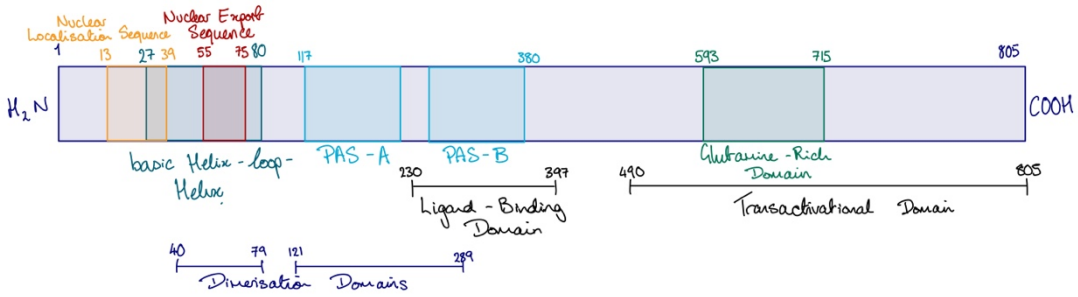

Figure 1.3 Schematic of the AhR. A representation of the distribution of conserved functional domains within the AhR.

Without a ligand bound, the AhR remains cytosolic in an inhibited state in complex with AhR-interacting Protein (AIP), p23, and Heat Shock Protein 90 (HSP90) (Cox & Miller, 2004; Gruszczyk et al., 2022) (Fig. 1.4). Upon binding of a ligand to the AhR's PAS-B domain, this complex undergoes conformational changes revealing the N-terminal Nuclear Localisation Sequence (NLS) (Ikuta et al., 1998) (Fig. 1.3) of the AhR which facilitates its nuclear translocation (Fig. 1.4). Once nuclear, this inhibitory complex is displaced (Tsuji et al., 2014) allowing the AhR to bind its transcriptional partner ARNT (also known as Hypoxia Inducible Factor 1B (HIF1B)), another bHLH TF. This heterodimeric TF may bind to AhR Response Elements (AhREs) in the genome. AhREs, also described as Xenobiotic Response Elements or Dioxin Response Elements, are hexameric sequences: 5'-TGCGTG-3' (Saatcioglus et al., 1990). Structural

studies have revealed the AhR forms contacts with the 5'-half of this sequence and ARNT forms the contacts with the 3'-half (Schulte et al., 2017). The AhR also bears an N-terminal Nuclear Export Sequence (NES), facilitating cytoplasmic shuttling of the AhR after mediating gene induction and clearance of the agonist that stimulated it (Ikuta et al., 1998, 2000).

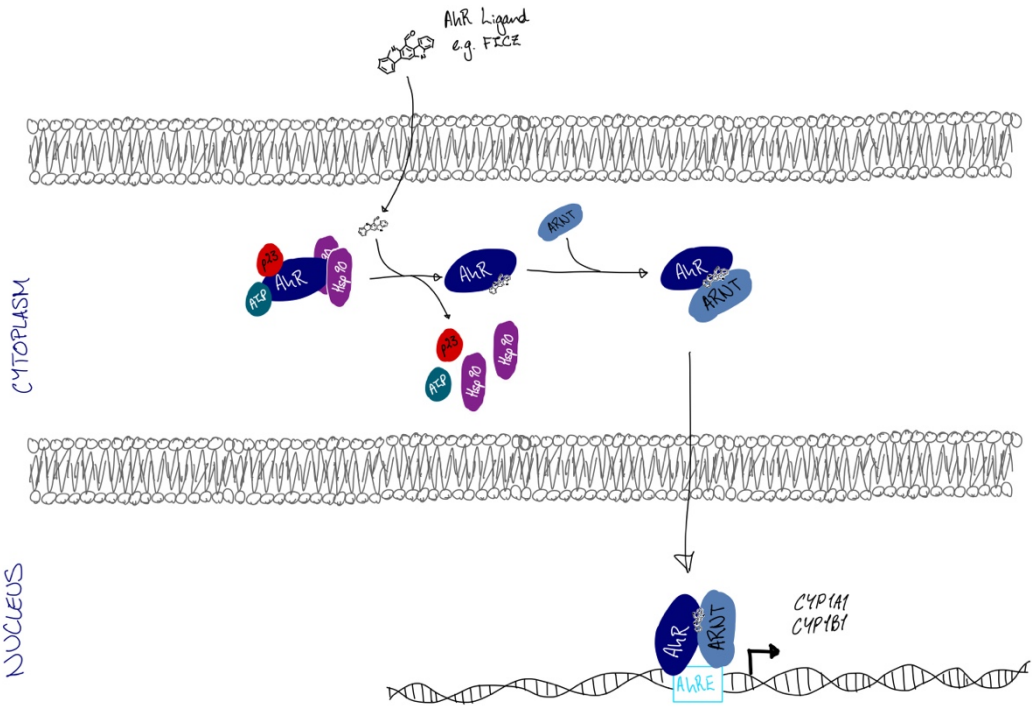

Figure 1.4 Schematic of the AhR Function. A representation of the processes following ligand binding to the AhR.

The AhR's expression in cells is autoregulated, with one of its key target genes being the *AHR repressor* (*AHRR*) (Mimura et al., 1999). The AhRR is a bHLH TF that associates with ARNT, competing with AhR suppressing its transcriptional activity (Sakurai et al., 2017). Furthermore, AhR activation stimulates expression of metabolising enzymes, the prototypical targets are *Cytochrome P450 (CYP) family 1 subfamily A member 1* (*CYP1A1*) (W. Ye et al., 2019a) and *CYP family 1 subfamily B member 1* (*CYP1B1*) (Jacob

et al., 2011). These are monooxygenases involved in the metabolism of polycyclic aryl hydrocarbons, which are agonists of the AhR (Wincent et al., 2012). The AhR forms a negative feedback loop wherein its activity is suppressed in response to stimulation.

Although *CYP1A1* and *CYP1B1* are canonical AhR target genes, the TFs that induce their expression are distinct. *CYP1A1* expression has been considered solely dependent on the AhR, with 4 AhREs in its promoter (Schulthess et al., 2015). However, there is evidence of multiple different TFs being involved in induction of this gene. The full extent of AhR-mediated activation of *CYP1A1* gene expression in human cells is dependent on the AhR-mediated recruitment of TF SP1 (Kobayashi et al., 1996; W. Ye et al., 2019b). In porcine cells, basal *CYP1A1* expression is mediated by AhR modulation but is dependent on SP1, suggesting a more complex network of regulation of *CYP1A1* expression than simply being solely mediated by the AhR (Xie et al., 2018). A Peroxisome Proliferator activated Receptor Alpha (PPARα) binding element in the *CYP1A1* promoter is sufficient to mediate induction of *CYP1A1* in response to fatty acids (Sérée et al., 2004; Villard et al., 2011). *CYP1A1* gene induction is also mediated by a T-Cell Factor (TCF) TF, integrating with AhR-mediated induction (Schulthess et al., 2015).

CYP1B1 expression is predominantly AhR-dependent, with 3 AhREs in its promoter (Shehin et al., 2000). However, the *CYP1B1* gene promoter also bears an E-box, which is the motif to which basic-helix-loop-helix (Leucine zipper) proteins may bind and mediate gene induction, amongst which are TCF3/4 (Shehin et al., 2000). Both *CYP1A1* and *CYP1B1* induction are therefore mediated by AhR:ARNT and TCF proteins (Schulthess et al., 2015; Shehin et al., 2000). The *CYP1B1* promoter also bears

sequences for Steroidogenic Factor 1 (SF1), SP1, and AP-2 family protein binding (Shehin et al., 2000). SP1 is an enhancer of *CYP1B1* expression (Tsuchiya et al., 2003). SF1's role is unclear, with it not being required for maximal *CYP1B1* gene induction and PKA mediating its effects on *CYP1B1* expression via the AhR:ARNT complex rather than through SF1 as expected (Tsuchiya et al., 2006).

The implications of these observations are that molecules that inhibit *CYP1A1* expression are indirect activators of the AhR due to the presence of tryptophan derivatives, *e.g.* FICZ, and Kynurenine-derived ligands being present and sufficient to activate the AhR (Seok et al., 2018) but then not efficiently cleared by CYP1A1 enzymatic activity (Wincent et al., 2012). FICZ is an inhibitor of CYP1A1 at very high concentrations, suggesting instances of high [FICZ], *e.g.* high UV may lead to prolonged AhR activation through inhibition of CYP1A1-mediated FICZ metabolism (Wincent et al., 2012).

1.3.1. AhR Ligands

The major ligands of the AhR are PAHs that are common in cigarette smoke and atmospheric pollutants from combustion engines. However, these are largely non-polar with limited diffusability through cells and tissues (Patel et al., 2020). Reactions catalysed by Cyp-family enzymes are key to catabolism of these compounds that increase their water solubility (Shimada & Fujii-Kuriyama, 2004). Enhanced water solubility of these compounds facilitates diffusion through the cell to the DNA where PAH-derivatives react with DNA driving mutagenesis (Shimada & Fujii-Kuriyama, 2004). An exemplary instance of this is B[a]P, bearing a conjugated system of five

benzene rings with poor water solubility that gets metabolised by first by CYP1A1 and subsequently by microsomal epoxide hydrolase 1 to yield B[a]P-7,8-dihydrodiol-9,10-epoxide (Gelboin, 1980). This bears 3 hydrophilic oxygen atoms increasing solubility and permitting diffusion to the DNA where it covalently binds to guanine to form bulky adducts, potentially perturbing key DNA processes driving mutations (Hargis et al., 2010).

Endogenous agonists of the AhR are often molecules related to tryptophan metabolism (Rannug et al., 1987). Two of further relevance in this thesis are 6-Formylindolo(3,2-b)carbazole (FICZ) and Kynurenine. FICZ: a photoproduct of tryptophan, produced upon UV exposure and a potent AhR agonist with a low nanomolar K_D (Rannug et al., 1987; Wincent et al., 2009). Kynurenine: the most common catabolite of tryptophan, is a weaker agonist of the AhR than FICZ with a low micromolar EC_{50} ($\leq 10^5$ times greater than FICZ) (Seok et al., 2018). Analysis of the chemical structure of Kynurenine against potent AhR agonists, FICZ/B[a]P, reveals significant differences: Kynurenine has a purine ring and extended carbon tail compared to the polycyclic conjugated aromatic rings found in FICZ and B[a]P. Spontaneous kynurenine derivatives, prevalent at picomolar concentrations in concentrated kynurenine solutions, are potent agonists of the AhR with structures considerably more analogous to FICZ/B[a]P (Seok et al., 2018). Kynurenine is better described as an AhR pro-ligand, with trace derivatives being true AhR ligands (Seok et al., 2018).

An important consequence both *in vivo* and *in vitro* of the AhR being stimulated by tryptophan derivatives is the basal stimulation of the AhR under almost all conditions.

Therefore, adding an AhR antagonist to cells not directly being treated with an AhR agonist will display inhibition of basal AhR activity, through antagonism of endogenous agonists.

There are also AhR antagonists, molecules binding the AhR, and inhibiting gene induction stimulated by agonists. One of the most common antagonist is 2-methyl-2H-pyrazole-3-carboxylic acid (CH223191) (Kim et al., 2006), with a low micromolar IC_{50} (Zhao et al., 2010). CH223191 is an antagonist, competing with AhR agonists, driving cytoplasmic retention of the AhR (Zhao et al., 2010) and suppression of transcription when AhR ligands are present.

The solvent used to suspend AhR modulators is also an effector of the AhR, albeit indirectly (Wincent et al., 2012). DMSO is often used to suspend non-polar compounds as it is miscible in both polar and non-polar solvents – essential for suspension and adding aromatic compounds to cell culture media. DMSO inhibits CYP-family enzyme activity including CYP1A1, which leads to AhR activation indirectly through reduced clearance of endogenous tryptophan-derived agonists of the AhR (David et al., 2012; Wincent et al., 2012).

Whilst early characterisation of the AhR was performed using exogenous toxins as AhR stimulants (Matsunawa et al., 2009; Pansoy et al., 2010), recent studies have demonstrated that AhR ligands can be endogenous (Rannug & Rannug, 2018; Opitz et al, 2011; Rannugs et al, 1987) or bacterial-derived (Moura-Alves et al., 2019). There are differences between the AhR-mediated transcriptional programs of different exogenous toxins (Pansoy et al., 2010). It is reasonable to assume that both the tumoral

context and the ligand stimulating the AhR affects its transcriptional program. To better understand mechanisms through which the AhR drives oncogenesis, one must study activity of the AhR under stimulation of physiologically relevant agonists in specific tumour types to accurately characterise the mechanisms of action in each context. The primary aim of this work is to better describe AhR's role under biological conditions in melanoma by using only physiological agonists rather than exogenous toxins to determine the AhR's role in oncogenesis. I focus on melanoma as a highly prevalent cancer type and a model for highly immunogenic cancers. Given the AhR modulates immunosuppression in this highly immunogenic tumour type *in vivo* (Paris et al., 2022a; Walczak et al., 2020), melanoma is a good model to study the AhR's immunomodulatory mechanisms.

1.3.2. The AhR in skin homeostasis

Expression of the AhR varies across cell types, however, it is highly expressed across the cells composing the skin: Keratinocytes, Melanocytes, Langerhans cells, Dendritic cells, and T cells (Esser et al., 2013). The AhR has three major roles in maintaining skin homeostasis: metabolism of aromatic compounds entering the skin, maintenance of skin barrier integrity, and modulation of immune systems in the skin.

Ligands stimulating the AhR in the skin may be exogenous toxins (TCDD, B[a]P, 3-MC), derived from plant flavonoids in the gut or from topical application, or Tryptophan derivatives from endogenous or microbial sources. Often, the metabolism of these compounds by CYP-enzymes, expressed in response to AhR activation, produces compounds causing inflammatory and carcinogenic effects in the

skin (Patel et al., 2020). As the skin is a barrier between body and environment, often exposed to dioxins amongst other AhR agonists, it must be able to catabolise these compounds to prevent diffusion into the blood and circulation through the body. The AhR mediates the expression of the Cyp-family monooxygenases catabolising the agonists and clearing them.

The AhR mediates expression of genes integral to keratinocyte differentiation. AhR:ARNT dimers induce expression of *OVO-like 1* (*OVOL1*), a TF, which subsequently induces key keratinocyte differentiation genes including the *Filaggrin* (*FLG*) and *Involucrin* genes (G. Tsuji et al., 2017). There are XREs in the promoter of *FLG*, which AhR:ARNT dimers directly bind to and enhance transcription from (Sutter et al., 2011). AhR-mediated induction of *FLG* after TCDD treatment enhances skin barrier formation, with enhanced differentiation of keratinocytes and cornification of cell envelopes, the process that generates the skin's outermost layer: the physical barrier to the outside world (Loertscher et al., 2001; Sutter et al., 2011). The precise role of the AhR in establishment of the barrier of skin remains unclear, with AHR^{KO} mouse models produced by independent research groups having either severe hyperkeratosis or no abnormal skin phenotype (Fernandez-Salguero et al., 1997; Mimura et al., 1997). Keratinocyte-specific ARNT-deficient mice display clear epidermal barrier defects with death <24-hours post-birth due to dehydration through the defective skin barrier which is a consequence of a failure of AhR:ARNT function (Takagi et al., 2003). The complexity of the AhR's role in cell differentiation in the skin is only further highlighted when considering that the AhR mediates commitment of epidermal stem cells to an undifferentiated cell fates (Rico-Leo et al.,

2021). Regardless of mechanism, the AhR plays an integral role across various cell types found in the skin with respect to physical structures of the skin's barrier.

The role of the AhR in skin regarding inflammation and immunity is two-fold; mediating expression of pro-inflammatory cytokines, and directly responding to microbes. The AhR modulates skin inflammation, evidenced by AhR activation being sufficient to reduce the severity of a psoriasis (an inflammatory skin disease) model (DiMeglio et al., 2014). In this instance, the AhR mediated its effects on skin inflammation through suppression of Interleukin-1β (IL-1β)-mediated-expression of AP-1 member JunB (known to mediate keratinocyte differentiation and immune cell activation in the skin) (DiMeglio et al., 2014; A. Wang et al., 2013). Constitutive expression of the AhR in skin, however, enhances IL-1β expression (Tauchi et al., 2005), which can be argued to be a consequence of prolonged AhR activation resulting in dysregulation (Bock & Köhle, 2006) – highlighting that the duration of AhR activation may also play a key role in AhR's effector function.

The AhR's response to microbes via microbiota-derived ligands points towards a clear protective role in the skin (Uberoi et al., 2021). Germ-free mice have impaired skin barrier structures. This, together with commensal microbes being activators of keratinocyte AhR, indicates that the AhR-microbiota axis is integral to skin barrier formation in healthy organisms (Uberoi et al., 2021). Furthermore, AhR activation in keratinocytes by microbial metabolites enhances the expression of *FLG* amongst other genes that contribute to barrier formation and the expression of antimicrobial peptides (Smits et al., 2020). Together, this points towards the AhR being a modulator of the skin barrier in response to changes in microbial composition, perhaps

reflecting that a microbial infection has the capacity to activate the AhR triggering reinforcement of the skin barrier and clearance of the deleterious microbes to restore a healthy microbiota in the skin (Smits et al., 2020).

The role of the AhR in skin homeostasis has largely been studied by assessing the role of the AhR in keratinocytes, not melanocytes. Keratinocytes outnumber melanocytes in the skin and are relevant to consideration of how the AhR modulates skin homeostasis (K. L. Sun et al., 2021). Unlike keratinocytes, which are derived from epidermal stem cells (Alcolea & Jones, 2014), melanocytes originate from neural crest cell derived melanoblasts (Mort et al., 2015b), and can give rise to melanoma, a highly skin cancer . Given the clear difference in lineages between these cell types and the repeated evidence of the context-specific nature of the AhR's behaviour, one wouldn't assume the behaviour of the AhR in these cells would be the same.

1.4. Pro- and Anti-tumorigenic mechanisms of the AhR

The following examples highlight some common aspects of cell biology and molecular processes the AhR mediates to promote or suppress tumour formation depending on cancer type. Broadly, the AhR mediates cell differentiation, immune signalling, and invasion/metastasis.

1.4.1. The AhR: a tumour suppressor

The AhR is a typical tumour suppressor in many contexts, with distinct mechanisms of action in each cancer type described (Elson & Kolluri, 2023). In Non-Small Cell Lung Carcinoma (NSCLC) murine and *in vivo* models, AhR-loss enhances activity of GF signalling cascade component Protein Kinase B (PKB/Akt) (Opitz et al., 2011) with concomitant elevated populations of cancer stem cells (Nacarino-Palma et al., 2021), although the specific mechanism through which this occurs is unclear. Invasion of NSCLC cells are also suppressed by the AhR, with AhR-mediated suppression of transcription of *MMP24* suppressing invasive capacities of NSCLC cells and driving proteasomal degradation of SMAD4: a known TF of invasive genes (C. C. Lee et al., 2016; Nothdurft et al., 2020; Tsai et al., 2017).

In brain cancers such as Medulloblastoma, Neuroblastoma, and Glioblastoma the AhR mediates its anti-oncogenic effects through a variety of mechanisms. In glioblastoma the AhR inhibits invasion and metastasis (Jin et al., 2019) through upregulation of *Interleukin-24* (*IL24*) expression (Y. Liu et al., 2021) which inhibits the expression of *ZEB1* (T. Lin et al., 2021), a driver of the EMT (P. Zhang et al., 2015). In Neuroblastoma,

the AhR is a positive transcriptomic modulator of cellular differentiation (P. Y. Wu et al., 2019), meaning that its loss facilitates dedifferentiation and oncogenesis. In Medulloblastoma, the AhR inhibits Tumour GF-β signalling, which blocks sonic hedgehog pathway activity on which, the majority of, these tumours depend for sustained cell proliferation and evasion of apoptosis (Rimkus et al., 2016; Sarić et al., 2020).

Intestinal cancers are suppressed by the AhR. AhR-mediated homeostasis of the intestinal tract has been well-studied (H. Han et al., 2021; Y. Li et al., 2011; Shah et al., 2022), it's expected that perturbation of the AhR in these tissues may contribute to disease. In the context of intestinal cancers, the AhR has been shown to down regulate immune inflammation (Díaz-Díaz et al., 2016; X. Zhang et al., 2021) which is a known risk factor for the formation and development of these tumours (Rubin et al., 2012).

Although these examples aren't exhaustive, they are demonstrative of the complexity of the mechanisms through which the AhR may be exacting its tumour suppressive roles. It also highlights the importance of the context in which I'm studying the AhR.

1.4.2. The AhR: an oncogene

The AhR has been demonstrated to be pro-oncogenic in oral squamous cell carcinoma (OSCC) (Kenison et al., 2021), Breast Cancer (BrCa) (Vogel et al., 2011), NSCLC (M. Ye et al., 2018), and melanoma (Corre et al., 2018; Mengoni et al., 2020). In these contexts, the AhR contributes to oncogenesis through immune modulation and dedifferentiation (Kenison et al., 2021; Mengoni et al., 2020; Vogel et al., 2011). Between

establishing a tolerant immune microenvironment and of EMT-associated proteins, the AhR contributes to tumour survival and progression towards late-stage disease phenotypes.

OSCC is a cancer derived from cells of the mucosal epithelia of the head and neck (Y. Tan et al., 2023), wherein the AhR, in murine models, is an immune modulator (Kenison et al., 2021). This demonstrates pro-oncogenic effects of the AhR in these mice is mediated through suppression of host immune interactions, with immune compromised mice developing tumours regardless of AhR presence in the tumour, but in those mice with competent immune systems, AhR-loss in tumour cells allows immune-mediated clearance of tumour cells. Presence of the AhR in tumour cells enhances expression of *CD274*; the gene encoding PD-L1, an immune-checkpoint inhibitor, which suppresses cytotoxic T cell activity (Y. Han et al., 2020), protecting OSCC tumour cells from elimination by the host immune system (Borcoman et al., 2021).

The role of the AhR in BrCa is somewhat unclear. Studies have demonstrated there's a pro-oncogenic link between the AhR and NF-κB signalling pathways (Fig. 1.5), which facilitate tumorigenesis of BrCa. The mechanism through which this drives cancer progression is unclear, but AhR agonist Benzo[a]pyrene (BaP) stimulates transformation of non-transformed breast cells in culture with concomitant elevated NF-κB activity (D. W. Kim et al., 2000). The role of the AhR in modulating NF-κB-mediated transcription is also unclear, however, interactions between the AhR and NF-κB subunit RelB have been demonstrated, forming a heterodimeric TF complex capable of binding distinct RelBAHRE motifs (Vogel et al., 2007). This AhR-RelB TF

complex is responsible for enhanced inflammation and tumour progression in BrCa (Vogel et al., 2011). Beyond this interaction, the AhR and NF-κB pathways are antagonistic of one another, with AhR stimulation suppressing tumour necrosis factor alpha (TNF)-stimulated NF-κB-mediated gene induction (Øvrevik et al., 2014; Tian et al., 1999).

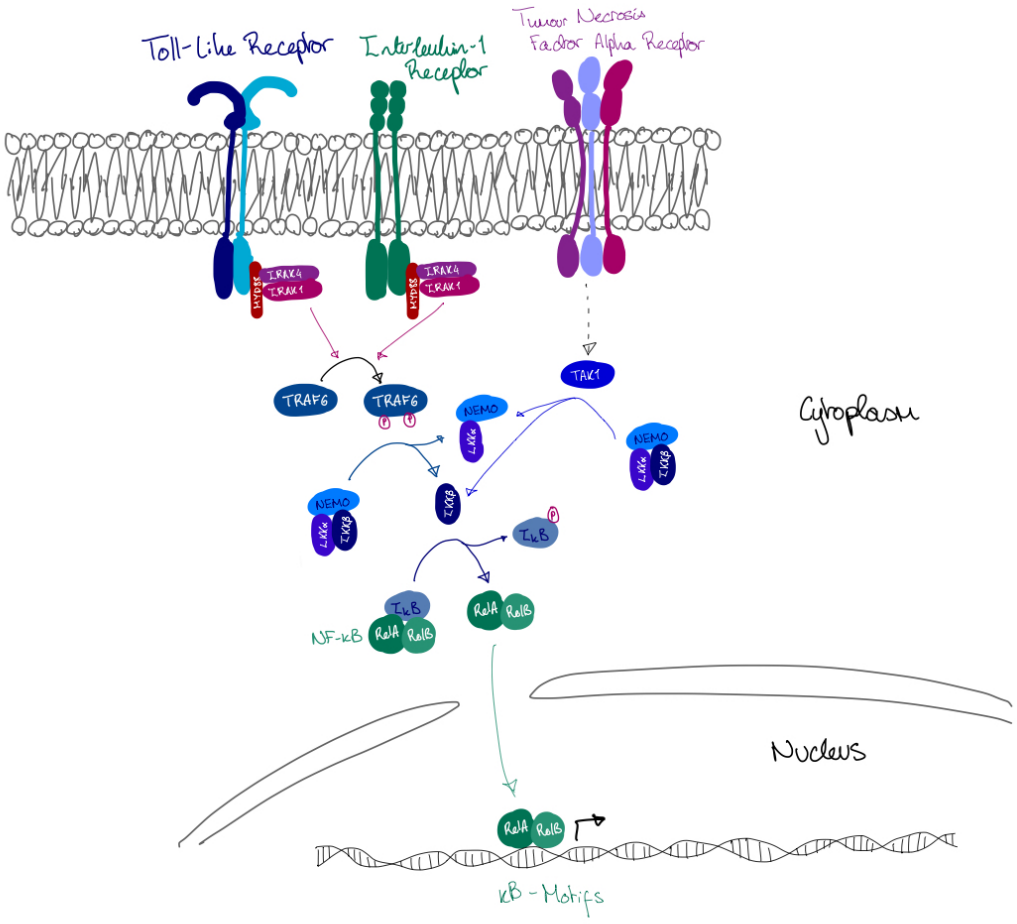

Figure 1.5 Schematic of the Nuclear Factor kappa B Signalling pathway. A representation of the signalling pathways that activate NF-κB mediated transcription in response to stimulation via TLRs, IL-1R, and the TNF receptor.

Although, the AhR has been described as a tumour suppressor in NSCLC through suppression of PKB/Akt signalling, under BaP-mediated stimulation, the AhR also drives invasion and metastasis of NSCLC cancer cells (Y. Wu et al., 2020). BaP-

stimulated AhR drives the expression of a long non-coding RNA (linc00673), which is a sink for the micro-RNA miR-150-5p (Lu et al., 2017). miR-150-5p expression drives degradation of *ZEB1* transcripts (Yokobori et al., 2013), meaning increased activity of the AhR depletes the free pool of miR-150-5p available to suppress *ZEB1* accumulation. This indirectly increases the amount of ZEB1 present in these cells, which as a pro-EMT TF, enhances expression of proteins facilitating invasion and metastasis (P. Zhang et al., 2015).

There's increasing evidence transformations that allow for growth of a tumour are distinct from those favouring dispersion of tumour cells away from the primary tumour. Broadly, mutations pushing a cell towards dysregulated division and growth in primary tumours are favouring phenotypic states distinct from the stressed/quiescent state that an invasive/metastatic cell would enter to disperse through the body (Hossain & Eccles, 2023). It's unsurprising a protein may drive tumour suppression in some stages of tumour development whilst being pro-oncogenic in other stages. It can be reconciled the AhR may be both pro- and anti-tumorigenic in NSCLC as the phenotype the AhR is driving is one of a stressed and invasive state, which would drive late-stage metastasis whilst being suppressive in early-stage development where rapid growth is the major selection pressure.

1.4.3. Genetic Risk Factors for cancer in the AhR Pathway

Often, cancer-associated genes bear consistent patterns of mutation across patients. This is reflective of certain mutations in genes producing specific functional changes

in the protein it encodes which drive oncogenesis, either through disruption of tumour suppressive capabilities or through acquisition of pro-tumorigenic mutations in proto-oncogenes. Meta-analyses studying the distribution of mutations across the *AhR*, *AHRR*, *ARNT*, *CYP1A1*, *CYP1B1*, and *IDO1* have been performed to assess whether there are genetic risk factors associated with cancer in this pathway.

While the *AhR* gene has several known polymorphisms that have been studied regarding the oncogenicity of the AhR; rs2066853, rs7796976, and rs2074113. Meta-analyses across more than 9,500 patient samples have revealed insignificant correlation between these polymorphisms and cancer rates across the entire population, sub-populations by ethnicity, and sub-populations by cancer type (Li et al., 2020). In the data available from The Cancer Genome Atlas there's a low frequency of mutation of the *AhR*, with only 4 available cancer datasets showing more than 15% of patients bearing *AhR* mutations (Paris et al., 2021a). Of those 4 cancer patient datasets exceeding 15% of patients with an *AhR* mutation, 2 are melanoma datasets where the most abundant mutation type is an amplification (Paris et al., 2021a). There is also evidence of that mutations resulting in expression of an AhR spliceoform missing exons 8 and 9, which disrupts its DBD, are drivers of urinary tract cancer-specifically (Vlaar et al., 2022). However, genetic lesions in AHR or its differential splicing will not be explored in this thesis.

While AhRR expression is associated with cancer development, relatively few polymorphisms in this gene have been identified within the coding region of this gene there's instead a clear relationship between the methylation of the *AhRR* and cancer incidence (Zudaire et al., 2008). 4 polymorphisms of the *AhRR* have been identified

although none of these are statistically significant in their effect on lung cancer incidence(Phane Cauchi et al., 2003). Hypomethylation of *AhRR* is a marker of smoking and lung cancer risk, a cancer type where the AhR behaves as a TSG suggesting the reduction in methylation at the promoter of the *AhRR* enhances its expression and thereby reducing AhR activity in these tumours (Tsuboi et al., 2022). This finding is contentious, with other studies identifying no such relationship between AhRR methylation and lung cancer rate (Grieshober et al., 2020).

The *ARNT* gene has more than 20 different single-nucleotide polymorphisms (SNPs), with only 6 predicted to have an effect of overall protein structure and function (Urban et al., 2011). Of these 6 SNPs predicted to influence ARNT function, their prevalence is incredibly low (Urban et al., 2011) and there are no available analyses of *ARNT* polymorphisms in cancer to assess whether these are significantly linked to cancer risk or incidence.

The *CYP1* family of genes bear SNPs associated with cancers. SNPs of *CYP1A1* affect cancer incidence in BrCa (C. Chen et al., 2007), Prostate Cancer (Zhu et al., 2019), Renal Cell Carcinoma (Meng et al., 2015), and Lung Cancer (Drakoulis et al., 1994). SNPs of *CYP1B1* have been associated with Lung Cancer (Liu et al., 2017; Sawrycki et al., 2018), Oral Squamous Cell Carcinoma (Moghadam et al., 2018), and BrCa (García-Martínez et al., 2017). The significance of the association of these SNPs with their corresponding cancer types varies with ethnicity, further emphasising the context in which the AhR is studied can have significant implications in the behaviour it displays regarding tumorigenesis.

IDO1 polymorphisms have been characterised in the context of human disease (Lee et al., 2014; Napolioni et al., 2019; Smith et al., 2011; Török et al., 2022), although with no evidence for these polymorphisms being linked to cancer incidence.

1.5. The AhR in melanoma

In melanoma, the AhR is oncogenic. The major pathway through which the AhR facilitates tumorigenesis in melanoma is modulation of the host immune system to establish a suppressive tumour immune microenvironment (Campesato et al., 2020; Y. Liu et al., 2017, 2018; X. Zhang et al., 2021). The AhR also is key a contributor to BRAF inhibitor (BRAFi) resistance, which encompasses a significant portion of the chemotherapeutics used against melanoma (Corre et al., 2018; Leclair et al., 2020; Paris et al., 2022a). Over 50% of melanomas are dependent on mutations in *BRAF*, which drives melanomagenesis (Section 1.2) and are acutely sensitive to BRAFi (Chapman et al., 2011; Maio et al., 2018). Generally, BRAFi drugs, such as vemurafenib, improve melanoma patient outcome compared to general chemotherapeutics (Chapman et al., 2011; Maio et al., 2018), however are ineffective in patients whose tumours do not rely on *BRAF* mutations. Equally, some melanomas may acquire resistance to BRAFi during treatment, as genetic or epigenetic changes which drive activation of components within MAPK signalling pathways downstream of BRAF have the same effect as $BRAF^{V600E/K}$ but aren't impacted by inhibition of BRAF (Johannessen et al., 2010; Nazarian et al., 2010; Villanueva et al., 2010).

The AhR contributes to BRAFi resistance in melanoma through activation of an alternative pathway responsible for independence from GF signalling. Src is a proto-oncogene whose protein product is a kinase involved in a multitude of signalling pathways (Guarino, 2010; Ortiz et al., 2021; Pelaz & Tabernero, 2022). Src directly interacts with the AhR *in vitro* with AhR activation contributing to enhanced phosphorylation of Src (G. Xie et al., 2012). Activation of Src alongside concomitant

AhR activity results in activation of MAPK pathways and independence from BRAF signalling for MAPK pathway activity, elevated Src and AhR activity in melanoma correlates with a more dedifferentiated phenotype with greater expression of genes associated with the EMT phenotypic switch (Paris et al., 2022a; M. Ye et al., 2018).

The role of the AhR in pro-oncogenic immunomodulation is more complex. In OSCC, the AhR is required for immune evasion and tumour survival in mice (Kenison et al., 2021). The mechanism through which the AhR mediates OSCC immune evasion was through elevated PD-L1 expression, this is not the predominant mechanism through which AhR mediates immunosuppression in melanoma. The current proposed mechanism of action is through the AhR-IDO1-kynurenine axis.

1.5.1. The AhR-IDO1-kynurenine axis

A landmark paper in the field of AhR immune oncology demonstrated that TCDD-mediated *IDO1* expression was dependent on the AhR (Vogel et al., 2008). Expression of *IDO1* is a well characterised driver of Treg cell fate adoption in the TME (Baban et al., 2009) across a spectrum of cancers (J. Y. Chen et al., 2014; M. Li et al., 2014; D. Shi et al., 2022). IDO1 converts tryptophan into kynurenine, and it's the depletion of tryptophan which drives Treg cell fate adoption and establishes a suppressive tumour immune microenvironment (Fallarino et al., 2002, 2006; Munn et al., 2005). Kynurenine is a polycyclic aryl hydrocarbon which also serves as an agonist of the AhR, stimulating expression of canonical AhR target genes *CYP1A1* and *CYP1A2* (DiNatale et al., 2010). It's hypothesised that together, the AhR forms a positive feedback loop wherein it stimulates *IDO1* expression, increasing the IDO1-mediated catabolism of

tryptophan to kynurenine, which in turn stimulates further AhR-mediated gene expression.

The AhR-*IDO1*-Kynurenine axis has been documented well in melanoma as the responsible mechanism for AhR-mediated immune suppression (Campesato et al., 2020; Y. Liu et al., 2017; X. Zhang et al., 2021). With IDO1 activity being shown to be mediated through the AhR in melanoma, and being an immune checkpoint dysregulated in many cancers independently of the AhR (Baban et al., 2009) it's essential to understand the mechanisms through which IDO1 expression is mediated in melanoma. While the evidence is very robust for the AhR being involved in mediating immunosuppression via regulation of *IDO1* expression, it's not without some doubt as to the physiological relevance of the AhR-*IDO1*-Kynurenine axis.

1.5.2. IFNγ signalling

is a canonical IFNγ-response gene, showing robust induction upon induction of the IFNγ-signalling pathway (Fig. 1.6) (W. Dai & Gupta, 1990). The IFNγ Receptor (IFNGR) is in complex with JAK1/2 without stimulation of the receptor, however, upon IFNγ binding to the receptor JAK1/2 are stimulated to phosphorylate each other and tyrosine 440 of the IFNGR1 (Müller et al., 1993). Phosphorylated tyrosine 440 is a binding site for STAT1 (Greenlund et al., 1995), and other STAT family members including STAT3 (Caldenhoven et al., 1999). Once recruited, JAK1/2 may phosphorylate and activate STAT family members. Phosphorylated STAT proteins may then dimerise and translocate to the nucleus where they interact with Gamma-activated sequences: 5'-TTCC(C/G)GGAA-3', where the bases in bold are the core sequence with variations in the intervening bases being tolerated (Horvath, 2000).

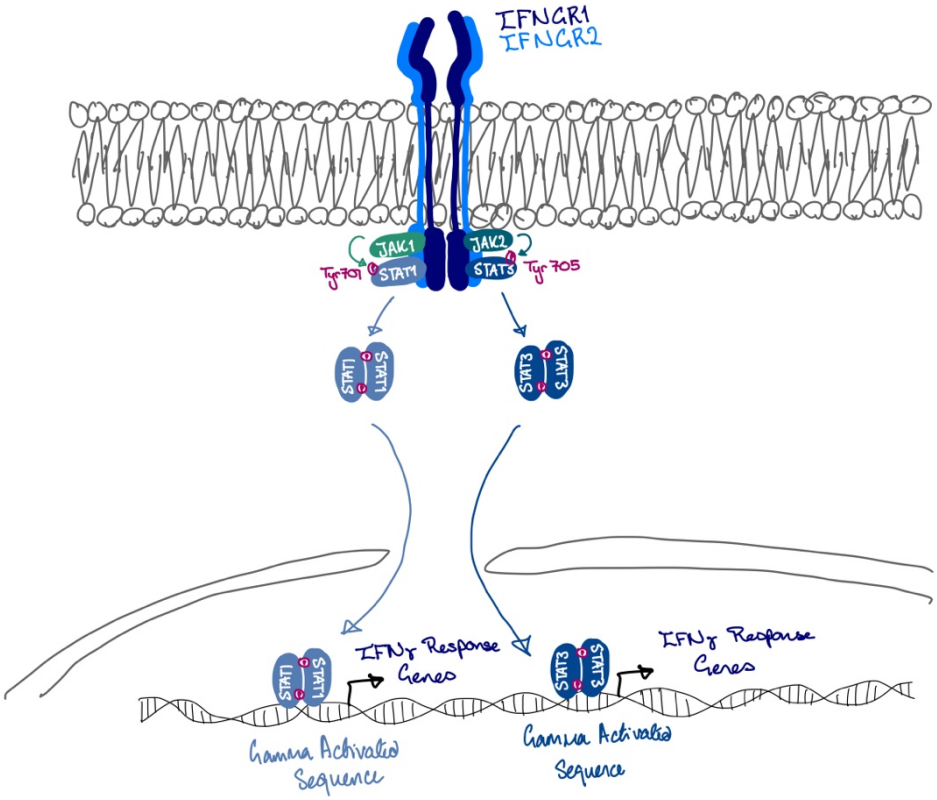

Figure 1.6 Schematic of the IFNγ Signalling pathway. A representation of the signalling pathways that lie downstream of activation of the Interferon Gamma Receptor by Interferon gamma.

The role of IFNγ-signalling in cancer is unclear with stimulation of IFNγ producing opposing effects on gene expression depending on, *e.g.* time course of treatment. These opposing effects of IFNγ on tumorigenesis have since been shown to be mediated through different STAT proteins, STAT1 and STAT3. STAT3 signalling is pro-tumorigenic, inducing expression of cell survival and proliferation genes (Hirano et al., 2000) while STAT1 induces cell-cycle arrest (Dimco et al., 2010). More recently, however, it has been shown *in vivo* that pro-tumorigenic IFNγ-signalling in melanoma is mediated by STAT1 not STAT3 (Zhou et al., 2022).

1.5.3. Speculation on the AhR-IDO1-kynurenine axis

Kynurenine is a physiological agonist of the AhR, it's rarely used in *in vivo* experiments assessing effects of the AhR. Instead, TCDD is generally used due to its greater affinity for the AhR and greater induction of target genes. In Vogel *et. al.* 2008, they demonstrate induction of *IDO1* with FICZ is 10-fold less than that observed with TCDD and 100-fold less than what is observed with IFNγ (Vogel et al., 2008). Furthermore, there's not a significant change in enzymatic activity of IDO1 in unstimulated cells and FICZ-stimulated cells but there's a 5-FI in response to TCDD treatment. This TCDD-mediated increase in IDO1 activity is AhR-dependent but is not observed in response to FICZ treatment. There's no evidence for kynurenine being sufficient to stimulate IDO1 expression at physiologically relevant levels without immune stimulation.

Hypothesising the AhR-*IDO1*-kynurenine axis is sufficient to explain immunosuppressive effects mediated by the AhR observed in vivo is, at best, incomplete. The role of the AhR as part of IDO1 mediated immunosuppression has been recapitulated both *in vivo* and *in vitro*, little evidence suggests that it's via this axis. Studying promoter regions of *IDO1* reveals the only known motifs found are bound by proteins involved in signalling downstream of interferons, chiefly IFNγ. The *IDO1* promoter contains multiple Interferon-stimulated response elements (ISREs) (Hassanain S et al., 1993) and IFNγ-activated sequences (GASs). These elements in IDO1's promoter are predominantly bound by Interferon regulatory factor-1 (IRF1) and STAT1, respectively. Binding and activation of *IDO1* transcription occurs in response to IFNγ binding to the IFNGR, which causes phosphorylation of STAT1 via

JAK1. Phosphorylated STAT1 dimerises and translocates to the nucleus where it may bind to GAS sequences. One of the genes with a GAS in its promoter is *IRF1*, IRF1 may then bind to ISRE sequences in the DNA 5'-TTTCNNTTTC-3' (Leviyang, 2021; Rettino & Clarke, 2013). There is little evidence of an AhRE/XRE/DRE in the promoter of *IDO1* nor at a nearby genomic locus wherein one could expect there to be a direct influence on its expression, unlike in the promoter of *IDO2* (Kado et al., 2023).

1.6. Aims of the thesis

1. **Determine the role of the AhR in IFNγ-signalling.**

   The mechanism through which the AhR is thought to drive immune suppression in melanoma is through expression of IFNγ-response gene *IDO1*. Evidence surrounding this mechanism fails to account for how physiological ligands could stimulate AhR-mediated expression of IDO1: central to the current model. I aimed to determine how the AhR is impacting expression of *IDO1*.

2. **Determine the role of the AhR in the binding of other TFs to melanoma-related genomic loci.**

   The AhR is a TF associated with oncogenesis in melanoma. As a TF, it may be exacting its pro-tumorigenic effects through binding to genomic loci affecting transcription directly or through regulation of other TFs. I aimed to determine whether the AhR is binding to genomic loci that may indicate roles of the AhR in mediating pro-melanomagenic gene expression.

3. **Determine the role of the AhR in shaping the transcriptome of melanoma cells.**

   As a cancer-associated TF in melanoma, there may be transcriptional regulation mediated by the AhR which could better characterise mechanisms

through which the AhR is contributing to melanomagenesis. I aimed to determine transcriptional changes mediated by the AhR in melanoma cells to assess whether there are currently uncharacterised mechanisms through which the AhR drives melanomagenesis.

2. Materials and Methods

2.1. Cell Lines and Cell Culture

2.1.1. Cell lines

The melanoma cell line used in this thesis is the human 501mel cell line derived from a cutaneous melanoma metastasis. With a melanocytic phenotype, representative of an early-stage tumour rather than a more dedifferentiated phenotype with loss of melanocyte identity generally coming in more developed tumours. This is a representative choice of melanoma phenotype at diagnosis, although derived from a metastasis it is not likely a genotypic representation of early-stage melanoma, although metastases can be driven by few mutations / epigenetic mechanisms (*TCGA Study of Genetic Drivers of Melanoma - NCI*, n.d.). 501mel are $BRAF^{V600E}$ driven melanoma cells, which is the most common driver mutation of melanoma in the clinic and representative of the most abundant melanomas diagnosed. Characterisation of this cell line in the Catalogue of Somatic Mutations in Cancer (COSMIC) database, reveals no characterised mutations associated with the AhR, inflammatory, or MITF-associated pathways. As such, I do not expect the behaviour of these pathways in these cells to be aberrant, however, this cannot be ruled out as there may be indirect effects mediated by other factors not directly in these pathways.

501mel and 501mel $AHR^{-/-}$ cell lines were gifts from Marie-Dominque Galibert, Université de Rennes and have been used in published work (Paris et al., 2021b, 2022b). The AHR-/- cell lines were generated using the GeneArt® CRISPR Nuclease Vector Kit, according to the manufacturer's protocol, including the $501mel^{WT}$ cell line

being treated with the GeneArt® Nuclease Vector and control oligonucleotide controlling for non-specific changes introduced by CRISPR when knocking-out the *AHR*. Cell lines we received were monoclonal.

The HaCaT cell line: a spontaneously immortalised human keratinocyte cell line, bearing a UV-induced *TP53* mutation. This cell line is used frequently within the field of skin biology due to their sustained non-tumorigenic phenotype allowing for representative studies of healthy keratinocyte function to be performed with these as a model (Boukamp et al., 1997). These cells have a propensity for spontaneous polyploidy although this doesn't appear to influence their nontumorigenic phenotype despite amplification of chromosomes (Boukamp et al., 1988, 1997).

The HaCaT *AHR*$^{-/-}$ and WT cell lines used in this work are also monoclonal. With both the 501mel and HaCaT AHR -/- cell lines used being monoclonal, the comparisons made between these cell lines and parental cells are at risk of being due to clonogenic differences, rather than differences driven by AhR status. Clonogenic differences between these cell lines may arise from random mutations in these cells ahead of selection and isolation of clones and mutations driven by non-specific cutting of the CRISPR-Cas9 system used to knock out the *AHR.* In this work, while the majority of differences in gene expression activity and behaviour between wild-type and *AHR*$^{-/-}$ cell lines may be driven by the difference in AhR status, clonogenic differences may exist and contribute to altered gene expression and biological properties of the derived cells. To improve reliability of these findings multiple monoclonal, polyclonal, and a variety of cell lines with the *AHR* gene knocked out should be examined to ensure these findings aren't artefacts of clonal differences. Alternatively,

the genomes of the AHR -/- and parental cells should be sequenced to determine genetic differences between wild-type and knock-out cell lines to avoid doubt regarding potential clonogenic differences and confirm their genetic similarity.

Together, the choice of these two cell lines provides *in vitro* models of typical skin cell behaviour from the HaCaT cell line and a melanoma cell line representative of melanoma cells as they are found in the dominant portion of tumours diagnosed. A significant benefit of the choice of the 501mel cell line, on which most of the work in this thesis was performed, was the availability of ChIP-Seq datasets on relevant genes that had been performed in this cell line previously, allowing for reliable comparisons between datasets to be made. Using only one melanoma cell line in which multiple genomic and transcriptomic studies have been performed allows for direct comparisons between these datasets is an advantage, although is also a clear limitation as the results may not be applicable to all melanomas, and especially not to melanomas with a de-differentiated or neural-crest like cell identity.

2.1.2. Culture conditions

501mel cells were cultured in Gibco DMEM with GlutaMAX supplement (Thermofisher, 10566016) supplemented with 10% fetal bovine serum (FBS, Biosera) at 37°C at 5% CO_2 which was thawed and distributed into 50 mL aliquots which were kept in a -20°C freezer until required. Given that many AhR ligands are photometabolites of cell culture components, media were stored in the dark as were all ligands. AhR ligands were suspended and aliquoted into microcentrifuge tubes then wrapped in aluminium foil before storage at -20°C to protect from UV or

degradation. For experiments comparing effects of FICZ, Kynurenine, or CH223191 on AhR activity, effects were measured compared to a control condition with an equivalent volume of DMSO added, DMSO is the solvent for FICZ, Kynurenine, and CH223191. HaCaT cells were cultured in RPMI 1640 medium with GlutaMAX™ supplement (Thermofisher, 61870010) supplemented with 10% FBS (FBS, Biosera) at 37°C at 5% CO_2. Cell lines were tested for mycoplasma ahead of RNA-Seq and ChIP-Seq sample collection and during culturing through assays and visualisation of DAPI in immunofluorescence.

2.2. Reagents

DMSO (Merck, 101900), FICZ (Cambridge Bioscience Ltd, 19529-1 mg-CAY), CH223191 (Stemcell Technologies, 72732), L-Kynurenine (Insight Biotechnology, sc-202688), Human Recombinant IFNγ (Bio-Rad, PHP050), Human Recombinant TNF (Abcam, ab30957),

2.3. Quantitative real-time reverse-transcription PCR (qRT-PCR)

1.2 x 10^6 cells were used/condition/replicate (three technical replicates per biological replicate). Total RNA was extracted using a RNeasy mini kit (Qiagen, 74104), as per manufacturer's protocol. RNA concentration was assessed using Nanodrop. cDNA synthesis was performed using GoScript™ Reverse Transcriptase (Promega, A5001) as per manufacturer's protocol using equal amounts of total RNA per sample. qPCR was performed using SYBR™ Select Master Mix (Thermofisher, 4472908) as per manufacturer's protocol using a LightCycler 480 Instrument II (Roche, 05015243001). Data was analysed in Microsoft excel (Version 16.87) using a

visual basic application integrating geNorm (Vandesompele et al., 2002) normalising relative transcript abundance using *GAPDH* as a house keeping gene and qBase (Hellemans et al., 2008) to generate relative quantities. This integrated VBA was developed by F. van Hauwermeiren (filipvh@dmbr.ugent.be). This method uses a developed version of the delta-delta-Threshold cycle method. The threshold cycle is the cycle number at which the fluorescence of the qRT-PCR reaction exceeds an arbitrary threshold value. Delta-Ct of samples are determined as difference between a true unknown or calibration sample and the gene of interest. This provides a relative concentration of starting material, allowing conversion into a normalised relative quantity (NRQ) with delta-delta-Ct calculations, where the delta-Ct of a gene of interest is divided by the delta-Ct of a house keeping gene (HKG). The qBase and geNorm models allow for calculations of NRQ using multiple HKGs and PCR efficiencies that aren't consistent. For this work, only one HKG was used, and PCR efficiencies were assumed to be 100%.

Table 1: List of primers used for qRT PCR.

Gene	Forward Primer (5' – 3')	Reverse Primer (5' – 3')
CYP1A1	ACATGCTGACCCTGGGAAAG	GGTGTGGAGCCAATTCGGAT
IDO1	GCCAGCTTCGAGAAAGAGTTG	ATCCCAGAACTAGACGTGCAA
ATF4	ATGACCGAAATGAGCTTCCTG	GGAGAACCCATGAGGT
PD-L1	TGGCATTTGCTGAACGCATTT	TGCAGCCAGGTCTAATTGTTTT
PKR	GCCGCTAAACTTGCATATCTTCA	TCACACGTAGTAGCAAAAGAACC
IRF1	ATGCCCATCACTCGGATGC	CCCTGCTTTGTATCGGCCTG
IL-6	ACTCACCTCTTCAGAACGAATTG	CCATATTTGGAAGGTTCAGGTTG
GAPDH	CATGAGAAGTATGACAACAGCCT	AGTCCTTCCACGATACCAAAGT

2.4. The Cancer Genome Atlas Dataset

The Cancer Genome Atlas (TCGA) dataset used (TCGA-SKCM) contains multi-omic data from 470 melanoma cases. 61.7% of cases were males, 38.3% of cases were females. 95.1% of cases were white individuals, 2.5% in Asian individuals, 2.1% did not report race, and 0.2% were black individuals. Age at diagnosis: 15.56 - 30.44 years

5.4%, 30.45 – 45.33 years 14.29%, 45.34 – 60.21 years 32.68%, 60.22 – 75.10 years 30.95%, 75.11 – 90 years 16.67%. For 89.36% of individuals, their primary diagnosis was melanoma, for 10.64% of individuals it was not.

2.5. CRISPR Gene Editing

HaCaT *AHR*$^{-/-}$ cells were established with AhR-specific TrueGuide™ Synthetic sgRNA (Thermofisher, A35533, CRISPR980378_SGM) (5'-CGGTCTCTATGCCGCTTGGA-3') with TrueCut™ Cas9 protein v2 (Invitrogen, A36498) according to manufacturer's protocol. Successful KO cell lines were validated with immunoblotting and qRT-PCR assessing FICZ-mediated *CYP1A1* and *CYP1B1* induction.

2.6. Immunoblotting

Using cells from 6 well-plates at confluency (approximately 1.2 x 10^6 cells) whole-cell lysates were collected by adding 500 µL 1X Laemlli Sampling Buffer (LSB) supplemented with cOmplete™ Protease Inhibitor Cocktail (Merck, 4693116001). Samples were incubated at room temperature (RT) for 10 minutes on a rocking platform, before transferring to microcentrifuge tubes and 5 minutes incubating at 95°C. Samples were centrifuged at 11,000 g at 4°C for 10 minutes with the supernatant carried forward. 20 µL of each sample was run on a 7.5% polyacrylamide gel at 100 V for 75 minutes. Proteins were transferred to nitrocellulose membranes via wet transfer at 400 mA for 75 minutes. Membranes were blocked using 5% semi-skimmed milk powder in phosphate buffered saline supplemented with 0.1% tween (PBS-T) on a rocking platform for 60 minutes at RT. Blots were washed for 3 x 5

minute washes using PBS-T. Samples were incubated with primary anti-bodies in PBS-T with 5% (w/v) Bovine Serum Albumin (Sigma, A3294-100G) overnight in an end-over-end rotator at 4°C. Samples were washed for 3 x 5 minute washes using PBS-T before adding Horseradish peroxidase-coupled secondary antibodies (anti-mouse 1:10000 and anti-rabbit 1:10000, BioRad) in PBS-T with 5% semi-skimmed milk and incubation at RT on an end-over-end rotator for 60 minutes. Antibodies were then removed, and blots were washed a further three times with PBS-T for 5 minutes each time before adding 500 µL of Cytiva Amersham™ ECL™ Western Blotting Detection Reagents (Fisher scientific, 10155854) and where luminescence was detected using X-ray film (Fuji film).

2.7. Immunofluorescence Microscopy

Cells were plated in 24 well-plates to reach confluency at the end of treatment (5 x 10^4 cells/well in 500 µL media 48-hours ahead) with cover glass (VWR, 631-0150) placed in each well. At the end of incubation, media was aspirated off and wells were washed with 500 µL of PBS, which was then aspirated off. 100 µL of 4% paraformaldehyde (PFA) in PBS was added and incubated at RT for 10 minutes, wells were quenched with 50 µL 2 M glycine in water. This was removed, then cells were incubated with 100 µL 0.2% Triton-X 100 in PBS on a rocking platform at RT for 10 minutes. This solution was removed, wells were washed with 500 µL PBS for 5 minutes on a rocking incubator at RT. 100 µL of primary antibody solution in PBS-T was added to each well and incubated at RT on a rocking platform. Primary antibody solutions were then removed before three 5-minute washes with PBS-T on a rocking platform. 100 µL of secondary antibody solution (Goat anti-Mouse IgG (H+L) Cross-

adsorbed Secondary Antibody, Alexa Fluor™ 488 (Thermofisher, A-11001) and Donkey anti-Rabbit IgG (H+L) Highly Cross-Adsorbed Secondary Antibody, Alexa Fluor™ 546 (Thermofisher, A10040)) with 0.1% 4',6-diamidino-2-phenylindole (DAPI) was added to each well and incubated on a rocking platform for a further 60 minutes whilst covered from light. Wells were then washed for 5 minutes in PBS-T a further three times before mounting on slides using 5 µL Mowiol as a mounting medium.

2.8. Antibodies

Table 2: List of antibodies used in experiments.

Target	Species	Provider	Catalogue Number	WB	IF
AhR	Mouse	Santa Cruz	A-3	1:300	1:300
AhR	Rabbit	Cell Signalling	D5S6H	1:300	1:300
HA-tag	Rabbit	Cell Signalling	C29F4	1:300	1:500
HA-tag	Mouse	Merck	12CA5	1:300	1:500
STAT1	Rabbit	Cell Signalling	9172	1:300	1:300
Phospho-STAT1 Tyr701	Mouse	Thermofisher	ST1P-11A5	1:300	1:300
STAT3	Mouse	Cell Signalling	9139	1:300	1:300
Phospho-STAT3 Tyr705	Rabbit	BioTeche R&D	9145S	1:300	1:300
IDO1	Rabbit	Thermofisher	711778	1:300	1:300

The choice of AhR-antibodies was made by sampling a variety of AhR antibodies available from major suppliers that had been used in published papers (Diedrich et al., 2023; Lafleur et al., 2023; Rudyak et al., 2023; Q. Tan et al., 2022) and selecting antibodies that gave western blots with limited non-specific bands, producing easily interpretable results when comparing 501mel AhR WT and 501mel *AHR*$^{-/-}$ cell lines.

2.9. Site-Directed Mutagenesis

Beginning with a plasmid with a cDNA *AHR* gene inserted upstream of an exogenous *MYC* NLS and 4xHA-tags flanked by PiggyBac transposon sequences. First, the exogenous NLS was removed using primer pair #1. From the resulting plasmid, nuclear localisation mutants were generated by deletion of the endogenous NLS (Δ13-39) and endogenous NES (Δ55-75) using primer pairs #2a and #2b, respectively.

Table 3: List of primers used for SDM.

Primer Pair	Forward (5'-3')	Reverse (5'-3')	Anneal. Temp.
1	TAGCGGCCGCTCGATAAG	AGCGTAATCTGGAACGTCATATG	58˚C
2a	AGAGACCGACTTAATACAG	GCGACTGGCGTAGGT	61˚C
2b	TACCTGAGAGCCAAGAG	CAGCAGGCTAGCCAAAC	61˚C

Primers were generated using NEBaseChanger®, and reactions were performed using Q5 Site-Directed Mutagenesis Kit (NEB, E0554S) according to manufacturer's protocols.

2.10. Transfections

To generate stable doxycycline-inducible cell lines, AhR construct-bearing plasmids were transfected into 501mel^{WT} and 501mel *AHR*$^{-/-}$ cell lines alongside vectors containing PiggyBac Transposase and Tet operator sequence. Constructs were introduced to cells using FuGENE6 Transfection Reagent (Promega, E2691) in OPTI-MEM (Thermofisher, 31985062) in 8:1:1 ratio ≤1 μg of DNA/well of 12 well-plate as per manufacturer's protocol. Cell lines were assessed for their doxycycline-inducible expression of constructs by immunoblotting and immunofluorescence.

2.11. Proximity-biotinylation affinity-purification coupled protein mass spectrometry.

These experiments were performed by collaborator JP. Lambert as per the protocol outlined in JP. Lambert et. al. 2015 (J. P. Lambert et al., 2015). 501mel cells were treated with FICZ and/or IFNγ for 4-hours before biotinylation and further processing. I received processed counts demonstrating enrichment of each hit compared to a baseline pulldown.

2.12. Gene ontology analysis

PantherDB's gene ontology (GO) web tool (https://geneontology.org) was used with relevant gene sets.

2.13. Chromatin Immunoprecipitation (ChIP)

For each of two repeats of 4 conditions (Control, FICZ 100 nM, IFNγ 10 ng/mL, FICZ 100 nM & IFNγ 10 ng/mL) two confluent 15 cm dishes of $501mel^{WT}$ cells were used. After 4-hours incubation with FICZ and/or IFNγ, paraformaldehyde was added directly to each dish to a final concentration of 1% and incubated for 12 minutes at 4˚C with agitation. Glycine was added to a final concentration of 125 mM and incubated for 10 minutes at 4˚C with agitation. Media was aspirated, and dishes were washed twice with 10 mL of ice-cold PBS, before adding 5 mL of ice-cold PBS to each. Cells were scraped off both dishes and collected into a 50 mL Falcon tube. Samples

were centrifuged at 800 rpm in an Eppendorf 5920 R centrifuge for 10 minutes at 4˚C. The supernatant discarded; the pellet resuspended in 1 mL of lysis buffer. Samples were incubated on ice for 10 minutes before adding 1 mL of ChIP-Dilution buffer then distributed evenly between two microcentrifuge tubes and sonicated for 15 minutes (15 seconds on / 15 seconds off, at high power in a Diagenode Bioruptor). Samples were centrifuged at 16,000 g for 10 minutes at 4˚C. Supernatants were combined, with 40 µL taken and frozen at -20˚C until reverse cross-linking and diluted with 10 mL of ChIP-Dilution buffer. 260 µL Millipore Protein A agarose 50% slurry (Merck, 16-157) was washed twice with 800 µL ChIP-Dilution buffer. After each wash, beads were sedimented by centrifugation for 3 minutes at 2840 G. 80 µL worth of beads were transferred to diluted samples and incubated at 4˚C for 60' on an end-over-end rotator for pre-clearing. Samples were centrifuged at 1000 rpm in an Eppendorf 5920 R centrifuge at 4˚C for 5 minutes to sediment the beads. Supernatants were transferred to a fresh 50 mL Falcon tube, where 20 µL of AhR antibody was added (D5S6H, Cell Signalling). Samples were incubated overnight at 4˚C on an end-over-end rotator. The remaining 180 µL worth of washed Millipore Protein A agarose beads were added to samples and incubated for 90 minutes on an end-over-end rotator at 4˚C. Samples were centrifuged at 380 g for 8 minutes at 4˚C. The supernatant discarded; the beads were collected and resuspended in 800 µL low salt buffer in a microcentrifuge tube. Post-inversion, samples were then centrifuged at 2840 g for 3 minutes at 4˚C (this sedimentation protocol is used for all subsequent washes until reverse cross-linking, after 5 minutes incubation at 4˚C in an end-over-end rotator). Samples were washed in 800 µL high salt buffer, 800 µL LiCl Wash-Buffer, 2 X TE buffer. After the second TE buffer wash, remaining liquid wash removed manually using a narrow loading-tip. 120 µL of elution buffer was added, resuspending beads, then placed on a shaking

incubator at 1400 rpm at RT for 15 minutes. Samples were centrifuged at 2840 g at RT for 3 minutes. Supernatant collected; the beads resuspended in a further 120 µL of elution buffer, placed in a shaking incubator at RT and 1400 rpm for a further 15 minutes. Samples were centrifuged again at 2840 g at RT for 15 minutes, the supernatants were combined for a total eluant volume of 240 µL.

Buffers:

Lysis Buffer

1% Sodium dodecyl sulphate (SDS), 10 mM Ethylenediaminetetraacetic acid (EDTA), 50 mM Tris buffer pH 8.1, 2X cOmplete™ Protease Inhibitor Cocktail (Roche, 11697498001) in MilliQ water.

ChIP-Dilution Buffer

0.01% SDS, 1.1% Triton X-100 (SLS, X100-100ML), 1.2 mM EDTA, 16.7 mM Tris pH 8.1, 167 mM NaCl in MilliQ water.

Low-Salt Wash-Buffer

0.1% SDS, 1% Triton X-100, 2 mM EDTA, 20 mM Tris pH 8.1, 150 mM NaCl in MilliQ water.

High-Salt Wash-Buffer

0.1% SDS, 1% Triton X-100, 2mM EDTA, 20 mM Tris pH 8.1, 500 mM NaCl in MilliQ water.

LiCl Wash-Buffer

1% Igepal® (MP Biomedicals®, 02198596-CF), 1 mM EDTA, 10 mM Tris pH 8.1, 250 mM LiCl, 1% Sodium deoxycholate in MilliQ water.

TE Wash-Buffer

10 mM Tris pH 8.0, 1 mM EDTA in MilliQ water.

Elution Buffer

0.1 M $NaHCO_3$, 1% SDS, in autoclaved water.

Reverse crosslinking:

The inputs were thawed and brought to a total volume of 240 µL with elution buffer. To both inputs and ChIP eluants: 12.5 µL of 4M NaCl was added, before incubation at 65˚C on a heated shaking incubator at 1400 rpm overnight. tubes were allowed to cool before adding 2 µL of 20 mg/mL Proteinase K (Invitrogen™, 25530049) in 50 mM tris buffer. Samples were incubated at 45˚C 1400rpm for 4-hours. Tubes were cooled to 37˚C and 1 µL of RNaseA (Qiagen, 19101) was added before 30 minutes of incubation at 1400 rpm. DNA was purified from samples using a Qiagen MinElute PCR purification kit (Qiagen, 28004), as per manufacturer's protocol.

2.14. qPCR

qPCR was performed using SYBR™ Select Master Mix (Thermofisher, 4472908) as per manufacturer's protocol using a LightCycler 480 Instrument II (Roche, 05015243001). Data was analysed in Microsoft excel (Version 16.87) to produce relative transcript abundance normalised to GAPDH (Same primers as in 2.3.3.).

Table 4: List of primers used for qRT PCR.

Gene	Forward Primer (5' – 3')	Reverse Primer (5' – 3')
CYP1A1	TTGAAGGATCGGAATGGATGG	GCGTTGCAATCAGACATAAG
CYP1B1	CGCTCCGGCGAACTTTAT	GATATGACTGGAGCCGACTTTC
IGF1R	CACGCATGACGTCTCTTCTT	GATGAGCGATGACCCTCTTTAC
NFE2L2	ATCTACACTCGCAACTCTTACC	TGTCTTTGGATTTAGCGTTTCAG

2.15. Library Preparation

DNA libraries were generated using NEBNext® Ultra™ II DNA Library prep kit for Illumina® with sample purification beads (NEB, E7103S) with NEBNext® Multiplex Oligos for Illumina® (NEB, E6440S) as per manufacturer's protocol.

2.16. Sequencing

Table 5: Number of reads for ChIP-Seq experiment

Sample	**Number of Reads** Pulldown	**Number of Reads** Input 2%
Control Rep. 1	58476572	39489140
Control Rep. 2	55211647	38703107
FICZ 100 nM Rep. 1	73130123	38524997
FICZ 100 nM Rep. 2	41759318	31941735
IFNγ 10 ng/mL Rep. 1	58830449	36077433
IFNγ 10 ng/mL Rep. 2	52804245	34531217
FICZ 100 nM + IFNγ 10 ng/mL Rep. 1	57058417	37560556
FICZ 100 nM + IFNγ 10 ng/mL Rep. 2	54515337	30230996

Sequencing of DNA libraries was performed on an Illumina® NextSeq 2000 for 50 bp paired end reads. Data has not yet been deposited into open access databases.

2.17. Bioinformatics for ChIP-Seq

2.17.1. Quality Control

Raw fasta files produced from sequencing were filtered for next generation sequencing errors and poor quality (short) reads using CutAdapt (v2.1) (Martin, 2011). Resulting files were quality controlled using FastQC (v0.12.1) (*Babraham Bioinformatics - FastQC A Quality Control Tool for High Throughput Sequence Data*, n.d.). Both paired-end reads were processed through CutAdapt together using their paired-end read function to ensure files could pair.

2.17.2. Sequencing Alignment

Both paired-end reads for each experiment were used for a single alignment output with Burrows-Wheeler Aligner (BWA) (v0.7.17) (H. Li & Durbin, 2009)*. Reads were aligned to GRCh38 (hg38). From this a single SAM file was produced per repeat per condition.

2.17.3. Converting SAM files into BAM files

* For analysis of MITF ChIP Seq data (GEO: GSE77437), the same packages were used however this data contains single-end reads, therefore were processed as such, not as paired-end reads.

SAM files were converted into BAM files for use in subsequent packages, this was completed using SAMtools (v1.17) (Danecek et al., 2021).

2.17.4. Peak Calling

For peak calling I used MACS3 (v3.0.1) (Zhang et al., 2008). combining each replicate at this point using their combining replicates functionality to produce a single peak set for each condition. i.e. 2% input replicate (rep) 1 and 2% input rep. 2 are averaged to give a single 2% input set of reads, IP rep. 1 and IP rep. 2 are averaged to give a single IP set of reads. Peaks are then called using these averaged reads, rather than producing a full set of peaks for each replicate separately. Reads were visualised as both input tracks and IP tracks, and a single Fold-Enrichment track.

2.17.5. Visualisation of peaks

Peaks were visualised using UCSC genome browser (Kent et al., 2002) from BigWig and BEDGraph files generated from MACS3 (v3.0.1) (Zhang et al., 2008).

2.17.6. Annotation of peaks

Peak annotation used ChIPpeakAnno (v1.40.0) (Wang et al., 2022; Yu et al., 2015) in RStudio (v2023.06.0), ChIPpeakAnno was used to generate graphs representing distribution of peaks across genomic features.

2.17.7. Heat maps of read density.

Heat maps of ChIP-Seq peak density and distribution were generated using EaSeq (v1.2) (Lerdrup et al., 2016).

2.17.8. Motif Analysis

Motif discovery and analysis was performed using MEME-Suite (Bailey et al., 2015), with their MEME-ChIP pipeline.

2.18. Gene Expression Profile Correlation

I established a list of genes regulated by the TF of interest through a literature review: gene expression profile (GEP). Then using transcriptomic data across a group of different biological samples, I rank each sample by expression of a gene. I then average ranks of each gene within my GEP to give overall GEP rank.

2.19. RNA Extraction

501mel^{WT} and *AHR*$^{-/-}$ cells were plated at 0.4 x 10^6 cells per well in a 6 well plate at time 0. At 24-hours, FICZ 100 nM and IFNγ 10 ng/mL were added, at 48-hours incubation was terminated with lysis and RNA extraction using a RNeasy® mini kit (Qiagen, 74104), as per manufacturer's protocol.

2.20. Library Preparation and Sequencing

Extracted RNA quality was assessed using a nanodrop for a 260 nM/280 nM ratio of ≥2.00. 3 μg of starting material for 3 replicates for each condition was provided to Wellcome Trust Genomic Service as part of the Oxford Genomic Consortium, Oxford. This material was used to generate a library with ERCC ExFold RNA Spike-In Mixes (Ambion) using QuantSeq 3' mRNA-Seq Library Prep Kit FWD (Lexogen, 015). Sequenced on HiSeq 4000 (Illumina), and data made available as FASTQ files.

RNA Seq data details: Read length 75bp, Single-End reads. Number of reads for each sample is detailed in table 6.

Table 6: Number of reads per conditions and replicate for RNA-Seq experiment

Cell Line	Treatment	Replicate 1	Replicate 2	Replicate 3
501mel WT	DMSO Control	18702741	19915248	16717550
501mel WT	FICZ 100 nM	18852474	19508661	19284034
501mel WT	IFNγ 10 ng/mL	18944482	19713269	22106948
501mel WT	FICZ 100 nM + IFNγ 10 ng/mL	22711579	20823939	20843452
501mel *AHR*$^{-/-}$	DMSO Control	21823233	20648475	20549037
501mel *AHR*$^{-/-}$	FICZ 100 nM	20042187	22131741	23203722
501mel *AHR*$^{-/-}$	IFNγ 10 ng/mL	17260303	16026960	17278783
501mel *AHR*$^{-/-}$	FICZ 100 nM + IFNγ 10 ng/mL	20044709	15764280	18725069

2.21. Bioinformatics for RNA-Seq

FASTQ files were trimmed of short reads, adapter sequences, and NGS errors using CutAdapt (v2.1) (Martin, 2011), then quality controlled using FastQC (v.0.12.1) (*Babraham Bioinformatics - FastQC A Quality Control Tool for High Throughput Sequence Data*, n.d.). Aligned to hg38 reference genome with ERCC spike-in using STAR (2.7.11b) (Dobin et al., 2013) determining number of reads per gene. Counts/gene files for each replicate of each condition were normalised using EdgeR (v4.4) (M. D. Robinson et al., 2010). Genes were filtered for genes with more than a normalised total count of 3 (Rationale: at least 1 count per replicate of an experimental condition). I performed gene set enrichment analysis (GSEA) using GSEA software (v3.0) provided by UC San Diego and the Broad Institute (Subramanian et al., 2005).

2.22. Statistical Analysis

Statistical analyses were performed using Prism (v10.0.3) (GraphPad). For each experiment, values are represented as the mean ± 1 Standard Deviation. Comparisons between multiple means were calculated by ordinary one-way ANOVA assuming a normal Gaussian Distribution followed by Tukey-Kramer test, correcting for multiple comparisons by invoking Tukey's Honestly Significant Difference test. Statistical significance was $P \leq 0.05$ for all experiments. For discontinuous data Spearman's Rank Correlation, for continuous data, Person's Correlation Coefficient was used.

2.23. Time Points for Experiments

Optimisation experiments (Section 3.2.1&3.2.2) were performed and a 24-hour time point was used for gene expression a 4-hour time point was used for protein-protein and genome binding assays.

3. Determining the role of the AhR in IFNγ Signalling

3.1. Background

As discussed in section 1.5.2., the AhR, in melanoma and other cancers, is an immune modulator. Presence of the AhR in tumours is sufficient to prevent host immune systems from efficiently recognising tumours cells and killing them (Kenison et al., 2021). The current proposed model for how the AhR contributes to an immunosuppressive TME: the AhR-*IDO1*-Kynurenine axis, a positive feedback loop. Action of this axis depletes the TME of tryptophan, sufficient to promote Treg cell fate adoption in turn preventing cytotoxic effects of T_{eff} cells. There are issues with details of how this mechanism functions.

There are no known AhR-binding sites in the promoter or enhancer regions of *IDO1*. While this is not an explanation for this mechanism's invalidity, it's evidence that is missing to explain how the AhR is affecting gene expression of *IDO1*. There are reports of the AhR being able to interact with non-canonical binding partners such as RelB forming heterodimeric TFs that bind distinct sequences (Vogel et al., 2007). It's possible the AhR is interacting with a non-canonical binding partner at a unique sequence, not previously characterised in the *IDO1* promoter.

Secondly, while there's evidence *IDO1* expression can be upregulated in response to TCDD (Vogel et al., 2008), there's little evidence of *IDO1* being upregulated in an AhR-dependent manner in response to physiological AhR ligands such as FICZ or Kynurenine. While FICZ and TCDD elicit strong AhR-dependent induction of canonical

AhR target genes, TCDD has significantly deleterious effects unseen with endogenous agonists. TCDD impacts DNA damage repair pathways and contributes to oxidative damage of DNA (Korkalainen et al., 2012; P. H. Lin et al., 2007). TCDD induces inflammatory signalling pathways independently of the AhR (Sciullo et al., 2009) by the same researchers who have demonstrated that *IDO1*, an inflammatory response gene, was induced by TCDD at a much higher level than FICZ (Vogel et al., 2008). It's possible the reason for TCDD's impact on *IDO1* induction is mediated through effects on inflammatory signalling not just through stimulation of the AhR's transcriptional activities. The differences between responses of *IDO1* induction upon TCDD/FICZ stimulation may be indicative of an integrative role between the AhR and inflammatory signalling rather than differences in AhR binding at the *IDO1* promoter.

The fact that the AhR mediates immunosuppression in melanoma is unambiguous, there's a requirement of better characterisation of the mechanisms underlying this. Improved mechanistic understanding of how the AhR is affecting immune signalling in the TME is likely to prove beneficial to improving therapeutic interventions, as IDO1 inhibitors are beginning to show promise in the clinic (Jung et al., 2019; X. Meng et al., 2017; Mitchell et al., 2018) and understanding drivers of *IDO1* expression will prove integral to assessing whether treatments are suitable for given patients as personalised therapeutic approaches advance.

3.2. Results

3.2.1. Induction of canonical AhR target gene: *CYP1A1,* is independent of changes in *AHR* expression in 501mel cells

To determine appropriate time courses for quantifying induction of *AHR* target genes, I stimulated 501mel cells with 100 nM FICZ, this should induce high expression of any AhR target genes. *CYP1A1* was chosen as the archetypal AhR target gene to gauge AhR activity as its expression is predominantly AhR-regulated in humans. DMSO was used as a control treatment as it is used as the solvent for dissolving FICZ and is known to inhibit CYP1A1 protein function, driving elevated basal activity of the AhR due to depressed clearance of endogenous agonists derived from the cell culture media.

All data are presented as fold-induction compared to induction by DMSO for each time point. This is to ensure any variation in gene expression caused by exposure to DMSO is controlled for. This experiment shows *CYP1A1* gene induction increases throughout the first 24-hours of treatment with FICZ (Fig. 3.1A), with relative amounts of *CYP1A1* transcripts 1.08-fold at 1-hour. This is insignificant from *CYP1A1* abundance after 2-hours (1.49-fold) (Fig. 3.1A). At 4-hours, there's 2.51-FI of *CYP1A1* transcript in FICZ-treated 501mel cells compared to DMSO-control, a significant increase from the induction at 1-hour (Fig. 3.1A). After 8-hours there's a further increase to 5.22-FI of *CYP1A1* in response to FICZ compared to that of DMSO (Fig. 3.1A). After 24-hours, FICZ-mediated *CYP1A1* induction is at its greatest, reaching 17.2-fold (Fig. 3.1A). To observe the most robust changes in AhR activity, a time course of at least 24-hours will be used, as to avoid false negative results which may be observed at shorter time points where expression of a gene is still accumulating.

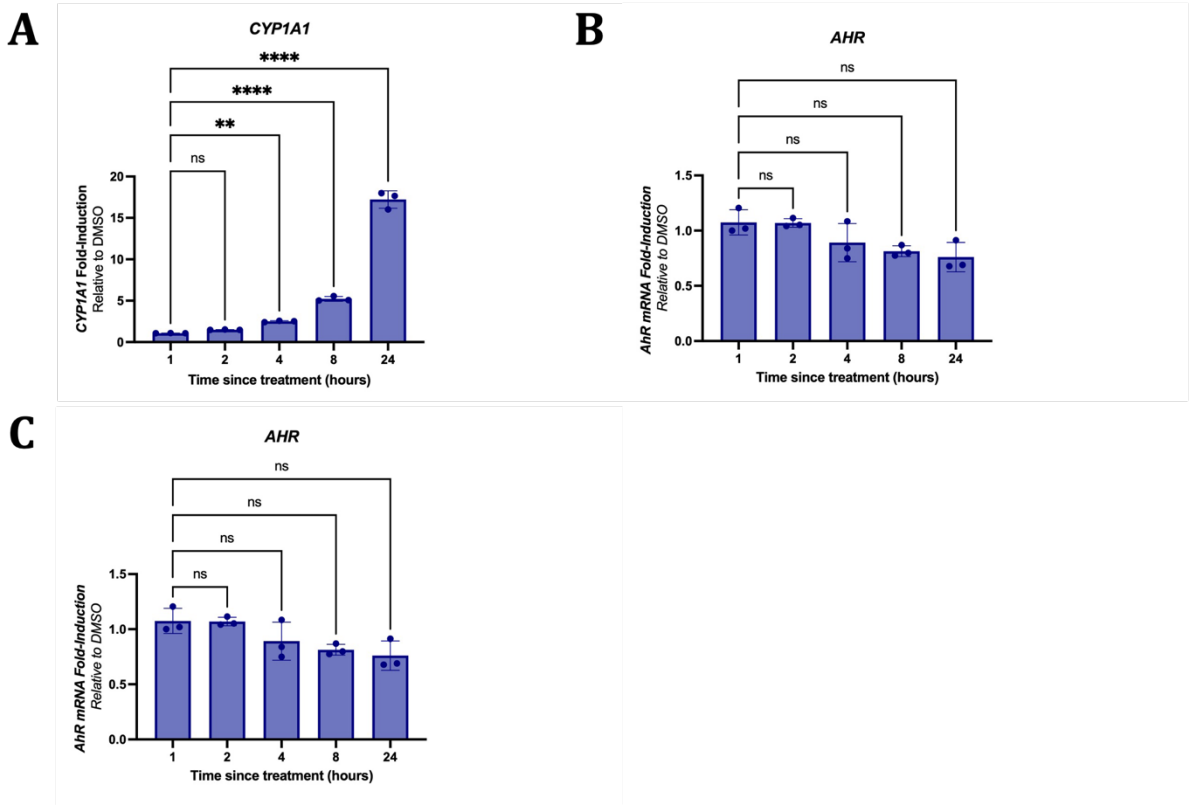

Figure 3.1 Time course induction of the *AHR*, *AHRR*, and *CYP1A1* genes in response to FICZ in 501mel cells. qRT-PCR determined fold-induction of (A) *CYP1A1*, (B) *AHR* and (C) *AHRR* in 501mel cells in response to up to 24-hours treatment with FICZ 100 nM. Ad-hoc test: Ordinary One-way ANOVA, post-hoc test: Tukey-Kramer test for multiple comparisons which inherently corrects for multiple comparisons, P > 0.05: ns, P < 0.05: *, P < 0.01: **, P < 0.001: ***, P < 0.0001: ****. Biological Replicates = 1, technical replicates = 3.

Under the same experimental conditions, I measured the relative amounts of transcripts of *AHR* and *AHRR*, to determine whether changes in AhR stimulation would be reflected in changes in *AHR* or *AHRR* expression. I observed insignificant difference in the expression of *AHR* (Fig. 3.1B) or *AHRR* (Fig. 3.1C) in response to FICZ suspended in DMSO or DMSO only at any time point during this experiment.

Given that in this cell line I did not observe significant changes in the amount of *AHR* or *AHRR* transcripts over the 24-hour time course, but I did observe a 17.3-FI of *CYP1A1* in response to FICZ compared to DMSO, I will not consider amount of *AHR* transcript as a

useful indicator of AhR activity in a cell or tissue and will instead rely on assessing the accumulation of AhR target genes such as *CYP1A1* and *CYP1B1*.

A limitation of this experiment is insufficient biological replicates were used, and this is a consistent limitation of my work throughout this chapter. This reduces reliability of my data and limits significance of any findings. Only one cell line was used in this experiment, thus I cannot be confident that results are representative of alternative cell lines. To increase confidence, I should have repeated this experiment in a panel of melanoma cell lines to be confident of its reproducibility *in vitro* and assessed in AHR activity in primary melanocytes for more confidence *in vitro* or in model organisms. There also should have been a 0-hours' time point in this experiment to determine a baseline of *CYP1A1* expression, however, given that I would have still normalised to DMSO-treatment I would expect no induction as the cells would have no opportunity to respond. It could be more indicative if these data were presented as ΔCt values to give absolute values of transcript abundance, but fold-induction provides a clearer representation that is easily understood. More known AhR target genes could also have been used to determine if there's a difference in the dynamics of AhR-mediated gene induction. Nevertheless, the induction of *CYP1A1* by FICZ over time in 501mel cells does reflect results of many other labs obtained using different cell lines or in vivo models *e.*g. (Wei et al., 1998) and I am therefore confident that, despite the limitations outlined above, the results obtained reflect induction of CYP1A1 by FICZ-activated AHR.

3.2.2. Accumulation of *CYP1A1* by FICZ does not continue to increase after 24-hours.

To confirm that 24-hours is an appropriate time point to observe effects of AhR agonists on transcription, I treated 501mel cells with FICZ and CH223191, using DMSO as a control as it is the solvent for both compounds. I measured accumulation of *CYP1A1* at 4-hours, 24-hours, and 48-hours and used CH223191 in this experiment to determine whether the degree to which it antagonises AhR activity varies throughout. This is important to observe as it impacts the time point chosen; if CH223191 is catabolised such that it is no longer significantly affecting AhR activity, it cannot be used.

Across all time points, DMSO is used as a control and all gene induction is represented as fold change relative to DMSO treatment; the induction by DMSO is always represented as 1.00-fold as it's the reference point. After 4-hours treatment, I observed 5.79-fold greater accumulation of *CYP1A1* compared to DMSO (Fig. 3.2A). When treated with CH223191, the difference in insignificant compared to DMSO treated cells (Fig. 3.2A). Although CH223191 is an AhR antagonist, I expect some marginal depression of AhR stimulation in this system as there's tryptophan, and likely its agonist derivates, present in the cell culture media. Co-treatment of 501mel cells with FICZ and CH223191 drives 3.52-FI relative to DMSO after 4-hours (Fig. 3.2A). Although mean induction of *CYP1A1* after FICZ and CH223191 treatment is lower than the mean-induction of FICZ-only treatment, this difference is not significant.

After 24-hours, there is 35.4-FI of *CYP1A1* in response to FICZ compared to DMSO (Fig. 3.2B). There's insignificant difference between DMSO and CH223191 treatments after 24-

hours (Fig. 3.2B). After 24-hours, accumulation of *CYP1A1* in response to FICZ and CH223191 is 24.4-fold compared to DMSO - significantly different to accumulation of either FICZ or CH223191 independently (Fig. 3.2B).

After 48-hours, there's 29.4-FI of *CYP1A1* under FICZ-treatment compared to DMSO only (Fig. 3.2C). This is only a moderate reduction compared to the induction of *CYP1A1* observed under the same conditions after 24-hours. There is insignificant change between the accumulation of *CYP1A1* under DMSO and CH223191 (Fig 3.2C). Interestingly, the accumulation of *CYP1A1* transcripts under FICZ and CH223191 co-treatment is not significantly different from that of CH223191 only (Fig. 3.2C). This could suggest the effect of CH223191 becomes greater with time, given the induction in response to FICZ doesn't alter much between 24 and 48-hours but that the degree of antagonism is greater after 48-hours – this is not a reasonable assumption though. CH223191 is a competitive inhibitor of the AhR: it is unlikely that its potency increases with time. The difference is insignificant between induction of *CYP1A1* between DMSO and CH223191 conditions at any time point, but I would expect to observe a depression if CH223191 were to become more potent in its inhibition with time as it would better antagonise the activity of endogenous ligands. The explanation for this result likely lies in the spread of values for FICZ-induced *CYP1A1* expression after 48-hours; there is one data point showing 64.9-FI, whereas all the other measured points are 31.7-fold or lower. This outlier could be omitted, but due to limited repeats for this experiment, I chose not to as it reduces reliability further. If this outlier was removed, induction of *CYP1A1* in response to FICZ treatment compared to DMSO is 22.3-fold (Fig. 3.2D), which indicates agonism by FICZ is diminishing between 24 and 48-hours: likely through FICZ catabolism, rather than changes in CH223191 potency.

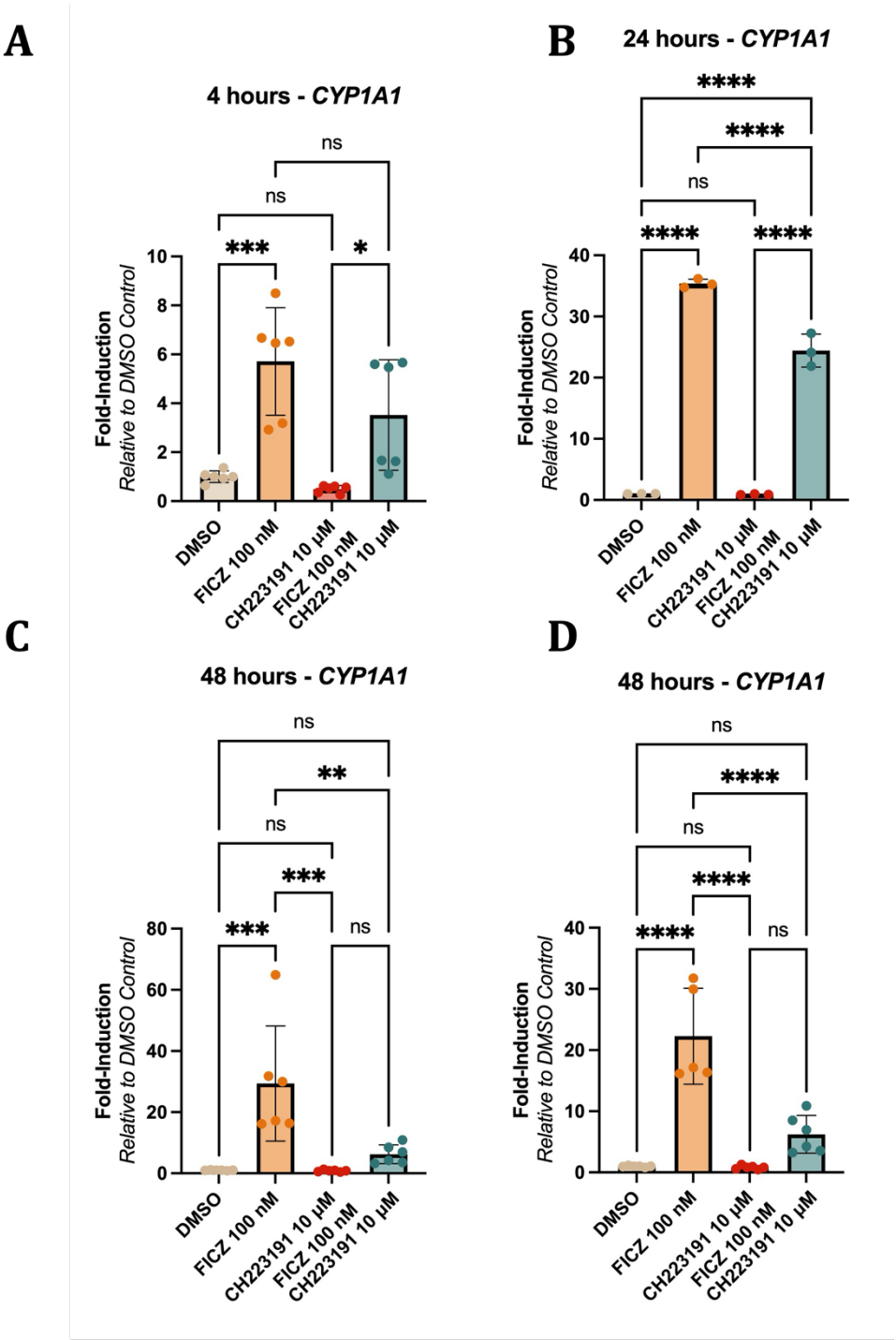

Figure 3.2 Time course induction of *CYP1A1* in response to FICZ in 501mel cells. qRT-PCR determined fold-induction of *CYP1A1* in 501mel cells in response to either FICZ 100 nM, CH223191µM, neither or both after (A) 4hours, (B) 24-hours, and (C&D) 48-hours. Ad-hoc test: Ordinary One-way ANOVA, post-hoc test: Tukey-Kramer test for multiple comparisons which inherently corrects for multiple comparisons, $P > 0.05$: ns, $P < 0.05$: *, $P < 0.01$: **, $P < 0.001$: ***, $P < 0.0001$: ****. Biological Replicates = 2, technical replicates = 3 (per biological replicate).

As *CYP1A1* induction increases ≤24-hours (Section 3.1) and falls between 24 and 48-hours, 24-hours is the time point for all experiments observing AhR-mediated gene induction in 501mel cells as it gives the greatest induction of *CYP1A1* and represents the point at which differences should be most apparent with least chance of false negatives. The weaknesses of this experiment include limited biological repeats, and using a single cell line, limiting generalization of the results to melanoma. Only *CYP1A1* is being used as an indicator of AhR activity, but there are other AhR target genes that could be measured that together would give better overview as to whether the pattern of AhR-induction observed is *CYP1A1*-specific or more general. *CYP1A1* expression is predominantly mediated by AhR activity, although there is evidence of PPARα being a mediator of *CYP1A1* expression in humans. CYP1A1 is therefore a good, but imperfect, proxy for canonical AhR activity. Using a reporter gene with a promoter driven uniquely by AHREs would be a good supplementary experiment to support these observations, removing ambiguity about effects of other TFs influencing expression of these genes.

3.2.3. AhR agonists modulate *IDO1* expression but aren't sufficient to induce it

To determine whether *IDO1* gene expression is induced by physiological agonists *in vitro* I treated 501mel^{WT} cells with FICZ , Kynurenine , and CH223191 for 24-hours and assessed gene induction by qRT-PCR. A DMSO control condition was used, as it is the solvent for compounds being examined. This important as DMSO is an indirect AhR activator, as discussed in section 1.3.1, via inhibition of CYP1A1. In the DMSO condition I expect a basal level of AhR stimulation as a product of endogenous tryptophan in the cell culture spontaneously forming derivates that excite the AhR, including FICZ and their reduced clearance by CYP1A1. First, I confirmed FICZ is a

more potent physiological agonist of the AhR than Kynurenine, (Fig. 3.3A) driving a 20-fold greater induction of canonical AhR target gene *CYP1A1* than Kynurenine, which doesn't drive a significant induction of *CYP1A1* expression compared to DMSO control (Fig. 3.3A). Limited induction of *CYP1A1* induction is in line kynurenine being an AhR pro-ligand, not ligand (Seok et al., 2018). FICZ-mediated induction of *CYP1A1* is also diminished by half in the presence of CH223191, demonstrating FICZ-mediated induction of *CYP1A1* is likely via the AhR, as it's diminished by AhR inhibitors (Fig. 3.3A). There's insignificant difference *CYP1A1* abundance with CH223191 or Kynurenine with CH223191 compared to no treatment (Fig. 3.3A). While CH223191 is an antagonist of the AhR, not an inhibitor, I would still expect to observe a depression in *CYP1A1* expression in response to CH223191 due to presence of tryptophan and its derivates in cell culture media causing basal AhR excitation. However, I couldn't detect any significant changes in accumulation of *IDO1* transcripts in response to FICZ-, Kynurenine-, or CH223191-treatment either compared to no treatment or each other (Fig. 3.3B). I conclude *IDO1* is not induced in response to FICZ or kynurenine alone in 501mel^{WT}.

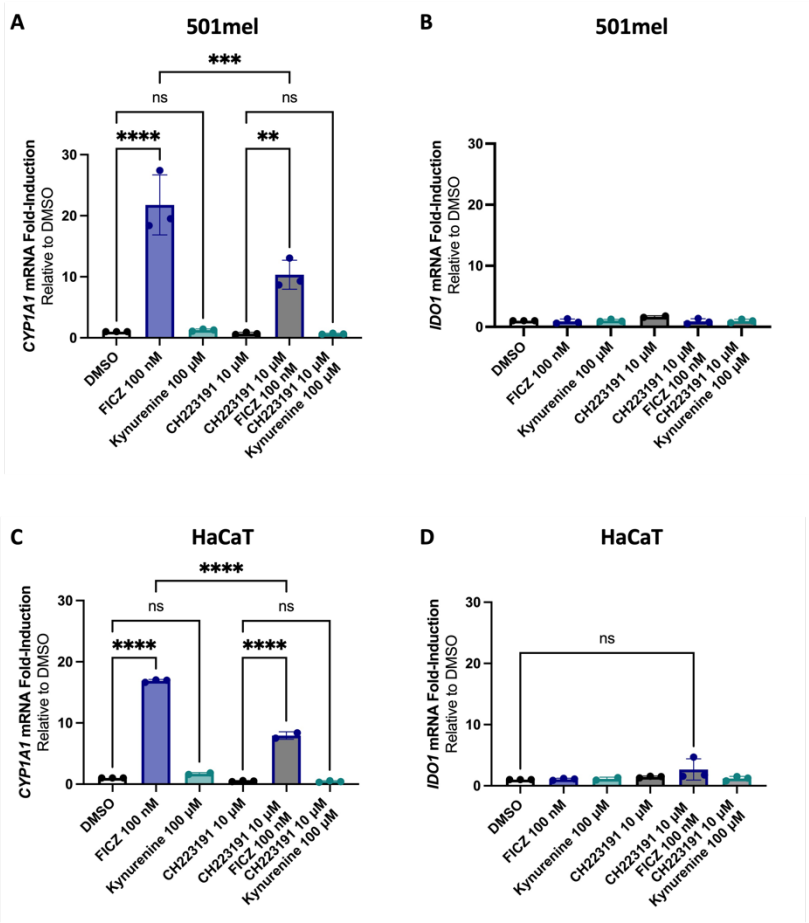

Figure 3.3 Induction of genes in response to physiological AhR agonists. qRT-PCR determined fold-induction of (A) *CYP1A1* and (B) *IDO1* in 501mel cells and of (C) *CYP1A1* and (D) *IDO1* in HaCaT cells in response to 24-hours treatment with; FICZ 100 nM, Kynurenine 100 µM, and CH223191 10 µM. Ad-hoc test: Ordinary One-way ANOVA, post-hoc test: Tukey-Kramer test for multiple comparisons which inherently corrects for multiple comparisons, $P > 0.05$: ns, $P < 0.05$: *, $P < 0.01$: **, $P < 0.001$: ***, $P < 0.0001$: ****. Biological Replicates = 3, technical replicates = 1.

To establish whether this effect was unique to this cell line or cell type I also assessed induction of *CYP1A1* and *IDO1* in response to AhR agonists in the HaCaT WT cell line, a keratinocyte cell line. I used a keratinocyte cell line as the primary melanoma TME is formed of transformed melanocytes and surrounding keratinocytes, if biopsies are taken demonstrating high levels of *IDO1*, it could be due to high *IDO1* expression in tumoural stromal cells rather than melanoma cells themselves.

FICZ-treatment induces *CYP1A1* expression in HaCaT WT cells, with a 16.9-FI compared to DMSO (Fig. 3.3C) but kynurenine induced an insignificant change in

CYP1A1 expression. There were insignificant changes in *IDO1* abundance in response to AhR modulators (Fig. 3.3D). Given I had been unable to induce *IDO1* expression in response to AhR ligands, I determined whether *IDO1* expression could be driven through IFNγ-stimulation: the canonical pathway through which *IDO1* expression is stimulated.

I stimulated 501mel^{WT} and HaCaT WT cells with 10 ng/mL IFNγ for 24-hours and quantified induction of the *IDO1* gene with qRT-PCR (Fig. 3.4A and 3.4B, respectively). In both cell lines, while FICZ was not sufficient to induce a significant change in the amount of *IDO1* transcripts, IFNγ induced strong accumulation of *IDO1* mRNA, with 20-FI (FI) in 501mel cells and 400-FI in HaCaT cells. These data demonstrate that whilst strong *IDO1* expression can be induced in these cells by IFNγ, FICZ and Kynurenine aren't sufficient to stimulate *IDO1* expression alone.

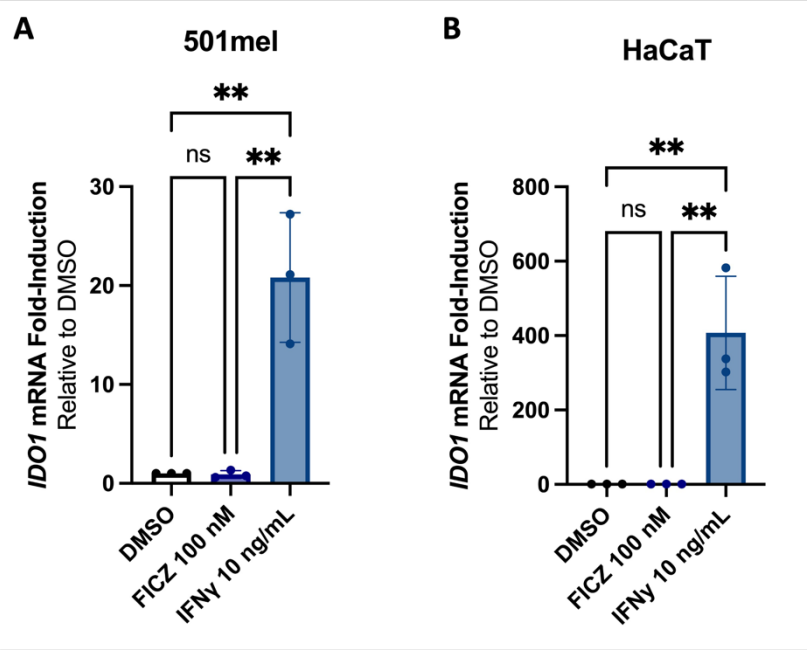

Figure 3.4 Induction of *IDO1* in response to treatment with IFNγ. qRT-PCR determined fold-induction of *IDO1* in (A) 501mel and (B) HaCaT in response to 24-hours treatment with FICZ 100 nM or IFNγ 10 ng/mL. Ad-hoc test: Ordinary One-way ANOVA, post-hoc test: Tukey-Kramer test for multiple comparisons which inherently corrects for multiple comparisons, P > 0.05: ns, P < 0.05: *, P < 0.01: **, P < 0.001: ***, P < 0.0001: ****. Biological Repeats = 1, Technical Repeats = 3.

Previous studies have clearly demonstrated the AhR is central to the expression of *IDO1* in melanomas *in vivo* (Campesato et al., 2020; Y. Liu et al., 2017), however, my data shows that AhR agonists cannot induce *IDO1* expression *in vitro*. I hypothesised that while agonists of the AhR may not be sufficient to induce *IDO1* expression, given the AhR is central to IDO1-medaited immunosuppression, they may modulate *IDO1* expression via other stimulants in an AhR-dependent manner.

To test this hypothesis, I treated 501mel cells with IFNγ which is known to induce *IDO1* expression (Dai & Gupta, 1990), alongside AhR agonist FICZ and antagonist CH223191, and used qRT-PCR to determine whether AhR modulation affects elevated *IDO1* expression. In 501mel^{WT} cells, treatment with FICZ induces 28.4-FI of *CYP1A1* compared to the DMSO control (from 4.77 ΔCt with DMSO to -0.06 ΔCt with FICZ), with insignificant change in *CYP1A1* abundance in response to CH223191 (5.18 ΔCt

)(Fig. 3.5A). This non-significant reduction of *CYP1A1* induction in response to CH223191 indicates there is basal AhR activation through ligands in the cell culture and media which is likely being exacerbated by the presence of DMSO and which is being antagonised by CH223191, albeit at a negligible level. The limited change in response to adding CH223191 is likely due to relatively low basal excitation of the AhR through these pathways. Co-treatment of FICZ and CH223191 reduces *CYP1A1* expression from -0.06 ΔCt to 1.08 ΔCt compared to FICZ alone, respectively (Fig. 3.5A). IFNγ synergises with AhR modulation of *CYP1A1*, increasing induction of *CYP1A1* with 3.23 ΔCt compared to 4.77 ΔCt of the DMSO control (Fig. 3.5A). This is further demonstrated with induction of *CYP1A1* in response to FICZ treatment rising from -0.06 ΔCt to -0.78 ΔCt on adding IFNγ. Similarly, induction of *CYP1A1* under co-treatment with FICZ and CH223191 rises from 1.08-fold to 0.21-fold upon adding IFNγ, 1.8-fold change in starting material (Fig. 3.5A).

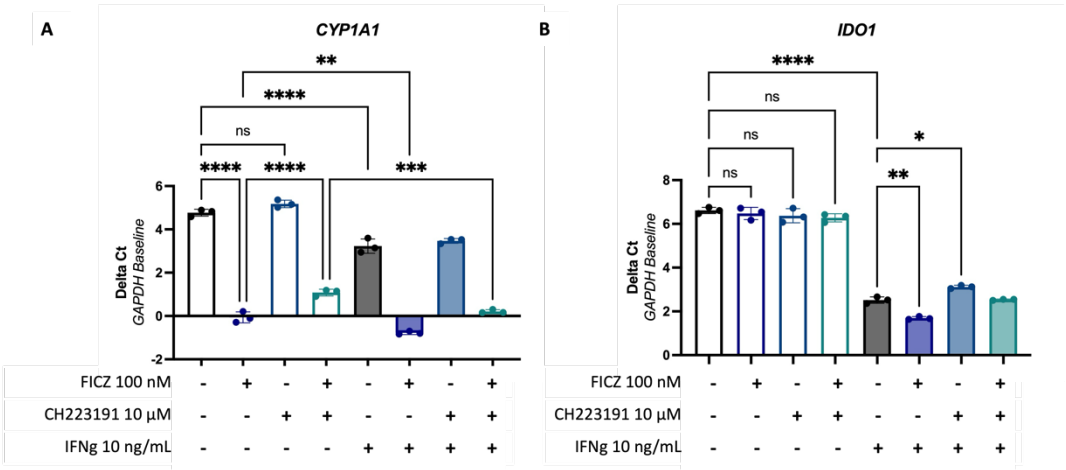

Figure 3.5 Cooperation between AhR agonists and IFNγ in gene expression. qRT-PCR determined ΔCt of (A) *CYP1A1* and (B) *IDO1* in response to 24-hours treatment with DMSO control, FICZ 100 nM, CH223191 10 µM, and IFNγ 10 ng/mL in 501mel WT cells. Ad-hoc test: Ordinary One-way ANOVA, post-hoc test: Tukey-Kramer test for multiple comparisons which inherently corrects for multiple comparisons, P > 0.05: ns, P < 0.05: *, P < 0.01: **, P < 0.001: ***, P < 0.0001: ****. Biological Repeats = 1, Technical Repeats = 3.

Treatment of these cells with FICZ, CH223191, or both, does not produce a significant change in the induction of *IDO1* compared to the DMSO control, confirming that AhR modulators aren't sufficient to drive expression of *IDO1* (Fig. 3.5B). IFNγ alone induces 17.1-FI of *IDO1*, with 6.62 ΔCt for DMSO to 2.52 ΔCt for treatment with IFNγ-treatment with FICZ enhances this, yielding 30.2-FI of *IDO1* compared to DMSO control and 1.7-FI compared to IFNγ alone, from 2.51 ΔCt to 1.70 ΔCt (Fig. 3.5B). There is also a depression of IFNγ-mediated induction of *IDO1* in response to treatment with AhR antagonist CH223191, decreasing *IDO1* expression from 2.51 ΔCt with IFNγ only to 3.12 ΔCt (Fig. 3.5B). This is likely due to CH223191 mediated antagonism of media-derived ligand-mediated activation of the AhR. *IDO1* expression is only significantly changed in the presence of IFNγ, but this induction is modulated by AhR ligands in the same pattern as *CYP1A1* induction (Fig. 3.5B). These data demonstrate that, while AhR agonists FICZ and Kynurenine aren't sufficient to induce *IDO1* expression, modulation of the AhR does affect IFNγ-mediated *IDO1* expression. A potential explanation for this is that IFNγ is inducing AhR expression, or alternatively the AhR is interacting with the IFNγ-signaling pathway to enhance IFNγ-mediated gene expression when AhR agonists are present.

In all three experiments discussed in this subchapter so far, their reliability is limited due to insufficient biological replicates. These experiments should've been performed in biological triplicate and technical triplicate rather than simply technical triplicate. Although two different cell lines of different cell types and cell lineage were used and they demonstrate the same dependency on IFNγ for induction of the *IDO1* gene, it would strengthen the observations if these experiments had been performed in

multiple melanoma and keratinocyte cell lines, and primary melanoma and primary keratinocyte cells – although, these weren't available at the time the work was completed.

Having observed a synergy in the induction of *CYP1A1* in response to IFNγ and FICZ, I wanted to examine whether this could be explained by IFNγ inducing changes in the expression of *AHR* and *AHRR.* Although section 3.1 indicated that FICZ doesn't affect the accumulation of *AHR* and *AHRR,* a possible explanation for how IFNγ enhances induction *CYP1A1* is that IFNγ induces *AHR* or suppresses *AHRR,* meaning there is a larger pool of AhR to be activated by FICZ. To examine this, I performed a time course experiment to examine relative transcript abundance at 1, 2, 4, 8, and 24-hours in 501mel cells after treatment with FICZ 100 nM, Ch223191 100 μM, and IFNγ 10 ng/mL or DMSO as a control.

After 1-hour, there was insignificant induction of *CYP1A1* under any treatment (Fig. 3.6A). After 2-hours, there was a significant induction of *CYP1A1* in response to FICZ, compared to DMSO both in the absence and presence of IFNγ (Fig 3.6B). There was insignificant difference between the abundance of *CYP1A1* in the DMSO vs. IFNγ or FICZ vs. FICZ + IFNγ, showing that at this time point there's not a significant effect of adding IFNγ on *CYP1A1 expression*. At 4-hours, FICZ drives 2.51-FI of *CYP1A1* compared to DMSO (Fig. 3.6C). There is a non-significant induction of *CYP1A1* when treated with IFNγ compared to DMSO of 1.15-fold (Fig. 3.6C), however, there is a significant difference in the induction of *CYP1A1* in response to FICZ (2.51-fold) vs. FICZ + IFNγ (3.41-fold). The difference between fold induction because of IFNγ in the

presence of FICZ is 1.36-fold, marginally greater than fold induction of IFNγ only (1.15-fold). After 8-hours, there's a greater difference between the induction of *CYP1A1* across these conditions. FICZ vs. DMSO yields 5.22-FI of *CYP1A1* and IFNγ vs. DMSO yields 2.08-FI (Fig. 3.6D). Co-treatment of FICZ and IFNγ produces 10.3-FI of *CYP1A1,* an IFNγ-dependent doubling of the FICZ-dependent 5-FI of *CYP1A1* (Fig. 3.6D). After 24-hours, induction in response to FICZ compared to DMSO is 17.2-fold, and in response to IFNγ compared to DMSO is 4.81-fold. In this instance, we do not see a multiplicative effect between induction of FICZ and IFNγ as observed at 8-hours, rather FICZ and IFNγ co-treatment causes 34.9-FI of *CYP1A1* (3.6E) whereas a multiplicative effect should yield around 82.7-FI.

After 1-hour of treatment, there is insignificant induction of *IDO1* in response to any treatment (Fig. 3.6F), nor after 2-hours (Fig. 3.6G) or 4-hours (Fig. 3.6H). It is only after 8-hours where we observe an induction of *IDO1,* with induction only observed in the presence of IFNγ, which compared to DMSO is 6.26-fold. There's a statistically significant increase in response to FICZ in the presence of IFNγ from 6.26-fold to 6.86-fold although this is unlikely to be biologically significant (Fig. 3.6I). There is insignificant difference after adding CH223191 in the presence of IFNγ (Fig. 3.6I). After 24-hours, the induction of *IDO1* in response to IFNγ compared to DMSO is 42.4-fold (Fig. 3.6J). The effect of IFNγ in addition to FICZ on *IDO1* expression that was observed in Fig. 3.5. is not recapitulated in this experiment, with FICZ not producing a significant induction irrespective of whether IFNγ is present (Fig. 3.6J). Interestingly, antagonism of the AhR with Ch223191 in the presence of IFNγ does produce a significantly diminished induction of *IDO1,* with 42.4-FI of *IDO1* falling to

27.5-fold (Fig. 3.6J). This result is difficult to explain: From the *CYP1A1* data there's a clear response to FICZ (Fig. 3.6A-E), meaning the explanation cannot be found in assuming there was an issue with the FICZ used in this experiment. Comparing fold-induction relative to DMSO in Fig. 3.5B to that in Fig. 3.6J reveals induction in response to FICZ and IFNγ co-treatment compared to DMSO was 30.2-fold in Fig. 3.5B but 41.1-fold in Fig. 3.6J. Induction in response to IFNγ-only compared to DMSO was 17.1-fold in Fig. 3.5B but 42.4-fold in Fig. 3.6J. It's possible that the experiment displayed in Fig. 3.6 may have had a much greater concentration of IFNγ used than intended, which is saturating the expression of *IDO1* in Fig. 3.6 due to errors performing the experiment. For example, pipetting errors due to miscalibration of pipettes when performing the experiment shown in Fig. 3.6, 1 µL of IFNγ solution in 10 mL of media giving the appropriate dilution and small errors in this step causing large differences in final concentration. This experiment could be repeated to determine whether this is the case.

Regarding induction of *AHR* expression across the time course of this experiment, there are insignificant changes regardless of treatment or time (Fig. 3.6K-O). As for *AHRR* induction, the only significant differences between conditions that differ by a single variable are observed after 24-hours of treatment (Fig. 3.6P-T) where there is a significant induction of *AHRR* in response to IFNγ of approximately 1.5-fold regardless of the status of FICZ and/or CH223191 (Fig. 3.6T). This is surprising, as I would have expected to observe no change or a depleted presence of *AHRR* in line with the data presented in Fig. 3.1 where there was no change in *AHRR* in response to FICZ. This observation does not explain synergism between FICZ and IFNγ in the induction of *CYP1A1* seen in Fig. 3.5 and Fig. 3.6. Perhaps, the accumulation of *AHRR*

mRNA is not yet translated and consequently the increase in AHRR mRNA is not reflected in an ability AHRR protein to repress the AhR. This experiment is limited by lack of sufficient repeats, and by being performed in only one cell line. Repetition in both this cell line and other melanoma cell lines is essential to understand whether it's representative of melanoma cells in general or is restricted to the 501mel cells.

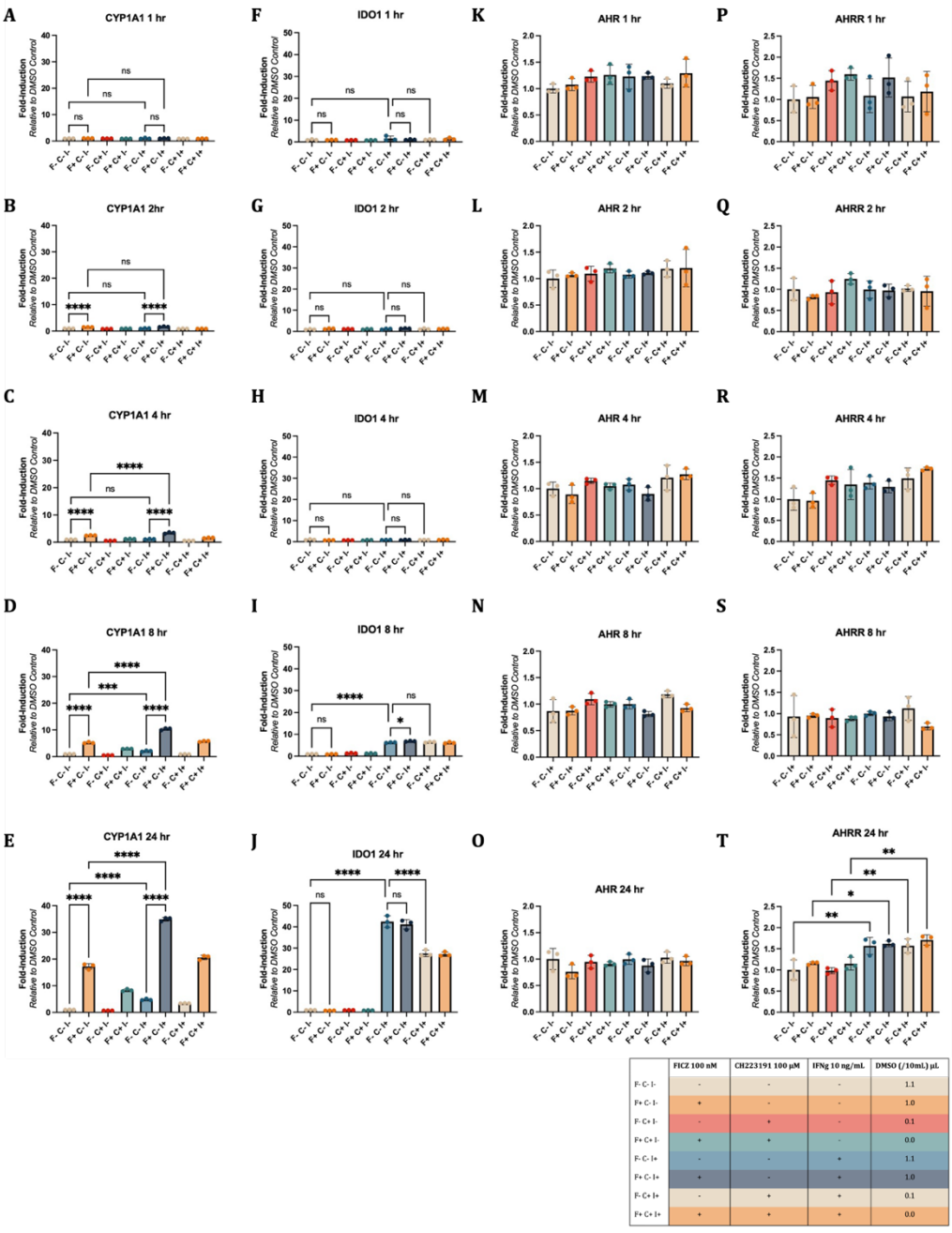

Figure 3.6 Gene induction in response to co-treatment with FICZ, CH223191, IFNγ. qRT-PCR determined fold-induction of *CYP1A1* (A-E), *IDO1* (F-J), *AHR* (K-O), and *AHRR* (P-T) in 501mel in response to up to 24-hours treatment with FICZ 100 nM, CH223191 100 µM, or IFNγ 10 ng/mL. Ad-hoc test: Ordinary One-way ANOVA, post-hoc test: Tukey-Kramer test for multiple comparisons which inherently corrects for multiple comparisons, P > 0.05: ns, P < 0.05: *, P < 0.01: **, P < 0.001: ***, P < 0.0001: ****. Biological Repeats = 1, Technical Repeats = 3.

3.2.4. *CYP1B1* expression correlates with IFNγ signalling in patients

Given the AhR modulates IFNγ-mediated *IDO1* expression in 501mel cells, I hypothesised the AhR might be modulating IFNγ-signalling broadly rather than just modulating *IDO1* induction. To determine whether this was likely, I analysed transcriptomic data available through the cancer genome atlas (TCGA) (www.cancer.gov/tcga) from melanoma patients, specifically.

To measure the relationship between AhR activity and induction of IFNγ target genes, I looked for a relationship between AhR target genes and IFNγ target genes, whilst also measuring correlations between *AHR* expression and these target genes expecting no relationship here, with *AHR* expression often remaining unchanged despite large changes in AhR activity (Fig. 3.1). With *CYP1A1* and *CYP1B1* being canonical target genes of the stimulated AhR, their expression can gauge AhR activity in patients' samples. As discussed in Section 1.3., *CYP1A1* has only been demonstrated to be under the control of the AhR and PPARα in humans and SP1 in porcine models, and *CYP1B1* expression is mediated by SF1, SP1 and the AhR. Given there's the possibility that either gene may be being regulated by other TFs, I included expression of both in following analyses and the expression of other TFs that can influence expression of these genes: *PPARA, SF1,* and *SP1*.

Genes being measured in these analyses can be grouped into Canonical AhR target genes (*CYP1A1*, *CYP1B1*), genes directly influencing AhR accumulation and potential activity that I do not expect to vary based on preliminary experiments (*AHR, AHRR*), IFNγ -associated genes (*IDO1, ATF4, CD274, IRF1, EIF2AK2*, *STAT1, IFNG*), and other

TFs that may influence accumulation of AhR target genes *CYP1A1* and *CYP1B1* (*PPARA, SP1, SF1*). *Activating TF 4* (*ATF4*) has been included in these analyses as a negative control of IFNγ-response genes, as it's part of the IFNγ-response, but its expression is not induced by IFNγ rather it's phosphorylated, so I would expect no correlation between *ATF4* expression and wider IFNγ-response gene induction.

Across all melanoma stages[†] (Fig. 3.7A-C) canonical AhR target gene expression is correlated with *IDO1, IRF1,* and *IFNG* expression. Considering only statistically significant comparisons ($p < 0.05$), *CYP1A1* expression is negatively correlated with these genes with Pearson coefficients of: *IDO1* -0.10; *CD274* -0.10; *IRF1* -0.12; and *IFNG* -0.09. *CYP1B1* expression is positively correlation with these genes with Pearson's coefficients of: *IDO1* 0.10; *CD274* 0.14; *IRF1* 0.14; and *IFNG* 0.12 (Fig. 3.7A-C). *CYP1B1* expression is also positively correlated with the expression of *STAT1* 0.14 (Fig. 3.7A-C). *CYP1A1* and *CYP1B1* expression aren't correlated, indicating there are other factors influencing one or both of their expression beyond the AhR, as if it were just the AhR responsible for their co-regulation then I would expect a strong positive correlation. The expression of *CYP1A1* is positively correlated with the expression

[†] Stage 0 – Melanoma cells are only in the top layer of skin. Stage 1 – Melanoma cells have penetrated layers of the skin without evidence of spread. Stage 2 – Tumour is larger than Stage 1, melanoma cells have penetrated layers of the skin without evidence of spread, Stage 3 – Melanoma has local metastases, Stage 4 – Melanoma has distant metastases

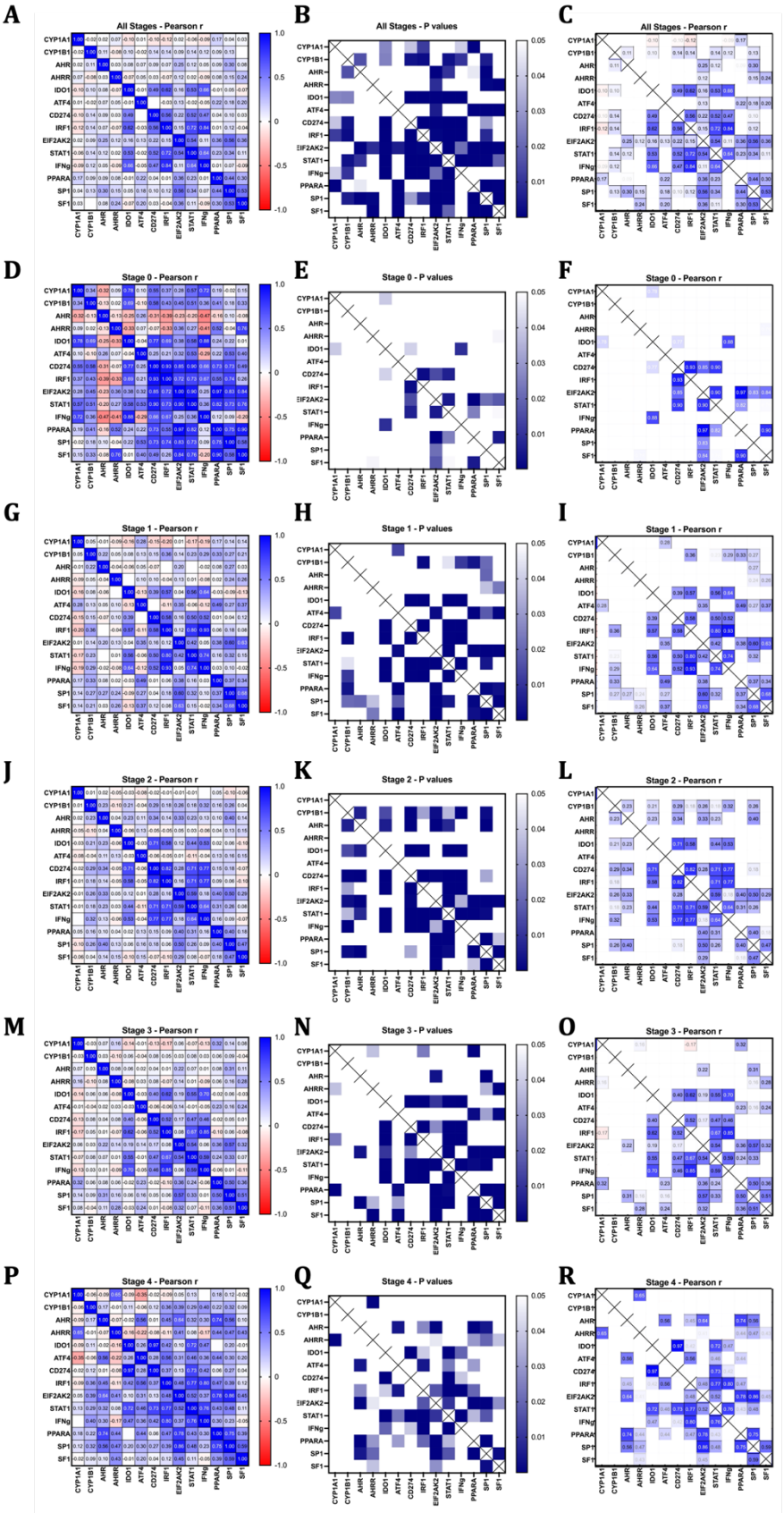

Figure 3.7 Correlation analysis between the expression genes in melanoma patients using TCGA data. Pearson's Correlation r-values (A, D, G, J, M, P), P-values for each correlation represented as a heat map (B, E, H, K, N, Q), and overlay highlighting only significant correlations (C, F, I, L, O, R). mRNA expression data of all patients n=472 (A-C), Stage 0 n=7 (D-F), Stage 1 n=76 (G-I), Stage 2 n=138 (J-L), Stage 3 n=175 (M-O), Stage 4 n=24 (P-R).

PPARA, r = 0.17, which agrees with the published relationship that PPARα is a positive

effector of *CYP1A1* expression (Fig. 3.7A-C). There's not a significant correlation between *CYP1A1* expression and the expression of either *SF1* or *SP1* (Fig. 3.7A-C), whereas *CYP1B1* expression is positively correlated with the expression of *SP1,* r = 0.13 (Fig. 3.7A-C). Together these data indicate that in these patient samples PPARα and SP1 are likely greater determinants of *CYP1A1* and *CYP1B1* expression than the AhR. Given *SP1* expression is positively correlated with the expression of; *AHR* (r = 0.30), *AHRR* (r = 0.15), *ATF4* (r = 0.18), *CD274* (r= 0.10), *IRF1* (r = 0.12), *EIF2AK2* (r = 0.56), *STAT1* (r = 0.34), and *SF1* (r = 0.53), it is possible that SP1 is a driver of expression of these factors, upstream of the AhR. However, this wouldn't explain the effects observed in the 501mel cell line I used to characterise an AhR-effector-dependent pattern of modulation of IFNγ-mediated *IDO1* expression. Furthermore, SP1 and AhR:ARNT dimers cooperate at the promoter of the *CYP1A1* gene to induce expression (Kobayashi et al., 1996; Ye et al., 2019b), meaning that I would expect a positive correlation between *SP1* and *CYP1A1* rather than *CYP1B1* if this were the case. Instead, it seems plausible that *SP1* expression and *CYP1A1* expression do not give a useful indication of AhR behaviour in these patient samples as they do not behave as one would expect based on the published data which suggests they should be positively correlated. Instead, in these patient samples it may be more reasonable to assume that PPARα is the greatest effector of *CYP1A1* expression rather than AhR:ARNT and SP1.

In stage 0 patients (Fig. 3.7D-F), expression of *IDO1* and *CYP1A1* are strongly positively correlated (r = 0.78), and expression of *CYP1A1* and *PPARA* aren't significantly correlated. Which agrees with current literature describing the AhR as a direct activator of *CYP1A1* and *IDO1*. This could be evidence of this relationship, or an

artifact of the limited sample size of Stage 0 patients in the TCGA cohort (n=7). There is no correlation between *CYP1A1, CYP1B1, AHR* or *AHRR* with any other IFNγ-response gene which would indicate the AhR is not an effector of IFNγ-response gene induction beyond *IDO1* in stage 0 melanoma patients.

In stage 1 melanomas, *CYP1A1* expression is only significantly correlated with the expression of *ATF4* (r = 0.28), the IFNγ-response gene that I'm using as a negative control given it's post-transcriptionally regulated with its translation stimulated by eIF2α with negligible effects on its transcription in response to IFNγ-stimulation (Fig. 3.7G-I). *CYP1B1* expression is positively correlated with the expression of *IRF1* (r=0.36), *STAT1* (r=0.23), *IFNG* (r=0.29) of the IFNγ-response genes (Fig. 3.7G-I), and *PPARA* (r=0.33) and *SP1* (r=0.27) which I wouldn't expect given that these TFs have not been previously characterised as mediators of *CYP1B1* expression. *SP1* expression is positively correlated with expression of several of the IFNγ-response genes examined in this analysis and could be mediating IFNγ-response genes independently of the AhR (Fig. 3.7G-I). The sample size of stage 1 melanoma is 76, making this a more reliable dataset than the Stage 0 dataset, although differences between these datasets may also arise due to epi/genetic differences in the cells that have developed throughout their oncogenesis, affecting gene expression.

In Stage 2 melanoma samples, *CYP1A1* expression is not correlated with any genes that I measured in this experiment (Fig. 3.7J-L). *CYP1B1* expression, however, is positively correlated with the expression of the *AHR* (r=0.23), *IDO1* (r=0.21), *CD274* (r = 0.29), *IRF1* (r=0.18), *EIF2AK2* (r=0.26), *STAT1* (r=0.18), *IFNG* (r=0.32) and *SP1*

(r=0.26) (Fig. 3.7J-L). The positive correlation with *AHR* expression is unexpected based on my *in vitro* studies where *AHR* expression is not correlated with expression of *CYP1B1,* and this TCGA correlation could be simply that or a causal relationship with greater *AHR* driving greater AhR in the cell increasing the expression of *CYP1B1*. Given that *AHR* expression correlates with *IDO1* (r=0.23), *CD274* (r = 0.34), *EIF2AK2* (r=0.33) and *STAT1* (r=0.23) it's possible the AhR is a driver of the expression of these or *vice versa,* it's also possible there is no connection in their regulation. The sample size of stage 2 melanoma samples is 138 making it a more statistically reliable dataset to draw from than the previous two stages examined, although differences between conclusions drawn may be due to differences in the physiology of the tumours rather than artefacts arising from sample sizes.

In Stage 3 melanoma samples, *CYP1A1* expression is negatively correlated with the expression of *IRF1* (r=-0.17) and positively correlated with *PPARA* (r=0.32) and *AHRR* (r=0.16) (Fig. 3.7M-O). The negative correlation with *IRF1* in stage 3 cancers (Fig. 3.7M-O) mirrors that of the correlation observed across all stages (Fig. 3.7A-C), which can be partially explained by stage 3 melanomas making up the greatest proportion of the melanoma samples in this dataset at 175/472 samples, it may also point to a common theme across other cancer stages but is only statistically significant with sufficiently large datasets. Regardless, this is not a particularly strong correlation ($|r| < 0.2$) and may not be indicative of a strong physiological relationship between the AhR and this IFNγ-response gene. There are insignificant correlations with *CYP1B1* expression (Fig. 3.7M-O), suggesting there's no relationship between AhR activity and IFNγ gene induction. Given that *IDO1* expression is not significantly correlated with the expression of *CYP1A1* or *CYP1B1* in these samples (Fig. 3.7M-O), it doesn't follow

the published pattern of behaviour in melanomas where AhR activity correlates with elevated *IDO1* (Zhang et al., 2021), and I am unsure as to whether the well-characterised relationship between the AhR and *IDO1* is applicable to all stages of melanoma or whether it's only relevant to early stages of melanoma.

In Stage 4 melanoma samples, there's a strong positive correlation between *CYP1A1* expression and *AHRR* expression (r=0.65) (Fig. 3.7P-R). This could be indicative of the AhR being highly active in these samples driving expression of two well-characterised target genes of the AhR. *CYP1B1* expression is not significantly correlated with expression of any IFNγ target genes (Fig. 3.7P-R). Interestingly, the expression of *AHR* is strongly positively correlated with *ATF4* (r=0.56), *IRF1* (r=0.45), and *EIF2AK2* (r=0.64) (Fig. 3.7P-R). This is surprising, given that I do not expect to observe any changes in expression of the *AHR*, but this correlation could be explained if the *AHR* gene was STAT1 target gene, resulting in *AHR* expression alongside these canonical IFNγ-response genes. This, however, is not wholly supported by this observation, as across all cancer stages there are limited positive correlations between the AhR and IFNγ-response genes which I would expect to be strongly positively correlated if this were true (Fig. 3.7A-C). It is, however, an interesting hypothesis and could explain the relationship between the expression of the *AHR* and *IDO1*, whilst not relying on the AhR-Kyn-IDO1 axis, which I have discussed the weaknesses of in Section 1.5.3.

Drawing clear conclusions from these data is difficult, especially when stratifying by melanoma stage. If considering *CYP1A1* expression to be a marker of AhR activity, which many consider to be the best proxy to do this with, then across all datasets AhR activity negatively correlates with *IDO1* expression (Fig. 3.7A-C). This disagrees with

almost all available research on mechanisms through which the AhR contributes to tumorigenesis. I must assume expression of *CYP1A1* is a poor marker of purely AhR activity, potentially explained by PPARα being the dominant regulator of *CYP1A1* expression in these datasets. *CYP1B1* expression can be used as a proxy for AhR activity even if it is an imperfect gauge of AhR activity due to being a target of multiple TFs. If *CYP1B1* is used as a proxy for AhR activity, however, it does at least agree with the published positive correlation relationship between the AhR and IDO1. This conclusion could have been supported by using a greater battery of AhR target genes, with the expression of the AhR gene set vs a broader IFNγ-response gene set used to control for any effect of other TFs acting on any of these genes individually. The effects of PPARα, SP1, and SF1 are referred to in these analyses regarding their effect on *CYP1A1* and *CYP1B1* expression, but this relationship has not been sufficiently examined. Introducing a gene set for each of these TFs to assess their overall activity to compare to that of an AhR and IFNγ gene set would be the most robust way of using this dataset.

3.2.5. Unstimulated AhR suppresses IFNγ signalling in these 501mel Cells

Given the correlations between *CYP1A1* and *CYP1B1* and the induction of IFNγ-response genes both *in vitro* and *in vivo* (based on TCGA data analysis), I hypothesised the AhR was responsible for mediating this interaction. To confirm this, I used both 501mel^{WT} and 501mel *AHR*$^{-/-}$ cell lines and treated them with both FICZ and IFNγ to assess whether the synergistic induction seen in WT cells is dependent on the AhR.

As a gift from Marie-Dominique Galibert, I received 501mel^{WT} and 501mel *AHR*$^{-/-}$ cell lines. I first confirmed by western blotting the 501mel cell lines I had received were/weren't expressing the AhR as expected (Fig. 3.8A). Further confirmation of the AhR status could've been performed, including qRT-PCR of *AHR* and other AhR target genes including *CYP1B1, TIPARP*, and *CYP1A2* would've increased the confidence in the AhR status of these cells. These experiments were not performed as I was sufficiently confident the AhR had been knocked out in these cells and they had already been used by the Galibert group who had performed their own validation of these cell lines. As I had only received a single clone of the 501mel *AHR*$^{-/-}$ cell line and had been unsuccessful in generating a 501mel *AHR*$^{-/-}$ cell line of my own up until this point, this and all further experiments comparing 501mel^{WT} and 501mel *AHR*$^{-/-}$ cells in this chapter are on these clones only. This is a major limitation of the work presented hereafter, with only one melanoma cell line used and only one clone of the knockout cell line. Consequently, all conclusions are limited in their applicability to melanoma in general, including whether regulation of genes by the AhR might be different in cell lines that reflect different phenotypic states. All work should be considered in this light, with conclusions drawn only being applicable to these cell lines, although perhaps indicative of wider biological patterns.

The use of a single *AHR*$^{-/-}$ clone in these experiments is a clear limitation of study, the clonogenic effects can be studied through re-introduction of an exogenous AhR construct, to determine whether this rescues all phenotypes. Later in this chapter the effect of re-introduction of multiple AhR constructs is performed, however none of these constructs are reconcile endogenous function exactly, as they bear mutations or tags affecting subcellular localisation. It's a weakness of the study as it's impossible

to certain that differences observed between the 501mel^{WT} and 501mel *AHR*$^{-/-}$ cell lines are in fact caused by AhR-loss or non-specific clonal differences.

Once AhR status of these cell lines was confirmed by western blot, I treated both cell lines with FICZ and IFNγ, separately and in combination, then assessed their induction of the AhR target gene *CYP1A1* and IFNγ-response genes through qRT-PCR. In 501mel^{WT} cells, I observed significant induction of *CYP1A1* in response to FICZ, causing ^#0.7-FI (Fig. 3.8B). Stimulation of 501mel^{WT} cells with IFNγ produced an insignificant change *CYP1A1* abundance (Fig. 3.8B). As in my preliminary studies, induction of *CYP1A1* is enhanced with co-treatment of FICZ and IFNγ compared to FICZ-only, with 17.1-FI compared to 10.7-FI (Fig. 3.8B). While there's an elevated basal level of *CYP1A1* in 501mel *AHR*$^{-/-}$ cells compared to 501mel^{WT}, 6.2-fold greater, expression of *CYP1A1* in 501mel *AHR*$^{-/-}$ cells is not significantly altered in response to FICZ (Fig. 3.8B). I am confident of the AhR status of these cells. Basal elevation of *CYP1A1* expression was a surprising finding, as I expected to see minimal *CYP1A1* expression in 501mel *AHR*$^{-/-}$ cells, as the AhR was expected to be the predominant mediator of its expression, although PPARα is also a driver of *CYP1A1* expression in humans. Elevated basal expression of *CYP1A1* expression in 501mel cells may arise from several possible mechanisms; 1) the AhR is a suppressor of *CYP1A1* expression in its unliganded form and the absence of AhR in 501mel *AHR*$^{-/-}$ cells allows for higher basal levels of *CYP1A1* but no greater induction in response to AhR effectors; 2) There are other mutations in these cells which drive an elevated basal level of *CYP1A1* expression independently of the desired knockout of the *AHR*, without any sensitivity to AhR ligands; 3) The expression of *CYP1A1* in the 501mel *AHR*$^{-/-}$ cells is predominantly driven by PPARα either as a direct consequence of *AHR* disruption or

other mutations not present in the parental cells. Other genes induced in response to the AhR should have been examined, to determine whether the elevated basal expression of *CYP1A1* in the 501mel *AHR*$^{-/-}$ cells is unique and likely a consequence of genetic lesions in these cells leading to aberrant expression of *CYP1A1*. Equally, other PPARα target genes should have been examined to determine whether there was elevated PPARα activity in these cells that may be driving *CYP1A1* expression without the AhR.. Without additional experiments designed to distinguish between these possibilities it is not possible to state unequivocally which of these possible explanations is likely to be true. Consequently, a weakness of the study, is the uncertainty around potential clonogenic effects being conflated with a true difference due to changes in the AhR status of the cells. Although research by the Galibert group using this cell line has been published (Corre et al., 2018), this work doesn't examine the cause of the elevated basal expression of *CYP1A1*. Given that proliferation of melanoma cells is likely to generate mutations and therefore genetic differences between parental and 501mel AHR$^{-/-}$ cells will very likely be present, assigning a role for any such mutations in regulating basal *CYP1A1* expression will be difficult. However, new 501mel *AHR*$^{-/-}$ cells have been isolated by another member of the lab, and in future testing these clones for changes in basal *CYP1A1* expression and their response to IFNγ will be informative.

Treatment of 501mel *AHR*$^{-/-}$ cells with IFNγ did induce 2.1-FI in the abundance of *CYP1A1* transcripts, rising from 6.2-FI without stimulation to 13.3-FI with IFNγ (Fig. 3.8B). This enhanced accumulation of *IDO1* transcripts in response to IFNγ in 501mel *AHR*$^{-/-}$ is not significantly affected by adding FICZ alongside IFNγ (Fig. 3.8B).

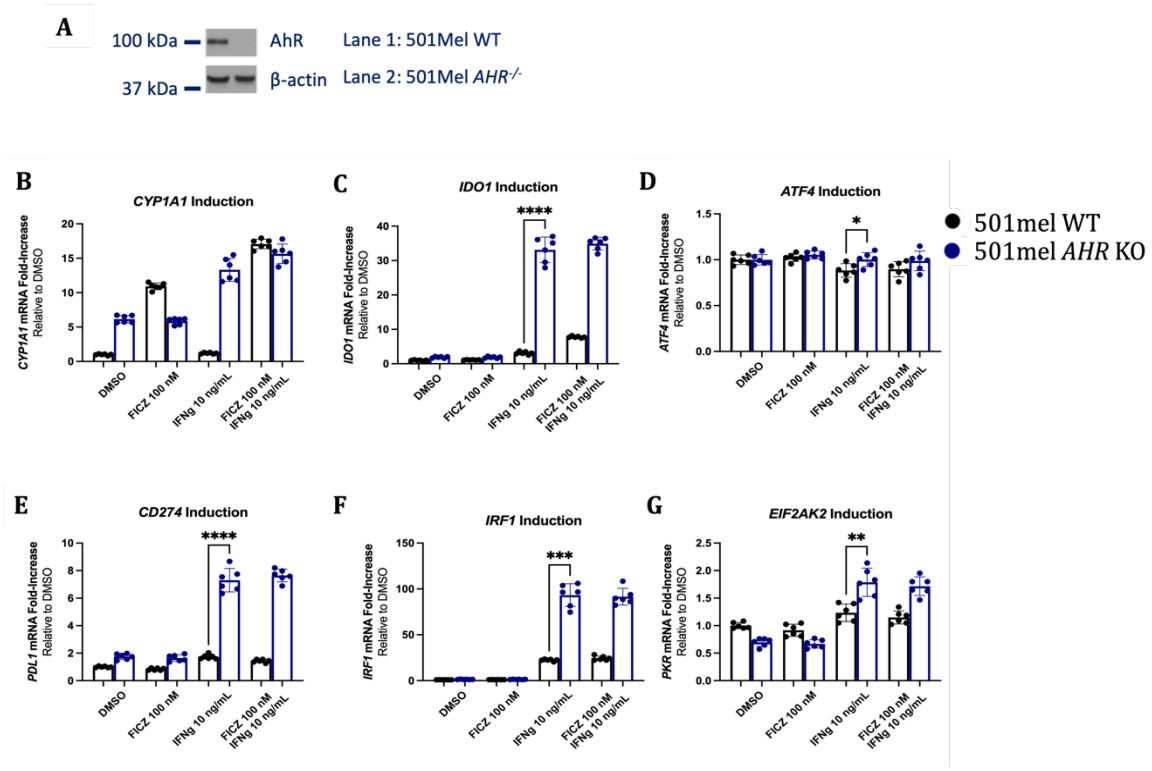

Figure 3.8 Expression of IFNγ response genes in 501mel WT and *AHR* KO. (A) Western blot of 501mel WT and 501mel *AHR* KO cell lines with immunoblotting for AhR and β-actin. Expression of (B) *CYP1A1*, (C) *IDO1*, (D) *ATF4*, (E) *CD274*, (F) *IRF1*, (G) *EIF2AK2* transcripts in 501mel WT and *AHR* KO cells after 24-hours treatment with either FICZ 100 nM, IFNγ 10 ng/mL, or both, assessed by qRT-PCR. Ad-hoc test: Ordinary One-way ANOVA, post-hoc test: Tukey-Kramer test for multiple comparisons which inherently corrects for multiple comparisons $P > 0.05$: ns, $P < 0.05$: *, $P < 0.01$: **, $P < 0.001$: ***, $P < 0.0001$: ****. Biological Repeats = 2, Technical Repeats = 3.

I expected AhR-loss would diminish synergistic induction of *IDO1* in response to both IFNγ and FICZ which I had previously characterised. Remarkably, I observed IFNγ-mediated *IDO1* induction was significantly greater in 501mel *AHR*$^{-/-}$ cells than WT cells (Fig. 3.8C). In 501mel^{WT} cells, IFNγ induced 3.1-FI of *IDO1*, whilst in 501mel *AHR*$^{-/-}$ cells I observed 33.1-FI of *IDO1*. While co-treating with IFNγ and FICZ increased 501mel^{WT} expression of *IDO1* from 3.1-FI to 7.8-FI, it had no effect on 501mel *AHR*$^{-/-}$ compared to IFNγ-treatment-only (Fig. 3.8C). It's likely the synergistic effect of combining FICZ with IFNγ on *IDO1* expression is AhR-mediated. However, with significantly greater expression of *IDO1* in these 501mel *AHR*$^{-/-}$ cells in response to IFNγ than in these 501mel^{WT}, one explanation for this is unstimulated AhR is

suppressing *IDO1*-induction, rather than stimulated AhR being an enhancer of *IDO1* induction, although further experiments are required to confirm this.

My current hypothesis, that the AhR is a broad modulator of IFNγ-signaling, assumes the AhR is a modulator of transcription of IFNγ-response genes beyond *IDO1* expression. I included the *ATF4* gene in the panel of IFNγ-response genes studied as a negative control. In normal responses to IFNγ, ATF4 is translated in response to IFNγ -induced phosphorylation of the translation initiation factor eIF2alpha, but its transcription is not induced. It is therefore included as a negative control to ensure there is only enhanced mRNA expression of genes induced by IFNγ-stimulation and not of genes that I wouldn't expect to be induced by IFNγ-treatment. I observe insignificant difference in the accumulation of *ATF4* mRNA between 501mel^{WT} and 501mel *AHR*$^{-/-}$ under no stimulation, FICZ treatment, or IFNγ with FICZ co-treatment. There's a small, albeit statistically significant, difference between *ATF4* accumulation in response to IFNγ only, with 501mel *AHR*$^{-/-}$ showing 1.00-FI compared to 501mel^{WT} with 0.88-FI, which is reflective of minor suppression of *ATF4* in response to IFNγ in 501mel^{WT} (Fig. 3.8D) although this is not likely to be biologically robust and the negative control has worked to demonstrate the effects on IFNγ gene induction aren't likely affecting genes associated with the pathway that I wouldn't expect to be differentially expressed.

Comparison of the IFNγ-mediated induction of IFNγ-response genes between 501mel^{WT} and 501mel *AHR*$^{-/-}$ cell lines (Fig. 3.8E-G) demonstrates a similar pattern of induction to *IDO1*. Induction of all IFNγ-response genes tested here upon IFNγ-

treatment was significantly greater in 501mel *AHR*$^{-/-}$ than 501mel^{WT}; *PDL1* (7.3-FI vs. 1.7-FI) (Fig. 3.5E), *PKR* (1.8-FI vs 1.2-FI) (Fig. 3.5F), and *IRF1* (93.2-FI vs 23.5-FI) (Fig. 3.8G). Given the positive correlation between AhR activity and IFNγ-response gene expression in patient data and my qRT-PCR data gained from this experiment, I hypothesise the unstimulated AhR is a suppressor of IFNγ-signalling broadly and has a role in mediating immune modulation of the TME of melanoma beyond affecting the expression of *IDO1*.

Given that most of the evidence for the AhR-IDO1-kyn axis lies in papers that used TCDD as a stimulant, I decided to test these 501mel^{WT} and *AHR*$^{-/-}$ cells for their induction of a limited number of IFNγ-response genes after stimulation with FICZ, IFNγ, and TCDD. The expectation here being that FICZ is a canonical AhR agonist, with no effect on expression of *IDO1* or other IFNγ-response genes in the work presented thus far and represents typical AhR activation. IFNγ is clearly going to induce the expression of IFNγ-response genes, and any effect of TCDD on expression of AhR target genes or IFNγ-response genes can be put in context of a strong physiological stimulus of either pathway.

Treatment of the 501mel^{WT} and *AHR*$^{-/-}$ cells with FICZ produces 4.68-FI of *CYP1A1* after 24-hours compared to DMSO control (Fig. 3.9A), and the amount of *CYP1A1* in the 501mel *AHR*$^{-/-}$ cells is not significantly different when treated with DMSO vs. FICZ (Fig. 3.9A). IFNγ induces *CYP1A1* expression in 501mel *AHR*$^{-/-}$ cells up to 6.70-fold compared to 501mel^{WT} which doesn't significantly change vs. DMSO-treatment (Fig. 3.9A). This aligns with previous data in this thesis. TCDD, however, significantly

induces *CYP1A1* compared to DMSO, driving 2.83-fold accumulation (Fig. 3.9A). However, this is not significantly different to the basal expression of *CYP1A1* in 501mel *AHR*$^{-/-}$ cells (Fig. 3.9A), although there is little information that can be gained from this comparison. TCDD and FICZ aren't used at equal concentrations which was intentional: the concentration of FICZ remained consistent between all other experiments in this thesis, and TCDD was limited to 10 nM owing to its toxicity and this concentration is reflective of the typical TCDD concentration used in previous studies *e.g.* (Vogel et al., 2008), but it does mean it's not possible to directly compare the potency of these compounds as activators of the AhR.

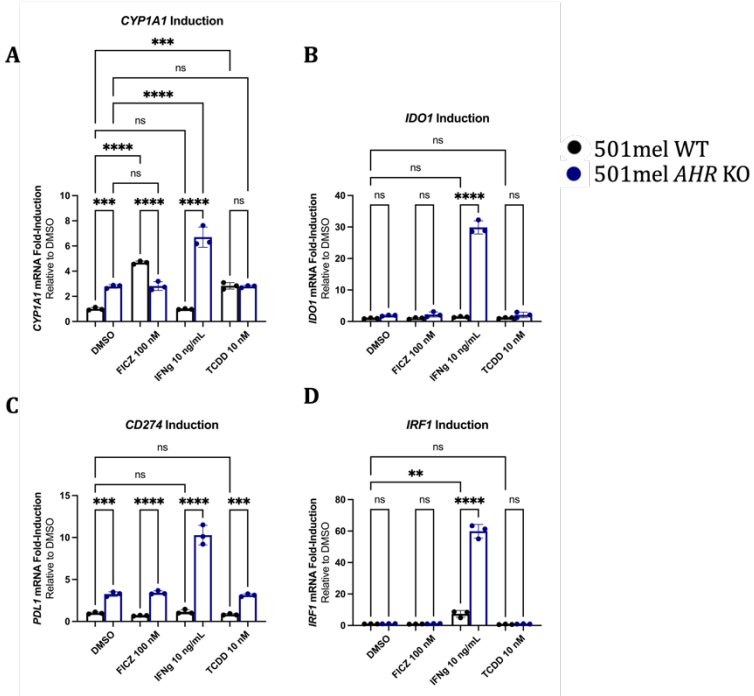

Figure 3.9 Expression of IFNγ response genes in 501mel WT and *AHR* KO. Expression of (A) *CYP1A1*, (B) *IDO1*, (C) *CD274*, (D) *IRF1* transcripts in 501mel WT and *AHR* KO cells after 24-hours treatment with either FICZ 100 nM, IFNγ 10 ng/mL, TCDD 10 nM, or DMSO as a control assessed by qRT-PCR. Ad-hoc test: Ordinary One-way ANOVA, post-hoc test: Tukey-Kramer test for multiple comparisons which inherently corrects for multiple comparisons P > 0.05: ns, P < 0.05: *, P < 0.01: **, P < 0.001: ***, P < 0.0001: ****. Biological Repeats = 1, Technical Repeats = 3.

There's insignificant difference in the induction of *IDO1* in 501mel^{WT} cells or 501mel *AHR*$^{-/-}$ cells under DMSO, FICZ, or TCDD (Fig. 3.9B), with no more than a non-

significant 2.2-FI in 501mel *AHR*$^{-/-}$ under FICZ being the greatest accumulation detected. This is surprising, previous literature describes TCDD as a driver of *IDO1* expression in melanoma cells, and in these cells in this experiment I do not observe this. This experiment is lacking sufficient biological replicates to be confidently relied upon, there's a reasonable chance that this absence of induction is an artefact of this run of this experiment or a clonogenic effect of this experiment using only a single 501mel *AHR*$^{-/-}$ and 501mel cell line. Equally, resuspending the TCDD in the laboratory was difficult, even in DMSO, leaving the possibility that a relatively small amount of the solid TCDD may have successfully dissolved into the solvent. This would mean the concentration of TCDD being used in this experiment is significantly lower than calculated to be 10 nM, this would account for the limited induction of *CYP1A1* compared to FICZ despite both concentrations of TCDD and FICZ being more than the EC_{50} value for each agonist. In this experiment, IFNγ induced robust expression of *IDO1* in 501mel *AHR*$^{-/-}$ cells but did not drive *IDO1* expression in 501mel^{WT} cells (Fig. 3.9B). Absence TCD-mediated effects on *IDO1* expression in this experiment, with IFNγ also failing to induce a response, suggests an issue with cells used in this experiment. However, failure of IDO1 to be induced by IFNγ in this experiment contrasts with all other experiments in these cells, raising the possibility that a technical error was made, given *IDO1* is a canonical IFNγ-response gene.

Across all conditions examined, *CD274* expression is greater in 501mel *AHR*$^{-/-}$ than 501mel^{WT} cells (Fig. 3.9C), with 3.26-fold greater expression under DMSO, 4.96-fold greater expression than WT cells under FICZ-stimulation, and 3.83-fold greater under TCDD-expression (Fig. 3.9C). Induction of *CD274* under IFNγ-stimulation yields the greatest induction at 8.96-fold that of 501mel^{WT} cells under the same stimulation (Fig.

3.9C). There's insignificant induction of *CD274* in 501mel^{WT} cells under FICZ- and TCDD-stimulation relative to DMSO (Fig. 3.9C). Together this suggests that a mistake had been made in the IFNγ-treatment of these cells, given that I do not observe induction of a known IFNγ target gene under treatment with IFNγ.

IRF1 induction in response to IFNγ yields the only significant induction of this gene under the conditions tested in either 501mel^{WT} or 501mel *AHR* WT cells (Fig. 3.9D). There was 7.34-FI of *IRF1* in 501mel^{WT} cells in response to IFNγ, and a significantly greater 59.9-FI of *IRF1* in 501mel *AHR*$^{-/-}$ under IFNγ (Fig. 3.9D). Although this reflects the same pattern as observed in Figure 3.5F, the magnitude of this induction is considerably lower, suggesting that perhaps the concentration of IFNγ used in this experiment might be lower than expected and this is the source of limited induction of *IDO1* and *CD274* in these cells under IFNγ-treatment. The absence of any induction in response to TCDD of any of these genes does, however, raise questions about the validity of using this cell line to examine the underlying mechanism of the AhR-IDO1-Kyn axis. However, IFNγ can induce the expression of these genes and modulation of the AhR affects the expression of these genes in these cells. Due to concerns regarding the IFNγ condition in this experiment and the solubility of TCDD and subsequent actual concentration of TCDD used, no substantial conclusions can be made from this experiment. Due to the difficulties regarding solubilising TCDD and the very high carcinogenic risk posed by using this compound and the difficulties in safely disposing of this compound I did not perform any subsequent experiments with TCDD.

To confirm whether these effects were cell line or cell type specific, I performed the same experiment in HaCaT cells. I generated HaCaT *AHR*$^{-/-}$ cells and validated their

AhR status through immunoblotting, which show a faint band in the HaCaT *AHR*$^{-/-}$ cell line, suggesting these cells are better considered AhR knockdowns, not knockouts (Fig. 3.10A). Alternatively, the faint 'AhR' band in the HaCaT *AHR*$^{-/-}$ lane could also be the product of a small population of HaCaT WT cells contaminating this cell line. If this were the case, there is the potential that this WT population could outgrow the HaCaT *AHR*$^{-/-}$ cell line, ultimately making this cell line unreliable and unrepresentative. The HaCaT 'KO' cells could be reselected for *AHR*$^{-/-}$ cells again outgrowing single clones and/or sequencing of the cells could be done to determine whether they are incomplete knockouts or a mixed population of cells. Unlike the 501mel cell lines where I did not observe any response to FICZ in *CYP1A1* induction in the *AHR*$^{-/-}$ cells, here I observe that FICZ induces a significantly depressed *CYP1A1* induction in HaCaT *AHR* KD compared to HaCaT WT (4.8-FI vs. 19.4-FI) (Fig. 3.10B). As observed in 501mel^{WT} and *AHR*$^{-/-}$ cell lines, expression of IFNγ-response genes after stimulation with IFNγ are elevated in HaCaT *AHR*$^{-/-}$ cells compared to HaCaT WT cells: *IDO1* (603.3-FI vs. 184.4-FI) (Fig. 3.10C), *IL-6* (422.9-FI vs. 11.5-FI) (Fig. 3.10D), *IRF1* (410.8-FI vs. 43.8-FI) (Fig. 3.10F), and *Eukaryotic Initiation Factor 2 alpha kinase 2* (*EIF2AK2*) (26.1-FI vs. 2.00-FI) (Fig. 3.10G). The fold change in *IDO1* transcripts in response to IFNγ in HaCaT *AHR*$^{-/-}$ compared to HaCaT WT is less than that observed in 501mel *AHR*$^{-/-}$ compared to 501mel^{WT}, which may be reflective of the HaCaT *AHR*$^{-/-}$ cell line being an *AHR* KD, not a true *AHR*$^{-/-}$. In contrast to expression profiles in 501mel cell lines, there's no significant difference in *CD274* (PD-L1) expression in HaCaT WT and HaCaT *AHR*$^{-/-}$ after IFNγ-treatment (Fig. 3.10E). This suggests, that although the AhR is modulating IFNγ-signalling broadly, there are potentially cell type specific differences in how this modulation manifests at the transcriptomic level. Furthermore, existing research demonstrates the AhR is a key modulator of pro-

inflammatory signalling in keratinocytes, suppressing IL-1b signaling in these cells (DiMeglio et al., 2014). This indicates a broader role of the AhR within modulation of

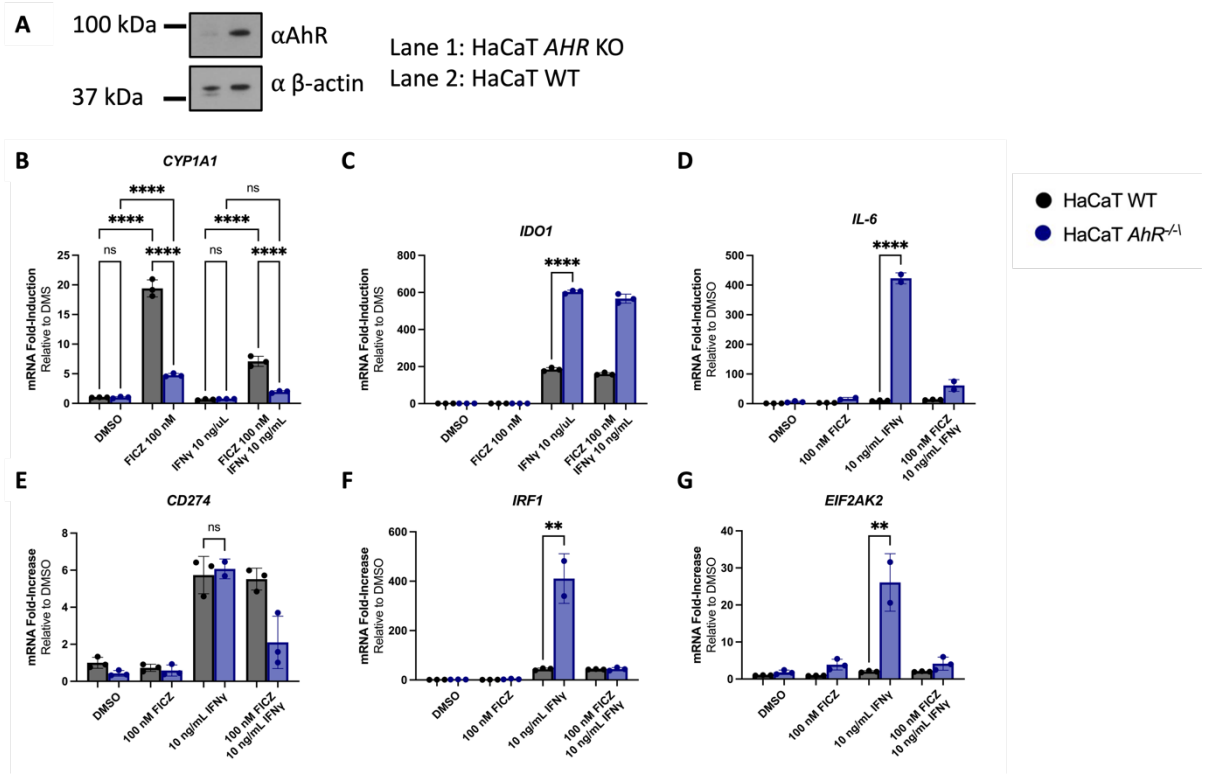

Figure 3.10 Expression of IFNγ response genes in HaCaT WT and *AHR* KO. (A) Validation of AhR status in HaCaT WT and HaCaT *AHR* KO. Expression of (B) *CYP1A1*, (C) *IDO1*, (D) *IL-6*, (E) *CD274*, (F) *IRF1* (G) *EIF2AK2* transcripts in HaCaT WT and *AHR* KO cells after 24-hours treatment with either FICZ 100 nM, IFNγ 10 ng/mL, or both, assessed by qRT-PCR. Ad-hoc test: Ordinary One-way ANOVA, post-hoc test: Tukey-Kramer test for multiple comparisons which inherently corrects for multiple comparisons $P > 0.05$: ns, $P < 0.05$: *, $P < 0.01$: **, $P < 0.001$: ***, $P < 0.0001$: ****. Biological Repeats = 1, Technical Repeats = 3.

the pro-inflammatory signaling in and around melanoma, with the AhR appearing to suppress pro-inflammatory signaling through multiple mechanisms in the cells of the melanoma TME. Although, my data is only applicable to these cell lines observed, and further work in more cell lines and primary cells is necessary to determine whether the role of the AhR in IFNγ-signaling is ubiquitous and relevant to the pathology of this disease.

Differences in transcription between WT and *AHR*$^{-/-}$ cell lines, while indicative, aren't necessarily reflected in protein levels. I used immunofluorescence to assess accumulation of IDO1 protein in 501mel cell lines in response to IFNγ. Without stimulation with IFNγ, 501mel *AHR*$^{-/-}$ cells have a greater accumulation of IDO1 than 501mel^{WT} cells, 131.8 AU compared to 52.1 AU (Fig. 3.11A, 3.11B, 3.11E). IFNγ-treatment of 501mel^{WT} cells drives an increase of IDO1 accumulation compared to no stimulation, 103.5 AU compared to 52.1 AU (Fig. 3.11C, Fig. 3.11A), again, this increase is greater in 501mel *AHR*$^{-/-}$, 131.8 AU compared to 156.8 AU (Fig. 3.11B, Fig. 3.11D). This supports my previous findings that *AHR*$^{-/-}$ cells have a greater induction of IDO1 in response to IFNγ than 501mel^{WT}.

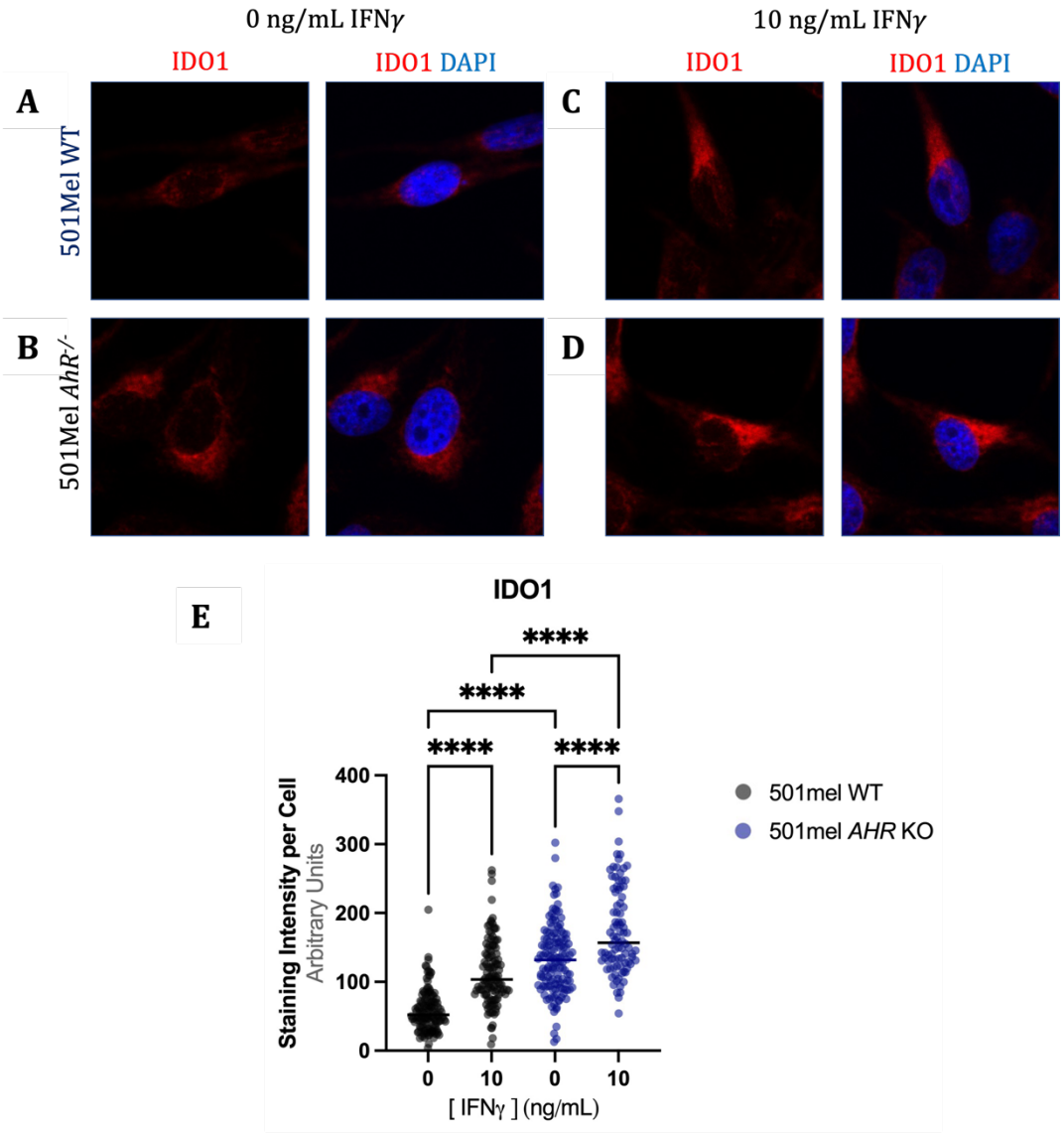

Figure 3.11 Accumulation of IDO1 protein in 501mel cell lines. Immunofluorescence microscopy with staining for IDO1 and DAPI in represented as red and blue, respectively. For representative images, cell lines used are (A & C) 501mel WT, (B & D). Cells were treated for 24-hours with or without 10 ng/mL IFNγ. (E) Quantification of IDO1 staining fluorescence per cell, where number of cells are WT 0 ng/mL: 139, WT 10 ng/mL: 122, *AHR* KO 0 ng/mL: 136, and *AHR* KO 10 ng/mL: 91. Ordinary One-way ANOVA, post-hoc test: Tukey-Kramer test for multiple comparisons which inherently corrects for multiple comparisons, $P > 0.05$: ns, $P < 0.05$: *, $P < 0.01$: **, $P < 0.001$: ***, $P < 0.0001$: ****.

To confirm whether these findings are AhR-dependent rather than clone specific, I generated an HA-tagged inducible *AHR* construct and transfected it into 501mel *AHR*$^{-/-}$ cells. Expression of this exogenous *AHR* construct is induced in response to treatment with doxycycline. In this inducible cell line, without doxycycline-mediated induction of the endogenous construct, which should be equivalent to the 501mel

AHR$^{-/-}$ cell line, there's greater IDO1 staining compared to doxycycline-treated cells (Fig. 3.12A, 3.12B). The basal expression of this AhR-construct, however, was not assessed and it's possible there's a basal expression of the AhR in these cells, meaning the effects may be the difference between low and high AhR expression rather than none and some. This pattern remains even with stimulation with IFNγ (Fig. 3.12C, 3.12D), where exogenous AhR expression depresses IDO1 accumulation. Quantification of these changes across more than 80 cells imaged show the average intensity of staining agrees with these representative images, although the differences between the groups are not statistically significant. While this is indicative of exogenous AhR being sufficient to drive changes in IDO1 accumulation in response to IFNγ-treatment, the result is not statistically significant across the cells I imaged. Consequently, the difference in means must be ignored and the conclusion must be the AhR is not sufficient. However, given the uncertainty whether this is a comparison between some and more AhR construct expression or if it's between none and some, the insignificance may be reflective of it being the former rather than the latter, and quantification of expression of this construct is required to confirm this and subsequent conclusions can be drawn depending on basal expression of the construct. Another issue with this experiment is there's insignificant change in the expression of IDO1 in response to IFNγ, something that should be detected regardless of AhR status as shown in Figure 3.11. This suggests that this experiment may not have been performed correctly , that there was an issue with the anti-IDO1 antibody, or there was an issue with the ability of the cells to respond to IFNγ and induce IDO1 expression. Consequently, drawing robust conclusion from this experiment is not possible. To be able to determine the effect of treating these cells with doxycycline on the expression of IDO1 to allow for a fairer comparison with the inducible cell lines

and the 501mel *AHR*$^{-/-}$ cell line, I should have included the 501mel *AHR*$^{-/-}$ cell line ±Doxycycline/±IFNγ to test whether there are differences in IDO1 expression being driven by doxycycline that are masking changes that are dependent on the constructs. The absence of this control limits the reliability of this experiment as it's not possible to discern effects of doxycycline on inducible cell lines that are independent of expression of these constructs.

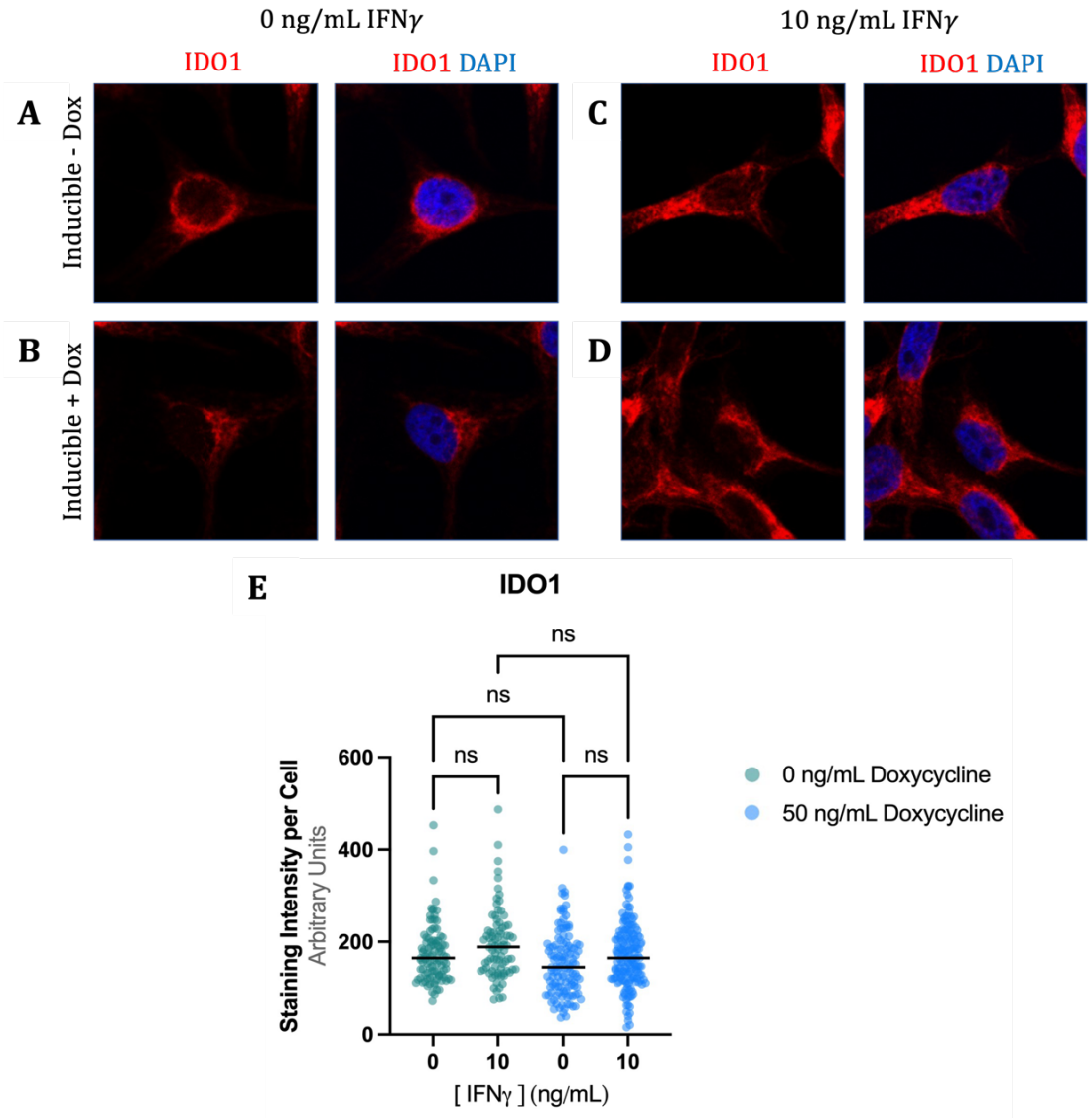

Figure 3.12 Accumulation of IDO1 protein in 501mel AhR inducible cell lines. Immunofluorescence microscopy with staining for IDO1 and DAPI in represented as red and blue, respectively. The cell line used is 501mel *AHR* KO transfected with an HA-tagged AhR^{WT} construct under a doxycycline-mediated promoter. (A & C) Without Doxycycline mediated induction, (B & D) with doxycycline mediated induction of AhR. Cells were treated for 24-hours with or without 10 ng/mL IFNγ, after 24-hours pre-treatment with 50 ng/mL Doxycycline before fixing and staining. (E) Quantification of IDO1 staining fluorescence per cell, number of cells: 0 ng/mL Dox 0 ng/mL IFNγ: 98, 0 ng/mL Dox 10 ng/mL IFNγ: 84, 50 ng/mL Dox 0 ng/mL IFNγ: 122, and 50 ng/mL Dox 10 ng/mL IFNγ: 165. Ordinary One-way ANOVA, post-hoc test: Tukey-Kramer test for multiple comparisons which inherently corrects for multiple comparisons, $P > 0.05$: ns, $P < 0.05$: *, $P < 0.01$: **, $P < 0.001$: ***, $P < 0.0001$: ****.

3.2.6. The AhR modulates phosphorylation of STAT1, not STAT3

The IFNγ-signalling pathway involves binding of IFNγ to its receptor, the IFNGR, which stimulates sequential association of JAK and STAT proteins, phosphorylated

STAT dimers translocate to the nucleus where they stimulate gene expression. The activated IFNGR may associate with JAK1 or JAK2, which stimulate STAT1 or STAT3 in response to IFNγ. Given the difference in roles of STAT1- and STAT3-mediated signalling in promoting tumorigenesis in melanoma (Zhou et al., 2022) as discussed in section 1.5.2. I wanted to determine whether the AhR affected STAT1 and/or STAT3 activation as upstream mediators of broad IFNγ-response gene activation.

I assessed activation of STAT1 and STAT3 proteins in response to IFNγ-treatment for 24-hours in 501mel^{WT} and 501mel *AHR*$^{-/-}$. Without stimulation with IFNγ 501mel^{WT} cells (Fig. 3.13A) had a lower accumulation of STAT1 than 501mel *AHR*$^{-/-}$ cells (Fig. 3.13B). Treatment with IFNγ‡ causes greater STAT1 and phospho-STAT1 accumulation in the 501mel^{WT} cells (Fig. 3.13C) than in untreated 501mel^{WT} cells (Fig. 3.13A). There's greater STAT1 accumulation in 501mel *AHR*$^{-/-}$ cells treated with IFNγ (Fig. 3.13D) than in the treated 501mel^{WT} cells (Fig. 3.13C), with an average staining intensity of 4.96 AU compared to 2.59 AU (Fig. 3.13E). There's also greater pY701 STAT1 accumulation in response to IFNγ in 501mel *AHR*$^{-/-}$ cells (Fig. 3.13D) than in 501mel^{WT} cells (Fig. 3.13C), with an average staining intensity of 2.55 AU compared to 1.72 AU (Fig. 3.13E). The immunofluorescence images were captured such that in the brightest images the sensors weren't saturated as to have a dynamic range that allowed for quantification of the brightest staining without concerns about

‡ Quantification of staining in the absence of IFNγ was not possible due to calibration of the microscope leading to staining intensities that were too weak to visualise the cytoplasm of cells surrounding nuclei. Consequently, it was not possible to reliably quantify the fluorescence intensity across the whole cell..

oversaturation, as a result the staining of STAT1 in the 501mel^{WT} cells is very faint in comparison as it's considerably lower than that of the brightest staining.

However, without IFNγ-treatment, STAT3 levels are higher in 501mel^{WT} (Fig. 3.13F) than in the 501mel *AHR*$^{-/-}$ cells (Fig. 3.13G). Upon IFNγ-treatment, there's little difference in the induction of STAT3 or pY705 STAT3 in either 501mel^{WT} (Fig. 3.13H) or 501mel *AHR*$^{-/-}$ cells (Fig. 3.13I), with insignificant difference between the average staining intensities (Fig. 3.13J). I conclude that this much greater induction of IFNγ-response genes in 501mel *AHR*$^{-/-}$ cells is likely mediated through effects of the AhR on STAT1 signalling rather than on STAT3 signalling.

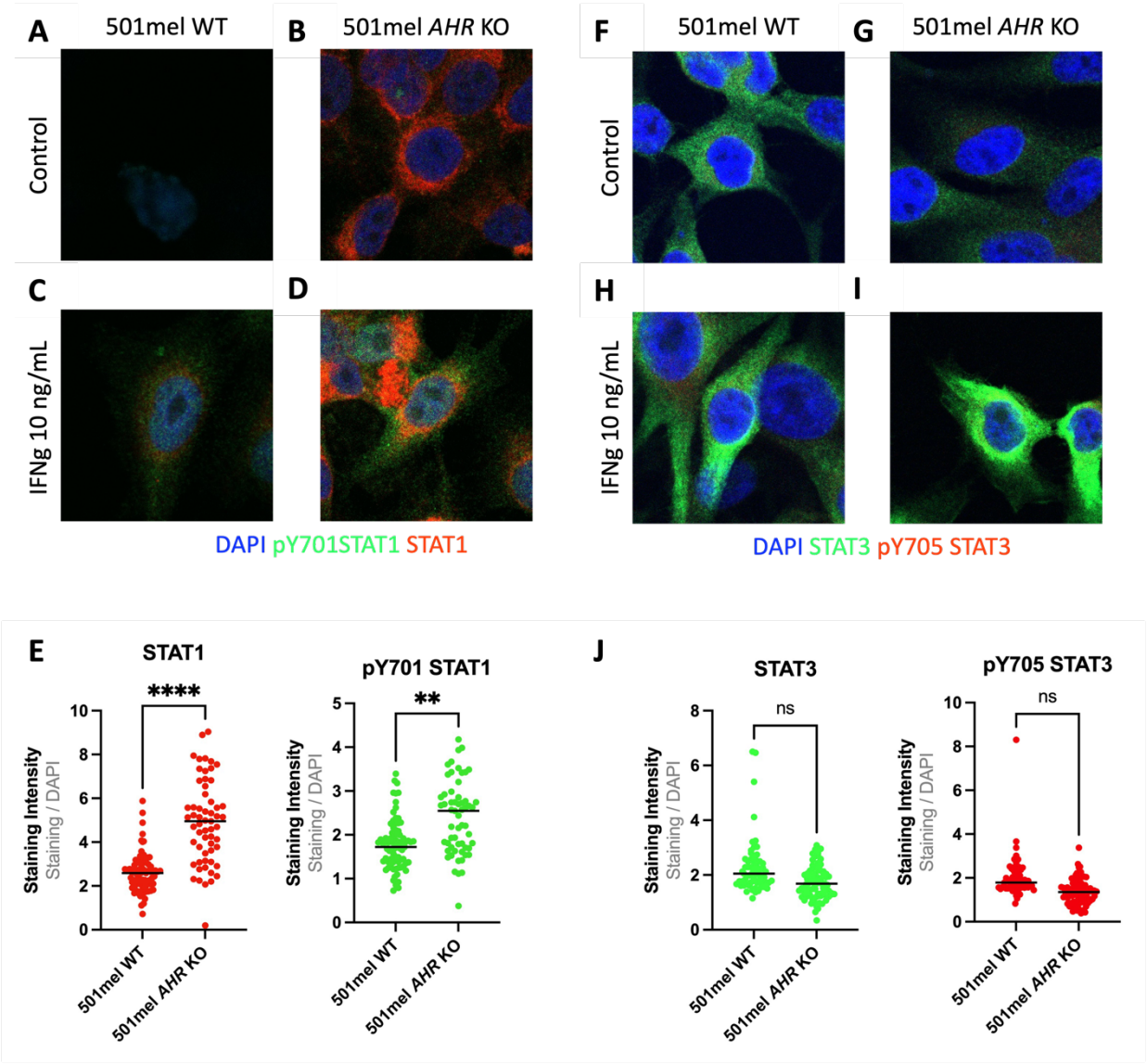

Figure 3.13 STAT1/3 signalling mediation by the AhR. Immunofluorescence microscopy of 501mel WT and *AHR* KO cells in response to 24-hours IFNγ 10 ng/mL stimulation. Staining for (A-D) STAT1 in red and pY701 STAT1 in green, and for (F-I) STAT3 in green and pY705 STAT3 in red. Quantification of the staining across all imaged IFNγ-treated cells for (E) STAT1 and pY701 STAT1(No. cells WT: 77, No. cells *AHR* KO: 59) and (J) STAT3 and pY705 STAT3 (No. cells WT: 61, No. cells *AHR* KO: 74). Ordinary One-way ANOVA, post-hoc test: Tukey-Kramer test for multiple comparisons which inherently corrects for multiple comparisons, P > 0.05: ns, P < 0.05: *, P < 0.01: **, P < 0.001: ***, P < 0.0001: ****. **NB:** data from panels A-E is repeated later in figure 3.16

3.2.7. Cytoplasmic AhR mediates IFNγ signalling suppression

Having determined that the AhR is affecting STAT1 signaling, not STAT3 signaling, I aimed to determine whether these effects are being mediated at the transcriptional or post-transcriptional level. Given the unstimulated AhR is not thought to be transcriptionally active, and the 501mel *AHR*$^{-/-}$ cells exhibit a greater accumulation of

both STAT1 and pSTAT1 in response to IFNγ, I do not think the mechanism underlying these effects is transcriptional as it would require unstimulated AhR to be a transcriptional repressor of *STAT1* in its inactive state, although this cannot be ruled out. This possibility, however, cannot yet be ruled out. It's more plausible, however, that cytoplasmic AhR is suppressing IFNγ-signalling, with some relief of inhibition coming with treatment with AhR agonists which drive nuclear localisation of the AhR and much greater loss of inhibition coming with *AHR*$^{-/-}$ – supporting my previous observations. I hypothesised confining AhR to the cytoplasm should be sufficient to suppress IFNγ-mediated gene expression, whereas confining AhR to the nucleus would recapitulate the effects seen in the 501mel *AHR*$^{-/-}$ cell lines.

To study this effect, I generated two deletion mutants of the AhR, lacking either the NLS (Δ13-39) or NES (Δ55-75) (Fig. 3.14). I generated these using my inducible AhR-HA tagged construct vector as a backbone and transfected these constructs into 501mel *AHR*$^{-/-}$ cells for doxycycline-induced expression, using a PiggyBac transfection system to produce an integrated transfection, with a puromycin resistance gene, where cells were maintained under 5 μg/mL of puromycin to select successfully transfected cells. Expression of my mutant AHR$^{\Delta NES}$ construct in the 501mel *AHR*$^{-/-}$ cell line is slightly 'leaky' with some baseline expression of the HA-tagged construct without doxycycline; however, expression of this construct is much greater in response to doxycycline treatment (Fig. 3.14). Given that ideally there should be no expression from this construct without doxycycline, I would rather overexpress AHR and be confident I'm using a cell line expressing the protein than relying on the basal expression observed and assuming the HA-AHR will be expressed, despite the level of expression without doxycycline in this experiment being closer to that of 501mel^{WT}

AhR expression. Furthermore, I did not successfully perform a western blot of the $AHR^{\Delta NLS}$ complemented cells to determine relative induction of the AHR mutant protein, so I could not determine baseline expression. However, subsequent immunofluorescence experiments demonstrate that it was expressed in these cells under doxycycline treatment. For further experiments I use 501mel $AHR^{-/-}$ cell lines as a comparison with doxycycline-treated inducible construct-complemented cell lines rather than the inducible cell lines with and without doxycycline-induction as the baseline expression is closer to WT levels of *AHR* expression (Fig. 3.14). A cell line that I tried but failed to generate a 501mel $AHR^{-/-}$ cell line complemented with an AHR^{WT} inducible construct. This cell line would have allowed for an important control to be used in this and other experiments by enabling me to determine using a single 501mel $AHR^{-/-}$ clone whether reintroducing WT AhR to it would restore the behaviours or target genes observed in the original parental $501mel^{WT}$ cell line. The absence of the complementation cell line here and in subsequent experiments means there always remains the possibility that differences between the 501mel $AHR^{-/-}$ cell line and cell lines derived from it with inducible constructs may differ from the parental $501mel^{WT}$ cells due to non-specific mutations rather than AhR-dependent mechanisms.

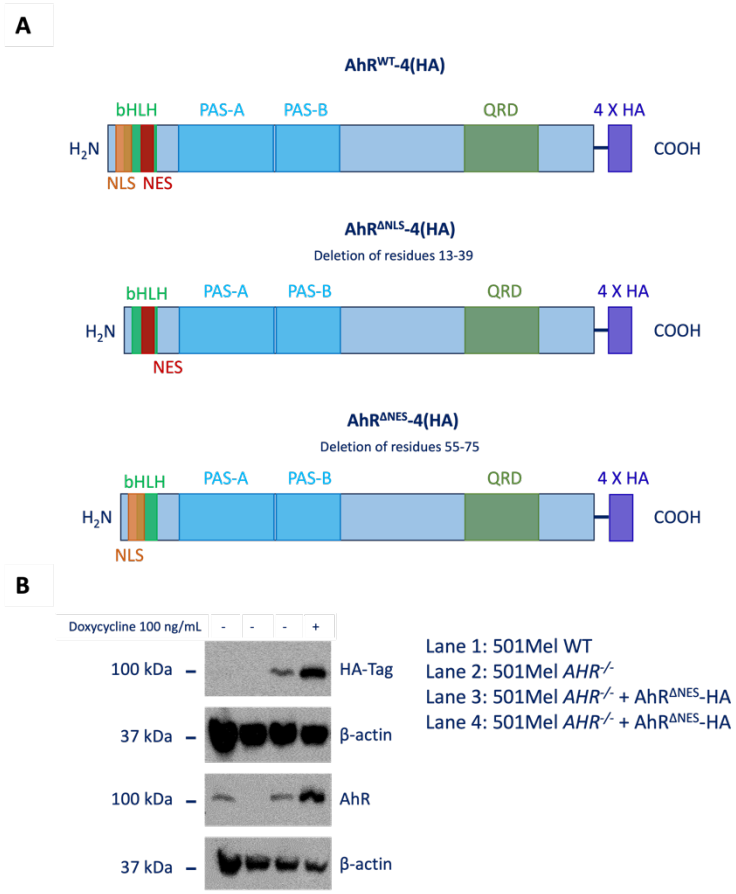

Figure 3.14 Generation of inducible mutant AhR cell lines. (A) Construct maps of AhR WT, AhR$^{\Delta NLS}$, and AhR$^{\Delta NES}$. (B) Immunoblotting of 501mel cell lines for HA-tagged constructs and the AhR, Doxycycline 100 ng/mL treated for 24-hours. β-actin is used as a loading control.

To assess whether these endogenous *AHR*$^{\Delta NLS}$-HA or *AHR*$^{\Delta NES}$-HA constructs localised within the cell as expected, I used immunofluorescence imaging to identify their subcellular localisation. Without doxycycline treatment, there's minimal expression of these constructs (Fig. 3.15Aii, 3.15Cii), which aligns with the immunoblotting data of these cell lines (Fig. 3.14). The images in this experiment were all captured using the same settings that were calibrated such that the sensor was not oversaturated in the brightest images. Consequently, the low basal expression of the constructs is not easily seen in the images (Fig. 3.15A&C). Expression of these constructs is then strongly induced in response to 24-hours of treatment with doxycycline (Fig. 3.15Bii,

3.15Dii). The *AHR*$^{\Delta NLS}$-HA (Cyt. AhR) construct is almost entirely excluded from the nucleus (Fig. 3.15B), whereas the *AHR*$^{\Delta NES}$-HA (Nuc. AhR) construct accumulates in the nucleus without stimulation, it's not entirely confined to the nucleus, with some cytoplasmic retention (Fig. 3.15D). However, these cell lines do provide a tool to compare effects of different nucleocytoplasmic distributions of the AhR on IFNγ-signalling.

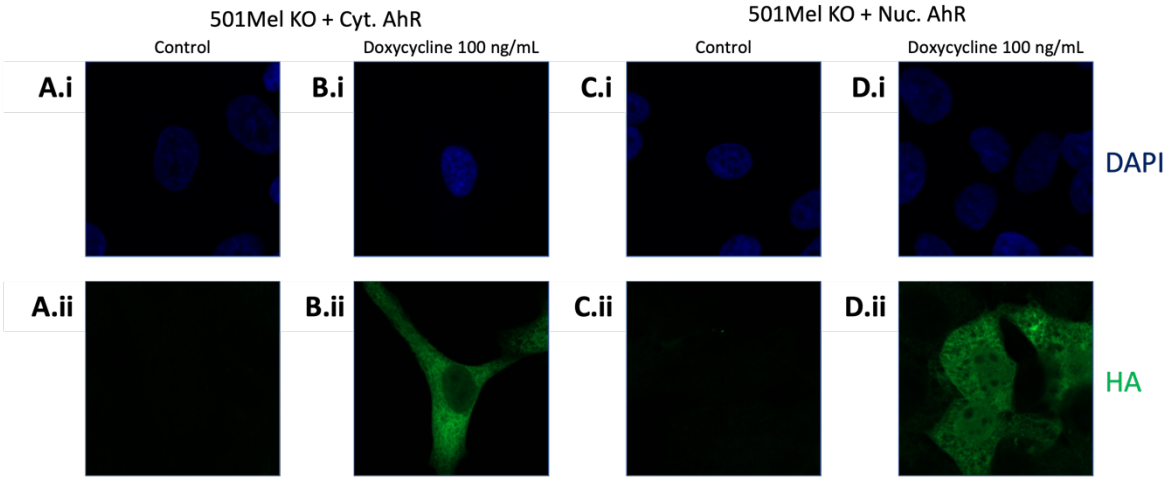

Figure 3.15 Cellular localisation ΔNES and ΔNLS AhR constructs. Immunofluorescent imaging of 501mel *AHR* KO cell lines reconstituted with either (A, B) inducible-*AHR*$^{\Delta NLS}$-HA or (C, D) inducible-*AHR*$^{\Delta NES}$-HA stained with (i) DAPI and an antibody against HA-tags, (ii) 12CA5 in green.

In 501mel^{WT} cells, STAT1 and pSTAT1 accumulation is lower than that of 501mel *AHR*$^{-/-}$ cells both with and without IFNγ-treatment (Fig. 3.16A-D, 3.16I, 3.16J)§. The apparent lack of STAT1 signaling in 501mel^{WT} cells may again be reflective of the calibration of the microscope such that the images captured are not saturated with the brightest images, but weak staining is barely visible. 501mel *AHR*$^{-/-}$ + Cyt. AHR cells have a similar baseline expression of STAT1 to 501mel *AHR*$^{-/-}$ cells (Fig. 3.16E),

§ Quantification of staining in the absence of IFNγ was not possible due to calibration of the microscope leading to staining intensities that were too weak to visualise the cytoplasm of cells surrounding nuclei. Consequently, it was not possible to reliably quantify fluorescence intensity across the whole cell.

however, IFNγ-treatment of 501mel *AHR*$^{-/-}$ + Cyt. *AHR* cells produces an accumulation of STAT1 and pSTAT1 equivalent to that of 501mel^{WT} cells (Fig. 3.16H). Whereas 501mel *AHR*$^{-/-}$ + Nuc. *AHR* cells have a weaker baseline expression of STAT1 than 501mel *AHR*$^{-/-}$ (Fig. 3.16G), the response to IFNγ in these cells is much more like that of 501mel *AHR*$^{-/-}$ (Fig. 3.16H, 3.16J). I believe that it's the cytoplasmic retention of AhR which mediates its suppressive effects on IFNγ-signalling with cytoplasmic AhR constructs producing the same effects as WT, and nuclear AhR producing the same effect as knocking-out the *AHR* on pY701 STAT1 accumulation.

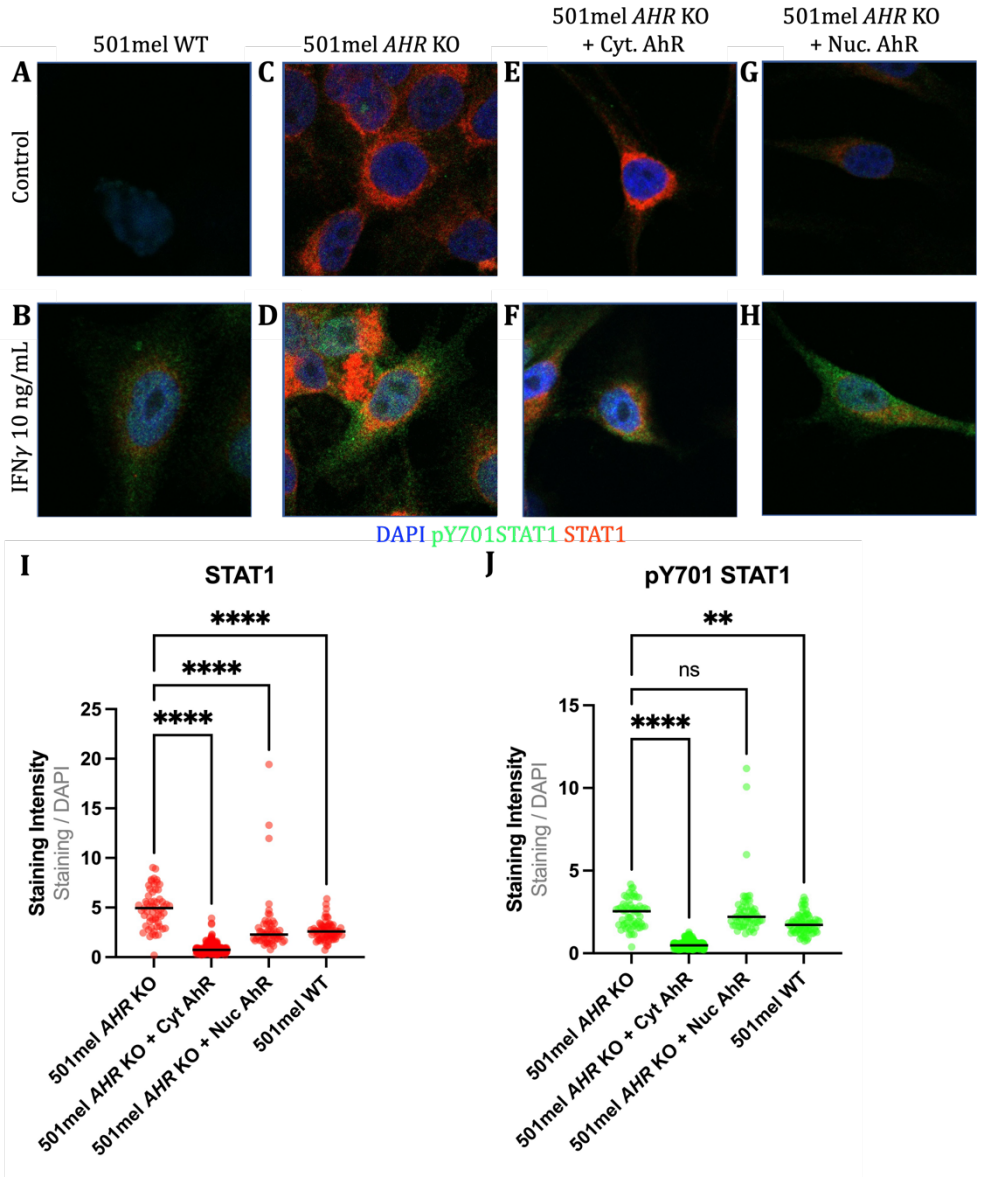

Figure 3.16 The effect of AhR subcellular localisation on pSTAT1 accumulation in response to IFNγ. Four 501mel cell lines were used (A, B) 501mel WT, (C, D) 501mel *AHR* KO, (E, F) 501mel *AHR* KO + Cyt. *AHR*, and (G, H) 501mel *AHR* KO + Nuc. *AHR*. The inducible cell lines were pre-treated for 24-hours with 100 ng/mL doxycycline before 24-hours of IFNγ 10 ng/mL treatment. Quantification of staining of (I) STAT1 and (J) pY701 STAT1 across all imaged cells. Ordinary One-way ANOVA, post-hoc test: Tukey-Kramer test for multiple comparisons which inherently corrects for multiple comparisons, $P > 0.05$: ns, $P < 0.05$: *, $P < 0.01$: **, $P < 0.001$: ***, $P < 0.0001$: ****. NB: As staining intensity is normalised to DAPI staining, when interpreting representative images, it is key to consider the intensities are relative to the DAPI staining not the absolute intensity. Furthermore, representative images were selected blinded of condition, therefore are not necessarily the best to display relative effects, rather what was considered the average when images were captured.

Given the NES is located slightly N-terminal to the DNA binding domain of the AhR, and the NLS is located within the DNA binding domain, I wanted to determine whether the effect I observed with the ΔNES and ΔNLS AhR mutant constructs were

solely dependent on subcellular localisation or if I had introduced off-target effects through disrupting DNA binding. I introduced an *AHR*^{WT}-eNLS-HA construct to 501mel^{WT} cells, where there was an exogenous NLS (eNLS) from *MYC* inserted downstream of the wild-type *AHR* coding sequence, also under control of a doxycycline inducible promoter.

The ΔNES and ΔNLS *AHR* constructs had biased the subcellular localisation of the AhR, with accumulation predominantly in the nucleus and cytoplasm, respectively. This localisation was not absolute, with presence of the AhR in both compartments of the cell, whereas the *AHR*^{WT}-eNLS-HA construct localised solely in the nucleus (Fig. 3.17A, 3.17B). As I increase expression of the *AHR*^{WT}-eNLS-HA construct in these cells, the total amount of AhR in the cell doesn't change (Fig. 3.17C). Unliganded AhR, without association with p23 is ubiquitinated and degraded by the proteosome (Pappas et al., 2018), as expression of exogenous AhR increases, p23 is likely sequestered away from the endogenous AhR leading to degradation of endogenous AhR. Consequently, as I increase the concentration of doxycycline, I increase AHR-eNLS-HA abundance which sequesters p23 from endogenous AhR causing its degradation, shifting the fraction of AhR in these cells from endogenous AhR to exogenous nuclear-only AhR as doxycycline concentration increases, with the overall concentration remaining constant. [Doxycycline] increase, the pool of AhR in these cells shifts from endogenous to exogenous, nuclear, AhR. As I increase the concentration of doxycycline in the presence of a fixed concentration of IFNγ, there's an increase in the accumulation of pSTAT1 (Fig. 3.17D). These data demonstrate that cytoplasmic AhR is a suppressor of STAT1 signalling in response to IFNγ-treatment, as unstimulated nuclear AhR yields

a greater accumulation of pSTAT1 in response to IFNγ than cytoplasmic-localised AhR or wild-type AhR.

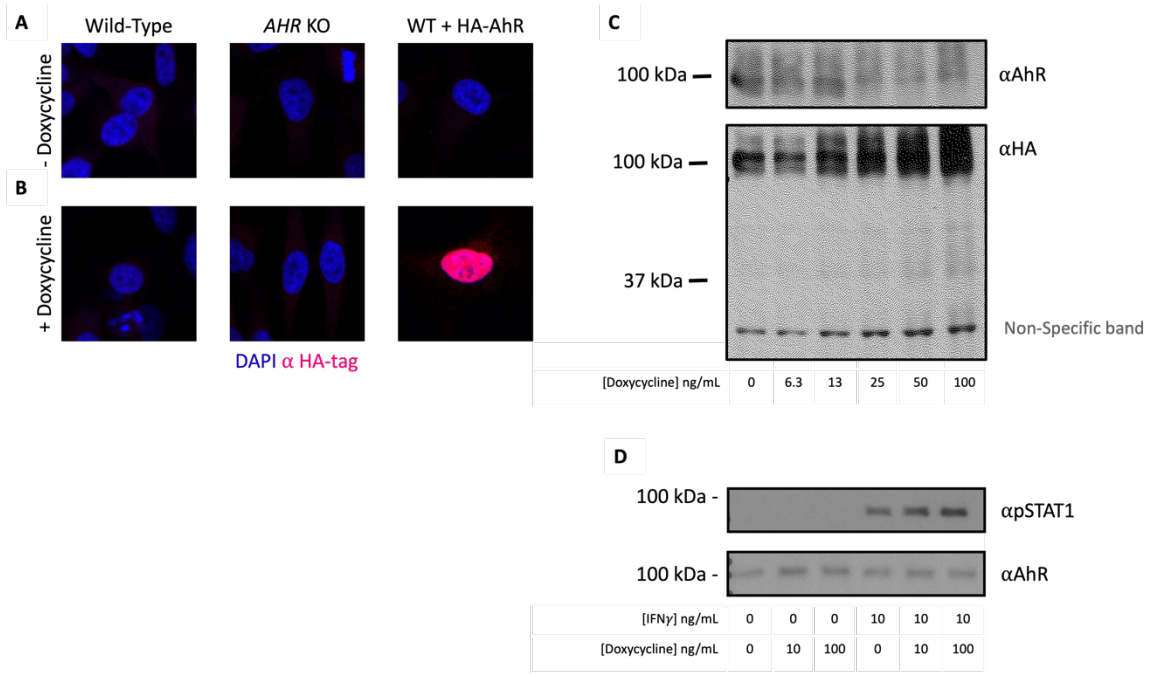

Figure 3.17 Nuclear localised ectopic AhR enhances pSTAT1 accumulation. Immunofluorescence Microscopy of 501mel WT, 501mel *AHR* KO, and 501mel WT with inducible *AHR^{WT}-eNLS-HA tag*, stained for DAPI and anti-HA tag antibodies in (A) the absence of 100 ng/mL doxycycline or (B) presence of 100 ng/mL doxycycline after 24-hours incubation. (C) Immunoblotting for the AhR (sc A-3) and HA-Tag (C29F4) in 501mel WT cells with inducible *AHR^{WT}-eNLS-HA tag* with a titration of doxycycline, with a non-specific HA band as a loading control. (D) Immunoblotting of pSTAT1 (ST1P-11A5) and AhR (sc A-3) after 24-hours incubation with 10 ng/mL IFNγ with a 24-hour pre-incubation with 0, 10, 100 ng/mL of doxycycline.

3.2.8. IRAK1 is a candidate for AhR-mediated effects on IFNγ signalling in these cells

My findings demonstrate that cytoplasmic AhR is a suppressor of IFNγ-signalling via STAT1 in the melanoma cell lines being examined, to determine how the AhR is mediating this effect my collaborator (Jean-Philippe Lambert, Lunefield, Canada) performed proximity biotinylation and affinity purification coupled mass

spectrometry of the AhR in 501mel cells. This method involves generation of a fusion protein, with the AhR being expressed with a biotin ligase domain, meaning that any protein the AhR is near at the point of a pulse of biotin will be tagged with a biotin moiety. Streptavidin beads may then be used to purify biotinylated proteins from the cell, the identities of which can be determined through mass spectrometry.

Given the AhR, when stimulated, translocates to the nucleus to mediate gene induction, I divided the BioID-identified interactors of the AhR into proteins enriched in the presence of FICZ to establish likely nuclear interactors of the AhR, and those enriched without FICZ which are the likely cytoplasmic interactors of the AhR (Fig. 3.18). To confirm validity the of the assumptions about sub cellular localisation of the AhR interactors in response to FICZ, I performed gene set enrichment analysis for cellular compartment enrichment on both lists of genes. Proteins from the FICZ-treated list showed 9.83-FE for the nuclear matrix ($P = 8.21 \times 10^{-4}$), and the untreated list showed 2.66-FE for the cytosol ($P = 2.36 \times 10^{-13}$), confirming these groups reflect a more nuclear and more cytosolic interactome, respectively.

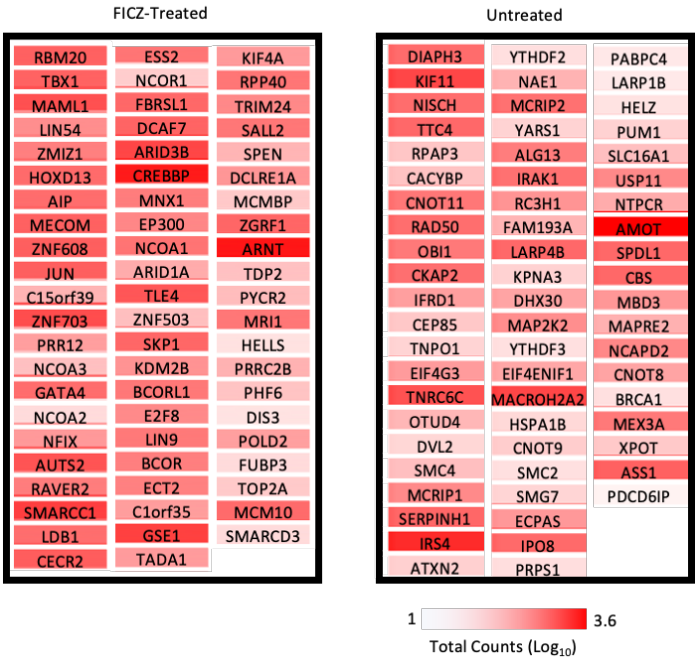

Figure 3.18 Summary of AhR-interacting proteins as assessed by BioID. A complete list of interacting proteins in each condition is found in Appendix 1 (8.1.). The hits were separated into two groups; FICZ-Treated and untreated, which reflects whether these hits were more abundant with or without FICZ 100 nM for 4-hours prior to biotin pulse. Ordered by descending fold-enrichment for the group it's in, colour coded by abundance of protein across all conditions.

I did not observe any association of the AhR with canonical IFNγ-signalling pathway components; IFNGR, JAK1/2, STAT1 in this experiment. Although this doesn't confirm there's not a direct interaction of the AhR with these proteins, it's unlikely there's a biologically-relevant direct interaction between them. There's also no evidence in the literature for a direct interaction of the AhR with components of the IFNγ-signalling pathway. I hypothesised the AhR is mediating effects on IFNγ-signalling through an indirect mechanism via a protein the AhR interacts with the cytosolic (untreated) fraction of AhR-associated proteins. Without presence of any clear candidates from within known IFNγ-signaling pathways, selection of any of these candidate genes to examine further is largely speculative. However, of cytoplasmic-interacting proteins there's IRAK1, a known modulator of NF-kB signaling via TNF which may interact with other inflammatory signaling pathways including IFNγ-signaling pathways.

3.2.9. TNF is sufficient to overcome AhR mediated suppression of IFNγ signalling

Considering limited potential candidate proteins that may interact with cytoplasmic AhR (Fig. 3.18) and having speculated IRAK1 is a protein worth further examination, I studied induction of *IDO1* in response to both IFNγ, TNF and CH223191. The rationale was that if IRAK1 interacts with cytoplasmic AhR it would be inhibited by the AhR. Consequently, antagonising the AhR by using with CH223191 would prevent activation by endogenous ligands, including kynurenine which would be produced by the expression of IDO1, and should reduce any induction of *IDO1* if the AhR is involved. If IRAK1 is being inhibited by the AhR directly interacting with it, then using TNF to increase its expression should overcome any inhibition by the AhR. I would therefore expect high TNF to produce a similar induction of *IDO1* in 501mel^{WT} to the induction of *IDO1* in 501mel *AHR*$^{-/-}$ cells in response to IFNγ, but with no difference without IFNγ. However, observation of these changes in response to these stimuli doesn't confirm this mechanism, rather suggests it's one possible explanation. IFNγ-mediated induction of *IDO1* in 501mel^{WT} cells is suppressed in response to co-treatment with AhR antagonist CH223191, 25.7-FI vs. 15.9-FI, 38% reduction in *IDO1* transcript abundance (Fig. 3.19). TNF alone doesn't stimulate *IDO1* expression (Fig. 3.19), however, co-treatment of TNF with IFNγ yields 58.3-FI of *IDO1*: 126% increase of induction compared to IFNγ-alone. CH223191 has a greatly diminished effect on *IDO1* expression in cell treated with both IFNγ and TNF than in cells treated with only IFNγ, causing 9.1% reduction in *IDO1* induction compared to 38% reduction. It's also worth noting that, in previous experiments, I showed that 501mel *AHR*$^{-/-}$ cells, treated with IFNγ, yielded 33.1-FI of *IDO1* (Fig. 3.5C). TNF treatment is sufficient to drive

elevated responses to IFNγ-signalling. This enhanced induction of *IDO1* in response to IFNγ and TNF co-treatment is like the induction observed in 501mel *AHR*$^{-/-}$ cells. This co-treatment also significantly diminishes the effects of AhR antagonism by CH223191, limiting the induction in response to endogenous ligands, including the IDO1 product Kynurenine on IFNγ-mediated induction of *IDO1*. This experiment should, however, be repeated with the inclusion of AhR agonists, to demonstrate a greater induction in response to their addition. This experiment should be performed in the 501mel *AHR*$^{-/-}$ cell line to demonstrate limited effects from adding TNF on enhanced induction of IFNγ target genes. This experiment would also be strengthened by measuring the expression of the same battery of IFNγ-response genes as examined elsewhere in this chapter to demonstrate that it affects IFNγ-signaling broadly as has been observed in the 501mel *AHR*$^{-/-}$ cell line.

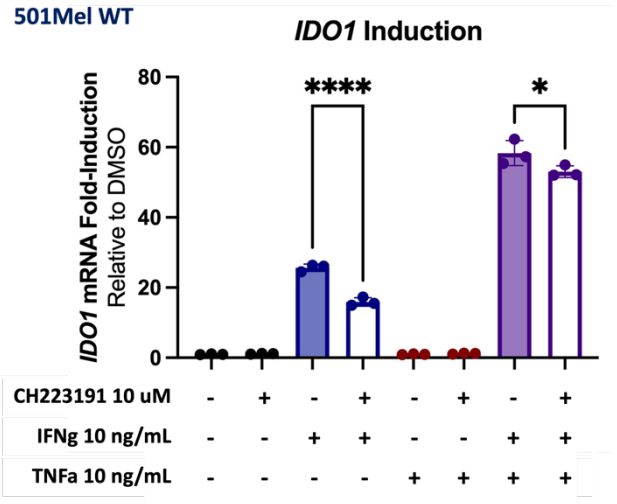

Figure 3.19 IFNγ and TNF mediated expression of *IDO1*. *IDO1* transcript abundance determined through qRT-PCR in response to 24-hour IFNγ 10 ng/mL, TNF 10 ng/mL, and CH223191 10μM treatment. Ad-hoc test: Ordinary One-way ANOVA, post-hoc test: Tukey-Kramer test for multiple comparisons which inherently corrects for multiple comparisons $P > 0.05$: ns, $P < 0.05$: *, $P < 0.01$: **, $P < 0.001$: ***, $P < 0.0001$: ****. Biological Repeats = 1, Technical Repeats = 3.

3.3. Discussion

Current understanding of the AhR's role in modulating immunosuppression in melanoma is dependent on the AhR-IDO1-Kynurenine axis (Anzai et al., 2022; Shi et al., 2019), through which the AhR directly stimulates expression of *IDO1* in melanoma cells in response to FICZ. In these cells, I did not detect changes in *IDO1* expression or other IFNγ-response genes examined in response to the physiological ligand, FICZ, the physiological pro-ligand Kynurenine, or the AhR antagonist, CH223191 (Fig. 3.3, 3.5, 3.6, & 3.8). However, IFNγ was sufficient to induce expression of *IDO1* and modulation of the AhR was a significant effector of this induction, suggesting the AhR is not directly responsible for induction of *IDO1,* rather that it affects IFNγ-mediated induction of *IDO1*. Previous studies have clearly demonstrated the centrality of the AhR in mediating immune suppression in cancer (Mengoni et al., 2020), and centre around the activity of IDO1. qRT-PCR analysis of several key IFNγ genes (Fig. 3.8) demonstrate that the AhR-effectors and AhR-status are sufficient to significantly affect induction of more than *IDO1* in response to IFNγ-treatment in 501mel cells. These cells, however, did not elicit a response in induction of *IDO1*, *CD274,* or *IRF1* in response to TCDD – the AhR agonist previously used to demonstrate AhR-dependency in induction of *IDO1* (Vogel et al., 2008). This necessitates repeating these experiments in more melanoma cell lines and primary melanoma cells, to determine whether effects observed in these 501mel cells are representative of melanoma more broadly.

Analysis of TCGA patient data from melanomas suggested a correlation between AhR activity and IFNγ-response gene expression (Fig. 3.7). However, it was not possible to conclude whether these correlations between *CYP1A1*/*CYP1B1* and IFNγ-response genes are reflective of AhR activity. While *CYP1A1* induction can be mediated by the AhR, PPARα, and TCF proteins (Schulthess et al., 2015; Sérée et al., 2004; Villard et al., 2011), and *CYP1B1* induction can be driven by the AhR, SF1, SP1, AP-2 and TCF proteins (Shehin et al., 2000; Tsuchiya et al., 2003, 2006), their expression is not significantly correlated (Fig. 3.7). Although there are significant positive correlations in patient data between *CYP1B1* expression and IFNγ-response gene expression, and some significant positive correlations between *CYP1A1* expression and some IFNγ-response genes, it is not possible to determine whether these are correlations between the AhR's activity and IFNγ-response genes or if there's another TF involved. qRT-PCR was used to examine the expression of IFNγ-response genes in response to AhR modulation and status and indicated there was an unliganded suppression of IFNγ-response gene induction by the AhR (Fig. 3.8). However, the qRT-PCR experiments in this chapter were poorly executed, lacking biological replicates, making true statistical certainty impossible to determine, and consequently it is possible the effects observed are not representative of true biological behaviour. Furthermore, an absence of results from other melanoma cell lines or primary melanocytes means it is impossible to confirm whether these effects are limited to 501mel cells or representative of melanoma cells more broadly. This is critical to understanding the value of this research in the wider context of melanoma, as the preliminary findings presented here represent a potential new understanding of how these genes are regulated. Moreover, with the 501mel cells used not responding to

TCDD whereas other melanocytes in the literature and *in vivo* models do respond, there could be cell line-specific effects (Kim et al., 2006; Vogel et al., 2008).

IFNγ-signalling in melanoma is central for immunosuppression by this cancer type. For example, STAT1-dependent signalling via the IFNGR is essential for anti-tumour responses by the host immune system (Zhou et al., 2022). IFNγ-signalling is a marker for anti-PD-1 melanoma therapy efficacy in the clinic (Cui et al., 2021), further supporting the role of IFNγ as a key mediator of tumour immune evasion in melanoma. My findings that the AhR could be a suppressor of IFNγ-signalling in its unliganded state raises the possibility of a central role in mediating tumour immune escape in melanoma. The consequence of this being that both over activation of AhR and loss of its expression may drive enhanced IFNγ-signalling and greater immune tolerance. However, without sufficient replicates in these experiments and analysis of these effects in other melanoma cell lines, it's not possible to determine whether the effects observed are melanoma- or 501mel-specific. It is necessary to perform transcriptomic analysis and genomic-binding analysis of the AhR in sufficient biological replicates of these cells to be confident of these effects in 501mel cells and to assess the extent of modulation of IFNγ-response gene regulation. Furthermore, as the experiments were performed in only a single clone of 501mel^{WT} (control gRNA) and 501mel *AHR*$^{-/-}$ cells, there is a very high risk the effects observed are not just 501mel-specific, but clone-specific, meaning that this research is potentially not representative of even the one cell type examined, let alone the cancer it's being used as a model for.

Ignoring the limitations of this research in its applicability beyond the 501mel clones and the limited statistical certainty, the implications of the proposed new model of activity for the AhR in modulating *IDO1* gene expression are potentially significant in developing novel immunotherapeutic approaches for melanoma. The introduction of anti-PD-L1 and anti-CTLA4 monoclonal antibodies into the clinic saw huge improvements in the prognosis of melanoma patients (Hodi et al., 2016, 2018; Tawbi et al., 2018; Wolchok et al., 2017). However, our current understanding of how immunosuppression is established in melanoma is that *IDO1* expression is the predominant mediator of tryptophan depletion-mediated immunosuppression in the TME. Yet, combinatorial therapies of anti-IDO1 monoclonal antibodies with anti-PD-L1 monoclonal antibodies are no more effective than anti-PD-L1 therapies alone (Jung et al., 2019). Furthermore, the specific IDO1 inhibitor Epacadostat failed to improve melanoma patient prognosis in Phase III clinical trials (Long et al., 2019). This, however, may be reflective of elevated *IDO1* expression in tumours being a component of the much broader immunosuppressive mechanism it's part of, with much higher activation of IFNγ pathways, which are immunosuppressive and pro-oncogenic (Zhou et al., 2022). Alternatively, using IDO inhibitors may not have a beneficial effect through restoring tryptophan levels as tumours are likely also deficient in other nutrients such as glucose and arginine that may also impact the activity of infiltrating immune cells. Considering these data, it might prove more efficacious to administer AhR inhibitors alongside anti-PD-L1 therapies to better suppress IFNγ-mediated immunosuppression in the TME, rather than specific inhibitors of IFNγ-response genes such as *IDO1*. The use of AhR inhibitors, however, would only be appropriate in instances of melanoma where the AhR is expressed, requiring biopsies of melanomas to determine AhRi applicability in patients.

qRT-PCR and Immunofluorescent experiments in this chapter indicating there may be a non-liganded role of AhR-mediated suppression of IFNγ-signaling. Using proximity-affinity mass spectrometry the interactors of the AhR were analysed in 501mel cells. In these analyses, there were no known components of the canonical IFNγ-signaling pathway (Fig. 3.18), meaning that I had to look to potential effectors of IFNγ-response pathways. There is a possibility that the effects being observed in the 501mel cells I used display clonogenic effects through interactions that aren't being replicated in the 501mel cells being used by the collaborator who performed these experiments. The absence of an IFNγ-response pathway interactor in these data may therefore arise through inter-clone variation. Assuming, however, these 501mel cell lines are behaving similarly, it suggests there must be a component of a non-canonical IFNγ-response pathway that the AhR is modulating. A literature review of the associating proteins of the 'cytoplasmic' fraction revealed that IRAK1 may be a candidate as a non-canonical modulator of the IFNγ-response. IRAK1 is a positive modulator of NF-κB signalling and mediates NF-κB activation via de-repression after phosphorylating and inactivating the Inhibitor of nuclear factor kappa B kinase (IκK), via Tumour necrosis factor receptor associated factor 6 (TRAF6), to release active NF-κB (Gottipati et al., 2008). Increases in NF-κB signalling predispose cells to greater responses to IFNγ, as positive mediators of IFNγ-signalling such as IRF1 are target genes of NF-κB and more highly expressed when NF-κB activity is stimulated by TNF (Hiroi & Ohmori, 2005; Ohmori et al., 1997).

My proposed mechanism through which the AhR mediates IFNγ-signalling is through direct interactions with the NF-κB signalling pathway. The AhR is antagonistic of the NF-κB pathway in response to TCDD stimulation (Tian et al., 1999). Crosstalk between the AhR and NF-κB signalling pathways has been described at the level of forming novel heterodimeric RelB-AhR TF complexes (Ishihara et al., 2019, 2021); although I provide evidence for a cytoplasmic interaction between these pathways, not a nuclear one. Stimulation of the AhR may have a synergistic effect with TNF-mediated signalling, as cytoplasmic unliganded AhR is suppressing immune-mediated induction of target genes. My evidence for this, however, is incomplete and due to limited replicates and analysis in various cell lines, it's not possible to be confident in this effect being representative of melanoma. I have only used *IDO1* gene expression in response to IFNγ, TNF, and CH223191 to demonstrate the role of the AhR in modulation of NF-κB signalling in this manner. To improve the robustness of this model, I should confirm whether the AhR is an effector of NF-κB signalling more broadly, and whether there's a marked increase in expression of NF-κB target genes without the AhR. However, the role of TNF in enhancing the induction of *IRF1* and increasing IFNγ-mediated responses in cancer has been characterised previously, remaining a likely mechanism through which the AhR is modulation IFNγ-signalling.

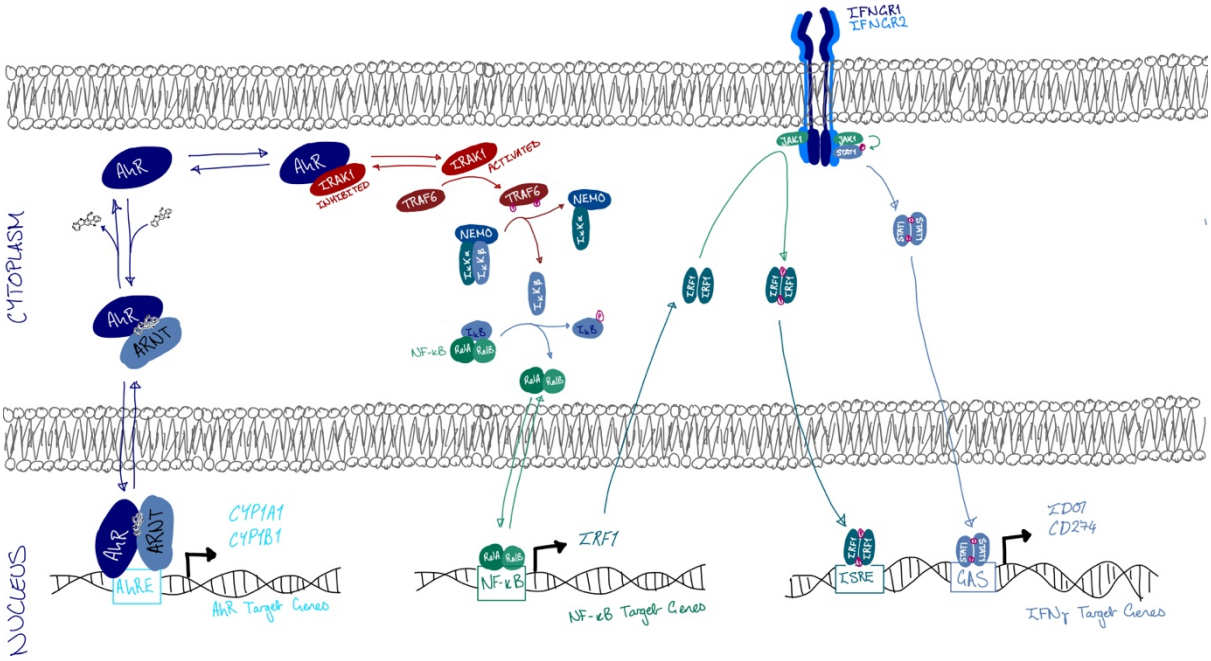

Figure 3.20 A graphical representation of my hypothesised mechanism This diagram demonstrates how modulation of the AhR could change its subcellular localisation, with agonism of the AhR driving it in to the nucleus. This removes the AhR from the cytoplasm, where it would otherwise inhibit IRAK1. This derepressed IRAK1 may then stimulate greater induction of *IRF1* via the NF-kB signaling pathway. The greater induction of *IRF1* would then allow for enhanced induction of IFNγ response genes in response to IFNγ.

Interestingly, my results indicate there may be cell-type specific mechanisms of how the AhR interacts with IFNγ-signalling. While in both 501mel cells and HaCaT cells, AhR-loss facilitates a greater induction of IFNγ-response genes, FICZ and IFNγ co-treatment produces opposing effects in either cell line. However, this may reflect as possible artefact of the HaCaT cell line as it appears to be an incomplete *AHR*$^{-/-}$ with residual AhR. While in 501mel cells I demonstrated that FICZ enhances IFNγ-mediated *IDO1* induction (Fig. 3.5), in HaCaTs, FICZ depresses this induction (Fig. 3.6). I have not explored these effects further, as I was predominantly concerned with the role of the AhR in melanoma, not in keratinocytes, it suggests a cell type specific behaviour of the AhR which may begin to reconcile how the AhR is both pro- and anti-tumorigenic in different cancer types (Liu et al., 2021; Liu et al., 2013; Tsai et al., 2017; Zhang et al., 2021). It's possible, however, these differences are clonogenic differences

rather than cell type specific differences. I have also not found other papers documenting the induction of *IDO1* in HaCaTs in response to solely physiological ligands, therefore, it is possible that these findings in HaCaTs are not representative of HaCaTs and Keratinocytes more broadly, highlighting the need for further work in a variety of keratinocyte cell lines to determine whether these effects are representative of keratinocyte biology or are cell type specific.

4. Determining the role of the AhR in the binding of other TFs to melanoma-related genomic loci

4.1. Background

Regulation of eukaryotic gene expression is highly complex, involving both general TFs to recruit RNA polymerase II to any given protein-coding gene and specific TFs, unique to given genes (Compe & Egly, 2021). Whether genes are expressed is dependent upon recruitment of both these specific and General TFs (GTFs) (Compe & Egly, 2021). Global transcription is regulated by GTFs, TFs II (TFII) B, TFIID, TFIIH, *etc.*, whereas gene-specific regulation occurs through specific TFs (Malik & Roeder, 2023). These specific TFs must contain at least two domains; a DNA-binding domain, and a transactivation/transrepression domain (S. A. Lambert et al., 2018). DNA binding domains (DBDs) are conserved regions of these proteins that form direct interactions with the nucleotides of a given sequence of DNA (Rohs et al., 2010). These interactions between the side chains of the amino acids within the protein confer specificity and affinity in tandem (Rohs et al., 2010). Any given organisation of amino acid side chains in a DBD, will favour binding to a specific DNA sequence based on the interactions the side chains can form with the exposed region of the nucleotides (typically in the major groove) (Rohs et al., 2010). The more interactions the DBD forms with a DNA sequence, the greater the affinity of the binding event and the greater the specificity of the interaction (Rohs et al., 2010). I can characterise TFs by the specific regions of DNA to which they bind, also known as motifs. Motifs can be ≥ 4 nucleotides long but are generally longer to confer greater specificity and affinity (Aptekmann et al., 2022). Presence of a given motif near a gene is not confirmation of

regulation by a given specific TF, but it does suggest the gene in question is regulated by that TF. This may be due to TF binding being dependent on the presence of another cofactor which is lacking from a given promoter (Inukai et al., 2017), chromatin architecture occluding protein binding from the motifs in the DNA (Saksouk et al., 2015), or flanking sequences of these motifs conferring specificity towards a different TF with a similar core motif (Aksan & Goding, 1998).

To determine whether a TF is potentially responsible for its regulation, one may capture direct binding of the TF to the motifs near a gene. This is possible through Chromatin immunoprecipitation-sequencing (ChIP-Seq). This technique is an unbiased approach to determine distribution of DNA-interacting proteins within a genome. In sheering DNA, purifying DNA fragments to which the protein of interest is bound, and sequencing these fragments, it's possible to assess the abundance of a protein of interest binding to specific regions within a genome by assessing the frequency that given regions are sequenced (regions of dense reads are described as peaks). From these data it's also possible to characterise motifs that are enriched amongst the sequenced regions of the genome (T. L. Bailey et al., 2015). Typically, motifs that are bound by the TF of interest are enriched centrally amongst the sequencing reads, whereas motifs of nearby TFs interacting directly or indirectly would be enriched non-centrally across reads. From these data, it's possible to establish where in a genome a TF binds and whether these binding events are likely related to any other TFs.

In the previous chapter, I investigated a novel mechanism through which the AhR regulated IFNγ-signalling in melanoma, through non-transcriptional mechanisms.

One of the key findings that supports this mechanism is that I couldn't induce *IDO1* expression, or expression of any of the IFNγ-response genes I examined, with a physiological agonist of the AhR: FICZ. Examination of the *IDO1* promoter revealed there were no AhREs to which activated AhR: ARNT dimers would likely bind to induce expression of these genes. However, the AhR can form non-canonical heterodimeric TF complexes such as the RelB:AhR dimer which binds to distinct motifs (RelBAHRE) (Vogel et al., 2007), it's possible there's a currently undescribed complex the AhR may form that binds to elements within the regulatory regions of *IDO1* and other IFNγ-response genes. Methods such as ChIP-seq would reveal these sites, if the anti-AhR antibody used bound to a region of the AhR not occluded by forming the transcriptionally active complex. Through use of a ChIP-seq experiment in the 501mel^{WT} cells, used in the previous chapter to establish the role of the AhR in IFNγ-signalling, I will be able to confirm whether the AhR is binding to the regulatory regions of IFNγ-response genes, and whether my previous conclusions the AhR is a non-transcriptionally active effector of these pathways remain a feasible hypothesis.

As eukaryotic gene expression regulation involves TFs binding to nearby promoters and intragenic and distal extragenic regions, the absence of a peak within the immediate bases upstream of a gene in ChIP-Seq data is not sufficient to confirm a given TF is not a potential regulator of its expression. Through long-range DNA looping, it's possible for TF up to 500 kilobases (kb) away from a transcription start site (TSS) to directly influence gene expression (van Arensbergen et al., 2014). It's important in analysis of ChIP-Seq data to search for peaks within 500 kb both upstream and downstream of a TSS, to identify whether there's likely influential TF binding occurring at a given gene.

The AhR is a protein with both pro- and anti-tumorigenic roles ascribed to it, depending on cell type (Section 1.4). One potential mechanism through which the AhR mediates its cell-type specific effects is through influencing cell-fate via LDTFs. Melanocyte cell lineage is defined through the activity of MITF, and loss of MITF activity has been shown to be a driver of late-stage melanoma invasion and metastasis (Section 1.2). A potential mechanism through which the AhR exerts melanoma-specific oncogenesis, perhaps through suppressing activity of MITF. For this to be a hypothesis worth pursuing, I would expect to see binding of both the AhR and MITF to key melanocyte-defining target genes. There's, however, the possibility that if there's a LDTF active in a cell, the open chromatin would be biased towards sites where said factor is bound, meaning there's a possibility the only genes for the AhR to bind to would be those also bound by MITF, as these genes are the only genes able to be bound. Even with this bias, it's not likely the only TF affecting chromatin state in a cell is a LDTF with the requirement to express a vast array of house-keeping genes, but it's a bias that should be considered when interpreting results from ChIP-Seq experiments.

4.2. Results

4.2.1. Endogenous AhR ChIP produces enrichment of AhR binding loci

For my ChIP experiments I wanted to compare the distribution of the AhR in response to both FICZ and IFNγ. This was to determine whether the synergistic effects I described in Chapter 2 were mediated through non-genomic events, as I had demonstrated, or if there were genomic binding events that could explain my results. Due to limited resources, I could only perform this experiment in one set of cell lines so did this in the 501mel^{WT} and 501mel *AHR*$^{-/-}$ cells as these are representative of melanoma cells – performing these experiments in HaCaT cells would've also allowed for comparison with a cell line not expressing MITF allowing for important comparisons as this could act as a negative control. For this ChIP-Seq experiment, I used an anti-AhR antibody that recognises residues near the C-terminus, far from the DBD (Cell Signalling, D5S6H), and performed the experiment in duplicate. I also used 4-hour time points as this was used for the proximity-affinity mass spectrometry experiment (Fig. 3.18) and transcript abundance from key AhR target genes is rising during this period up to 24-hours (Fig. 3.6) suggesting the AhR is actively bound to and facilitating the expression of genes at this time.

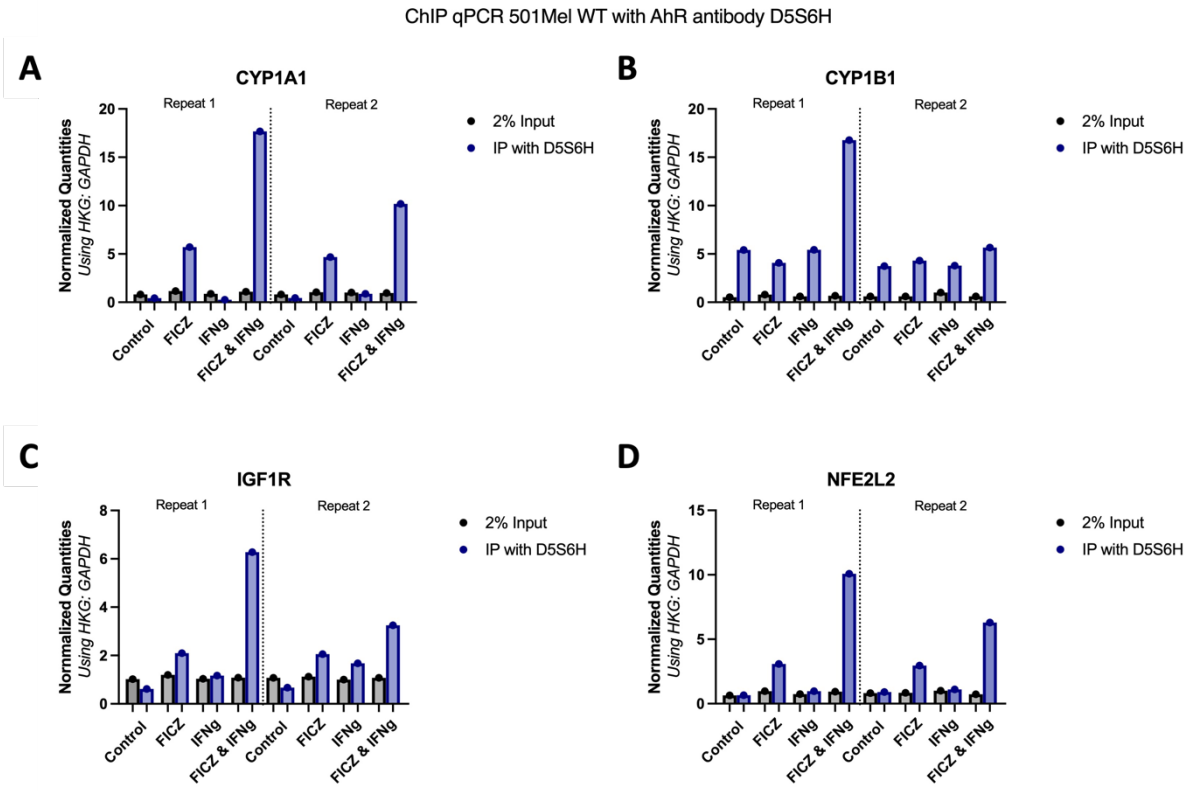

Figure 4.1. Abundance of known AhR binding loci in ChIP-collected DNA from 501mel WT cells. Abundance of target DNA sequences were determined through qPCR. Target sequences were in the promoters of (A) *CYP1A1*, (B) *CYP1B1* (C) *IGF1R*, and (D) *NFE2L2*. FICZ 100 nM, IFNγ 10 ng/mL, incubation 4-hours. Biological Repeats = 1, Technical Repeats = 3 (Each dot represents the average of the three technical repeats). Normalised quantity was performed as delta-delta Ct to determine relative amounts of starting material.

I demonstrated significant binding of the AhR to its AhRE in the promoter of *CYP1A1* in response to FICZ treatment, with ChIP-ed *CYP1A1* increasing from 0.43 – normalised quantity (NQ) without any treatment to 5.7 NQ with FICZ, which is 13.3-FI of AhR binding (Fig. 4.1A). This is to be expected as the AhR is predominantly in a transcriptionally inactive state in the cytoplasm until there's ligand binding, which is reflected in low binding of the AhR to the *CYP1A1* promoter without ligand. The binding of the AhR to the promoter of *CYP1B1* is present at low levels without stimulation with FICZ, with the 2% input fraction showing 0.52-NQ but 10.4-fold greater accumulation in the ChIP-ed fraction, 5.4-NQ (Fig. 4.1B). Interestingly, I do not see the same significant increase in AhR binding to the AhRE in *CYP1B1* in response to FICZ treatment that I observed in *CYP1A1* (Fig. 4.1A, 4.1B). However, I do observe

in both *CYP1A1* and *CYP1B1* promoter binding that co-treatment of FICZ and IFNγ results in a greater binding of AhR, *CYP1A1*: FICZ 5.7 NQ to FICZ and IFNγ 17.7 NQ, *CYP1B1*: FICZ 4.1 NQ to FICZ and IFNγ 16.8 NQ. This pattern of moderate AhRE binding in response to FICZ and an enhanced binding in response to FICZ and IFNγ is observed in other AhR target genes *IGF1R* (Fig. 4.1C) and *NFE2L2* (Fig. 4.1D) with FICZ-treated abundances of 2.1-NQ and 3.1-NQ, respectively, which rise to 6.3-NQ and 10.1-NQ in response to FICZ and IFNγ-treatment. There were insignificant increases in binding of the AhR to AhREs in these genes in response to IFNγ-alone, with IFNγ-mediated fold-inductions of 0.60, 1.0, 1.9, and 1.4 for *CYP1A1*, *CYP1B1*, *IGF1R*, and *NFE2L2*, respectively (Fig. 4.1A-D). Given the strong FICZ-mediated and FICZ and IFNγ-mediated enrichment of AhRE pulldown both compared to the input control and the control pulldown samples I'm confident that this ChIP protocol works successfully in precipitating AhR-bound DNA sequences.

Of the unstimulated cells, only *CYP1B1* shows enrichment of AhR binding. It was unexpected that any of these genes should be bound differently to any other given they contain canonical AhR binding sites. The greater binding of the AhR to *CYP1B1* compared to the other genes may be the product of induction of the AhR by endogenous ligands derived from tryptophan in the media driving nuclear import where it's more stabilised at *CYP1B1* than the other genes due to interactions with SF1 and SP1 that are known to bind to the *CYP1B1* gene. Interaction with these factors and stabilization of AhR at the promoter would enhance its induction (Tsuchiya et al., 2003, 2006).

This experiment would be improved if a negative control was used to confirm these data, such controls include performing the same process in 501mel *AHR*$^{-/-}$ cells where there should be no protein to interact with the DNA and no DNA pulldown. Use of primers for a known site the AhR should not bind to would also confirm that this pulldown is specific, providing no material is pulled down. Use of another antibody rather than the AhR antibody would also be a good negative control as it would demonstrate the enrichment of these genes is AhR-specific rather than a non-specific effect of the experimental procedure.

Across all these genes there's a greater enrichment of binding in repeat 1 compared repeat 2 (Fig. 4.1). This suggests that, due to differences in sample preparation, the first repeat has a more efficient pulldown and sample preparation process when compared to the second. As these qPCRs were performed as validation of the ChIP ahead of sequencing, I would expect to see parallel effects in the peaks identified, with greater ChIP efficiency in repeat 1 than repeat 2.

4.2.2. Characterising peak calling from AhR ChIP-Seq

To characterise the differences in binding between replicates in this experiment, I compared the mean intensity of peaks with a peak height above 10 (Fig. 4.2A). Between the replicates of DMSO-, FICZ-, and FICZ & IFNγ-treated cells, there are significant differences in the mean signal, 106 vs. 266, 180 vs. 274, and 350 vs. 300, respectively (Fig. 4.2A). There was not a significant difference in the average peak height between the IFNγ-only treated cells 247 vs. 216 (Fig. 4.2A). Given the differences between rep. 1 and rep. 2 in the pulldown efficiency (Fig. 4.1), I compared

the difference between conditions from the same replicate to determine whether there are likely robust biological differences between the binding in response to various stimuli. In the first replicate, all conditions were significantly different in their average peak height except for FICZ- and IFNγ-treated conditions (Fig. 4.2A). In the second replicate, where the efficiency was lower (Fig. 4.1), the only significant difference in the average binding intensity was between IFNγ– and FICZ & IFNγ-treated conditions.

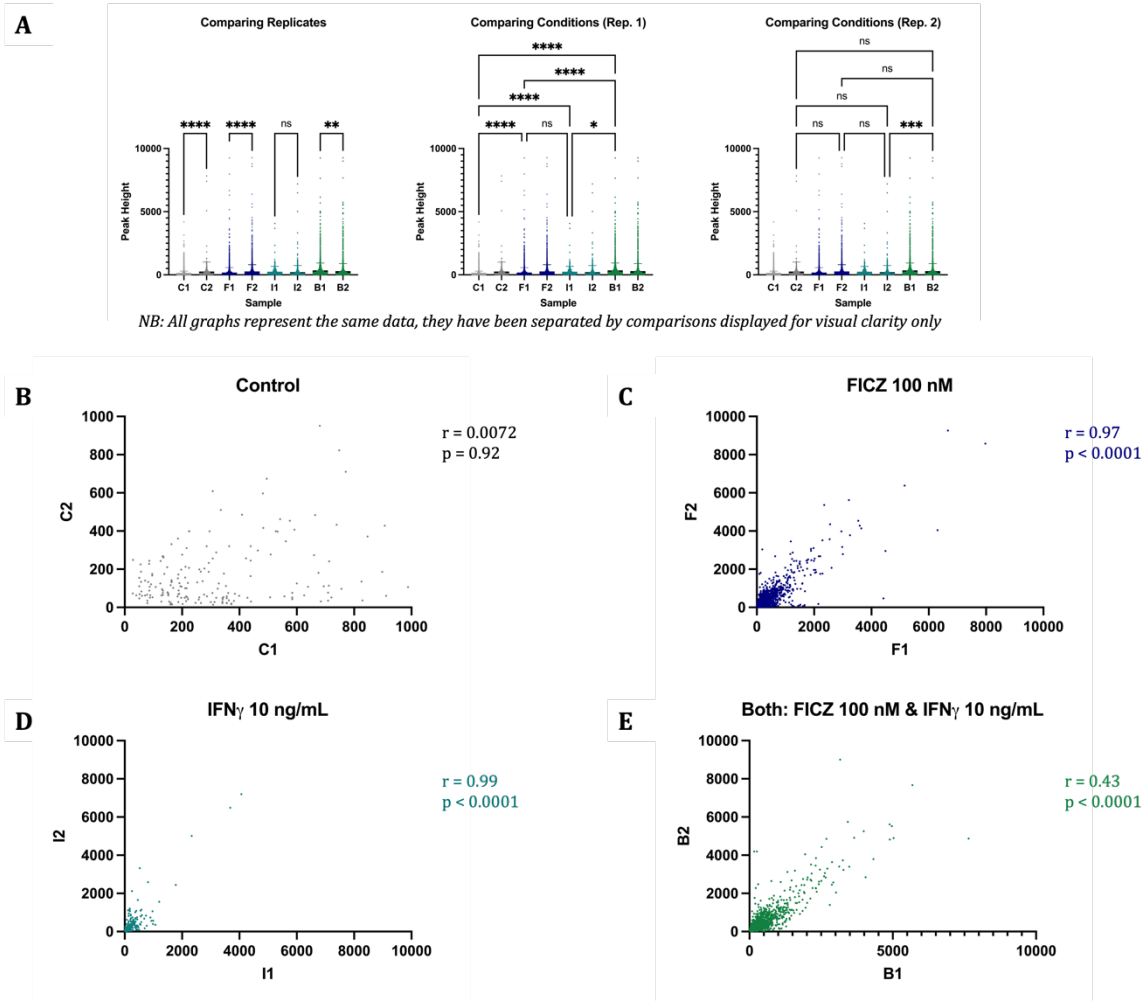

Figure 4.2. Comparison of peaks between replicates and conditions. Peaks were identified from MACS3 through comparison of the pile up in the 2% input and pile up for the IP sequences. (A) Peak intensity across all peaks in each replicate. Ad-hoc test: Ordinary One-way ANOVA, post-hoc test: Tukey-Kramer test for multiple comparisons which inherently corrects for multiple comparisons P > 0.05: ns, P < 0.05: *, P < 0.01: **, P < 0.001: ***, P < 0.0001: ****. Biological Repeats = 1, Technical Repeats = 3. Correlations analysis of the intensity of peaks that overlap in both replicates after stimulation with; (B) DMSO Control, (C) FICZ 100 nM, (D) IFNγ 10 ng/mL, and (E) Both FICZ 100 nM and IFNγ 10 ng/mL. r and p values determined by Pearson's rank correlation.

Considering these differences between the average binding intensities between the replicates, I analysed the correlation between the peak height in the peaks across both replicates of each condition. In the Control replicates, there was not a significant correlation between the two replicates, suggesting the binding observed using only endogenous agonists is not robust and the peaks found in this condition are largely

representative of noise rather than true binding, but without the pulldown in the 501mel *AHR*$^{-/-}$ cells, it's not possible to be confident of this (Fig. 4.2B). In the FICZ and IFNγ treated replicates, there are very strong positive correlations of nearly 1 (Fig. 4.2C, 4.2D), representing that although the height of the of the peaks are significantly difference, the pattern of enriched binding in both is consistent. In the FICZ & IFNγ treated cells, there's a weaker, albeit statistically significant, correlation, suggesting there are more differences between these replicates in the peak height underlying them (Fig. 4.2E).

As indicated in the ChIP-qPCR data (Fig. 4.1), at the loci tested there was little AhR binding to the DNA without an AhR agonist, which is reflected in my ChIP-seq data with only 220 peaks being present in both replicates (Fig. 4.3A). Treating cells with FICZ, however, produces an 8.9-FI in the number of peaks called in both replicates, 1950 peaks (Fig. 4.3B). IFNγ-treatment, however, did not produce a robust change in the number of peaks, with only 200 peaks being called in both replicates (Fig. 4.3C). Stimulating cells with both FICZ and IFNγ resulted in a significant increase in the number of peaks called in both replicates compared to no treatment or IFNγ only, 1630 vs. 220 or 200, respectively (Fig. 4.3D). However, co-stimulation with FICZ and IFNγ resulted in 16.4% fewer peaks called in both replicates than treatment with FICZ alone. These data demonstrate that IFNγ doesn't induce a robust change in the amount of binding of the AhR to the genome on its own, however, it does perturb FICZ-mediated binding of the AhR to the genome. Peaks are called when the difference between the 2% input pile up and the ChIP pile up differ with a q-value of $q < 0.01$, q-

values are like p-values but are adjusted to consider the False Discovery Rate and are more reliable in complex comparisons.

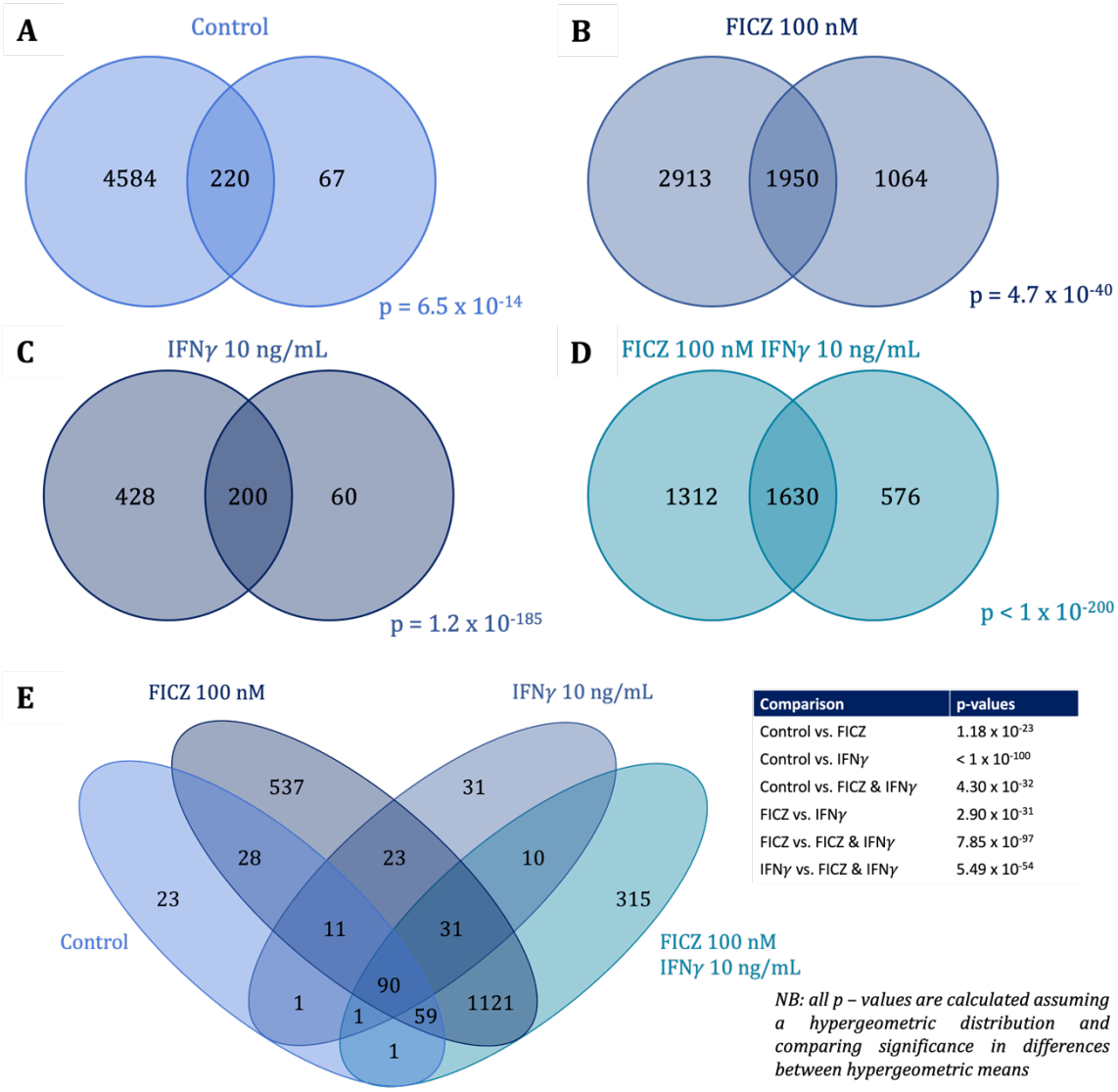

Figure 4.3. Overlap of peaks between replicates and conditions. Peaks were identified from MACS3 through comparison of the pile up in the 2% input and pile up for the IP sequences. Overlap of peaks between each replicate are shown for the (A) DMSO Control, (B) FICZ 100 nM Treated, (C) IFNγ 10 ng/mL Treated, and (D) FICZ 100 nM and IFNγ 10 ng/mL Co-treated. Using only the peaks that occur in both replicates, overlap between each treatment condition was determined and presented in (E) a Venn Diagram with accompanying p-values for whether groups overlap significantly determined by the hypergeometric mean. Comparison of the peaks of overlapping conditions by peak height can be found in Appendix 8.2.

To determine whether there's a difference between the loci bound by the AhR when 501mel cells are treated with IFNγ, I compared the overlaps of the peaks called in both replicates between conditions (Fig. 4.3E, App. 8.2.). There's a significant difference

between the peaks called in all comparisons between groups (Fig. 4.3E), showing the loci bound by the AhR in each treatment condition are distinct, despite some overlap between conditions. This suggests the AhR does bind some genes under stimulation with endogenous agonists with 23 peaks in only the control peaks, and 220 peaks in total (Fig 4.3A&E). There are also peaks bound only under stimulation with IFNγ, with 31 peaks of 200 peaks being identified in only the IFNγ treated cells (Fig. 4.3C&E). Interestingly, co-treatment with IFNγ and FICZ drives 315 unique peaks, compared to overlap between FICZ and the co-treated group which share 1121 peaks (Fig. 4.3E). These data suggest introduction of IFNγ to these cells drives distinct binding loci by the AhR beyond that of those bound in response to FICZ. However, without a true negative control in the form of a pulldown in 501mel *AHR*$^{-/-}$ cells, it's not possible to determine whether the peaks are truly dependent on the AhR. The total number of peaks called between control and IFNγ-treated samples differ by 20% (Fig. 4.3A, C), however, analysis of the overlap between these peaks reveals the composition of both groups differ significantly.

An alternative way of combining replicates in ChIP-Seq experiments involves averaging the pile up at each base across both reads to provide a single '2% input' and a single 'Pulldown' file from which to call peaks. More details on the rationale and process of this method are in Section 4.2.5. When peaks are called from these data, there are considerably more peaks called (Fig. 4.4A) across all conditions, which may be the product of less noise in the input file, with non-specific binding averaging to very low values from which smaller peaks can be called from.

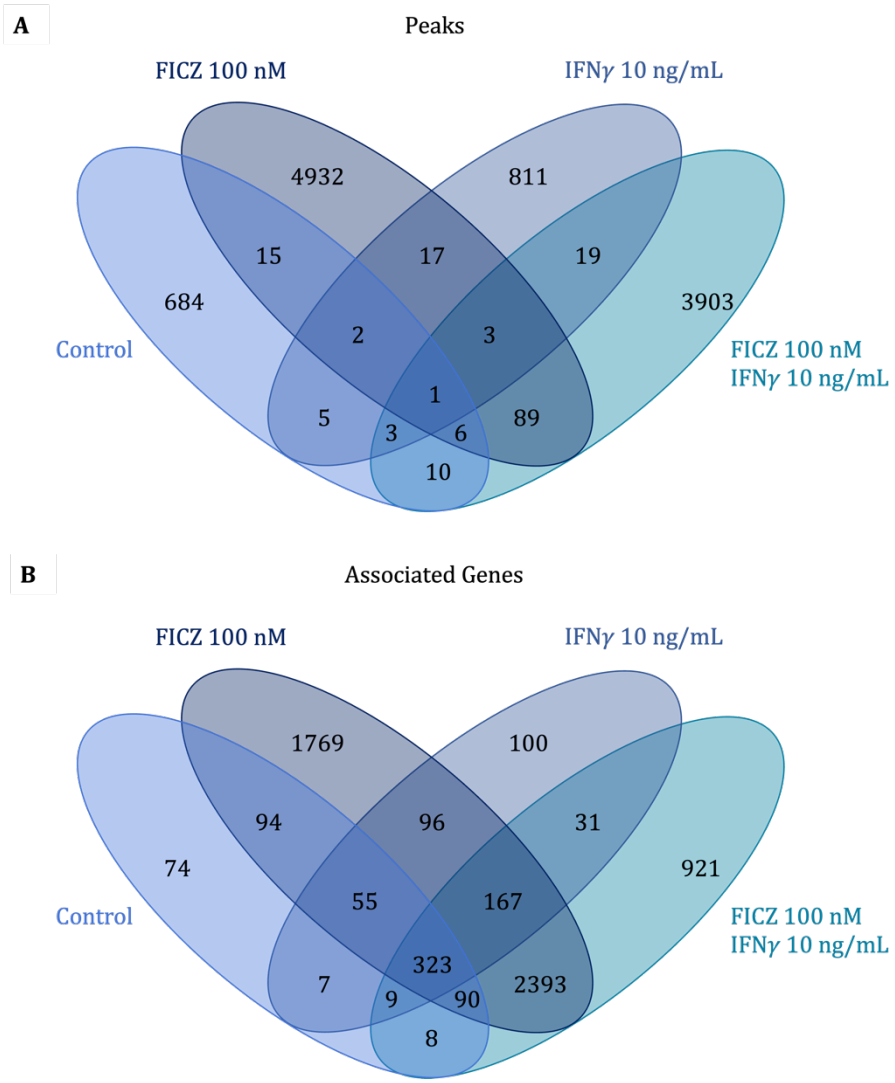

Figure 4.4. A Venn diagram describing overlap of genes bound by the AhR. Called peaks from integrated peaks (A) were annotated and overlap between genes bound (B) by the AhR after FICZ 100 nM and/or IFNγ 10 ng/mL treatment for 4-hours are described above. Statistical analysis was performed to determine if there's significant overlap between peaks called (not genes) between replicates, for all pairwise comparisons between conditions $p > 0.05$ when determined using the hypergeometric mean, meaning that overlap between conditions in (A) is not significant. Similar analysis cannot be performed for called genes in panel (B).

Peaks were associated with genes by reporting the gene closest the peak, it's not necessarily a correct annotation of the gene it influences expression of. Of 660 annotated peaks (not all peaks) from the control sample and 788 annotated peaks from the IFNγ-treated sample, only 394 peaks overlap (Fig. 4.4B). This suggests that IFNγ could be stimulating some specific genomic binding events compared to the unstimulated AhR with 60% of control sample bound genes and 50% of IFNγ-treated sample bound genes sharing identity. Of the FICZ-treated samples, 2393 genes are

found in both, comprising 60% of FICZ-treated annotated genes and 82% of FICZ and IFNγ treated annotated genes (Fig. 4.4B). These data demonstrate that only a small proportion of genes bound by the AhR are bound specifically in an IFNγ-dependent manner. With 40% of FICZ-bound genes not being bound when co-treated with IFNγ, this suggests that IFNγ-stimulation of cells where the AhR is activated could be driving a reduced AhR-transcriptional program. A potential explanation for the very distribution between the overlap of peaks These overlaps have been established through determining which genes have associated peaks, rather than where the binding event is relative to these genes. To understand whether there's a biological consequence to these binding events, it's essential to determine where the AhR is binding relative to these bound genes identified in the ChIP-Seq, and how this differs between experimental conditions.

4.2.3. Distribution of AhR ChIP peaks

To determine the likely biological consequences of FICZ and/or IFNγ-treatment-mediated changes to AhR binding, I characterised the locations of the peaks relative to genomic features. FICZ treatment produces a very similar distribution of peaks relative to transcription start sites (TSS) as the distribution of peaks observed without treatment (Fig. 4.5A). This demonstrates the AhR is likely binding in a similar manner in both conditions which agrees with 85.1% of the control condition peaks overlapping with FICZ-treated peaks (Fig. 4.4). The much greater number of peaks in FICZ-treated samples compared to control, however, indicates the major difference between the AhR's binding under FICZ-treatment is much greater binding to the genome rather than a change in the specificity of the genes bound by the AhR (Fig. 4.3,

4.4). This binding observed in the FICZ-treated sample is characterised by approximately half of the peaks being located within 1 kb of the TSS. The most notable difference between no treatment and FICZ treatment is greater binding of the FICZ-stimulated AhR to regions 5-10 kb from the TSS compared to unstimulated AhR (Fig. 4.5A).

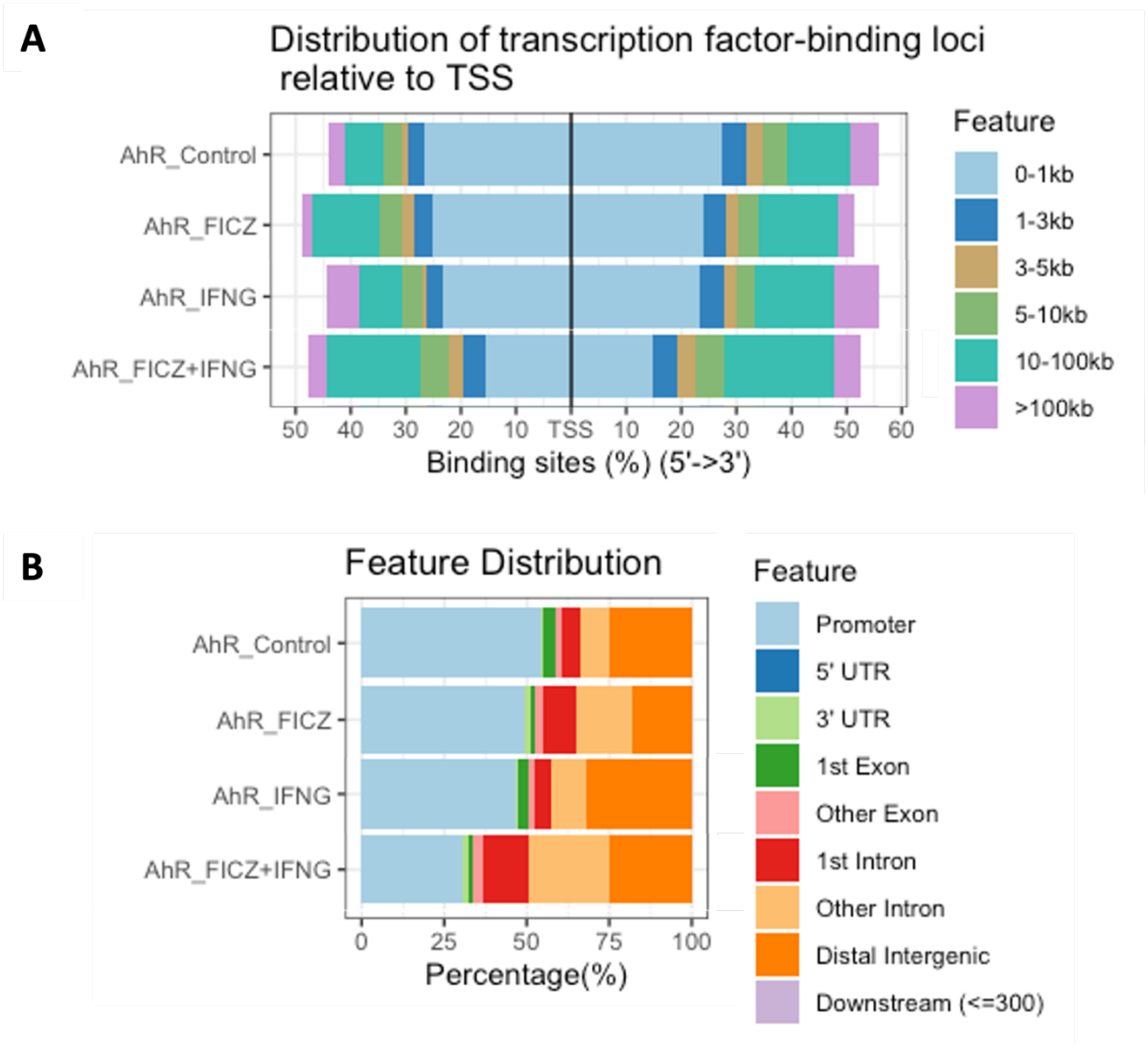

Figure 4.5. Distribution of AhR peaks relative to genomic features. Bar charts representing the distribution of (A) AhR peaks relative to transcription start sites and (B) AhR peaks in various annotated genomic regions. 501mel cells treated for 4-hours with FICZ 100 nM and IFNγ 10 ng/mL.

The distribution of the AhR under IFNγ-mediated stimulation is like that of both unstimulated and FICZ-stimulated AhR relative to the TSS (Fig. 4.5A). Which is

reflective of 81.3% of IFNγ-treated AhR peaks overlap with FICZ-treated AhR peaks (Fig. 4.4). There's a greater proportion of peaks in the IFNγ-treated samples than in the FICZ-treated or unstimulated located in very distal regions (>100 kb), the function of which is uncertain, however, there's evidence of enhancers within topologically associated domains (TADs) being more than 100 kb from the promoter (van Arensbergen et al., 2014).

Co-treatment of IFNγ with FICZ produces a distinct distribution of binding events relative to the TSS, with proportionally fewer peaks within 1 kb of the TSS than treatment with either individually (Fig. 4.5A). Treatment with FICZ or IFNγ results in approximately 50% of peaks being located within ± 1kb of the TSS, but approximately 30% of peaks being within ±1 kb after stimulation with both FICZ and IFNγ (Fig. 4.5A). This is associated with concomitant increases of the number of peaks within the ± 5-10 kb from 25% in FICZ only to 35% in FICZ and IFNγ-treatment. These peaks in the ± 5-10 kb region are unevenly distributed across upstream and downstream, with 20% of total peaks being located + 5-10 kb from the TSS compared to 15% being located – 5-10 kb from the TSS. This distinct binding profile is reflected in 23.4% of peaks in the co-stimulated samples being unique to this treatment.

The distribution of AhR binding across genomic features parallels the distribution of peaks relative to the TSS. The unstimulated sample shows > 50% of peaks being located within the promoters (≤ 3kb upstream of the TSS) of genes (Fig. 4.5B). There is a similar distribution of AhR peaks across genomic features in response to FICZ treatment as in the untreated sample, with approximately 50% of peaks being within the promoter regions of genes (Fig. 4.5B). There's, however, a greater proportion of

binding events in introns which aren't the first intron in the FICZ-treated samples, approximately 17%, compared to 10% in control samples (Fig. 4.5B) which is coupled to a change in the proportion of distal intergenic peaks.

IFNγ-treatment slightly depresses promoter region binding to 45% compared to 55% in control samples (Fig. 4.5B). The most significant change is in, proportionally, much greater distal intergenic binding in response to IFNγ-treatment than in response to FICZ treatment, 30% compared to 20%. The consequence of this is unknown as distal binding events may be regulatory but requires large scale chromatin organisation to facilitate bringing these distal elements in proximity of the promoter of the gene.

Binding of the AhR in response to FICZ and IFNγ together, again produces a distinct distribution profile across genomic features. Compared to no treatment and FICZ and IFNγ individually, co-stimulation depressed promoter binding to 30% compared to 50% ± 5% (Fig. 4.5B). This is coupled to an increase in binding of the AhR to introns (1st and other) compared to all other conditions with 37.5% of all peaks being in introns of genes when co-treated, compared to 27% of peaks in FICZ-treated, 20% in IFNγ treated, and 17% in untreated (Fig. 4.5B). Without statistical analyses of the differences, it's not possible to be confident whether differences in distribution are significant making this a purely qualitative assessment.

4.2.4. Binding of the AhR to canonical targets

Visualisation of input and ChIP-seq tracks from both replicates for each condition demonstrates enrichment of AhR binding at canonical target genes after undergoing

ChIP. Dynamics of AhR binding in response to FICZ stimulation is well demonstrated by the accumulation of sequencing reads at the *CYP1A1* gene. Without any stimulants, the AhR is not enriched at the *CYP1A1* gene with no peaks in either the 2% input fraction or the ChIP fraction in either replicate (Fig. 4.6A). FICZ treated cells demonstrate enrichment of AhR binding with the presence of a peak with height 354 Rep. 1 and 231 Rep. 2 in the ChIP samples and no peaks in the input samples (Fig. 4.6A). This highlights the potency of FICZ as an AhR agonist, with significant accumulation at the *CYP1A1* promoter only after both treatment with FICZ and ChIP for AhR. There's no accumulation of the AhR at the *CYP1A1* promoter in response to IFNγ-treatment, which reflects the observed gene induction in response to treating 501mel^{WT} cells with FICZ and IFNγ as assessed by qRT PCR with significant *CYP1A1* mRNA induction being FICZ-dependent and IFNγ-independent in 501mel^{WT} cells (Fig. 3.3A). Furthermore, I see enhanced binding of the AhR to the *CYP1A1* promoter in response to both FICZ and IFNγ-treatment compared to FICZ only treatment, 421 vs. 354 (Rep. 1) and 281 vs 231 (Rep. 2) (Fig. 4.6A). This too is reflective of the induction of *CYP1A1* expression in the same cells under the same conditions, with 46.7-FI of *CYP1A1* in response to treatment with IFNγ and FICZ compared to 28.7-FI in response to FICZ alone. The double peak observed here is likely the result of some looping or folding of the DNA, as there are two XRE motifs in this region (chr15:74726419 and chr15:74726506), but both are found under the most upstream peak raising the possibility that the downstream peak is produced by interactions with the AhR bound to the upstream peak.

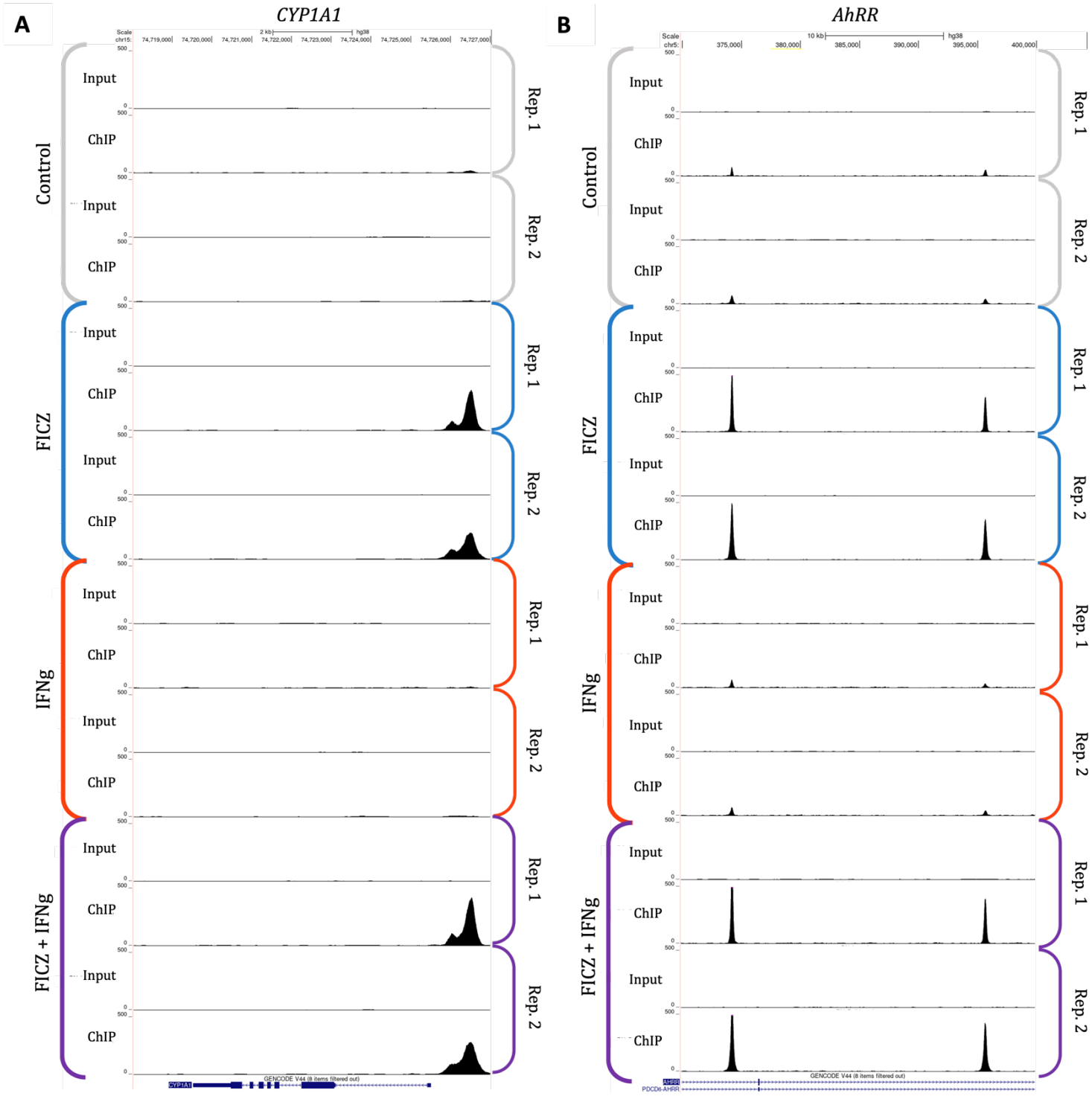

Figure 4.6. Visualisation of AhR ChIP Peaks. UCSC Genome Browser generated visuals of sequencing tracks from the 2% input and ChIP fractions for each replicate of each condition for (A) *CYP1A1* and (B) *AhRR* after 4-hours treatment with FICZ 100 nM and/or IFNγ 10 ng/mL.

AhR binding to the *AHRR* gene demonstrates the same pattern of AhR accumulation in response to FICZ and IFNγ. Focussing on the most upstream of the two peaks: under all conditions there's no enrichment of sequencing reads in the input fractions with

enrichment in the ChIP fractions demonstrating AhR specific binding at this locus (Fig. 4.6B). In the untreated control samples, there's a slight enrichment of AhR binding with peak heights 80 (Rep. 1) and 78 (Rep. 2), however there's much greater enrichment in response to FICZ treatment with peak heights of 570.5 (Rep. 1) and 523.5 (Rep. 2) (Fig. 4.6B). For examination of binding to the *AHRR* gene, I will focus on the upstream peak. There's similar binding of the AhR to the *AHRR* gene in response to IFNγ as in the control sample with peak heights of 73 (Rep. 1, IFNγ) and 75 (Rep. 2, IFNγ) compared to 80 (Rep. 1, Control) and 78 (Rep. 2, Control) (Fig. 4.6B). Further confirming the limited induction of the AhR transcriptional activity in response to IFNγ alone. There's also enhanced binding of the AhR to the *AHRR* gene in response to FICZ and IFNγ compared to FICZ alone, with peak heights of 763 (Rep. 1, FICZ & IFNγ) and 643 (Rep. 2, FICZ & IFNγ) compared to 570.5 (Rep. 1, FICZ) and 523.5 (Rep. 2, FICZ) (Fig. 4.6B). The two distinct peaks observed in the *AHRR* gene overlap with distinct XRE motifs (chr5:373950 and chr5:399964), suggesting that AhR:ARNT can bind to both sites, rather than binding directly to one and looping to interact with the other.

Given the difference between conditions and the difference between replicates regarding mean peak height is significantly different (Fig. 4.2), I performed correlation analysis of the peaks bound in both the FICZ and FICZ & IFNγ treated samples to determine if they correlate more between conditions or between replicates to determine whether the differences (Fig. 4.6) are reflective of differences in treatment or experimental variation. The correlation between FICZ treated samples has an r-value of 0.97, and in the co-treated sample r = 0.43, but the correlation between the two conditions gives r = 0.64 (Fig. 4.7). This reveals the

difference between conditions is greater than the difference between FICZ-treated replicates but not co-treated replicates.

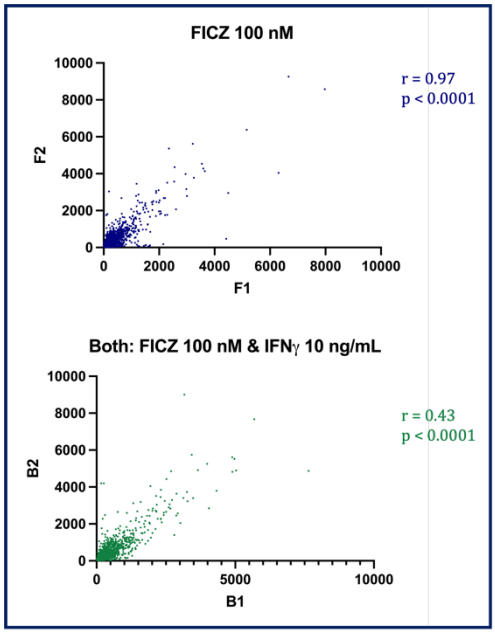

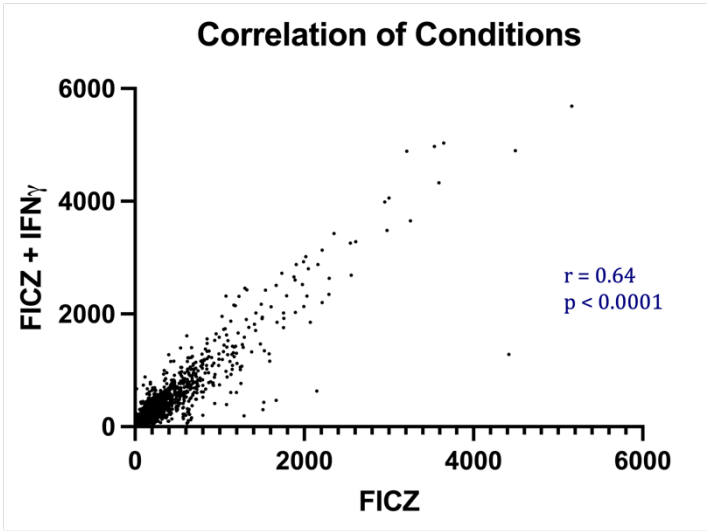

These data have been presented previously in Fig. 4.2.

Figure 4.7. Correlations within and between replicates . Pearson's rank correlation analysis between the FICZ 100 nM and FICZ 100 nM & IFNγ 10 ng/mL 24-hours treated samples, comparing peak height at the peaks that overlap in both replicates of both conditions.

4.2.5. Simplifying UCSC data

To make analysis of the UCSC track data simpler, I instead chose to represent the data as a FE of read depth of the ChIP sample over the input sample. Using the peak calling files (MACS3) where both 2% input replicates were combined to produce a single 2% input sequencing read for each condition and similarly both replicates of the ChIP reads were combined to give a single ChIP sequencing read. Comparison of both sets of tracks reveals the information presented in the simplified version is a faithful representation of the information contained in the more detailed version. In the

CYP1A1 control samples I see no accumulation of reads in either the 2% input fractions or ChIP Seq fractions (Fig. 4.8A) which is reflected in no accumulation of reads in the Control track in the combined representation (Fig. 4.8B). In the FICZ treated 2% input tracks I see no accumulation of reads and in the ChIP Seq tracks there's a peak of height 354 (Rep. 1, FICZ) and 231 (Rep. 2, FICZ) (Fig. 4.8A), which is

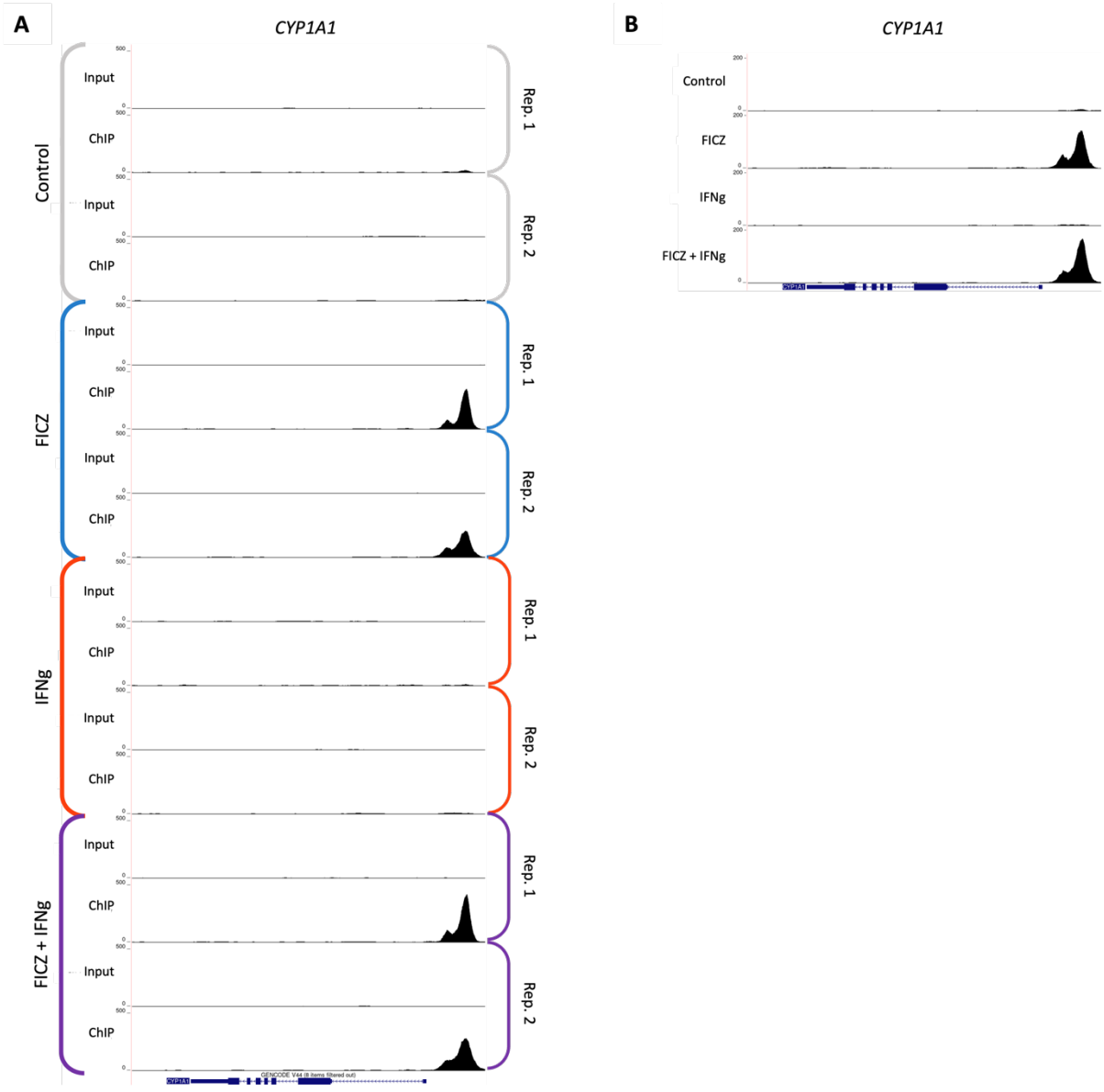

Figure 4.8. Visualisation of AhR ChIP Peaks. UCSC Genome Browser generated visuals of sequencing tracks for the *CYP1A1* associated peak represented as (A) 2% input and ChIP Tracks for each replicate for each condition and (B) Fold enrichment for ChIP Sample binding over 2% input co-processing each replicate to generate a single 2% input pile up and a single ChIP pile up for each condition. Treatment with FICZ 100 nM and IFNγ 10 ng/mL for 4-hours.

summarised in the simplified track data as a peak with height 131.7-FE (Fig. 4.8B). While there's a depression in the peak height in the simplified representation due to the 2% input read depth being, on average, between 1 and 2 reads there's no loss of information as far as the visualisation of the peak is concerned with the pattern of accumulation being equivalent in both the detailed (Fig. 4.8A) and simplified representations (Fig. 4.8B). This simplified model demonstrates the enhanced accumulation of AhR in response to IFNγ and FICZ co-treatment in comparison to FICZ-only. While the individual tracks show a peak of 763 (Rep. 1, FICZ & IFNγ) and 643 (Rep. 2, FICZ & IFNγ) compared to 570.5 (Rep. 1, FICZ) and 523.5 (Rep. 2, FICZ) (Fig. 4.8A) the simplified representation shows 154.5-FE compared to 131.7-FE for the same information (Fig. 4.8B). This corresponds to an average enhanced binding in the individual replicates of 1.29-fold (Fig. 4.8A) and an enhancement of 1.17-fold in the simplified peaks (Fig. 4.8B), the value from the simplified model is lower, however, it does account for non-specific changes in input read pile up so is a more reliable reflection of the AhR binding than comparison of raw pileup, the biological significance of which is highlighted in the statistically significant difference in *CYP1A1* induction (Fig. 3.5).

4.2.6. The AhR doesn't bind to IFNγ-response genes enriched in *AHR*$^{-/-}$ cells

In the previous chapter, I described a novel role of the AhR in mediating IFNγ-signalling which involved non-genomic activities of the AhR. I demonstrated that cytoplasmic AhR was an inhibitor of STAT1 activation and claimed the effect of the AhR on IFNγ-signalling wouldn't involve binding of the AhR to the IFNγ-response

genes I observed to be highly affected by AhR-loss. I did not, however, provide direct evidence for the absence of AhR binding to these genes. From these ChIP-Seq data I have demonstrated there's insignificant accumulation of the AhR at key IFNγ target genes. I demonstrated IFNγ-mediated induction of *IDO1*, *ATF4*, PDL1 (*CD274*), PKR (*EIF2AK2*), and *IRF1* was significantly higher in 501mel *AHR*$^{-/-}$ than in 501mel^{WT} cells (Fig. 3.5C-G). Using my ChIP-seq data, I examined loci of these genes for AhR binding. I found a very small peak in the 7th intron of the *IDO1* gene with a peak height of 9.49-FE in the untreated sample and up to 14.2-FE in the FICZ treated sample (Fig. 4.9A). Under IFNγ-stimulation, the peak height is 10.4-FE and with FICZ co-treatment 10.5-FE (Fig. 4.9A). While this is direct evidence of AhR interaction with the *IDO1* gene, the sequence of DNA under the peak identified is 5' – GTGGTTTTAAGTCCCGAAAAAAAAAAAATA - 3', which doesn't contain an AhRE, and the peak height is relatively low in comparison to the binding I observe at canonical AhR genes with significant AhR-mediated induction. Equally, there's insignificant change in the binding of the AhR to *IDO1* in response to IFNγ or IFNγ and FICZ compared to the control sample which doesn't align with the AhR-mediated modulation of IFNγ-response gene induction where co-treatment of IFNγ and FICZ produces a much greater induction of *IDO1* expression in comparison to no stimulation or IFNγ-only. Together, it's unlikely that this small peak in *IDO1* is a significant binding site of the AhR with which could explain the changes in *IDO1* expression that I have observed in the previous chapter.

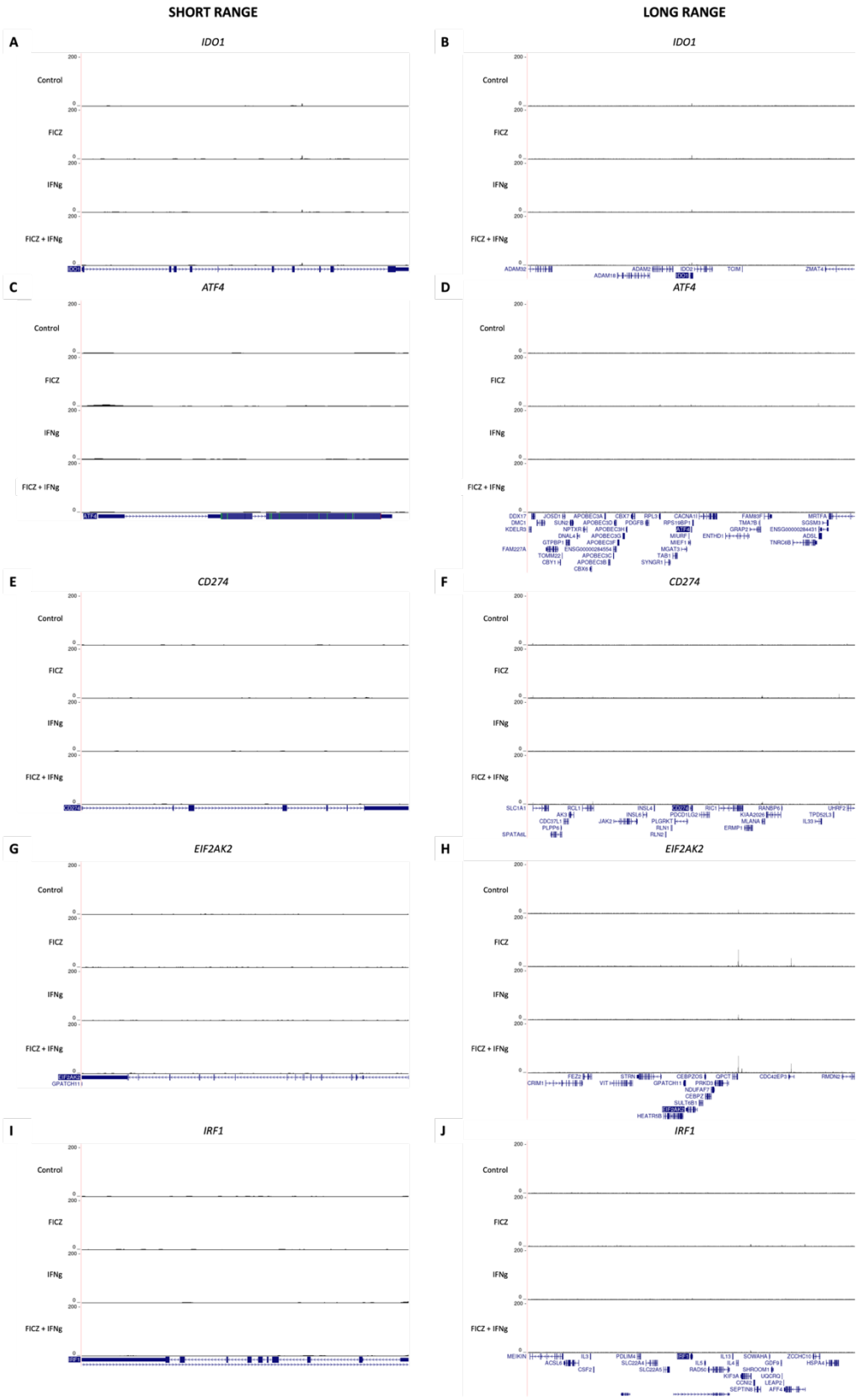

Figure 4.9. ChIP Seq track visualisation at IFNγ response genes. UCSC Genome Browser generated visuals of sequencing tracks for (A, B) *IDO1*, (C, D) *ATF4*, (E,F) *CD274*, (G,H) *EIF2AK2*, (I,J) *IRF1*. Left-hand side panels are of only the respective gene and right-hand side panel are of ± 700 kb – 1.05 Mb regions flanking the gene. FICZ 100 nM, IFNγ 10 ng/mL, 4-hours treatment.

Interactions between enhancers and promoters are typically within 500 kb with the

average distance being 125 kb, with chromatin looping generating topologically associated domains where there may be up to 1 Mb of DNA looped together, it's not sufficient to simply look at genes themselves for binding events that may be regulatory (van Arensbergen et al., 2014). I looked at large surrounding regions of each gene between ±700 kb - ±1.05 Mb for any substantial peaks in my ChIP-seq data that could be influencing gene expression. There are no substantial AhR binding events within ± 700 kb of the *IDO1* gene (Fig. 4.9B).

ATF4 gene expression was enhanced in the 501mel *AHR*$^{-/-}$ cells treated with IFNγ compared to 501mel^{WT} treated with IFNγ, yet there are no peaks within the *ATF4* gene (Fig. 4.9C) or within ±1.05 Mb (Fig. 4.9D). PD-L1, a protein involved in mediated immunosuppression in melanoma whose expression is modulated by the AhR shows no AhR binding to its gene, *CD274* (Fig. 4.9E), or within ±1.0 Mb (Fig. 4.9F). PKR is the product of the *EIF2AK2* gene, a gene without AhR binding to it (Fig. 4.9G). There's a peak of AhR binding 222 kb upstream of the *EIF2AK2* promoter which (Fig. 4.9H), with an average peak height of 17.3-FE without FICZ and 64.8-FE with FICZ, with insignificant dependence on IFNγ-treatment. While this is a substantial peak, it lies directly downstream of *Glutaminyl-peptide cyclotransferase* (*QPCT*) a gene whose expression is directly mediated by the AhR (Appendix 2, 8.2.) and doesn't display an IFNγ-associated change in binding. It's also significantly above the average distance for a promoter-enhancer interaction. There's no binding of the AhR to *IRF1* (Fig. 4.9I) or within ±700 kb of *IRF1* (Fig. 4.9J). The absence of significant AhR binding to any of these genes or binding that would likely regulate within the average distance of a long-range enhancer suggests the role of the AhR in mediating IFNγ-signalling is not modulated at the point of genomic binding. This supports the model proposed at the

end of the Chapter 2, wherein the AhR is a cytoplasmic suppressor of IFNγ-signalling in these 501mel cells.

It would be a valuable addition to these data to have ChIP-Seq data for STAT1- and/or IRF1 in 501mel AhR WT/ *AHR*$^{-/-}$ cell lines. Analysis of changing intensity of these factors or changing bound loci in response to perturbations in AhR status, would enable analysis of whether the AhR sufficient to drive significant changes in the binding of IFNγ-response-mediating TFs, as proposed in this thesis. No experiments with publicly available data in 501mel cells that have analysed the binding of STAT1 or IRF1 binding has been performed to allow for direct comparison and should be performed as further work to this thesis.

4.2.7. Enrichment Analysis

Given the AhR has a cell type specific role in modulating oncogenesis (Section 1.4.), I performed Gene Ontology (GO) analysis on the gene lists produced from each set of stimuli in the ChIP-seq experiment. I determined which biological processes were enriched using GO analysis, as this would elucidate likely biological effects the AhR modulates in response to FICZ and IFNγ.

In the DMSO-treated samples, where I had 220 peaks called in both replicates there were no significantly enriched gene sets. This may be the product of biological factors, *i.e.* there's no enrichment of pathways amongst these genes because there's no enrichment in these cells, or that, without sufficient negative controls, there are false-positive peaks being called which are masking any enrichment of pathways. Without

sufficient negative controls and repetition in other melanoma cells / cell lines, it's not possible to conclude there truly is an absence of enrichment in DMSO treated melanoma cells. In the IFNγ-treated peaks, the only significantly enriched pathway was positive regulation of cyclic-nucleotide phosphodiesterase activity, albeit only due to having 3 associated genes in the gene set (Fig. 4.10). Across the FICZ treated samples ±IFNγ there were many statistically enriched pathways detailed in Supp. 9.1. in their entirety. I focussed on pathways that are likely reflective of AhR- and melanoma-relevant processes; EMT, differentiation, cell-cycle, metabolism, and pigmentation (Fig. 4.10). I summarised the enrichment scores of pathways that were significantly enriched in both FICZ ± IFNγ genes nearest called peaks in both replicates and plotted their fold-enrichment (Fig. 4.10). From the plot of these data, the trend is close to a y=x line, with enrichment of pathways in FICZ + IFNγ trending slightly lower than that of FICZ-only, with no pathways over 10 FE having a greater enrichment in the co-treated gene set (Fig. 4.10). With fewer peaks and subsequent fewer genes from which to analyse, it's possible the difference in FE is an artefact of enrichment analysis being susceptible to small changes in number of genes in a pathway producing large changes in fold-enrichment, it could also be reflective of IFNγ driving a reduced number of AhR binding events across the genome, but without adequate negative controls it's not possible to be certain of the reason for the changes in fold-enrichment.

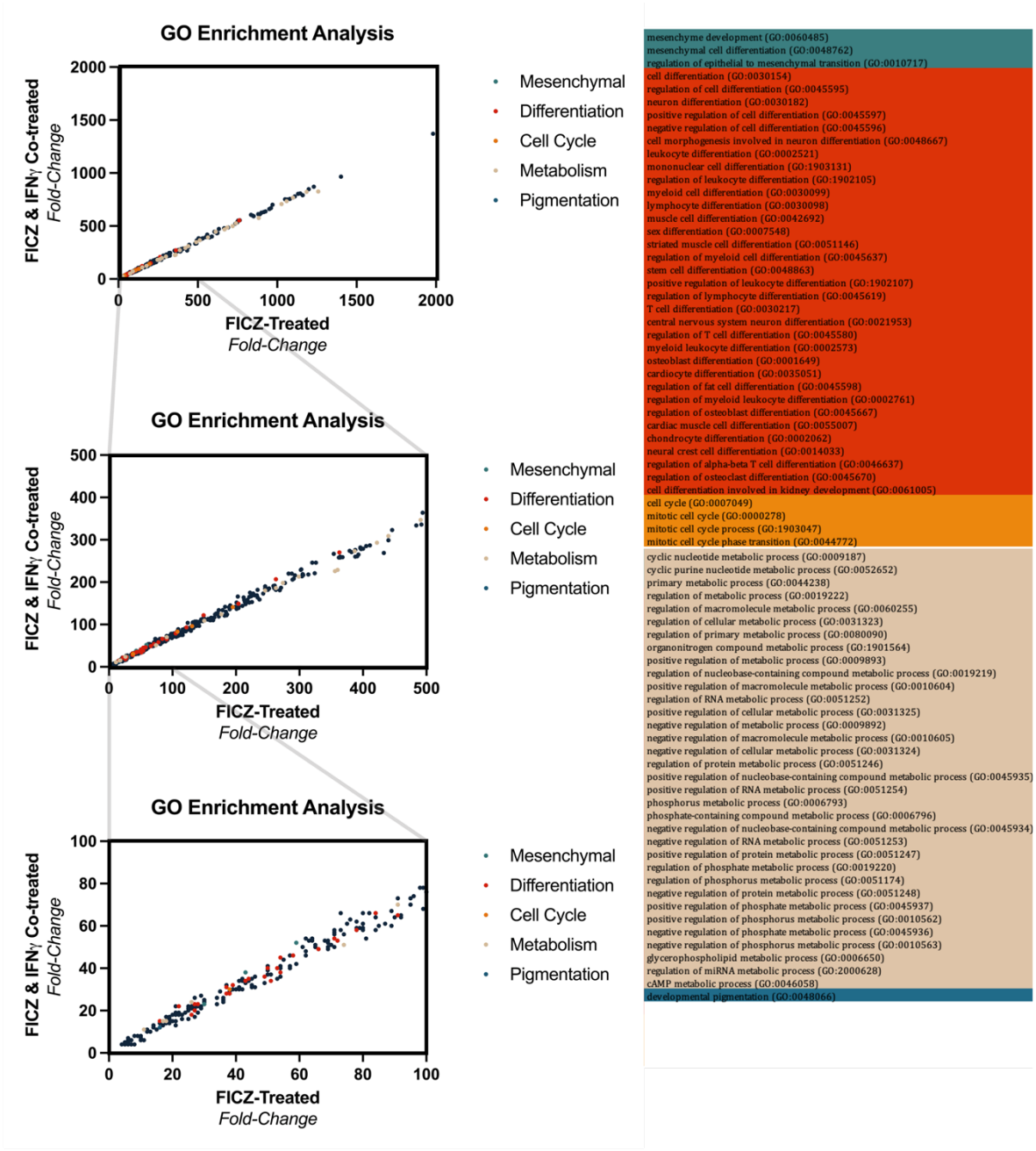

Figure 4.10. GO Enrichment of biological processes of AhR bound genes. GO Enrichment analysis of biological processes showing enrichments where FDR $p < 0.05$ only. using gene list generated from the nearest gene to peaks in both replicates AhR ChIP-seq from 501mel WT cells under FICZ 100 nM and FICZ 100 nM and IFNγ 10 ng/mL for four-hours. There were no significantly enriched pathways in the Control list and only GO:0051343 in the IFNγ 10 ng/mL treatment list. Complete lists in Supp. 9.1.

In 501mel cell treated with FICZ ± IFNγ, there's enrichment of peaks near genes that are associated with pathways associated with mesenchymal cell fate and the EMT (Fig. 4.10). These pathways are enriched to similar extents independent of IFNγ, with

GO:0060485 59 FE vs. 52 FE, GO:0048762 43 FE vs. 38 FE, and GO:0010717 30 FE vs. 23 FE in FICZ and Co-treated cells, respectively. With the EMT being a phenotypic transition associated with dedifferentiation, I examined enrichment of pathways associated with differentiation (Fig. 4.10). Many of the pathways enriched are specific to cell types that aren't melanocytic, except for 'Neural Crest Cell Differentiation', which is 27 FE vs. 23 FE in FICZ/+ IFNγ (Fig. 4.8). There are also general pathways relating to differentiation; 'Cell Differentiation' (762 FE vs. 552 FE), 'Regulation of Cell Differentiation' (363 FE vs. 270 FE), 'Positive Regulation of Cell Differentiation' (204 FE vs. 149 FE), and 'Negative Regulation of Cell Differentiation' (149 FE vs. 122 FE), in FICZ/+ IFNγ, respectively. Without transcriptomic data or adequate negative controls for this experiment, it's not possible to be certain of any biological consequences of these enrichments, however, it allows for speculation on the role of the AhR in mediating differentiation with these pathways being very highly enriched amongst the genes nearest peaks found in 501mel FICZ-stimulated cells.

As the AhR is oncogenic in melanoma (Section 1.5), I also examined cell-cycle-related GO pathways (Fig. 4.10), 5 of which are enriched in these gene sets. The 'Cell-cycle' pathways is 195 FE vs. 141 FE, and the 'Mitotic Cell-cycle' is 131 FE vs. 96 FE in FICZ/+ IFNγ, respectively. The robust enrichment of both cell-cycle-associated and differentiation-associated pathways suggests the possibility the AhR is driving oncogenic phenotypes at the transcriptomic-level in 501mel cells.

Given the AhR is responsible for the induction of metabolising proteins in response to dioxins *etc.,* I also examined pathways associated with metabolism as a positive control, expecting high enrichment of these pathways in response to FICZ-

stimulation, reflective of broad induction of metabolising enzymes. Focussing on broad pathways; 'primary metabolic process' (1258 FE vs. 826 FE), 'Regulation of cellular metabolic process' (1059 FE vs. 734 FE), 'positive regulation of metabolic process' (740 FE vs. 525 FE), in FICZ/+ IFNγ, respectively.

I also searched for pathways associated with 'melanocytes'/'pigmentation', and only 'developmental pigmentation' was enriched in both conditions, to 16 FE vs. 12 FE in FICZ/+ IFNγ, respectively. This limited enrichment may be a consequence of the AhR binding to and expression pigmentation-associated genes, which are generally hallmarks of melanocyte cell-fate, and influencing melanocyte cell fate, however this cannot be concluded from these data. MITF is a LDTF, it's possible that a large proportion of all accessible chromatin is bound by MITF and most genes the AhR could bind to will be bound by the MITF. Thus, the enrichment of these pathways being enriched for pathways associated with MITF could be a product of majority of available genes being MITF-driven, especially those involved in melanocyte cell fate phenotypes. An *AHR*$^{-/-}$ pulldown would help confirm whether there's enrichment of MITF associated genes in general or whether this is AhR-specific. The 501mel cell line is a melanocytic SKCM-derived cell line and is phenotypically like healthy melanocytes, further supporting the potential for the enrichment of these pathways being enriched in these cells and in this dataset due to these genes being biased in the open chromatin.

4.2.8. The AhR is associated with dedifferentiated melanoma phenotypes

Tsoi et. al. 2018 performed bulk RNA sequencing of 54 melanoma cell lines across a variety of phenotypic states grouped into 4 categories from differentiated 'melanocytic' through 'transitory', 'neural crest like', to 'undifferentiated' (Tsoi et al., 2018). Their work confirmed that MITF expression is high in the more differentiated 'melanocytic' and 'transitory' cell lines and low in the more dedifferentiated 'neural crest like' and 'undifferentiated' cell lines. I hypothesised that if the AhR is causally involved in melanoma de/differentiation then I should observe a strong correlation with MITF activity across these cell lines. If the AhR is a contributor to differentiation then this should be a positive correlation with high AhR in the 'melanocytic' and 'transitory' cell lines, and if the AhR is a driver of dedifferentiation then I should see a strong anti-correlation of AhR and MITF activity with elevated AhR activity in the 'neural crest like' and 'melanocytic' cell lines. To determine AhR and MITF activity, I established gene expression profiles (GEPs) of both the AhR and MITF and determined the correlation between the GEPs in each of the melanoma cell lines (Table 7).

AhR GEP	**MITF GEP**
AHR	*DCT* (Kawakami & Fisher, 2017)
AHRR (Mimura et al., 1999)	*GPNMB* (Hoek et al., 2008)
CREB5 (De Abrew et al., 2010)	*GPR143* (Hoek et al., 2008)
CYP1A1 (W. Ye et al., 2019a)	*HEXA* (Louphrasitthiphol et al., 2020)
CYP1B1 (Jacob et al., 2011)	*MITF* (Hartman et al., 2014)
INHBA (Corre et al., 2018)	*MLANA* (Kawakami & Fisher, 2017)
ITGA6 (Teino et al., 2020)	*OCA2* (Dilshat et al., 2021)
LRRC49 (Corre et al., 2018)	*PMEL* (Kawakami & Fisher, 2017)
OSMR (Corre et al., 2018)	*RAB38* (Racioppi et al., 2019)
PMAIP1 (Corre et al., 2018)	*SLC45A2* (Hartman et al., 2014)
PTPN13 (Merches et al., 2020)	*TRPM1* (Hoek et al., 2008)
RUNX2 (Corre et al., 2018)	*TYR* (Kawakami & Fisher, 2017)
THBS1 (Corre et al., 2018)	*TYRP1* (Kawakami & Fisher, 2017)
TIPARP (Teino et al., 2020)	

Table 7: List of genes constituting AhR and MITF GEP.

Comparison of the AhR GEP and the MITF GEP reveals a strong negative correlation with a Pearson's correlation score of -0.80 (Fig. 4.11). This strong negative correlation, if causative, indicates there may be a mechanistic link between MITF activity and AhR activity, with one antagonising the other. These data also demonstrate that high MITF and low AhR activity are characteristic of the more differentiated melanocytic and transitory cell phenotypes which are representative of early-stage disease. Conversely, low MITF and high AhR activity are characteristic of the more dedifferentiated Neural Crest-like and Undifferentiated cell phenotypes representing late-stage disease. A potential consequence of this is, if causative, the AhR may be a contributing factor to melanoma dedifferentiation and disease progression through antagonism of MITF activity. These data could, however, be

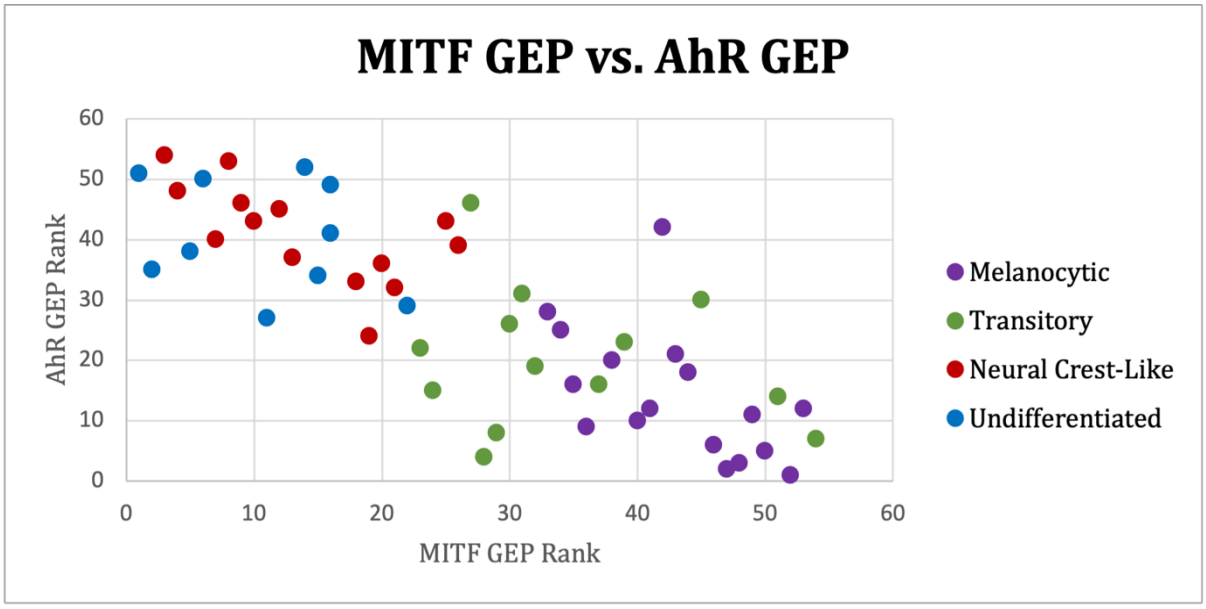

Figure 4.11. GEP analysis of AhR and MITF activity. A scatter graph representing the AhR GEP rank and MITF GEP rank for each of the 54 melanocyte cell lines coloured by phenotypic state as determined in Tsoi *et. al.* 2018. Pearson's rank -0.80, $P < 0.0001$.

reflective of independent mechanisms of action of MITF loss and AhR overactivation both manifesting in more dedifferentiated phenotypes.

4.2.9. Expression of the AhR and LDTFs in patient data

While there's a strong negative correlation of AhR and MITF expression in this panel of melanoma cell lines, it's not the only available database. I demonstrated this negative correlation is found across melanoma cell lines from the cancer cell line encyclopaedia (CCLE) with a Spearman's rank correlation coefficient of -0.4079 (Fig. 4.12). The reduced strength of the negative correlation in this instance may be reflective of these data being the correlation of AhR and MITF expression rather than use of a gene expression profile which would be reflective of activity. Using the

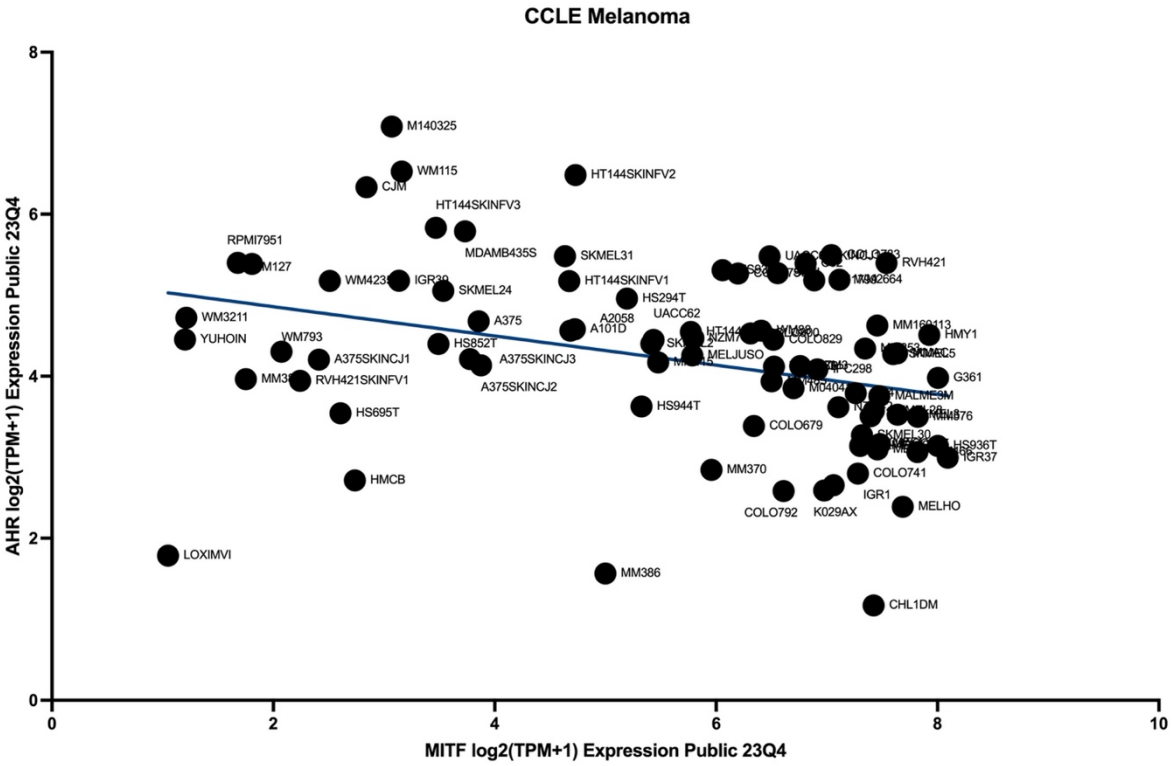

Figure 4.12. Expression of MITF and AhR in CCLE melanoma cell lines. Scatter graph representing the distribution of 'MITF Expression' vs 'AhR Expression' with data from the 'Cancer Cell Line Encyclopaedia' (R = -0.4079, P = 0.0001, Spearman's Rank Correlation Coefficient).

expression of the single *AHR* and *MITF* genes rather than the GEP of both is because the raw data not being available and only being able to access the CCLE data via their visualisation tool which is limited to pairwise gene comparisons.

Using data available from TCGA, I performed the same GEP analysis as I had done in the Tsoi *et. al.* melanoma cell line dataset in 420 available sequenced melanoma samples[**]. Across of stages of melanoma there's a negative correlation between the AhR GEP and MITF GEP of r = -0.2990 (Fig. 4.13A), which aligns with the data in the Tsoi *et. al.* dataset. In stage 0 melanomas there's not a significant correlation between AhR GEP and MITF GEP (Fig. 4.13B), the absence of significance may represent no biological relationship in these tumours and/or very few samples being used, and the relationship is missed. In stage 1 melanomas, there's a negative correlation between AhR GEP and MITF GEP of r = -0.3497 across 76 samples (Fig. 4.13C). There's also a significant negative correlation between AhR GEP and MITF GEP in stage 2 and stage 3 tumours, with Pearson correlation coefficients of r = -0.3869 and r = -0.2853, respectively (Fig. 4.13D&E). There's no correlation between AhR GEP and MITF GEP in stage 4 tumours (Fig. 4.13F). From these data, it's evident there's a correlation between AhR activity and MITF activity across melanoma samples from patients, although this is only significant in Stage 1-3 tumours. This could be due to these stages having the greatest number of samples and giving significant correlations where Stage 0&4 samples were fewest. It could also be reflective of a difference in behaviour of these tumours being the least transformed and the most transformed where, this relationship exists in most tumours but not in healthy cells or very late-stage disease.

[**] Total datasets available: 472. 52 datasets were omitted as they did not have an attributed stage.

The difference between stage 0 and stage 1-3 correlations between AhR GEP and MITF GEP may be indicative of this correlation not being present in untransformed healthy cells, analysis of this correlation should be performed in healthy melanocytes as well, to determine if this is a cancer-specific relationship.

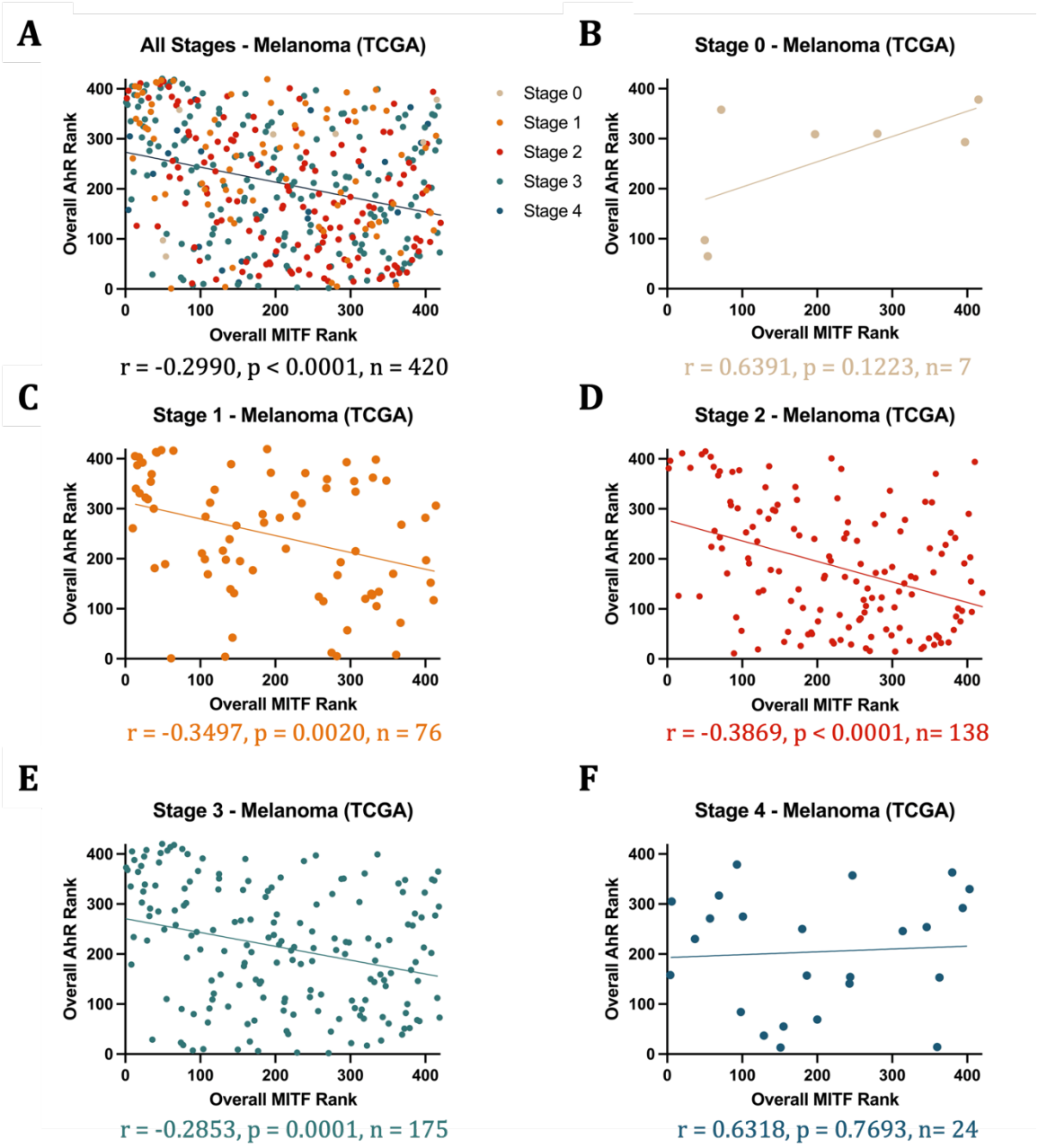

Figure 4.13. GEP Analysis of AhR and MITF activity in TCGA Melanoma. Scatter graphs representing the AhR GEP Rank and MITF GEP Rank of TCGA melanoma samples in (A) All Patients, (B) Stage 0 Patients, (C) Stage 1 Patients, (D) Stage 2 Patients, (E) Stage 3 Patients, and (F) Stage 4 Patients. Simple linear regression is shown on each graph and the statistics beneath are Pearson Rank Coefficients with corresponding p values and number of samples.

A potential mechanistic explanation for the negative correlation observed between AhR and MITF expression/activity is the AhR is antagonising the binding of MITF and expression of lineage-defining genes. I explored whether there were similar correlations between the AhR and the expression of LDTFs in a small array of cancers the AhR is known to influence the tumorigenesis of: BrCa, *TRPS1* (Witwicki et al.,

2018); NSCLC, *SOX2* & *NKX2-1* (Mollaoglu et al., 2018); Glioma, *SPI1* (Heinz et al., 2010); Myeloid cancers, *GATA2* (Y. Li et al., 2021). In melanoma, *MITF* and *AHR* expression negatively correlate, r = -0.1554 which aligns with the previous data showing their activity is negatively correlated (Fig. 4.14A). In BrCa, *TRPS1* and *AHR* expression positively correlates, r = 0.1709 (Fig. 4.14B). Lung cell lineage is determined by the expression of *SOX2* and *NKX2-1*, in NSCLC TCGA datasets *AHR* expression negatively correlates with *SOX2* expression, r = -0.08857 (Fig. 4.14C), but doesn't correlate with *NKX2-1* expression (Fig. 4.14D). Glial cell lineage is partially determined by *SPI1* expression, which positively correlates with *AHR* expression in Glioma TCGA data, r = 0.2925 (Fig. 4.14E). *GATA2* is a LDTF in myeloid cells and its expression negatively correlates with *AHR* expression in myeloid cancers in TCGA datasets, r = -0.1268 (Fig. 4.1F). In BrCa, the AhR is oncogenic (Section 1.4.) I'd expect a negative correlation with AhR expression, the opposite is observed here, if there's a mechanistic link between the AhR and LDTFs in differentiation status. In glioma, where expression of *AHR* and *SP1* are positively correlated and the AhR is thought to be a tumour suppressor (Section 1.4.), which aligns with what would be expected if there was a mechanistic link between these factors. In AML, a cancer of myeloid cells, the AhR is tumour suppressive (Ly et al., 2019) a positive correlation is expected between *AHR* and LDTF *GATA2,* there's a negative correlation between their expression in myeloid cancers. In NSCLC, the AhR has been shown to be both pro- and anti-tumorigenic (Section 1.4.) and in these data there's a very weak negative correlation between lung LDTF *SOX2* and no correlation with *NKX2-1*. From these

data, it doesn't suggest the AhR could be a regulator of LDTF expression in cancers, beyond melanoma, examined in this work.

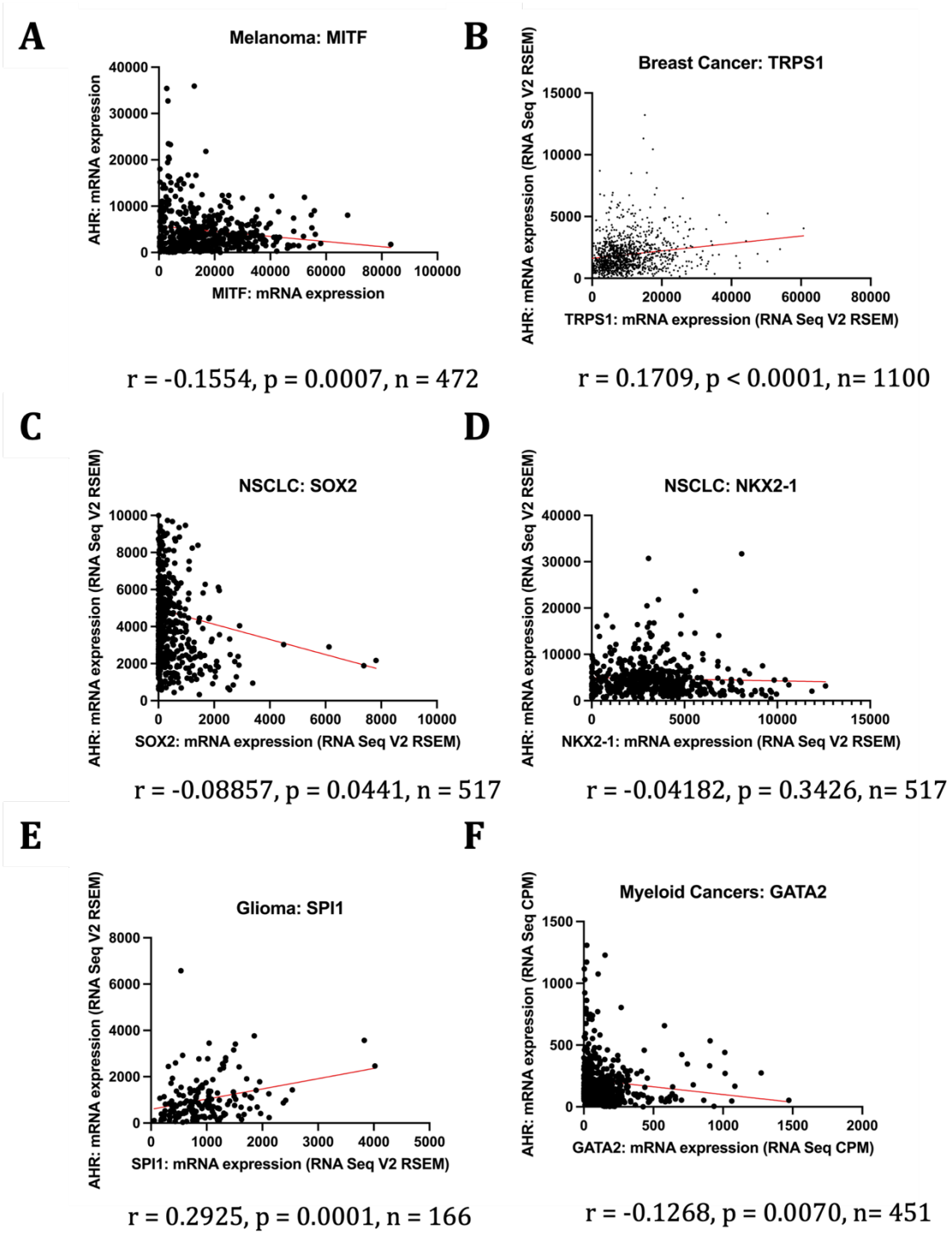

Figure 4.14. Expression of AhR and LDTFs in their corresponding cancers. Scatter graphs representing *AHR* mRNA expression and expression of LDTFs in their corresponding cancers with data from TCGA. (A) Melanoma and *MITF,* (B) Breast Cancer and *TRPS1*, (C) NSCLC and *SOX2*, (D) NSCLC and *NKX2-1*, (E) Glioma and *SPI1*, and (F) Myeloid Cancers and *GATA2*. Simple linear regression is shown on each graph and the statistics beneath are Pearson Rank Coefficients with corresponding p values and number of samples.

4.2.10. MITF motifs are enriched near AhR binding sites

Motif enrichment analysis of my ChIP-Seq data demonstrated the most enriched DNA-sequence across my peaks is the AhR:ARNT binding sequence: AhRE, $p = 1.3 \times 10^{-1572}$ (Fig. 4.15A). The AhRE motif is enriched centrally across all reads which is expected and supports the validity of the ChIP-seq data processing pipeline. I determined there was also a significant enrichment of TFE-family motifs, TFEC ($p = 2.3 \times 10^{-143}$), TFEB ($p = 3.0 \times 10^{-113}$), TFE3 ($p = 1.0 \times 10^{-103}$), and MITF ($p= 1.8 \times 10^{-75}$) (Fig. 4.15A). Where AhRE motifs are centrally enriched, TFE-family binding motifs are enriched in the regions flanking the centre point of reads with regular subpeaks of greater probability of these sequences approximately every 25 bp from the centre of the AhR:ARNT binding site (Fig. 4.15A). This binding of the AhR nearby potential TFE-family binding sites, could be the basis of a mechanism of antagonism between AhR activity and MITF activity. For this to be likely, one would expect these sites to be distributed such that TFs binding to them would bind on the same face of the DNA. The most frequently observed distribution of the AhR:ARNT and MITF motifs is 28 bp upstream, $p = 2.16 \times 10^{-5}$ (Fig. 4.15B-D), with this specific distribution occurring in 16 of the reads but across many more reads with differing numbers intervening base pairs. Given a single turn of the double helix contains 10 bps, 28 bp would place these sites on very similar faces of the DNA given the MITF motif is bound at the 5'-CACGTG-3' element located 31 bp away, just over 3 complete turns. I examined the genes closest to the 16 occurrences of the 5'-MITF-28bp-AhR:ARNT-3' (Fig. 4.15E). Although the closest genes are likely candidates to be regulated by binding of these TFs, it's not necessarily the case. From this list of genes there are ER components (*EIF2AK3, STX18-AS1, SARAF*), Global Translation Regulators (*EIF2AK3, LARP1*) and a cancer-associated

gene (*KLF10*). Although, the enrichment of the MITF motifs near AhR motifs doesn't necessarily reflect binding or regulation of expression of the nearby genes. Furthermore, there's an expected bias of MITF binding sites in open chromatin in melanocytes and melanoma cells, so this enrichment may simply be an artefact of this bias rather than a biological mechanism.

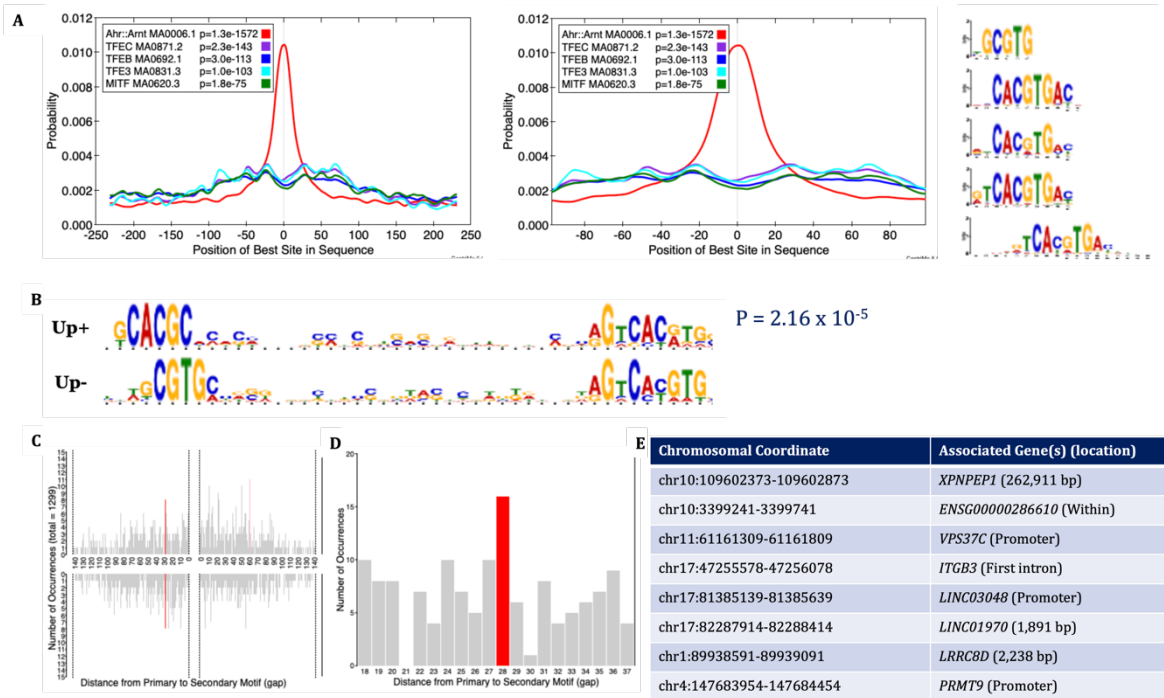

Chromosomal Coordinate	Associated Gene(s) (location)
chr10:109602373-109602873	*XPNPEP1* (262,911 bp)
chr10:3399241-3399741	*ENSG00000286610* (Within)
chr11:61161309-61161809	*VPS37C* (Promoter)
chr17:47255578-47256078	*ITGB3* (First intron)
chr17:81385139-81385639	*LINC03048* (Promoter)
chr17:82287914-82288414	*LINC01970* (1,891 bp)
chr1:89938591-89939091	*LRRC8D* (2,238 bp)
chr4:147683954-147684454	*PRMT9* (Promoter)
chr18:3758526-3759026	*DLGAP1* (Other Intron)
chr2:88627997-88628497	*EIF2AK3* (Promoter)
chr3:48564022-48564522	*COL7A1* (5'-UTR)
chr4:4580864-4581364	*STX18-AS1* (Other Intron)
chr5:154682413-154682913	*LARP1* (Promoter)
chr7:767470-767970	*DNAAF5* (Other Intron)
chr8:102662857-102663357	*KLF10* (7,388 bp)
chr8:30000613-30001113	*SARAF* (61,407 bp)

Figure 4.15. Motif Enrichment Analysis. Motif enrichment analysis of all AhR peaks using MEME-ChIP showing (A) Canonical AhR-ARNT binding motifs and TFE-family member binding motifs. Motif distribution analysis between the AhR:ARNT and MITF motifs (B) showing sequences, (C) bi-directional distribution and (D) uni-directional distributions (E) list of sequences contributing to the most frequent observed distance from primary to secondary motif.

To assess whether the proximity of these sites to one another in these cells could be biologically relevant, binding of MITF to these sites should be examined via MITF ChIP-Seq (App. 8.4.) or ChIP-qPCR, and co-binding of these factors to these sites could

be examined via ChIP-re-ChIP to capture sequences bound by both factors. Performing gene expression analysis (RNA-Seq / qRT-PCR) of these genes in response to AhR modulation/Status (App. 8.5.) and in the presence or absence of MITF using *MITF* KO cell lines could also be an approach to determining whether there is any regulatory interaction between AhR and MITF.

To determine whether there's a mechanistic link between these TFs, a further ChIP-Seq experiment could also be performed, examining the effect of FICZ treatment on MITF binding in an MITF ChIP in these cells. This would demonstrate whether excitation of the AhR was sufficient to drive differential binding of the MITF to its target sequences in the genome.

4.2.11. MITF binding occurs near AhR sites in key genes

Using available ChIP-Seq data produced from MITF IP in 501mel cells (Louphrasitthiphol et al., 2020) (GEO: GSE77437) I determined whether the AhR and MITF bind to the same genes. For comparison, I used the FICZ-stimulated AhR list of annotated peaks, as this reflects activated AhR binding under canonical physiological ligands. I also used ChIP-Seq data from ARNT-IP in 501mel cells (Louphrasitthiphol et al., 2019) (GSE: GSE132624) to determine which sites of the genome in these cells were also bound by ARNT, assuming that sites that were occupied by both the AhR and ARNT represented canonical AhREs bound by AhR:ARNT dimers. Without performing ChIP-re-ChIP experiments it's not possible to be confident that both factors are binding at the same time, without using appropriate IP controls in knockout cell lines it's also not possible to be certain that peaks being studied are

bound by either factor. Assuming these peaks are reliable, I'm speculating that AhR peaks without associated ARNT peaks represent non-canonical binding events of the AhR.

The MITF ChIP experiment used over 15-fold more material than the AhR ChIP-Seq experiment and, when analysed through my pipeline, gave over 100000 peaks that were more than 2-fold enriched in binding and were statistically significant ($p < 0.05$). with only approximately 30000 genes in the human genome, this shows that almost all genes being expressed in 501mel would be expected to have an MITF peaks nearby. This is reflected in most genes with FICZ-treated AhR-associated peaks have MITF associated peaks (Fig. 4.16A). This overlap is not significant ($p > 0.05$) and is likely due to MITF peaks vastly outnumbering the AhR peaks meaning that only a small fraction of total MITF peaks could be bound by the AhR or ARNT at most. The discrepancy in starting material and pulldown method could accounts for the greater number of MITF peaks than AhR or ARNT peaks. Despite no statistical significance in the overlap of the MITF peaks with the AhR/ARNT peaks, there may still be a biological significance to the peaks to which AhR/ARNT does overlap with MITF if this subset drives distinct phenotypic programmes.

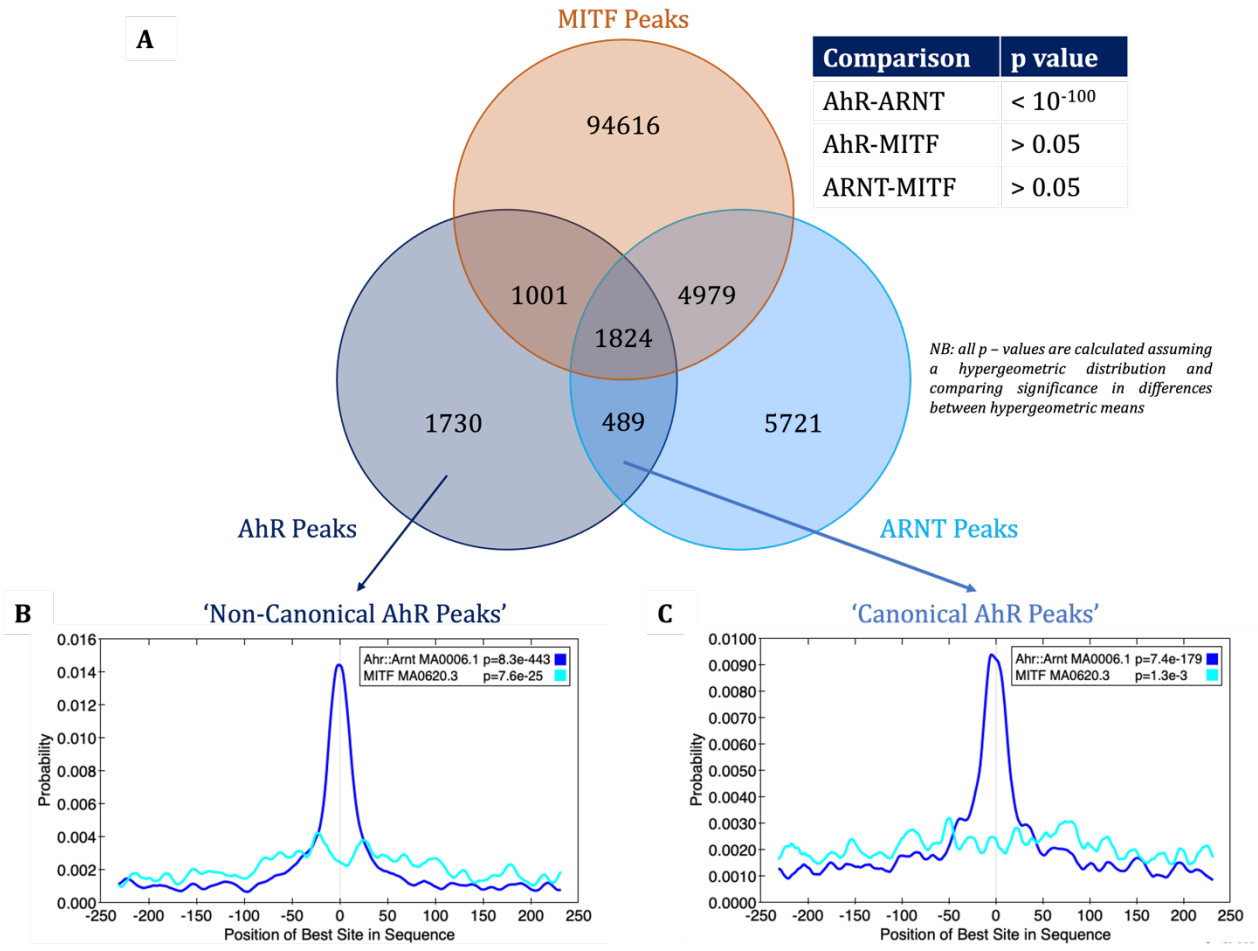

Figure 4.16. Analysis of called peaks from AhR, ARNT, and MITF ChIP Seq experiments. (A) The overlap of peaks called from an AhR IP (After FICZ 100 nM-stimulation), MITF IP peaks, and ARNT IP peaks determined by ChIP Seq, data for MITF and ARNT ChIP Seq experiments from papers cited in text, with all IPs performed in 501mel WT cells. (B) Central motif enrichment analysis from peaks from the AhR-IP that do not overlap with peaks called in the ARNT-IP and (C) peaks that do overlap from the AhR-IP and the ARNT-IP, labelled as 'Non-Canonical' and 'Canonical' peaks, respectively.

The overlap between the AhR-IP peaks and the ARNT-IP peaks is significant, and of 5065 AhR-peaks, 2313 peaks are called in both pulldowns. The assumption made here is these 2313 peaks represent canonical binding events, and the remaining 2752 peaks are non-canonical binding events, where the AhR is associating with DNA independently of ARNT. MEME-ChIP analysis of the two groups shows the canonical sequences are 6-fold more likely to occur over a canonical AhRE sequence (Fig. 4.16B) than the non-canonical sequences, with both sets being enriched for the AhRE motif centrally.

Despite overlap of the peaks between the AhR and MITF not being statistically significant, the MITF binding motif is significantly enriched again in both sets of peaks. While this could be due to random chance, in the non-canonical peaks it's enriched at ±30bp from the centre of the reads in a greater proportion of reads (0.4%) (Fig. 4.16B) compared to the canonical peaks where there's no distinct enrichment at any position and occurs in 0.3% of reads (Fig. 4.16C). This could be entirely due to random chance and would require a repeat of this experiment with a proper negative control to be confident of the AhR peaks, and a repeat of the ARNT ChIP-seq using the same experimental set up to be confident in the comparisons between experiments. It would also be valuable to perform a ChIP-re-ChIP of the AhR then ARNT in these cells to confirm the co-binding of these factors to the 'canonical sites'.

To determine whether there's a likely biological consequence of these non-/canonical AhR binding sites, I performed GO analysis of all FICZ-treated AhR peaks, then of each subset (Fig. 4.17)[††]. There's enrichment of the EMT of 2.40FE in 'canonical' genes, and of regulation of EMT across all peaks of 1.82 FE (Fig. 4.17A&B). This suggests the genes associated with the EMT to which the AhR binds are predominantly bound by AhR:ARNT rather than non-canonical AhR complexes. Across all peaks there's 2.84 FE of 'melanocyte differentiation' however, only in non-canonical AhR peaks is there a similar pathway enriched: 'pigment cell differentiation' 3.89 FE (Fig 4.17A&C). This suggests that specific genes associated with melanocyte differentiation are bound by non-canonical AhR complexes. Across all-peaks there's 1.25 – 2.29 FE of cell-cycle-

[††] A full list of GO analysis results for all 3 sets are available in Supp. 9.1.

associated pathways, with 1.57 – 2.72 FE of similar pathways in canonical peaks and no significant enrichment in similar pathways in non-canonical peaks (Fig. 4.17A-C). There are many differentiation-associated pathways across all AhR peaks, with 1.31 – 5.2 FE, and enrichment of fewer related pathways in non-/canonical peaks ranging from 1.63 – 6.68 FE and 2.05 – 3.34 FE, respectively. With these differentiation pathways being across many non-melanocyte cell types they reflect proteins that may have roles in melanocyte differentiation or cellular differentiation broadly, and their enrichment in both subsets suggests these potential general effects of the AhR on expression of differentiation-associated genes aren't specific to AhR complexes. Although without proper controls and ChIP-re-ChIP it's not possible to confirm any of these potential effects of non-canonical binding on specific behaviour. Furthermore, binding of the AhR to these genes doesn't reflect their expression and these enrichments may be biologically irrelevant. Furthermore, these FE-values are relatively low, so it's uncertain whether these binding events, even if they are regulating expression, can generate significant phenotypic changes.

A

AhR+FICZ All	FE	FDR
regulation of epithelial to mesenchymal transition (GO:0010717)	1.82	1.96E-02
mesenchyme development (GO:0060485)	1.51	2.82E-02
mesenchymal cell differentiation (GO:0048762)	1.56	4.82E-02
melanocyte differentiation (GO:0030318)	2.84	2.87E-02
developmental pigmentation (GO:0048066)	2.32	1.81E-02
pigmentation (GO:0043473)	1.77	3.24E-02
G2/M transition of mitotic cell cycle (GO:0000086)	2.29	1.62E-02
cell cycle G2/M phase transition (GO:0044839)	2.08	4.68E-02
positive regulation of mitotic cell cycle (GO:0045931)	1.81	1.28E-02
positive regulation of mitotic cell cycle phase transition (GO:1901992)	1.8	4.55E-02
regulation of viral life cycle (GO:1903900)	1.66	3.14E-02
mitotic cell cycle phase transition (GO:0044772)	1.62	4.40E-02
regulation of mitotic cell cycle (GO:0007346)	1.42	3.57E-03
mitotic cell cycle (GO:0000278)	1.37	4.11E-03
mitotic cell cycle process (GO:1903047)	1.31	4.77E-02
regulation of cell cycle process (GO:0010564)	1.29	2.45E-02
regulation of cell cycle (GO:0051726)	1.26	5.37E-03
cell cycle (GO:0007049)	1.25	1.88E-02
inhibition of neuroepithelial cell differentiation (GO:0002085)	5.2	1.63E-02
type I pneumocyte differentiation (GO:0060509)	4.68	1.13E-02
regulation of timing of cell differentiation (GO:0048505)	3.64	2.70E-02
positive regulation of T-helper cell differentiation (GO:0045624)	3	6.54E-03
lung epithelial cell differentiation (GO:0060487)	2.64	3.28E-02
lung cell differentiation (GO:0060479)	2.64	3.28E-02
macrophage differentiation (GO:0030225)	2.55	2.87E-03
regulation of CD4-positive, alpha-beta T cell differentiation (GO:0043370)	2.41	1.64E-03
positive regulation of CD4-positive, alpha-beta T cell differentiation (GO:0043372)	2.36	2.89E-02
regulation of T-helper cell differentiation (GO:0045622)	2.27	3.29E-02
positive regulation of alpha-beta T cell differentiation (GO:0046638)	2.27	8.78E-03
regulation of alpha-beta T cell differentiation (GO:0046637)	2.16	3.56E-03
cell differentiation involved in kidney development (GO:0061005)	2.12	4.55E-02
cardiocyte differentiation (GO:0035051)	2.05	4.16E-04
chondrocyte differentiation (GO:0002062)	2.01	8.38E-03
positive regulation of muscle cell differentiation (GO:0051149)	1.96	4.53E-02
cardiac muscle cell differentiation (GO:0055007)	1.94	1.28E-02
osteoblast differentiation (GO:0001649)	1.92	7.28E-04
regulation of osteoclast differentiation (GO:0045670)	1.91	4.29E-02
regulation of stem cell differentiation (GO:2000736)	1.87	4.25E-02
regulation of myeloid leukocyte differentiation (GO:0002761)	1.86	4.11E-03
neural crest cell differentiation (GO:0014033)	1.85	3.36E-02
stem cell differentiation (GO:0048863)	1.85	2.41E-04
myeloid leukocyte differentiation (GO:0002573)	1.8	3.38E-03
regulation of osteoblast differentiation (GO:0045667)	1.79	8.61E-03
regulation of fat cell differentiation (GO:0045598)	1.78	9.97E-03
central nervous system neuron differentiation (GO:0021953)	1.76	1.61E-03
T cell differentiation (GO:0030217)	1.75	1.82E-03
positive regulation of leukocyte differentiation (GO:1902107)	1.73	1.82E-03
cell morphogenesis involved in neuron differentiation (GO:0048667)	1.72	8.46E-08
regulation of myeloid cell differentiation (GO:0045637)	1.7	2.36E-03
positive regulation of T cell differentiation (GO:0045582)	1.7	3.97E-02
fat cell differentiation (GO:0045444)	1.67	4.34E-02
regulation of T cell differentiation (GO:0045580)	1.65	8.60E-03
positive regulation of lymphocyte differentiation (GO:0045621)	1.65	4.44E-02
myeloid cell differentiation (GO:0030099)	1.64	3.03E-04
striated muscle cell differentiation (GO:0051146)	1.63	3.86E-03
regulation of leukocyte differentiation (GO:1902105)	1.62	2.71E-04
mononuclear cell differentiation (GO:1903131)	1.57	4.12E-04
muscle cell differentiation (GO:0042692)	1.56	3.37E-03
lymphocyte differentiation (GO:0030098)	1.56	3.69E-03
leukocyte differentiation (GO:0002521)	1.55	2.36E-04
regulation of lymphocyte differentiation (GO:0045619)	1.53	2.79E-02
glial cell differentiation (GO:0010001)	1.52	3.64E-02
neuron differentiation (GO:0030182)	1.52	1.32E-10
regulation of cell differentiation (GO:0045595)	1.48	2.98E-13
positive regulation of cell differentiation (GO:0045597)	1.47	5.23E-07
sex differentiation (GO:0007548)	1.47	2.70E-02
negative regulation of cell differentiation (GO:0045596)	1.44	1.86E-04
cell differentiation (GO:0030154)	1.31	2.91E-15

B

AhR+FICZ and ARNT	FE	FDR
epithelial to mesenchymal transition (GO:0001837)	2.4	0.0445
positive regulation of epithelial to mesenchymal transition (GO:0010718)	2.92	0.027
mesenchymal cell differentiation (GO:0048762)	2.06	0.0241
cellular pigmentation (GO:0033059)	2.9	0.0187
melanosome organization (GO:0032438)	3.58	0.0154
pigment granule organization (GO:0048753)	3.49	0.0185
positive regulation of melanin biosynthetic process (GO:0048023)	6.81	0.0185
regulation of melanin biosynthetic process (GO:0048021)	5.1	0.0275
cell cycle (GO:0007049)	1.57	0.000206
cell cycle checkpoint signaling (GO:0000075)	2.07	0.02
cell cycle G1/S phase transition (GO:0044843)	2.72	0.0219
cell cycle phase transition (GO:0044770)	2.23	0.0058
cell cycle process (GO:0022402)	1.61	0.000139
G1/S transition of mitotic cell cycle (GO:0000082)	2.6	0.0433
mitotic cell cycle (GO:0000278)	1.58	0.00886
mitotic cell cycle phase transition (GO:0044772)	2.14	0.0252
mitotic cell cycle process (GO:1903047)	1.65	0.00591
negative regulation of cell cycle (GO:0045786)	1.63	0.0489
regulation of cell cycle (GO:0051726)	1.62	0.00000593
regulation of cell cycle phase transition (GO:1901987)	1.72	0.006
regulation of cell cycle process (GO:0010564)	1.71	0.0000676
myeloid leukocyte differentiation (GO:0002573)	2.14	0.0199
negative regulation of fat cell differentiation (GO:0045599)	3.34	0.00531
negative regulation of striated muscle cell differentiation (GO:0051154)	3.31	0.042
osteoclast differentiation (GO:0030316)	3.29	0.00374
regulation of epithelial cell differentiation (GO:0030856)	2.05	0.0352
regulation of fat cell differentiation (GO:0045598)	2.46	0.00242
regulation of myeloid cell differentiation (GO:0045637)	2.13	0.00351
regulation of osteoclast differentiation (GO:0045670)	2.65	0.0275

C

AhR+FICZ not ARNT	FE	FDR
pigment cell differentiation (GO:0050931)	3.89	0.0421
cell morphogenesis involved in neuron differentiation (GO:0048667)	1.77	0.00829
immature B cell differentiation (GO:0002327)	6.68	0.0309
muscle cell differentiation (GO:0042692)	2.03	0.00552
myotube differentiation (GO:0014902)	2.88	0.0204
neuron differentiation (GO:0030182)	1.63	0.000111
regulation of muscle cell differentiation (GO:0051147)	2.41	0.0123
stem cell differentiation (GO:0048863)	2.38	0.00361

Figure 4.17. GO Analysis of AhR-IP determined genes. Subsets of GO pathways enriched across the genes closest to the called peaks from; (A) all AhR-IP 501mel after 24-hours treatment with FICZ 100 nM, (B) the 'Canonical' peaks that overlapped the AhR-IP and ARNT-IP, and (C) the 'Non-Canonical' peaks from the AhR-IP that did not overlap with the ARNT-IP called peaks. These subsets are limited to significantly (FDR < 0.05) enriched GO pathways associated with; 'Epithelial to Mesenchymal', 'Melanocyte/Pigment', 'Cell Cycle', and 'Metabolism'. A complete list of significantly (FDR < 0.05) enriched GO pathways are found in Supplementary 9.1.

Given there's enrichment of 'pigment cell differentiation'-associated genes in the non-canonical peaks list and 'melanocyte-differentiation'-associated genes across all peaks, I examined loci of these genes to determine whether there was a discernible

relationship between AhR/ARNT binding with MITF, the TF responsible for melanocyte cell fate. Within the non-canonical gene set there's *Solute Carrier Family 24 member 5 (SLC24A5), Ras-related protein 32 (RAB32),* and *KIT* which are associated with these pathways. The *SLC24A5* gene has an associated AhR 23.5 kbp upstream of its TSS, which overlaps with one of two neighbouring MITF peaks with no nearby ARNT peaks (Fig. 4.18A). Interestingly, the summits of these peaks are 10 bp apart, which represents a single turn of the helix, placing both binding sites on the same face of the DNA. The *RAB32*-associated peak is slightly downstream of the 2nd exon, again with the NC-AhR peak overlapping with an MITF peak and no nearby ARNT peak (Fig. 4.18B). The summits of these peaks are approximately 85 bp apart, placing them on opposite sides of the helix. The *KIT*-associated AhR peak is downstream of 7th exon, and again overlaps with an MITF peak and no ARNT peaks (Fig. 4.18C). The summits of these peaks are displaced by approximately 32 bp which places these factors on roughly the same side of the helix and aligns with the distribution of MITF motifs relative to AhR peaks (Fig. 4.17).

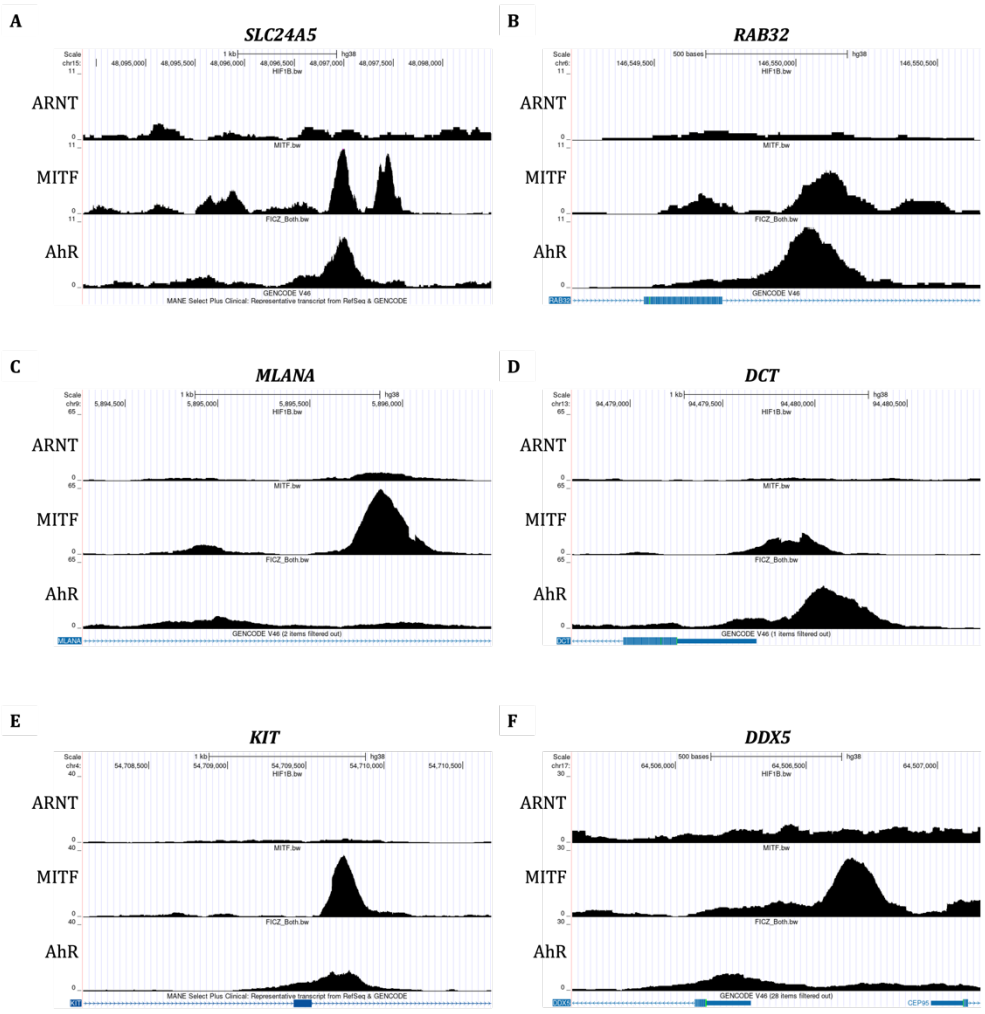

Figure 4.18. UCSC Genome Browser tracks of Melanocyte-defining genes. UCSC genome browser-generated visuals of the ChIP-Seq data from the AhR-IP after 24-hours of FICZ 100 nM stimulation (AhR), the ARNT-IP, and the MITF-IP all in 501mel cells. 3 of these genes comes from those in the 'pigment cell differentiation' pathway in the 'Non-canonical' AhR peaks (A) *SLC24A5,* (B) *RAB32,* (C) *MLANA.* The remaining 3 are genes associated with melanocyte cell-fate that are in the 'Canonical' peaks of the AhR-IP at (D) *DCT*, (E) *KIT*, and (F) *DDX5*.

With the AhR potentially binding to several melanocyte-defining genes, I examined some genes within the 'Pigment Cell Differentiation' that are bound in the canonical-AhR fraction of genes: *(DCT), (MLANA),* and *DEAD-box Helicase 5 (DDX5)*. In all these instances, the AhR and MITF-associated peaks are far more enriched than the ARNT-associated peaks (Fig. 4.18D-F). In the ARNT tracks, the signal doesn't appear to have a clearly defined peak at these loci, rather is more akin to noise from the sequencing runs, which may be reflective of non-specific binding at these loci as they are open chromatin in 501mel cells. To control for this, it would've been good to have had an

ARNT pulldown and sequencing in 501mel *ARNT* KO cells, to determine whether this presence of signal is ARNT-specific and reflective of a canonical AhR peak or whether these loci should be classified as NC-AhR peaks. The AhR and MITF peaks in *DCT* are 170 bp apart (Fig. 4.6D), which is much greater than observed in the other NC-AhR and MITF peaks (Fig. 4.18A-C). In *MLANA* the ARNT track appears to have 2 very small peaks that overlap with 2 MITF peaks and 2 very small AhR peaks (Fig. 4.18E). Interestingly, the most enriched AhR peak overlap with upstream MITF peak, which is the least enriched MITF peak, and the most enriched MITF and ARNT peaks overlap. Without proper controls and ChIP-re-ChIP experiments, it's not possible to discern whether these observations are likely to be biological relevant or artefacts of the experimental process. In *DDX5,* there's a large 466bp displacement between the AhR and MITF peaks, without clear indication of any peaks in the ARNT-track beyond noise (Fig. 4.18F). Together, these data could be interpreted to show the AhR binds nearby MITF peaks on key melanocyte-cell fate-defining genes which may have a biological consequence. However, without proper controls and further experiments, detailed previously, it's not possible to be certain of this. Furthermore, RNA-seq across WT/*AHR*$^{-/-}$/*ARNT*$^{-/-}$/*MITF*$^{-/-}$ 501mel cells would be required to demonstrate effects on the expression of these associated genes.

4.3. Discussion

In the first chapter I proposed a novel mechanism through which the AhR mediates IFNγ-signalling via STAT1 through inhibitory interactions with the cytoplasmic components of the NF-κB signalling pathway. Previous work on the AhR in melanoma tumour immunity depended on the AhR being a direct transcriptional agonist of the *IDO1* gene, without providing evidence of either robust induction of *IDO1* in response to physiologically relevant ligands, or of the AhR binding to the *IDO1* promoter (Vogel et al., 2008). The first chapter of this thesis provided evidence, albeit severely limited by the caveats highlighted previously, for a wider role of the AhR in IFNγ-signalling, affecting induction of many IFNγ-response genes beyond that of *IDO1*. Given the absence of robust induction of *IDO1* in response to physiological agonists of the AhR (Fig. 3.3, 3.5, 3.6, 3.8), the AhR modulating induction of IFNγ-response genes beyond *IDO1* (Fig. 3.8 and 3.10), and the suppressive effects of the AhR being mediated by cytoplasmic AhR not nuclear (transcriptionally active) AhR (Fig. 3.15, 3.16, 3.17, 3.18), the AhR is not likely inducing *IDO1* expression via the AhR-IDO1-kyn axis. However, due to the persistent lack of sufficient controls to rule out non-specific or clonogenic effects, these data aren't sufficient to confirm this, rather these experiments should be repeated with appropriate controls and in a broader number of melanoma cell WT and *AHR* -/- cell lines and in primary melanocytes, if possible, to determine whether the observations in these cell lines are applicable to melanoma.

My observations in the previous chapter, however, do not provide evidence to support or reject the hypothesis the AhR is not a direct transcriptional agonist of the

IDO1 gene and the other IFNγ-response genes I studied. For this, I performed a ChIP-Seq experiment which demonstrated the AhR does not bind at the *IDO1* promoter or within a genomic distance where one would expect even a very distal enhancer could bind (Fig. 4.7) (van Arensbergen et al., 2014). Not only is this true at the *IDO1* locus, but also across the same panel of IFNγ-response genes that I showed to be modulated by the AhR by qRT PCR in the first chapter (Fig. 3.8, 4.7). Together, these support my contention that the previous studies that suggested the AhR was a direct transcriptional agonist of *IDO1* (Vogel et al., 2008) may not be the case in the 501mel cells used here. Furthermore, it suggests the AhR-IDO1-Kynurenine axis as the model of establishing tumour immune evasion in melanoma may be incorrect. Although much more work will be needed to generalize the observations made, the data presented here instead indicate the AhR is potentially a component of a much broader mechanism of AhR-mediated immunosuppression through modulation of IFNγ-signalling.

I have yet to confirm the AhR is affecting either NF-κB signalling or IFNγ-signalling broadly across the transcriptome rather than at specific target genes in these cells. An RNA-Seq experiment with sufficient biological replicates is essential to further characterise the mechanism through which I propose the AhR to be mediating immunosuppression in the TME in these cells. This should then be repeated in other melanoma cell lines and primary melanocytes to determine if this mechanism is worth pursuing as a route of therapies in the clinic. The data from such an experiment would enable me to determine the global effects of AhR status on the transcriptome and assess whether the AhR is a mediator of immune signalling pathways in the broad manner which I suggest may operate.

I performed GO enrichment analyses on the AhR ChIP Seq samples which showed the genes bound by the AhR are implicated in many cancer-related biological processes and pathways. In the gene lists from the FICZ and FICZ + IFNγ samples (Fig. 4.8), there was a strong enrichment of biological processes of cellular differentiation and EMT-associated pathways. These enriched pathways were indicative of a role of the AhR in mediating cell differentiation in melanocytes, which would be consistent with the AhR acting as an oncogene in melanoma (Paris et al., 2022b; Walczak et al., 2020). Since phenotypic heterogeneity is a major contributor to immune escape and therapy-resistance (Benboubker et al., 2022; Hossain & Eccles, 2023), the role of AhR in melanoma de-differentiation could further contribute to disease progression. As melanoma cells become more dedifferentiated as they transition from differentiation through proliferation to invasion, the AhR may be having a cell-type specific effect in melanoma with an ability to suppress pigment production/differentiation in these cells consistent with enrichment of AhR binding sites near developmental pigmentation-associated genes (Fig. 4.8). The enrichment of the AhR across cell fate and multiple specific cancer-related genes suggests the AhR may be playing a broad role in dedifferentiation of cancer cells, and a specific role in melanomas, where pigment production is a key biological function of these cells when differentiated.

MITF is the master regulator of melanocyte cell fate, as such loss of MITF activity in melanoma contributes to invasion and metastasis of melanoma cancer cells (Carreira et al., 2006; Dilshat et al., 2021). As such, I hypothesised the AhR may be suppressing the activity of MITF at cell fate genes contributing to loss of phenotypic identity and invasion of melanoma cells. To explore this relationship, I analysed my AhR ChIP-Seq

data and available MITF ChIP-Seq data in 501mel cells and demonstrated that both the AhR and MITF bind to the promoters of genes involved in melanocyte cell fate and differentiation. These data suggest the pro-oncogenic roles of the AhR in melanoma extend beyond the modulation of the host immune system and influence progression of melanoma to metastatic disease. However, an investigation as to whether modulation of the AhR in melanocytes, melanoma cell-lines, or primary melanoma cells affects invasion and cell differentiation would be required to confirm any meaningful biological relationship. Further experiments including measuring expression of *MITF* and other key melanocyte-defining genes including *PMEL, OCA2,* and *TYR* in response to AhR status/stimulation would be valuable, as a depression in their expression in the presence of stimulated AhR would suggest possible dedifferentiation. This should also be performed alongside assays measuring cell viability and division rate, with differentiated cells generally dividing at a slower rate than less-differentiated cells. Performing cell invasion assays in response to AhR status would also demonstrate whether its stimulation or presence drives enhanced invasion and metastasis *in vivo*. Furthermore, if AhR status drives very large-scale effects on dedifferentiation, traditional light microscopy would reveal morphological changes driven by AhR-mediated dedifferentiation.

Using transcriptomic data from both a panel of melanoma cell lines, the CCLE, and TCGA, I discovered a strong anti-correlation between AhR and MITF activity and expression. An anti-correlation between the AhR and MITF showed that AhR activity is greatest in the most dedifferentiated cell phenotypes from the melanoma cell lines. These observations further supported the GO enrichment analyses which showed enrichment of AhR binding across genes involved in cell fate and differentiation.

Together, these data suggest a novel role of the AhR in regulating cell differentiation in melanoma, with increased AhR activity correlating with cell dedifferentiation and binding of the AhR to genes involved in cell fate. Dedifferentiation associated with the AhR in these cells may be a contributor to the observed relationship between dedifferentiation and melanoma progression (Benboubker et al., 2022; Hossain & Eccles, 2023).

An anti-correlation between MITF activity and AhR activity also provides preliminary indirect evidence for the AhR being a broad modulator of tumour immunosuppression. T_{reg} infiltration in melanoma has been shown to be negatively correlated with MITF expression (Chauhan et al., 2022), which my results suggest would positively correlate with AhR activity. Not only is there a greater infiltration of T_{reg} cells, but there is a greater infiltration of many immune cell types in $MITF^{LOW}$ melanomas, which suggests that in these cancers there's a highly suppressive TME wherein tumour cells may infiltrate but not react with the tumour (Chauhan et al., 2022). My data suggests the $MITF^{LOW}$ state would be positively correlated with the AhR. Furthermore, melanoma cells in dedifferentiated states would have reduced sensitivity to immune checkpoint blockade therapies and reduced antigen presentation (Pozniak et al., 2024).

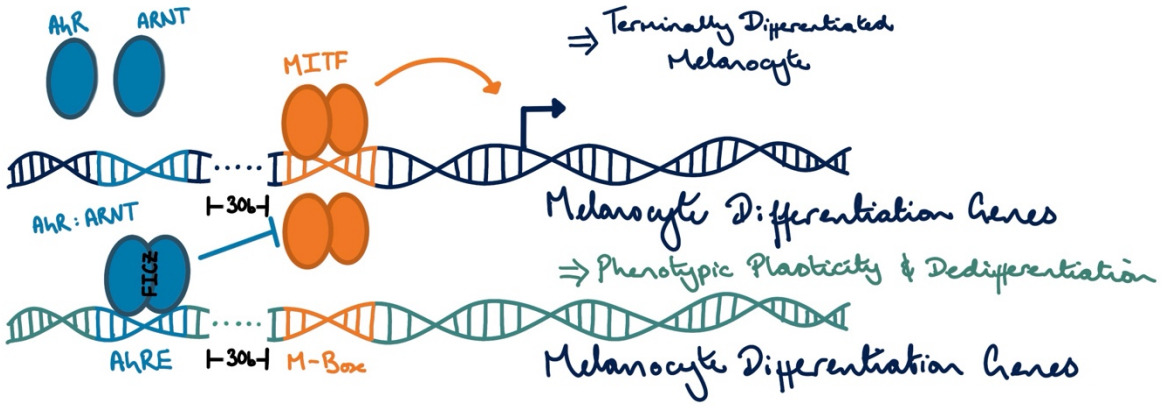

Figure 4.19 A graphical representation of proposed mechanism of AhR and MITF mechanism. Without stimulation of the AhR, MITF binds to M-Box motifs that regulate Melanocyte cell fate genes. Upon stimulation of the AhR, it associates with ARNT and binds to AhREs near MITF binding sties, antagonising MITF-mediated expression of the associated gene.

This negative correlation in melanomas and melanoma cell lines between the AhR and MITF suggests there may be a mechanistic link between MITF-mediated cell differentiation and AhR-mediated cancer cell dedifferentiation. Motif analysis of the AhR ChIP seq demonstrated enrichment of the E-box DNA motif, to which all the TFE family TFs bind, including MITF. With these enriched E-box motifs, there's also enrichment of the M-box motif which is associated with MITF binding to melanocyte cell fate and differentiation genes. Enrichment of these sequences near AhR binding sites, however, is not sufficient to confirm a biological interaction. Using ChIP Seq data in 501mel for MITF IP, I showed there are many genomic loci to which both the AhR and MITF bind. Analysis of the distribution of MITF E/M-box motifs around AhR binding locations reveals the MITF motifs flank the AhR binding events, most frequently at roughly 30 bp from the AhR binding sites. This would place AhR:ARNT and MITF on the same face of the double helix. If this is reflective of sites to which MITF binds, then it allows for a mechanism through which binding of AhR:ARNT could occlude, or otherwise prevent MITF binding and subsequent stimulation of transcription. Analysis of MITF ChIP-Seq in these cells reveals there are nearby peaks

associated with AhR and MITF binding, suggesting the enrichment of these M-box motifs amongst AhR peaks may be biologically relevant, and not an artefact of MITF binding to many sites of open chromatin in melanocytes. However, without a ChIP-re-ChIP experiment, MITF ChIP Seq in response to FICZ, or MITF ChIP seq in 501mel *AHR*$^{-/-}$ cells, it's not possible to determine whether there's a biologically relevant mechanism occurring here.

Furthermore, these data aren't sufficient to confirm this role as to demonstrate transcriptional antagonism between these factors. There are very few reported instances of the AhR behaving as a transcriptional repressor (Krishnan et al., 1995), and those instances are contentious with the evidence supporting indirect mechanisms of suppression of gene expression rather than by the AhR directly (Beischlag et al., 2008). Furthermore, there are limited instances of MITF acting as a direct transcriptional repressor, although it has been documented (Berico et al., 2021). With limited instances of transcriptional repression by either TF being documented, the proposed mechanism of antagonism requires much further study, as this model depends on the AhR being a transcriptional repressor, assessing expression of these melanocyte-defining genes in response to AhR modulation is essential to determine whether this hypothesis is worth further study. Equally, mechanistic interactions between the AhR and MITF could be demonstrated through transcriptomic analysis of 501mel cells when treated with FICZ and 501mel^{WT} and *AHR*$^{-/-}$ cells. Transcriptomic analysis of 501mel cells, WT and *AHR*$^{-/-}$, treated with IFNγ and FICZ would also reveal mechanistic information about how the AhR is modulating IFNγ-signalling.

5. AhR and the Melanoma Transcriptome

5.1. Background

Regulation of gene expression in cells is mediated by a complex network of interactions, often with many specific TFs interacting synergistically and antagonistically through the mediator complex with RNA Polymerase II at the promoters of protein-encoding genes (Compe & Egly, 2021). Determining the effects of a given TF within a cell can be made increasingly complex with perturbations in the activity of one TF driving subsequent expression of other TFs or regulators thereof. There are also instances of TFs having non-genomic effects, such as I described in Chapter 2 with the AhR mediating suppression of IFNγ-response genes through cytoplasmic effectors. To fully understand consequences of activation, suppression, or loss of a TF, one must also consider the transcriptome of cells rather than expression of singular genes.

High-throughput RNA sequencing (RNA-Seq) has been integral to characterising the wider effects of TFs across the genome rather than at specific target genes only (Kukurba & Montgomery, 2015). Non-biased sequencing of transcripts within cells have revealed both novel direct gene regulation events and indirect gene regulation (Ishikawa et al., 2023). RNA-Seq is a key experiment to perform when trying to characterise the effect of the AhR in both mediating IFNγ-signalling and cell differentiation and invasion in melanoma.

My hypothesised model of AhR modulation of IFNγ-signalling suggests that I should detect transcriptome-wide changes in both NF-κB signalling and IFNγ-response genes when I stimulate or lose the AhR in melanocytes. This is due to the proposed interaction of the AhR upstream of NF-κB with IRAK1 likely effecting the expression of NF-κB targets and predisposing the cells to greater IFNγ-responses through baseline elevation of *IRF1* and other IFNγ-signalling pathway components. The breadth of expected transcriptional changes positions RNA-Seq, as an unbiased high-throughput method, the most well-suited experiment for characterising the AhR's role in these pathways. Equally, transcriptomic analysis of 501mel cells with stimulated AhR or the absence of AhR, should demonstrate a depression of MITF activity or an increase in MITF activity respectively, should there be a biologically relevant antagonism between these factors affecting cell differentiation or invasion.

5.2. Results

5.2.1. Validation of RNA-seq

In this experiment I treated 501mel^{WT} and *AHR*$^{-/-}$ cell lines with either 100 nM FICZ, 10 ng/mL IFNγ, or neither for 24-hours, with three replicates for each condition of each cell line. In this experiment, as in each of the results chapters in this thesis, only a single 501mel *AHR*$^{-/-}$ clone was used. Differences observed in gene expression may be the result of clonogenic differences between this *AHR*$^{-/-}$ cell line and the non-targeting CRISPR treated 501mel^{WT} cell line rather than AhR-dependent differences. Results presented in this chapter should be considered cautiously and this experiment should be repeated in multiple 501mel *AHR*$^{-/-}$ clones to improve confidence in results observed, then repeated in more melanoma cell lines for confident in their applicability to melanoma. To determine whether data generated from this experiment are reliable, I assessed expression of the canonical AhR target gene *CYP1A1* after treatment with ±FICZ/±IFNγ. qRT PCR data is displayed as Fold-Induction relative to DMSO which is possible due to detectable transcript abundance of *CYP1A1* and *IDO1* in the DMSO condition. However, in the RNA seq data there are no detectable *IDO1* transcripts in the DMSO condition. Consequently, fold-induction is not possible as each value would've to be divided by 0, thus RNA Seq data is presented as normalised abundance. From RNA-Seq data, there's 3.57-fold greater abundance of *CYP1A1* transcripts in 501mel *AHR*$^{-/-}$ than in 501mel^{WT} without stimulation (Fig. 5.1A), which is reflected in the qRT PCR data where there's 6.16 greater abundance of *CYP1A1* in 501mel *AHR*$^{-/-}$ than in the 501mel^{WT} without stimulation (Fig. 5.1B). In neither the RNA-seq or qRT PCR data is there a significant

difference in the *CYP1A1* induction in response to FICZ in the 501mel *AHR*$^{-/-}$ (Fig. 5.1A, 5.1B). However, there's a response in the 501mel^{WT} cells with 6.05-FE compared to no stimulation, demonstrated in the RNA-Seq data (Fig. 5.1A) and 10.9-FE demonstrated in the qRT PCR data (Fig. 5.1B). The baseline expression of *CYP1A1* in 501mel *AHR*$^{-/-}$ cells is greater than that in 501mel^{WT} cells in both the qRT-PCR and RNA-Seq data, supporting my earlier observation the unliganded AhR may be a transcriptional repressor of *CYP1A1* (Fig. 5.1A, Fig. 5.1B). There's not a significant induction of *CYP1A1* in response to IFNγ-stimulation in the 501mel^{WT} cells detected in either data set (Fig. 5.1A, 5.1B). In 501mel *AHR*$^{-/-}$ cells, there's 2.03-FE of *CYP1A1* induction in response to IFNγ compared to WT in the RNA-Seq data (Fig. 5.1A) and 3.16-FE between the same conditions in the qRT-PCR dataset (Fig. 5.1B). In both datasets there's not a significant change between the *CYP1A1* abundance in either dataset when treating 501mel *AHR*$^{-/-}$ with IFNγ compared to co-treatment with IFNγ and FICZ (Fig. 5.1A, 5.1B). in the 501mel^{WT} cells, however, I do see an increase in *CYP1A1* expression in response to co-treatment with FICZ and IFNγ compared to treatment with only IFNγ with 5.66-FE in the RNA-Seq dataset (Fig. 5.1A). The congruency in patterns of *CYP1A1* induction between the qRT PCR and RNA-Seq datasets confirms the validity of the RNA-Seq dataset with respect to AhR target gene induction.

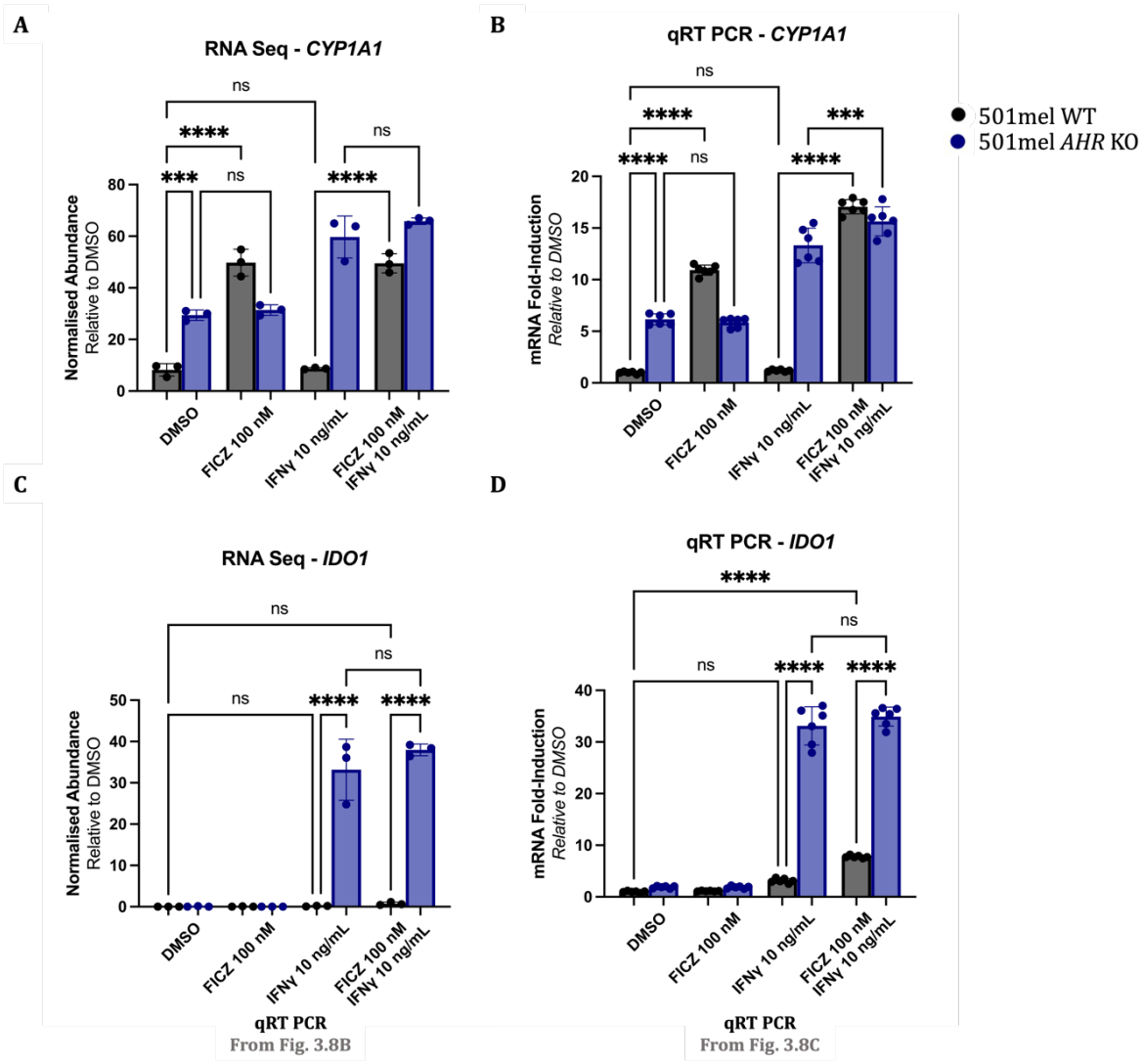

Figure 5.1. Expression of *CYP1A1* in response to FICZ and IFNγ in 501mel cell lines. *CYP1A1* mRNA abundance as determined through (A) RNA-Seq and (B) qRT PCR after 24-hours incubation with FICZ 100 nM and/or IFNγ 10 ng/mL. *IDO1* mRNA abundance as determined through (C) RNA-Seq and (D) qRT PCR after 24-hours incubation with FICZ 100 nM and/or IFNγ 10 ng/mL. Ad-hoc test: Ordinary One-way ANOVA, post-hoc test: Tukey-Kramer test for multiple comparisons which inherently corrects for multiple comparisons P > 0.05: ns, P < 0.05: *, P < 0.01: **, P < 0.001: ***, P < 0.0001: ****. For RNA-Seq data, Biological Replicates = 3. For qRT PCR data, Biological Repeats = 2, Technical Repeats = 3 (Each dot represents a single technical repeat across two biological repeats).

In the RNA-Seq dataset there's no detectable abundance of *IDO1* transcripts in either cell line without treatment of IFNγ (Fig. 5.1C). This is reflected in the qRT PCR dataset, where there's not a significant enrichment in the abundance of *IDO1* transcripts compared to the 501mel^{WT} untreated cells in either cell line without stimulation with IFNγ (Fig. 5.1D). In the RNA-Seq dataset, there's an increase in abundance of *IDO1* transcripts in response to IFNγ, with the 501mel^{WT} cells increasing to 0.16 NQ and to

33.2 NQ in the 501mel *AHR*$^{-/-}$ cells (Fig. 5.1C), although this is a low absolute accumulation of *IDO1* in 501mel^{WT} cells in response to IFNγ, it does represent a clear increase from no detection of any *IDO1* transcripts in the unstimulated 501mel^{WT} cells, albeit not statistically significant due to the variation in the dataset being greater than the difference from the observed induction and 0. There's a similar pattern of *IDO1* induction in the qRT PCR dataset, with IFNγ driving 3.1-FE in 501mel^{WT} and 33.1-FE in 501mel *AHR*$^{-/-}$ cells compared to no treatment (Fig. 5.1D). In the RNA Seq data set, there's not a significant difference in the induction of *IDO1* in 501mel *AHR*$^{-/-}$ cells between IFNγ-treatment and IFNγ+FICZ-treatment (Fig. 5.1C), nor is there a significant difference in the qRT PCR dataset (Fig. 5.1D). In the RNA Seq dataset, the abundance of *IDO1* transcripts increases from 0.24 NQ to 1.15 NQ in 501mel^{WT} when treated with IFNγ and FICZ compared to IFNγ-only (Fig. 5.1C), with 2.52-FI in the co-treatment sample compared to IFNγ-only sample of 501mel^{WT} in the qRT PCR dataset (Fig. 5.1D). With *IDO1* patterns of induction being congruent between the RNA-Seq and qRT PCR datasets, the validity of the RNA-Seq dataset with respect to *IDO1* induction has been confirmed which is reflective of the changes in IFNγ-response between these cells and conditions being equivalent in both.

5.2.2. The effect of FICZ on 501mel^{WT} and 501mel *AHR*$^{-/-}$ cell lines

501mel^{WT} cells, when treated with FICZ, respond with changes in gene expression. This is demonstrated with 117 (80 up, 37 down) statistically significant changes in the expression of genes in 501mel^{WT} cells before and after treatment with FICZ (Fig. 5.2A). While there are many genes whose changes in expression are statistically significant, there are only 15 (14 up, 1 down) genes with a significant change in expression in response to FICZ that is above 2-fold (Fig. 5.2A). This shows the AhR, in response to a canonical ligand, only affects the expression of a small battery of genes in 501mel^{WT} cells. In 501mel *AHR*$^{-/-}$ cells, however, there are no statistically significant changes in gene expression with and without FICZ (Fig. 5.2B). This is to be expected, as FICZ is thought to mediate all its effects on gene expression through the AhR, cells without the AhR should not show significant changes in gene expression. The relatively small number of genes induced in 501mel WT cells in response to FICZ-treatment may be due to basal excitation of the AhR from media-derived ligands driving low AhR-target gene expression in the absence of FICZ, reducing the number of significantly induced genes as their baseline expression may not be negligible in the absence of FICZ (Fig. 5.2E). Furthermore, this could also be a product of clonogenic differences between the WT and KO cell lines.

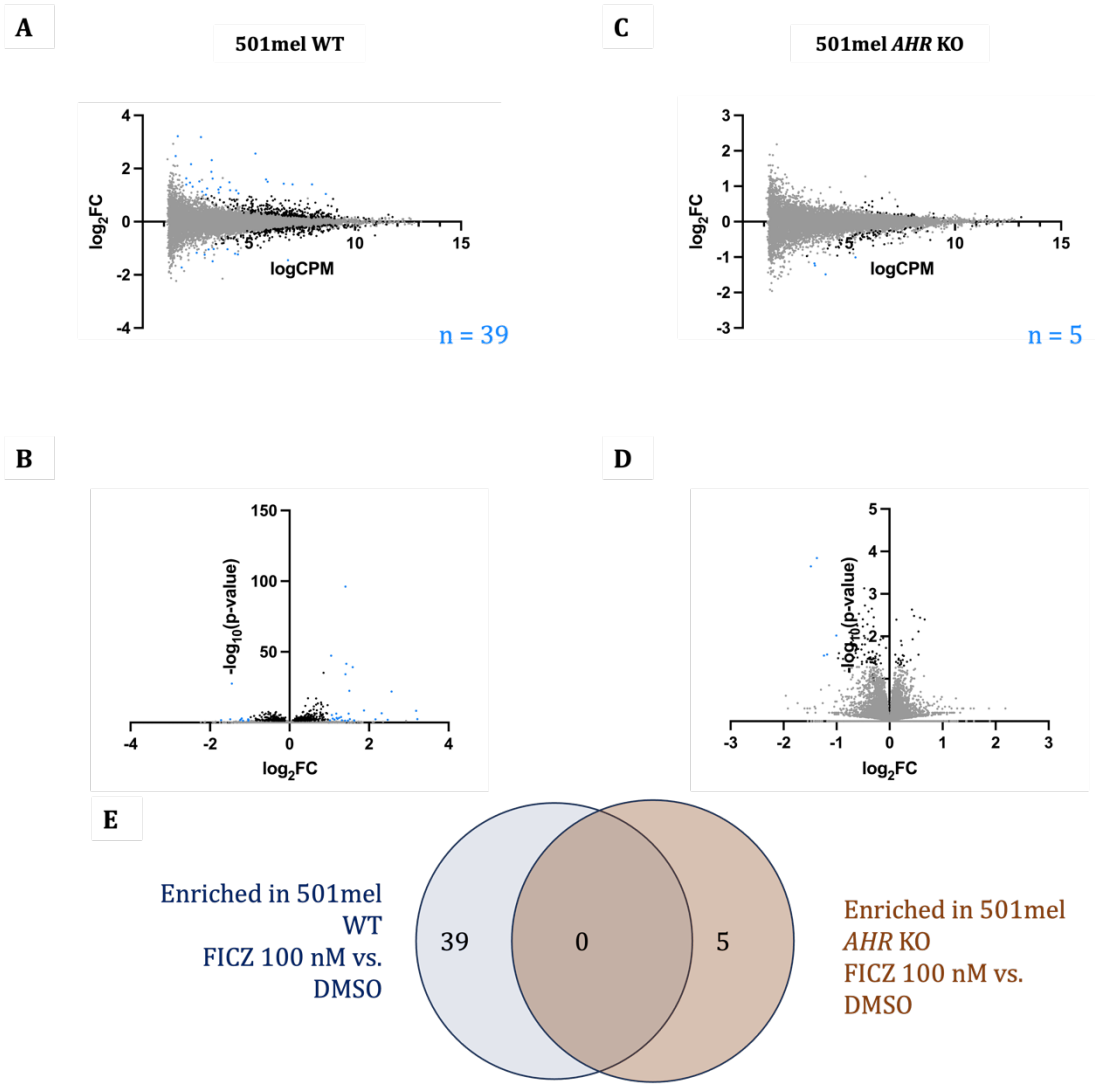

Figure 5.2. Distribution of differential gene expression in response to FICZ. Representations of differential expression of the transcriptome in response to 24-hours of FICZ 100 nM treatment in (A & B) 501mel WT and (C & D) 501mel *AHR* KO cells. Grey points are non-significant changes $p > 0.05$, Black points are statistically significant ($p < 0.05$) but not robustly effected ($FC < 2$), Blue points are statistically significant and robustly effected ($FC > 2$). A Venn diagram representing the overlap between significant and robustly induced genes between 501mel WT and *AHR* KO in response to FICZ 100 nM (E).

501mel^{WT} cells compared to 501mel *AHR*$^{-/-}$ cells without any stimulation, have 3184 significantly differentially expressed genes (1245 up, 1939 down) with some showing up to a 590-fold change (Fig. 5.3A). This result is surprising as it suggests the AhR is involved in regulation of expression of a significant proportion of the genome in its unstimulated state. This may be reflective of a combination of AhR transcription without stimulation, which was indicated as a possibility in the ChIP-Seq data with

genomic binding of the AhR without ligand in Chapter 3, and non-genomic interactions with components of signalling pathways, such as the NF-κB and IFNγ-signalling pathways as described in Chapter 2. Together, these data show the AhR has a central role in the homeostasis of cells, rather than simply acting as a ligand-activated environmental sensor triggered to mediate metabolism of toxins amongst other compounds. There are a greater number of statistically significant differences in gene expression between 501mel^{WT} and 501mel *AHR*$^{-/-}$ cells when stimulated with FICZ compared to no stimulation, 3184 (1328 down, 2084 up) vs. 3321 (1352 down, 2191 up) (Fig. 5.3B), with only 2634 of these being the same in both comparisons (Fig. 5.3C). It's, however, important to consider that due to these experiments being performed in a single clone, these differences may represent clonogenic differences between these samples rather than true biological differences driven solely by AhR-loss. To improve the reliability of these data, this experiment should be repeated in both more clones of 501mel *AHR*$^{-/-}$ cells and a greater variety of melanoma cell lines to ensure they are more relevant to melanoma. Of these differentially expressed genes between 501mel^{WT} and 501mel *AHR*$^{-/-}$ cells stimulated with FICZ, there are also more differences of greater magnitude with more genes showing at least 2-FC in expression between the transcriptomes of the two cell lines, 998 genes FICZ-treated vs. 882 untreated. This is expected, as 501mel^{WT} respond to FICZ and 501mel *AHR*$^{-/-}$ cells do not, one expects a greater difference between these cell lines when stimulated with an AhR ligand than without stimulation. Considering these data in light of the ChIP-Seq data of the previous chapter, it demonstrates that if these differences in gene expression between the 501mel^{WT} and *AHR*$^{-/-}$ cells are due solely to the AhR, the number of genes whose expression is affected by AhR-loss aren't likely being directly regulated by the AhR binding to their promoter, as only 725 peaks were observed in

the DMSO control condition. While a single binding event may regulate multiple genes, it's unlikely that 4,000 genes are differentially regulated by direct AhR binding to them. Rather at least some genes will be regulated indirectly by the AhR modulating expression of other TFs or transcriptional regulators.

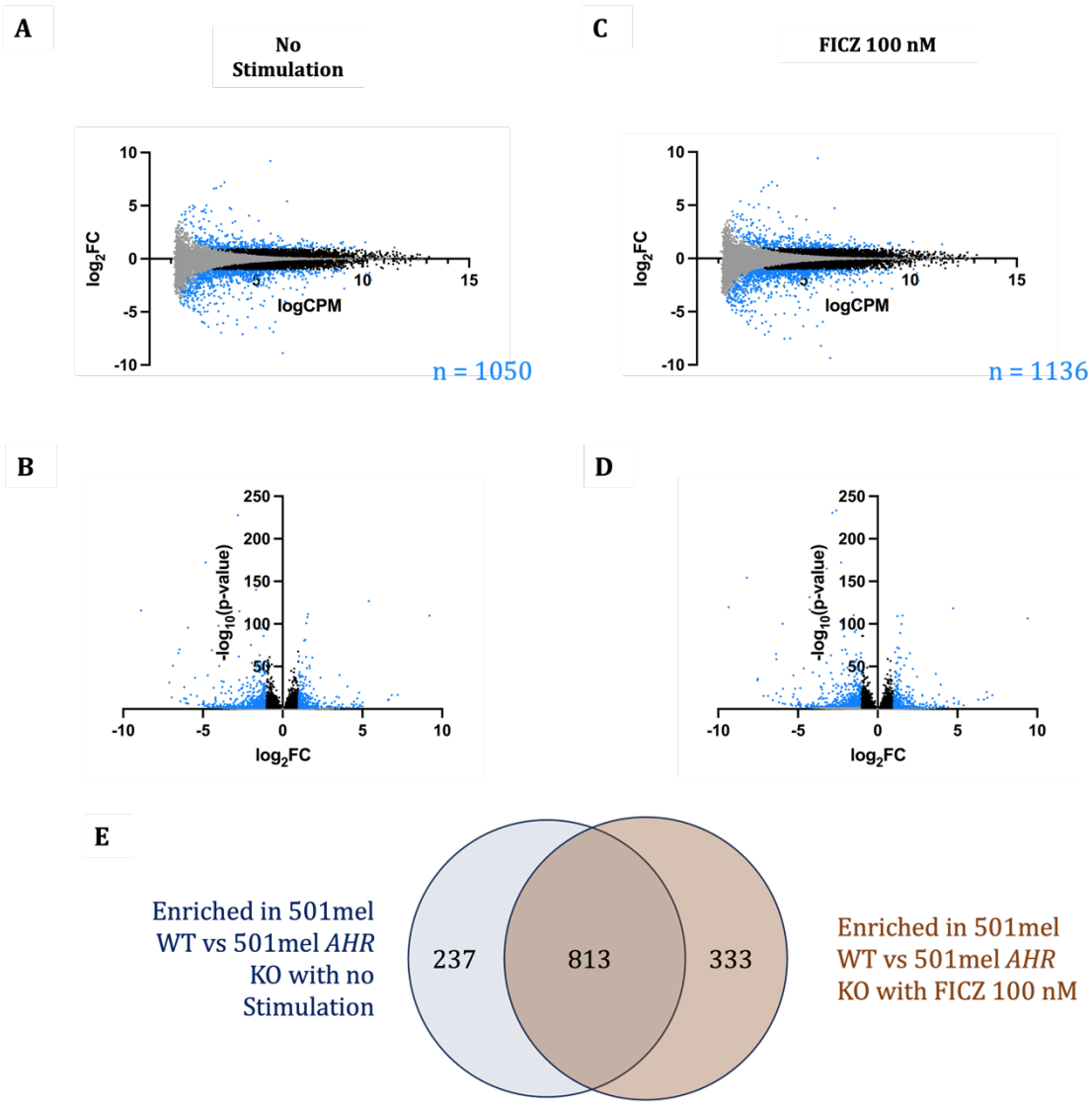

Figure 5.3. Distribution of differential gene expression between 501mel WT and *AHR* KO. Representations of differential expression of the transcriptome between 501mel WT and 501mel *AHR* KO under (A & B) no stimulation and (C & D) 24-hours of FICZ 100 nM stimulation. Grey points are non-significant changes $p > 0.05$, Black points are statistically significant ($p < 0.05$) but not robustly effected ($FC < 2$), Blue points are statistically significant and robustly effected ($FC > 2$). A Venn diagram representing the overlap between significant and robustly induced genes between 501mel WT and *AHR* KO in response to DMSO or FICZ 100 nM (E).

5.2.3. The effect of IFNγ on 501mel^{WT} and 501mel *AHR*$^{-/-}$ cell lines

When treated with IFNγ, 501mel^{WT} cells significantly upregulated the expression of 162 genes compared to unstimulated cells and significantly downregulated the expression of 57 genes (Fig. 5.4A). This is reflective of the canonical response to IFNγ in these cells, which is much more dysregulated in 501mel *AHR*$^{-/-}$ cells. In 501mel^{WT} cells, the most differentially expressed genes have no more than 120-FI in response to IFNγ-treatment, but in 501mel *AHR*$^{-/-}$ cells I see 21 genes with at least 120-FI in response to IFNγ-treatment (Fig. 5.4B). There are also more genes with significantly changed expression in response to IFNγ in the 501mel *AHR*$^{-/-}$ cells, with 765 significantly induced genes and 805 significantly repressed genes (Fig. 5.4B). There are also many more genes in the 501mel *AHR*$^{-/-}$ cells displaying at least 2-FC in response to IFNγ (261 up and 75 down) than in the 501mel^{WT} cells (70 up and 1 down) (Fig. 5.4B). Together, these data demonstrate the AhR is clearly modulating the IFNγ-response which, in turn, is regulating many genes across the transcriptome, likely beyond direct targets of the IFNγ pathway. There are few IFNγ-response genes only differentially expressed in 501mel WT, which indicates that these effects are not directly mediated by the AhR, but as alluded to in Chapter 3, I believe this is indicative of a role of the AhR in modulating the magnitude of the AhR response in it's unstimulated state which would manifest as a greater dysregulation of IFNγ-response gene expression in 501mel *AHR*$^{-/-}$ cells rather than in 501mel WT cells (Fig. 5.4F).

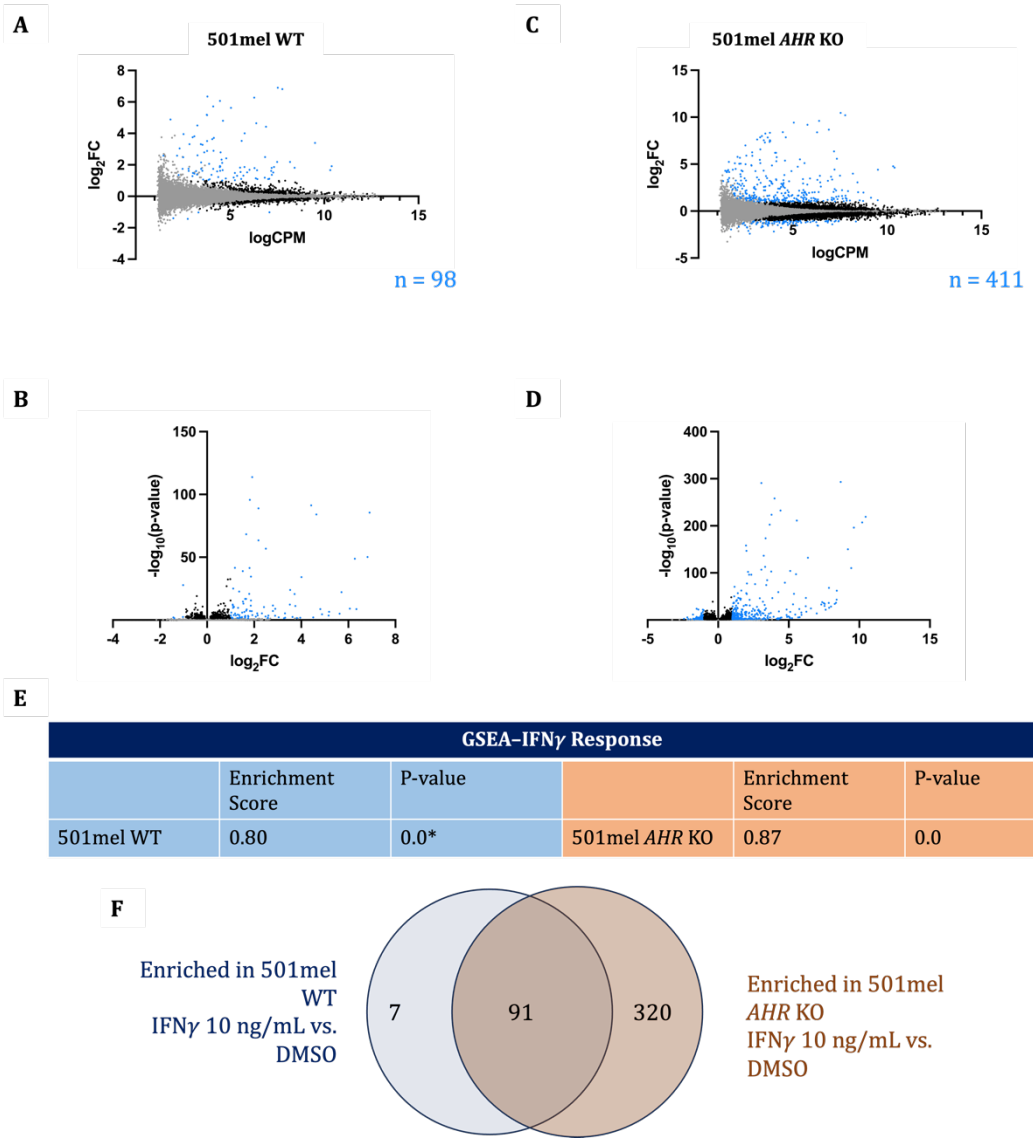

E

GSEA–IFNγ Response					
	Enrichment Score	P-value		Enrichment Score	P-value
501mel WT	0.80	0.0*	501mel *AHR* KO	0.87	0.0

Figure 5.4. Distribution of differential gene expression in response to IFNγ. Representations of differential expression of the transcriptome in response to 24-hours of IFNγ 10 ng/mL treatment in (A & B) 501mel WT and (C & D) 501mel *AHR* KO cells. Grey points are non-significant changes $p > 0.05$, Black points are statistically significant ($p < 0.05$) but not robustly effected ($FC < 2$), Blue points are statistically significant and robustly effected ($FC > 2$). A table of GSEA of the IFNγ -response pathway in 501mel WT and 501mel *AHR* KO in response to IFNγ (E). A Venn diagram representing the overlap between significant and robustly induced genes between 501mel WT and *AHR* KO in response to IFNγ 10 ng/mL (F).

Comparison between the transcriptomes of 501mel^{WT} and 501mel *AHR*$^{-/-}$ cells under no stimulation revealed there's a huge baseline difference in the transcriptomes of both cell lines, 3184 genes differentially expressed, 882 genes with more than 2-fold change (Fig. 5.5A). This is reflected in their response to IFNγ, with 3320 genes

significantly differentially expressed, but more importantly, many genes displaying at least 2-FC in their induction between the cell lines, 965 genes with more than 2-fold change (Fig. 5.5B). Between these two groups, only 2217 of the more than 3000 genes are the same, representing differences between the cell lines independent of stimulation (Fig. 5.5C), with 967 genes uniquely enriched in the unstimulated comparison vs. 1103 uniquely enriched genes in the IFNγ-treated comparison (Fig. 5.5C). These data demonstrate the AhR is an integral part of the transcriptome, both in the absence and presence of stimulants.

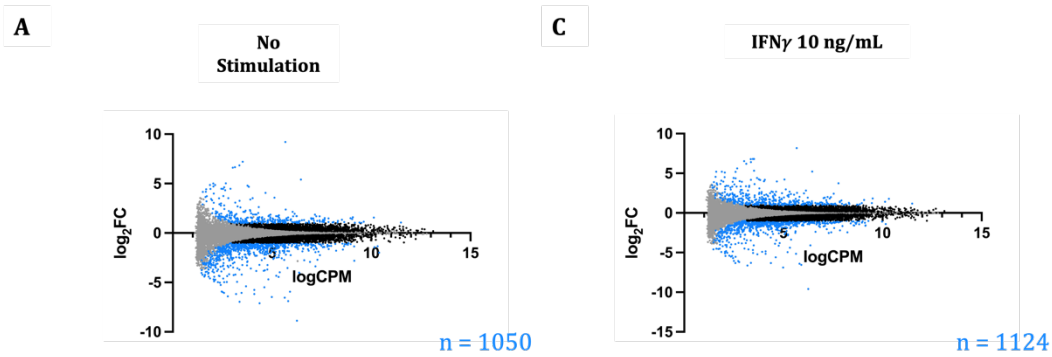

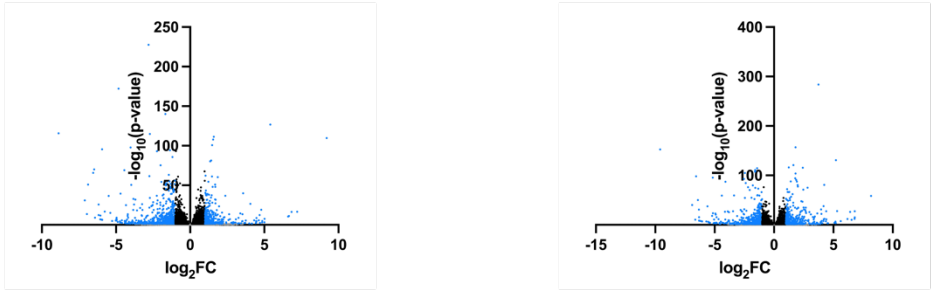

E

GSEA–IFNγ Response					
	Enrichment Score	Nominal P-value		Enrichment Score	Nominal P-value
DMSO	-0.43	0.0*	IFNγ 10 ng/mL	0.67	0.0

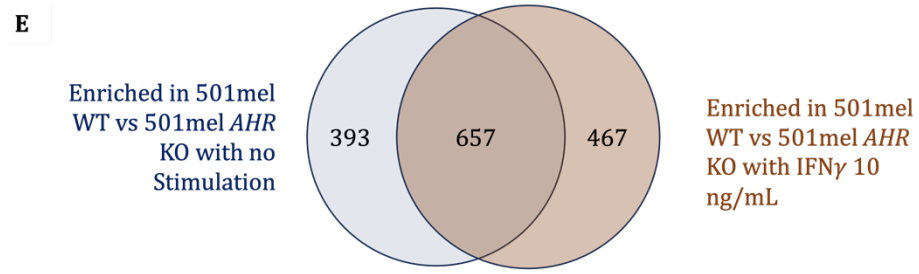

Figure 5.5. Distribution of differential gene expression between 501mel WT and *AHR* KO. Representations of differential expression of the transcriptome between 501mel WT and 501mel *AHR* KO under (A & B) no stimulation and (C & D) 24-hours of IFNγ 10 ng/mL stimulation. Grey points are non-significant changes $p > 0.05$, Black points are statistically significant ($p < 0.05$) but not robustly effected ($FC < 2$), Blue points are statistically significant and robustly effected ($FC > 2$). A table of GSEA of the IFNγ -response pathway in response to DMSO and IFNγ comparing 501mel*AHR* KO to 501mel WT (E). A Venn diagram representing the overlap between significant and robustly induced genes between 501mel WT and *AHR* KO in response to IFNγ 10 ng/mL (F).

501mel^{WT} cells co-treated with IFNγ and FICZ have a greater number of significantly differentially expressed genes than when treated with either stimulant, FICZ and

IFNγ: 387 genes, FICZ: 117 genes, IFNγ: 219 genes (Fig. 5.6A, 5.2A, 5.4A). Co-treatment of FICZ and IFNγ-stimulated a greater number of genes to undergo at least 2-FC in expression than either stimulant separately, 111 genes compared to 71 genes in response to IFNγ and 15 genes in response to FICZ. There was a larger magnitude change in gene expression with co-treatment in 501mel^{WT} cells driving at least a maximum fold change of 131.9 in *Guanylate Binding Protein 1 (GBP1)* compared to 119.5-fold change in *GBP1* in the FICZ-only treated cells, whereas the highest magnitude of differential expression in 501mel^{WT} cells in FICZ is 9.08-fold change in *Leucine Rich Glioma Inactivated 3 (LGI3)*. This demonstrates that stimulation of WT cells with both IFNγ and FICZ produces a synergistic effect on the transcriptome rather than an additive effect, showing the AhR is an effector of both pathways. The response to FICZ-only in 501mel^{WT} cells also significantly suppresses the expression of 1 gene (*Matrix Gla Protein*) with at least a two-fold change (Fig. 5.2A), which is the same sole gene to be suppressed by at least 50% in response to FICZ in IFNγ-treated cells (Fig. 5.6C). This is further demonstrated by the response of 501mel *AHR*$^{-/-}$ cells, where treatment with FICZ-only doesn't produce a significant change in the expression of any genes (Fig. 5.2B). 501mel *AHR*$^{-/-}$ cells treated with IFNγ-only and IFNγ with FICZ generates similar patterns of gene expression with 1 significantly differentially expressed gene, *Promythosin Alpha* (Fig. 5.6D) and with IFNγ driving a greater upregulation of more genes in 501mel *AHR*$^{-/-}$, 765 genes, than IFNγ-treatment

of 501mel^{WT} cells, 162 genes (Fig. 5.4B, 5.6B). There's not a significant difference of any gene with more than 2-FC between 501mel *AHR*$^{-/-}$ IFNγ and 501mel *AHR*$^{-/-}$ FICZ

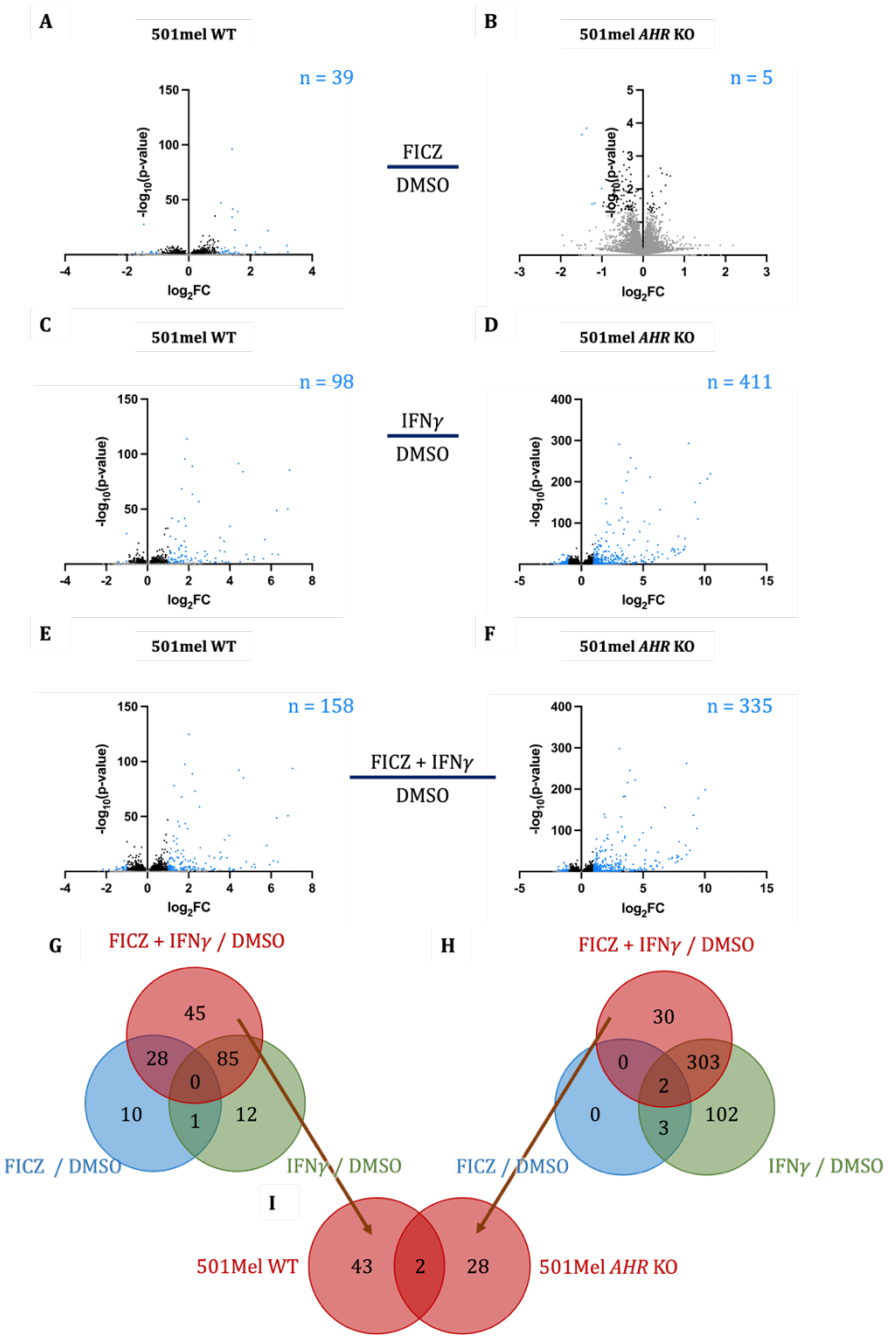

Figure 5.6. Distribution of differential gene expression in response to IFNγ and FICZ. Representations of differential expression of the transcriptome in response to 24-hours of FICZ 100 nM compared to DMSO in 501mel WT (A) and 501mel *AHR* KO (B), in response to 24-hours of IFNγ 10 ng/mL compared to DMSO in 501mel WT (C) and 501mel *AHR* KO (D), and in response to 24-hours of FICZ 100 nM IFNγ 10 ng/mL co-treatment in 501mel WT (E) and 501mel *AHR* KO (F). Grey points are non-significant changes $p > 0.05$, Black points are statistically significant ($p < 0.05$) but not robustly effected ($FC < 2$), Blue points are statistically significant and robustly effected ($FC > 2$). Venn diagrams demonstrating the overlap between significantly ($p < 0.05$) and robustly ($FC > 2$) induced genes in response to each treatment compared to DMSO in 501mel WT (G) and 501mel *AHR* KO (H) cells. A Venn diagram showing the overlap between the genes significantly ($p < 0.05$) and robustly ($FC > 2$) induced genes that are only enriched under co-treatment with FICZ 100 nM and IFNγ 10 ng/mL (I).

an IFNγ treated cells (Fig. 5.6D).

5.2.4. Co-validation of RNA-Seq and ChIP-Seq data

To confirm validity and compliance of my ChIP-Seq and RNA-Seq data, both of which are approaches to characterising the action of TFs, I examined how congruent they are at target genes. I generated a gene set of AhR Bound genes, defined as genes nearest peaks found in both FICZ-treated ChIP-Seq replicates from the previous chapter. I performed GSEA on the 501mel^{WT} cells treated with FICZ compared to DMSO treated cells and found enrichment of 1.60 NES (Fig. 5.7A). I generated a heat map of the 100 most differentially up and down regulated genes with associated ChIP-seq peaks between the 501mel^{WT} control and FICZ-treated samples (Fig. 5.7B). Analysis of transcriptomic changes in 501mel^{WT} in response to FICZ shows there are only 10 statistically significant ($p < 0.05$) substantially (>2FC) downregulated gene in response to FICZ (Fig. 5.2A) none of which appear in the AhR bound gene set. The difference in downregulated genes in response to FICZ reflects a small change in gene absolute induction which is statistically insignificant, but high relative induction in the heat map (Fig. 5.7A). However, more genes are significantly upregulated in response to FICZ treatment in 501mel^{WT} cells (Fig. 5.2A), which aligns with my understanding of FICZ being an AhR agonist that stimulates expression of polycyclic aryl hydrocarbon-metabolising enzymes. I examined genomic loci of the top 4 most enriched genes in response to FICZ treatment in 501mel^{WT} cells using the UCSC genome browser to visualise my ChIP-Seq data.

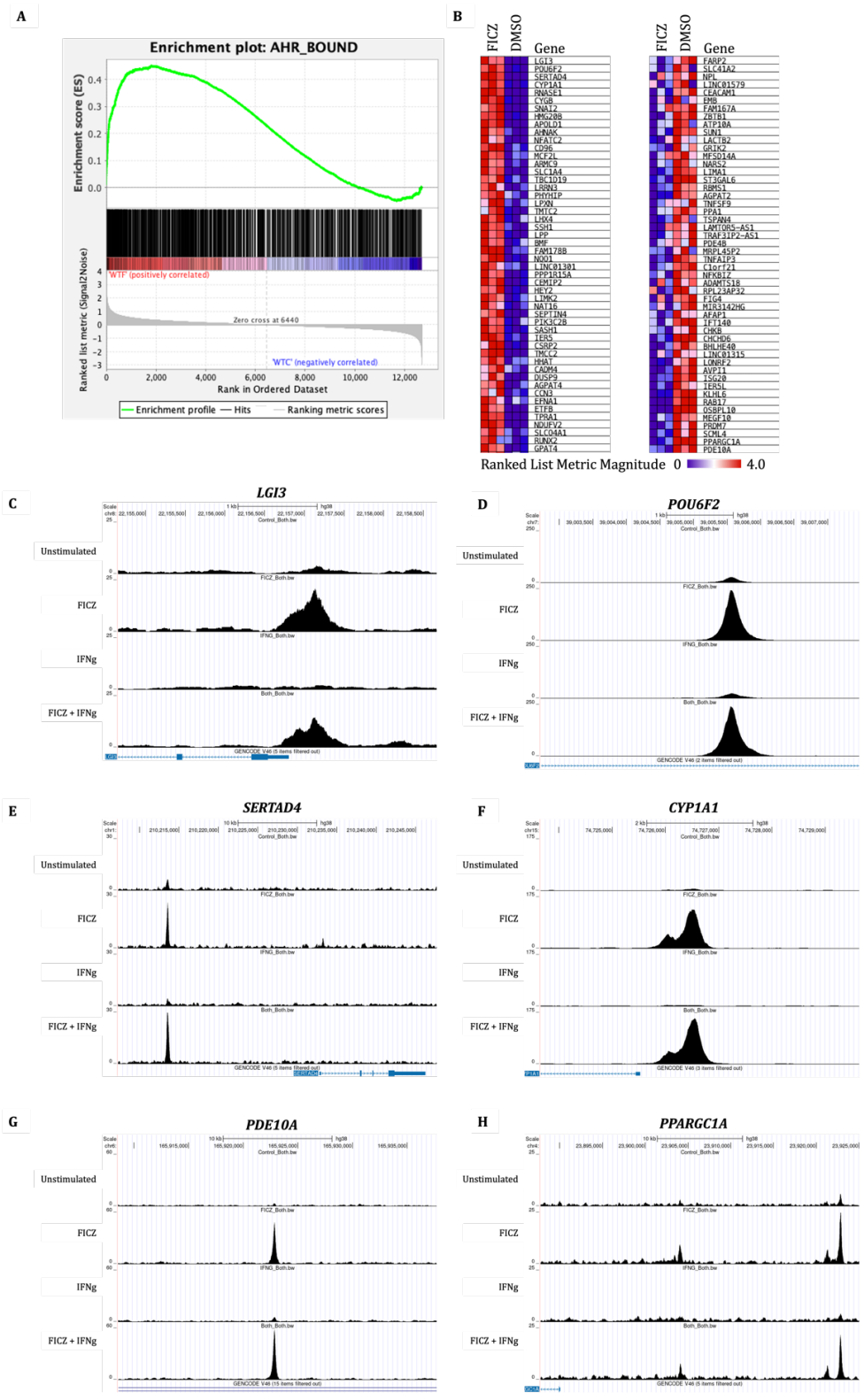

Figure 5.7. Co-validation of RNA-Seq and ChIP-Seq data. A GSEA plot of 501mel WT cells treated with FICZ 100 nM or DMSO using a gene list from the genes with associated peaks in both replicates of the 501mel FICZ treated ChIP-seq experiment (A). A heat map of the 50 most positively ascending and most negatively differentially expressed genes descending between 501mel WT DMSO and FICZ 100 nM 24-hours stimulated cells, left- and right-hand sides, respectively (B). UCSC track data from the AhR ChIP Seq experiment for the 4 most positively enriched genes in the FICZ treated samples compared to the control samples in 501mel WT cells *LGI3* (C), *POU6F2* (D), *SERTAD4* (E), and *CYP1A1* (F). UCSC track data from the AhR ChIP Seq experiment for the 2 most negatively enriched genes in the FICZ treated samples compared to the control samples in 501mel WT cells *PDE10A* (G), *PPARGC1A* (H),

The most upregulated gene in response to FICZ treatment is *Leucine Rich Repeat LGI*

family member 3 (*LGI3*). The AhR shows significant FICZ-dependent accumulation at the promoter of *LGI3*, with peak magnitude rising from 4-Fold Enrichment (FE) without stimulation to 21-FE upon FICZ-treatment (Fig. 5.7B). This is a 5.3-fold change in AhR accumulation at this locus which is driving average abundance of *LGI3* transcripts from 1.44 NQ to 14.2 NQ, 10-FC in gene induction. Binding of the AhR to *POU class 6 homeobox 2* (*POU6F2*) increases 9.4-fold in response to FICZ treatment, rising from a peak of 26-FE to 244-FE in 501mel^{WT} (Fig. 5.7C), this is reflected in 12.5-fold change in gene expression from 0.33 NQ to 4.15 NQ upon FICZ treatment (Fig. 5.7A). FICZ treatment drives 4-fold greater accumulation of the AhR at an enhancer of *SERTA Domain Containing 4* (*SERTAD4*) (Fig. 5.7D) which drives 5.2-FI in *SERTAD4* transcript accumulation. Binding of the AhR to the *CYP1A1* promoter upon FICZ-treatment compared to no stimulation is 21.2-fold greater (Fig. 5.7E) which stimulates 6-FI in *CYP1A1* transcript abundance from 8.23 NQ to 49.8 NQ.

Increases in binding of the AhR to these genes in response to FICZ detected through ChIP-Seq and concomitant increase in the abundance of transcripts of these genes detected through RNA-Seq, demonstrates data from these experiments align and reflect both datasets being reliable to draw conclusions from on the biological role of the AhR. Discrepancies between the magnitude of AhR binding to the gene and observed changes in transcript abundance are to be expected, as it's well documented that magnitude of ChIP-seq peak is not directly correlated to its effects on transcription initiation, with gene expression regulation being an integrative process between multiple specific and general TFs (Compe & Egly, 2021; Lickwar et al., 2012). However, these data provide exemplar instances of genes with direct induction of transcription in response to the AhR. Genes significantly differentially expressed in

response to FICZ, IFNγ, or AhR-loss which do not have any associated peaks in the corresponding ChIP-seq data, I'm confident reflects instances of indirect gene regulation.

5.2.5. Indirect regulation of IFNγ-response genes

I assessed expression of IFNγ-response genes in the RNA-Seq data, whose expression I had shown to be modulated by the AhR in qRT PCR data previously (Fig. 3.5), to confirm the pattern of AhR-mediated expression I had observed is maintained in the RNA-seq dataset. *IDO1* expression is not inducible in either 501mel^{WT} or 501mel *AHR*$^{-/-}$ cell lines without IFNγ-treatment (Fig. 5.8A). There's a much greater induction of *IDO1* in 501mel *AHR*$^{-/-}$ cells than in 501mel^{WT} cells (Fig. 5.8A). The expression of *ATF4*, however, is not significantly altered in response to IFNγ or FICZ, except for between the induction in response to FICZ in 501mel^{WT}, 1336 relative abundance, compared to 955.3 relative abundance in 501mel *AHR*$^{-/-}$ cells (Fig. 5.8B). The largely non-responsive expression of *ATF4* was also demonstrated in my qRT PCR data on these cells (Fig. 3.5C). Expression of *CD274* is greater in 501mel *AHR*$^{-/-}$ cells compared to 501mel^{WT} cells under all conditions (Fig. 5.8C). There's a greater relative induction of *CD274* expression in response to IFNγ in these cells also, with IFNγ-treatment of 501mel *AHR*$^{-/-}$ producing 2.57-FI of *CD274*, and only a 1.5-FI in 501mel^{WT} cells (Fig. 5.8C). *EIF2AK2* expression is significantly different between 501mel^{WT} and 501mel *AHR*$^{-/-}$ cells under all conditions, however, expression is lower in 501mel *AHR*$^{-/-}$ cells than 501mel^{WT} cells without IFNγ-stimulation, but greater in the presence of IFNγ-stimulation (Fig. 5.8D). This pattern of depressed expression in the 501mel *AHR*$^{-/-}$ compared to WT without IFNγ is also demonstrated in the qRT-PCR data (Fig. 3.5F).

Expression of *IRF1* is not detected at significant levels in the 501mel^{WT} or 501mel *AHR*$^{-/-}$ cell lines without IFNγ-stimulation, however, there's significantly greater induction of *IRF1* expression in response to IFNγ in 501mel *AHR*$^{-/-}$ cells compared to 501mel^{WT} cells (Fig. 5.8E). As I demonstrated Chapter 3, the AhR doesn't bind to the promoter or within a genomic distance one would expect to find an enhancer element of any of these genes (Fig. 4.7). I'm confident the effects of the AhR on IFNγ-signalling in 501mel cells aren't mediated through the AhR directly activating transcription of these genes and is instead evidence of an indirect effect. My hypothesised model of indirect IFNγ-signalling pathway regulation via the AhR is summarised in Fig. 3.16 and involves the interaction of the AhR with the NF-κB signalling pathway to affect the expression of components of the IFNγ-signalling pathway, not through direct genomic binding events, as evidenced here.

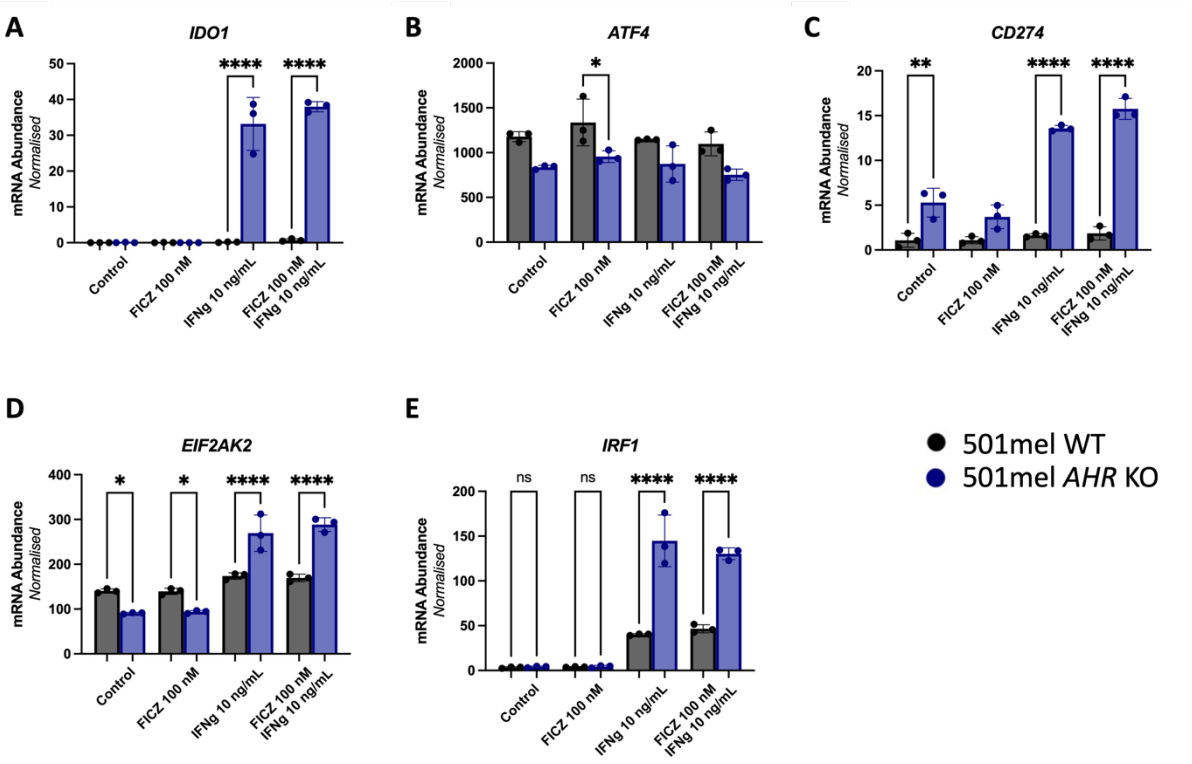

Figure 5.8. Accumulation of IFNγ response gene transcripts in response to stimulation of 501mel WT and 501mel *AHR* KO cell lines. Using the read data from the RNA-Seq experiment I determined the relative abundance of reads of each treatment condition; control, FICZ 100 nM, IFNγ 10 ng/mL, and FICZ 100 nM IFNγ 10 ng/mL in 501mel WT and 501mel *AHR* KO cell lines. Genes assessed are (A) *IDO1*, (B) *ATF4*, (C) *CD274*, (D) *EIF2AK2*, and (E) *IRF1*. Ad-hoc test: Ordinary One-way ANOVA, post-hoc test: Tukey-Kramer test for multiple comparisons which inherently corrects for multiple comparisons P > 0.05: ns, P < 0.05: *, P < 0.01: **, P < 0.001: ***, P < 0.0001: ****. Biological repeats = 3.

5.2.6. Gene Set Enrichment Analysis: Inflammatory Signalling

To analyse pathways that may be differentially expressed between each cell line or between conditions, GSEA was performed. GSEA provides information on how 50 hallmark pathways, each composed of multiple genes associated with a biological process, are enriched between two sets of expression data. GSEA is a useful tool for assessment of the expression of these pathways but can be flawed with these Hallmark gene set names often being misleading regarding the genes contained within. Comparison of gene expression in response to IFNγ in 501mel^{WT} cells, demonstrates the IFNγ-response in these cells is intact and behaving as expected.

Analysis of the 50 most upregulated genes in 501mel cells in response to IFNγ-treatment shows significant increases in the expression of canonical IFNγ-response genes; *Interferon-induced transmembrane protein 1* (*IFITM1*), *Serpin family G member 1* (*SERPING1*), *IRF1*, and *IFITM2* as a non-exhaustive list (Fig. 5.9A). A summary of all GSEA hallmark pathways, their normalised enrichment and p-values is provided (Fig. 5.9B). GSEA of 501mel^{WT} cells treated with IFNγ shows a strong enrichment of the IFNγ-response pathway in response to IFNγ, 1.51 NES (Fig. 5.9C). There's also enrichment of the TNF signalling via NF-κB pathway in response to IFNγ-stimulation, 1.44 NES, albeit to a lesser extent than the IFNγ-response pathway[‡‡] (Fig. 5.9D). Stimulation of 501mel cells with IFNγ does produce enrichment of a broad inflammatory response signature with a score of 1.74 NES, which demonstrates the broad range of gene induction occurring in response to IFNγ in WT cells[§§] (Fig. 5.9E). There's also enrichment of the IFN-alpha (IFNα) response in 501mel^{WT} cells to IFNγ, weaker than the IFNγ-response, 1.42 NES vs. 1.51 NES (Fig. 5.9F). This is likely due to overlaps between the two gene sets, with 60/81 IFNα genes being also found in the 141 genes that define the IFNγ gene set. This may be indicative of both signalling pathways being mediated through activation of STAT1 downstream of IFNGR1/2 in IFNγ-signalling and IFNAR1/2 in IFNα-signalling, although, this wouldn't account for the difference in magnitude of enrichment of these pathways. There's also enrichment of other STAT signalling pathways IL2 STAT5 signalling, 1.34 NES (Fig. 5.9G) and IL6-JAK-STAT3 signalling 1.63 NES (Fig. 5.9H) in response to IFNγ, which may be reflective of crosstalk between STAT signalling pathways which is a known behaviour

[‡‡] IFNγ gene set, 141 genes. TNF gene set, 143 genes. 19 genes are present in both gene sets.
[§§] IFNγ gene set, 141 genes. Inflammatory Response gene set, 91 genes. 21 genes are present in both gene sets.

of IFN signalling pathways given there's limited overlap between the gene lists of each of these hallmarks pathways[***]. The IL2-STAT5 pathway shows enrichment in both the DMSO and IFNγ-treated cells, suggesting that this is not a reliable enrichment to consider (Fig. 5.9G).

[***] IFNγ gene set, 141 genes; Il2-STAT5, 135 genes; 13 genes are present in both gene sets. IFNγ gene set, 141 genes; Il6-JAK-STAT3, 51 genes; 14 genes are present in both gene sets. Il2-STAT5, 135 genes; Il6-JAK-STAT3, 51 genes; 7 genes are present in both gene sets.

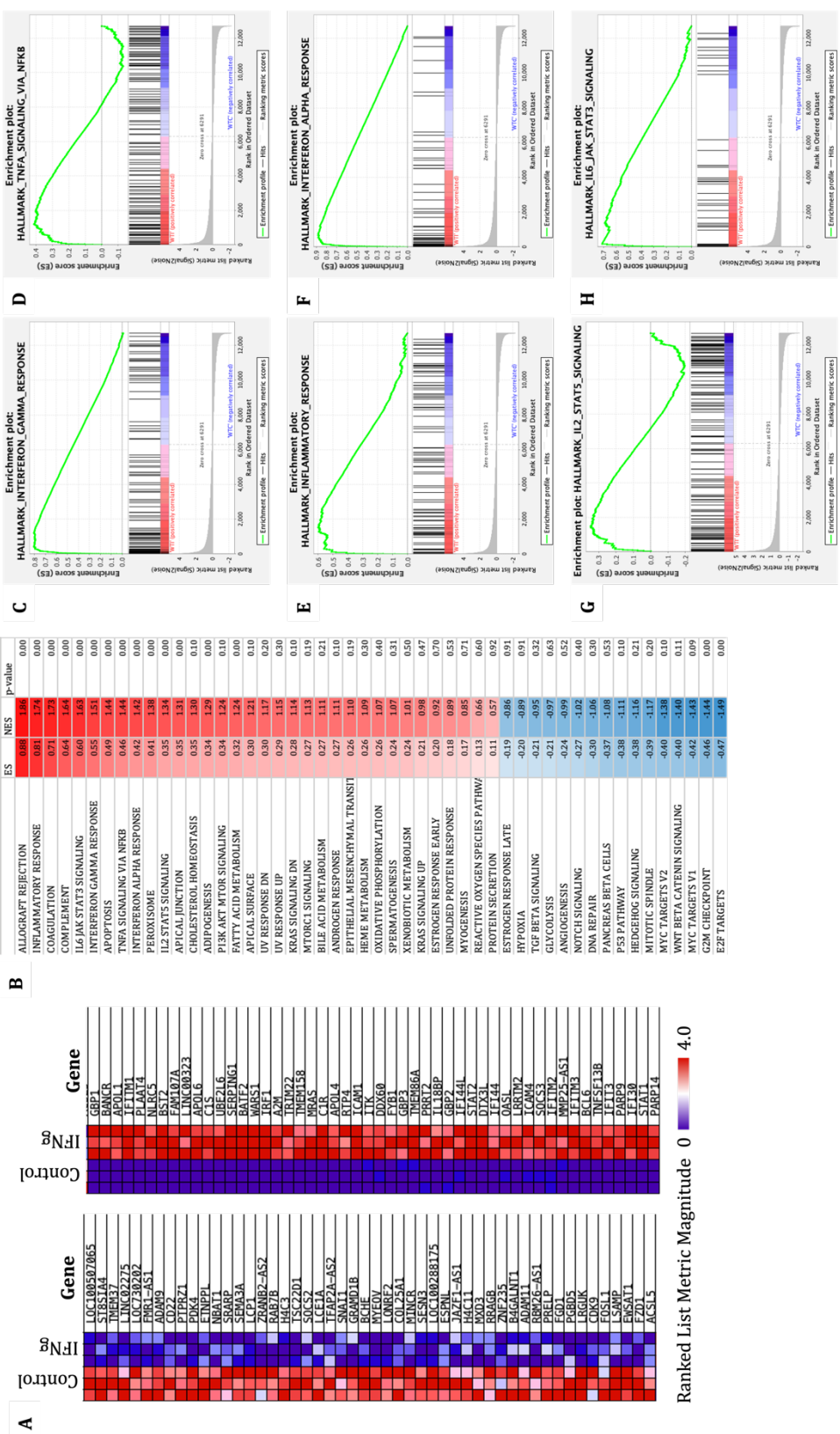

Figure 5.9. GSEA of 501mel WT cells in response to IFNγ stimulation. GSEA of 501mel cells with and without 24-hours of IFNγ 10 ng/mL treatment. (A) LHS 50 most enriched genes in 501mel WT unstimulated cells compared to IFNγ-treated cells RHS 50 most enriched genes in 501mel WT cells in response to IFNγ treatment compared to no treatment. Enrichment Score: ES, Normalised Enrichment Score: NES. Summary of all 50 GSEA Hallmark Gene Sets (B). GSEA hallmark summaries of (C) Interferon Gamma Response, (D) TNF Signalling via NF-κB, (E) Inflammatory Response, (F) Interferon Alpha Response, (G) IL2-STAT5 Signalling, and (H) IL6-JAK-STAT3 Signalling, where a positive score represents an enrichment in the IFNγ-treated sample (WTI) in red, and a negative score represents an enrichment in the DMSO control cells (WTC) in blue.

The response of 501mel *AHR*$^{-/-}$ cells to IFNγ compared to no treatment is similar to changes observed in 501mel^{WT} cells, albeit with greater expression of genes associated with IFNγ-responses. This is evident in greater numbers of key IFNγ-

response genes being amongst the most highly differentially enriched in 501mel *AHR*$^{-/-}$ treated with IFNγ (Fig. 5.10A) when compared to changes in 501mel^{WT} cells. This includes *IDO1* being one of 50 most upregulated genes in response to IFNγ in 501mel *AHR*$^{-/-}$ cells, but not in 501mel^{WT} (Fig. 5.10A). Summary of all GSEA hallmark pathways, their normalised enrichment and p-values is provided (Fig. 5.10B). Enrichment of the IFNγ-response in 501mel *AHR*$^{-/-}$ has a magnitude of 1.64 NES, representing a very robust induction of this hallmark pathway (Fig. 5.10C), more so than in 501mel^{WT} cells with 1.51 NES (Fig. 5.9C). Magnitude of TNF signalling via NF-κB is also slightly more robustly enriched in the IFNγ treated 501mel *AHR*$^{-/-}$ compared to WT cells with a magnitude of 1.78 NES (Fig. 5.10D) compared to 1.44 NES (Fig. 5.9D). Enrichment of the general inflammatory in 501mel *AHR*$^{-/-}$ cells treated with IFNγ compared to no treatment is 1.88 NES (Fig. 5.10E) greater than in 501mel^{WT} cells (Fig. 5.9E). Enrichment of the IFNα pathway in IFNγ-treated cells is the same in both 501mel *AHR*$^{-/-}$ and 501mel^{WT} cells, (1.40 NES (Fig. 5.10F) vs. 1.42 NES (Fig. 5.10F)), highlighting AhR-mediated effects on IFNγ-signalling appears to be limited to significant changes in IFNγ and NF-κB signalling pathways. This is supported with similar relative enrichments of other STAT signalling pathways: IL2-STAT5 and IL6-JAK-STAT3, between the 501mel^{WT} and *AHR*$^{-/-}$ cell lines with a magnitude of 1.34 NES and 1.63N ES in response to IFNγ in the 501mel^{WT} cells (Fig. 5.9G, 5.9H) and 1.59 NES and 1.67 NES in the 501mel *AHR*$^{-/-}$ cells (Fig. 5.10G, 5.10H). These data support my previous finding, where AhR-loss drives a greater response to IFNγ which may be mediated through perturbations in the NF-κB signalling pathways.

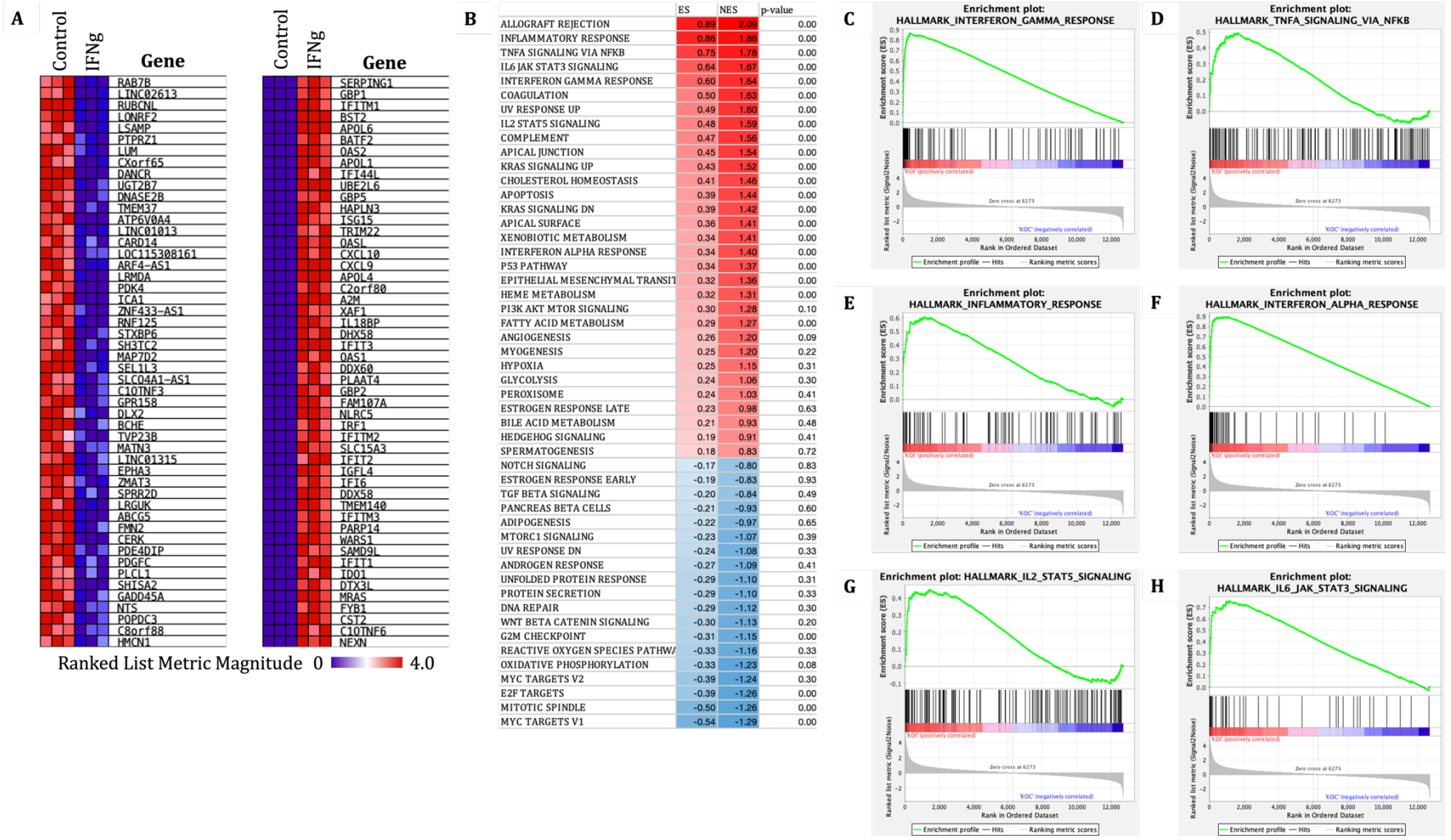

	ES	NES	p-value
ALLOGRAFT REJECTION	0.89	2.09	0.00
INFLAMMATORY RESPONSE	0.86	1.88	0.00
TNFA SIGNALING VIA NFKB	0.75	1.78	0.00
IL6 JAK STAT3 SIGNALING	0.64	1.67	0.00
INTERFERON GAMMA RESPONSE	0.60	1.64	0.00
COAGULATION	0.50	1.63	0.00
UV RESPONSE UP	0.49	1.60	0.00
IL2 STAT5 SIGNALING	0.48	1.59	0.00
COMPLEMENT	0.47	1.56	0.00
APICAL JUNCTION	0.45	1.54	0.00
KRAS SIGNALING UP	0.43	1.52	0.00
CHOLESTEROL HOMEOSTASIS	0.41	1.46	0.00
APOPTOSIS	0.39	1.44	0.00
KRAS SIGNALING DN	0.39	1.42	0.00
APICAL SURFACE	0.36	1.41	0.00
XENOBIOTIC METABOLISM	0.34	1.41	0.00
INTERFERON ALPHA RESPONSE	0.34	1.40	0.00
P53 PATHWAY	0.34	1.37	0.00
EPITHELIAL MESENCHYMAL TRANSIT	0.32	1.36	0.00
HEME METABOLISM	0.32	1.31	0.00
PI3K AKT MTOR SIGNALING	0.30	1.28	0.10
FATTY ACID METABOLISM	0.29	1.27	0.00
ANGIOGENESIS	0.26	1.20	0.09
MYOGENESIS	0.25	1.20	0.22
HYPOXIA	0.25	1.15	0.31
GLYCOLYSIS	0.24	1.06	0.30
PEROXISOME	0.24	1.03	0.41
ESTROGEN RESPONSE LATE	0.23	0.98	0.63
BILE ACID METABOLISM	0.21	0.93	0.48
HEDGEHOG SIGNALING	0.19	0.91	0.41
SPERMATOGENESIS	0.18	0.83	0.72
NOTCH SIGNALING	-0.17	-0.80	0.83
ESTROGEN RESPONSE EARLY	-0.19	-0.83	0.93
TGF BETA SIGNALING	-0.20	-0.84	0.49
PANCREAS BETA CELLS	-0.21	-0.93	0.60
ADIPOGENESIS	-0.22	-0.97	0.65
MTORC1 SIGNALING	-0.23	-1.07	0.39
UV RESPONSE DN	-0.24	-1.08	0.33
ANDROGEN RESPONSE	-0.27	-1.09	0.41
UNFOLDED PROTEIN RESPONSE	-0.29	-1.10	0.31
PROTEIN SECRETION	-0.29	-1.10	0.33
DNA REPAIR	-0.29	-1.12	0.30
WNT BETA CATENIN SIGNALING	-0.30	-1.13	0.20
G2M CHECKPOINT	-0.31	-1.15	0.00
REACTIVE OXYGEN SPECIES PATHWA	-0.33	-1.16	0.33
OXIDATIVE PHOSPHORYLATION	-0.33	-1.23	0.08
MYC TARGETS V2	-0.39	-1.24	0.30
E2F TARGETS	-0.39	-1.26	0.00
MITOTIC SPINDLE	-0.50	-1.26	0.00
MYC TARGETS V1	-0.54	-1.29	0.00

Figure 5.10. GSEA of 501mel *AHR* KO cells in response to IFNγ stimulation. GSEA of 501mel *AHR* KO cells with and without 24-hours of IFNγ 10 ng/mL treatment. (A) LHS 50 most enriched genes in 501mel *AHR* KO unstimulated cells compared to IFNγ-treated cells RHS 50 most enriched genes in 501mel *AHR* KO cells in response to IFNγ treatment compared to no treatment. Enrichment Score: ES, Normalised Enrichment Score: NES. Summary of all 50 GSEA Hallmark Gene Sets (B). GSEA hallmark summaries of (C) Interferon Gamma Response, (D) TNF Signalling via NF-κB, (E) Inflammatory Response, (F) Interferon Alpha Response, (G) IL2-STAT5 Signalling, and (H) IL6-JAK-STAT3 Signalling, where a positive score represents an enrichment in the IFNγ-treated sample (KOI) in red, and a negative score represents an enrichment in the DMSO control cells (KOC) in blue.

Direct comparison between 501mel *AHR*$^{-/-}$ and 501mel^{WT} cells in response to IFNγ demonstrates that 501mel *AHR*$^{-/-}$ cells are enriched for their response to IFNγ and related pathways (Fig. 5.11). Amongst the top 50 most differentially enriched genes in 501mel *AHR*$^{-/-}$ cells treated with IFNγ, compared with 501mel^{WT} cells treated with IFNγ, are many canonical IFNγ-response genes including, but not limited to; *CXCL10*, *SERPING1*, *2'-5'-oligoadenylate synthetase 2* (*OAS2*), *IDO1*, and *IFITM1* (Fig. 5.11A). A summary of all GSEA hallmark pathways, their normalised enrichment and p-values is provided (Fig. 5.11B). Presence of these canonical IFNγ target genes amongst the most differentially enriched between 501mel^{WT} and 501 *AHR*$^{-/-}$ cells in response to IFNγ, highlights the IFNγ-response is highly regulated by the AhR. This is further supported by the strong enrichment of the IFNγ-response pathway in 501mel *AHR*$^{-/-}$ cells compared to 501mel^{WT} cells with enrichment score of 1.58 NES (Fig. 5.11C). There's no statistically significant difference in the enrichment of TNF signalling via NF-κB between these cells in response to IFNγ as demonstrated in each cell line in response to IFNγ individually (Fig. 5.11B&D). The Hallmark inflammatory response pathway is not significantly enriched in the 501mel *AHR*$^{-/-}$ IFNγ-treated cells compared to the 501mel^{WT} IFNγ-treated cells, with 1.25 NES and $p > 0.05$ (Fig. 5.11B&E), which shows that although the differences between the response of these cells to IFNγ, there's a strong IFNγ-response pathway-specificity to these perturbations. The IFNα-response pathway is significantly enriched in the 501mel *AHR*$^{-/-}$ cells treated with IFNγ compared to the 501mel^{WT} cells treated with IFNγ, with enrichment score of 1.48 NES (Fig. 5.11B&F), this however may be due to the significant identity of the two gene sets. IL2-STAT5 signalling pathway is not significantly enriched in either cell line (Fig. 5.11B&G). IL6-JAK-STAT3 signalling

pathway is significantly enriched in the 501mel *AHR*$^{-/-}$ IFNγ-treated cells compared to the 501mel^{WT} IFNγ-treated cells, 1.70 NES (Fig. 5.11B&H), which may be the consequence of JAK-STAT3 pathways also being downstream of IFNγ binding to IFNGR1/2 and downstream of IL6. Together, these data demonstrate that IFNγ-signalling is broadly modulated by the AhR, with AhR-loss driving an enhanced response to IFNγ with concomitant upregulation of IFNγ, IFNα, and inflammatory signalling in 501mel *AHR*$^{-/-}$ cells compared with 501mel^{WT} cells treated with IFNγ. This supports my hypothesis the AhR supresses IFNγ-signalling beyond *IDO1* induction in these 501mel cell lines.

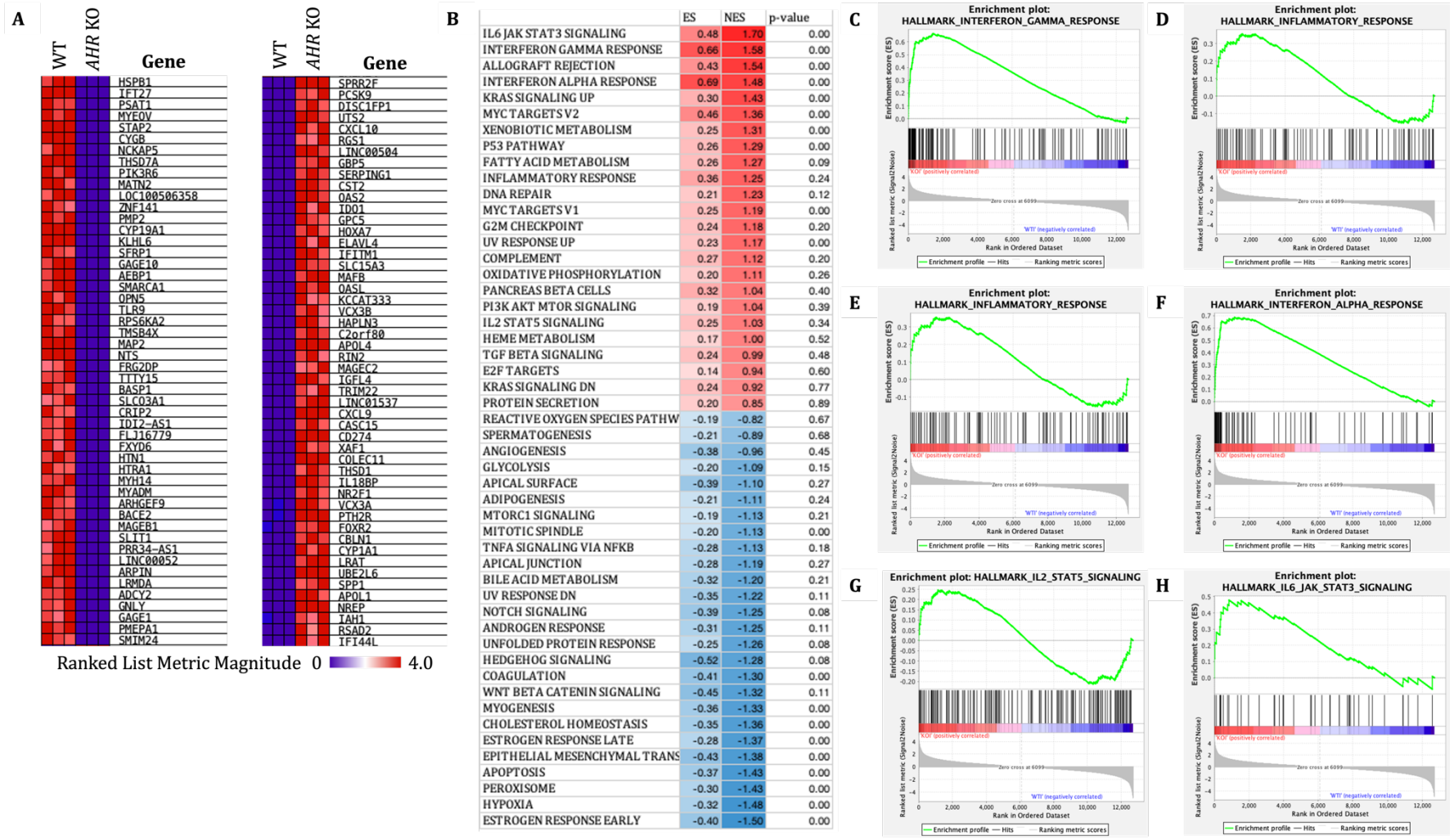

	ES	NES	p-value
IL6 JAK STAT3 SIGNALING	0.48	1.70	0.00
INTERFERON GAMMA RESPONSE	0.66	1.58	0.00
ALLOGRAFT REJECTION	0.43	1.54	0.00
INTERFERON ALPHA RESPONSE	0.69	1.48	0.00
KRAS SIGNALING UP	0.30	1.43	0.00
MYC TARGETS V2	0.46	1.36	0.00
XENOBIOTIC METABOLISM	0.25	1.31	0.00
P53 PATHWAY	0.26	1.29	0.00
FATTY ACID METABOLISM	0.26	1.27	0.09
INFLAMMATORY RESPONSE	0.36	1.25	0.24
DNA REPAIR	0.21	1.23	0.12
MYC TARGETS V1	0.25	1.19	0.00
G2M CHECKPOINT	0.24	1.18	0.20
UV RESPONSE UP	0.23	1.17	0.00
COMPLEMENT	0.27	1.12	0.20
OXIDATIVE PHOSPHORYLATION	0.20	1.11	0.26
PANCREAS BETA CELLS	0.32	1.04	0.40
PI3K AKT MTOR SIGNALING	0.19	1.04	0.39
IL2 STAT5 SIGNALING	0.25	1.03	0.34
HEME METABOLISM	0.17	1.00	0.52
TGF BETA SIGNALING	0.24	0.99	0.48
E2F TARGETS	0.14	0.94	0.60
KRAS SIGNALING DN	0.24	0.92	0.77
PROTEIN SECRETION	0.20	0.85	0.89
REACTIVE OXYGEN SPECIES PATHW	-0.19	-0.82	0.67
SPERMATOGENESIS	-0.21	-0.89	0.68
ANGIOGENESIS	-0.38	-0.96	0.45
GLYCOLYSIS	-0.20	-1.09	0.15
APICAL SURFACE	-0.39	-1.10	0.27
ADIPOGENESIS	-0.21	-1.11	0.24
MTORC1 SIGNALING	-0.19	-1.13	0.21
MITOTIC SPINDLE	-0.20	-1.13	0.00
TNFA SIGNALING VIA NFKB	-0.28	-1.13	0.18
APICAL JUNCTION	-0.28	-1.19	0.27
BILE ACID METABOLISM	-0.32	-1.20	0.21
UV RESPONSE DN	-0.35	-1.22	0.11
NOTCH SIGNALING	-0.39	-1.25	0.08
ANDROGEN RESPONSE	-0.31	-1.25	0.11
UNFOLDED PROTEIN RESPONSE	-0.25	-1.26	0.08
HEDGEHOG SIGNALING	-0.52	-1.28	0.08
COAGULATION	-0.41	-1.30	0.00
WNT BETA CATENIN SIGNALING	-0.45	-1.32	0.11
MYOGENESIS	-0.36	-1.33	0.00
CHOLESTEROL HOMEOSTASIS	-0.35	-1.36	0.00
ESTROGEN RESPONSE LATE	-0.28	-1.37	0.00
EPITHELIAL MESENCHYMAL TRANS	-0.43	-1.38	0.00
APOPTOSIS	-0.37	-1.43	0.00
PEROXISOME	-0.30	-1.43	0.00
HYPOXIA	-0.32	-1.48	0.00
ESTROGEN RESPONSE EARLY	-0.40	-1.50	0.00

Figure 5.11. GSEA between IFNγ response in 501mel WT and 501mel *AHR* KO cell lines. GSEA of 501mel WT vs. 501mel *AHR* KO cells after 24-hours of IFNγ 10 ng/mL treatment. (A) LHS 50 most enriched genes in 501mel WT IFNγ-stimulated cells compared to 501mel *AHR* KO IFNγ-stimulated cells RHS 50 most enriched genes in 501mel *AHR* KO compared to 501mel WT cells in response to IFNγ. Enrichment Score: ES, Normalised Enrichment Score: NES. GSEA hallmark summaries of (B) Interferon Gamma Response, (C) TNF Signalling via NF-κB, (D) Inflammatory Response, (E) Interferon Alpha Response, (F) IL2-STAT5 Signalling, and (G) IL6-JAK-STAT3 Signalling where a positive score represents an enrichment in 501mel *AHR* KO (KOI) in red, and a negative score represents an enrichment in the 501mel WT cells (WTI) in blue.

5.2.7. The AhR likely mediates IFNγ signalling via STAT1, not STAT3

IFNγ-signalling may be mediated through STAT1 or STAT3 depending on the context of the cells and the genes targeted by these factors aren't identical. Although there's overlap between targets of both TF complexes, STAT1 and STAT3 mediate opposing effects on the expression of some key IFNγ-response genes; *Cyclin D1* (*CCND1*), *MYC*, and *IFITM1*. STAT1 suppresses expression of *CCND1* and *MYC* and enhance the expression *IFITM1*, whereas STAT3 drives an increase in *CCND1* and *MYC* expression and suppresses the expression of *IFITM1*. *CCND1* RNA abundance is lower in all 501mel *AHR*$^{-/-}$ cell conditions compared to WT by approximately half (Fig. 5.12A). *MYC* mRNA abundance is also significantly lower in 501mel *AHR*$^{-/-}$ cells under all conditions except FICZ treatment (Fig. 5.12B). Furthermore, *IFITM1* expression is 10-fold greater in 501mel *AHR*$^{-/-}$ cells compared to 501mel^{WT} cells in response to IFNγ (Fig. 5.12C). Given that, throughout this thesis, there has been an elevated induction of IFNγ-response genes in 501mel *AHR*$^{-/-}$ cells compared to 501mel^{WT}, I expect the STAT protein responsible would be more active in the 501mel *AHR*$^{-/-}$ cell line than in the 501mel^{WT} cell line. Depression of *CCND1* and *MYC* and increased *IFITM1* expression in 501mel *AHR*$^{-/-}$ cells compared to 501mel^{WT} suggest that STAT1 is more active than STAT3, although, this is an indirect observation and requires further quantification of the activation of both TFs in both cell lines in response to IFNγ.

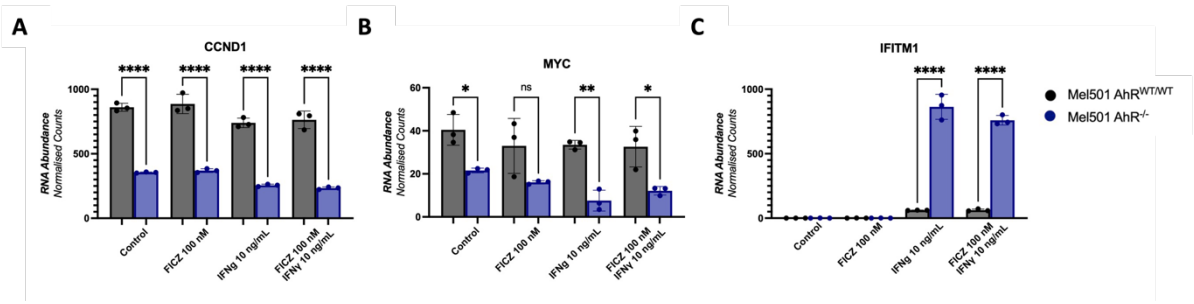

Figure 5.12. Expression of IFNγ Target genes. Bar charts representing the relative abundance of IFNγ target genes (A) *CCND1*, (B) *MYC*, (C) *IFITM1* in 501mel WT and 501mel *AHR* KO cell lines in response to 24-hours stimulation with FICZ 100 nM, IFNγ 10 ng/mL, neither, or both. Ad-hoc test: Ordinary One-way ANOVA, post-hoc test: Tukey-Kramer test for multiple comparisons which inherently corrects for multiple comparisons $P > 0.05$: ns, $P < 0.05$: *, $P < 0.01$: **, $P < 0.001$: ***, $P < 0.0001$: ****. Biological Repeats = 3.

To better characterise the binding of the AhR to target genes within the IFNγ-Response pathway, I generated lists of the closest genes to peaks that were present in both replicates of each of the ChIP-Seq experiment (Supp. 9.2.) and examined the overlap between these genes and the genes in GSEA gene set. Only 9 of the 141 genes within this gene set are bound by the AhR under any condition in these cells (Fig. 5.13). This reflects that most of the effects on the IFNγ-Response pathway are mediated indirectly by the AhR. Interestingly, *STAT1* has an associated peak in both conditions with IFNγ-treatment (Fig. 5.13). This could explain the elevated response of the IFNγ-response pathway, with the AhR driving induction of the *STAT1* gene under IFNγ-treatment, potentially driving further induction when co-treated with FICZ. This would explain the elevated expression of IFNγ-response genes in co-treatment compared to IFNγ-only, and the dependency on IFNγ for any expression of these genes. It doesn't, however, provide an explanation for the effects of knocking out the AhR. Further study is required to determine whether this mechanism is responsible for the observed effects of AhR on IFNγ-signaling, including determining why the AhR is binding to genes in the presence of IFNγ only.

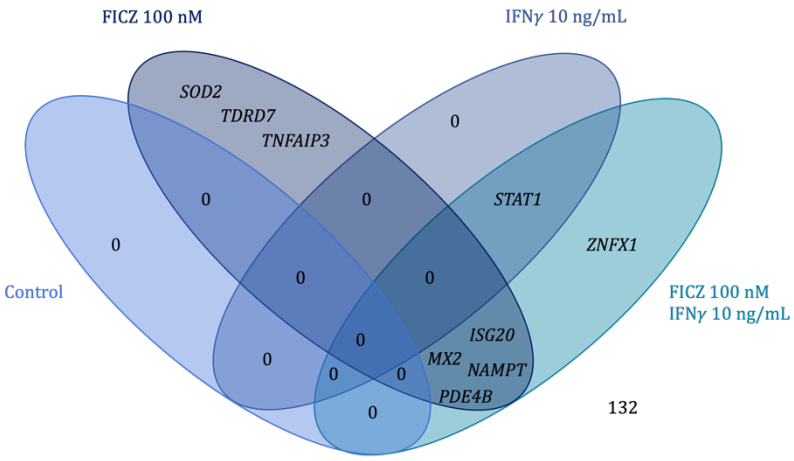

Figure 5.13. Binding of the AhR to IFNγ-Response Pathway Gene Set Genes. A Venn Diagram of the 141 genes within the IFNγ Response Gene Set from the GSEA showing the conditions with which there were associated peaks in both replicates of each condition in the ChIP-Seq Data.

To examine the nature of this binding I visualised the ChIP-Seq data presented in Chapter 4 at the *STAT1* promoter (Fig. 5.14A&B). Examining each pulldown and unput track separately (Fig. 5.14A&B) shows there are two peaks in the promoter region of *STAT1* which overlaps with the promoter region of *STAT4-AS1*. To simplify the visualisation of the data I used the ChIP-Seq tracks determined as per the protocol in Section 4.2.4. combining data from both replicates to produce a single fold-change track (Fig. 5.14B). From these data, it appears there's some binding of the AhR to this locus under all conditions, only becoming significant in both replicates of the ChIP-Seq after treatment with IFNγ (Fig. 5.14A&B). However, the peak nearest the *STAT4-AS1* gene appears to have the greatest accumulation only with treatment with FICZ, whereas the peak nearest the *STAT1* gene appears to be predominantly affected by IFNγ (Fig. 5.14). Together, these data suggest the AhR may be accumulating at this locus, but in this experiment, it's not robust without IFNγ. RNA-Seq of these cells, reveals that expression of *STAT1* is mediated in the same manner as most examined IFNγ-Response genes, with FICZ having limited effect, with no significant changes being due to FICZ (Fig. 5.14C). However, there's a 3.53-FI of *STAT1* in 501mel^{WT} in

response to IFNγ compared to DMSO, and an 8.28-FI between the same conditions in 501mel *AHR*$^{-/-}$ cells (Fig. 5.14C). This demonstrates the IFNγ-mediated induction of *STAT1* in these cells is greater without the AhR.

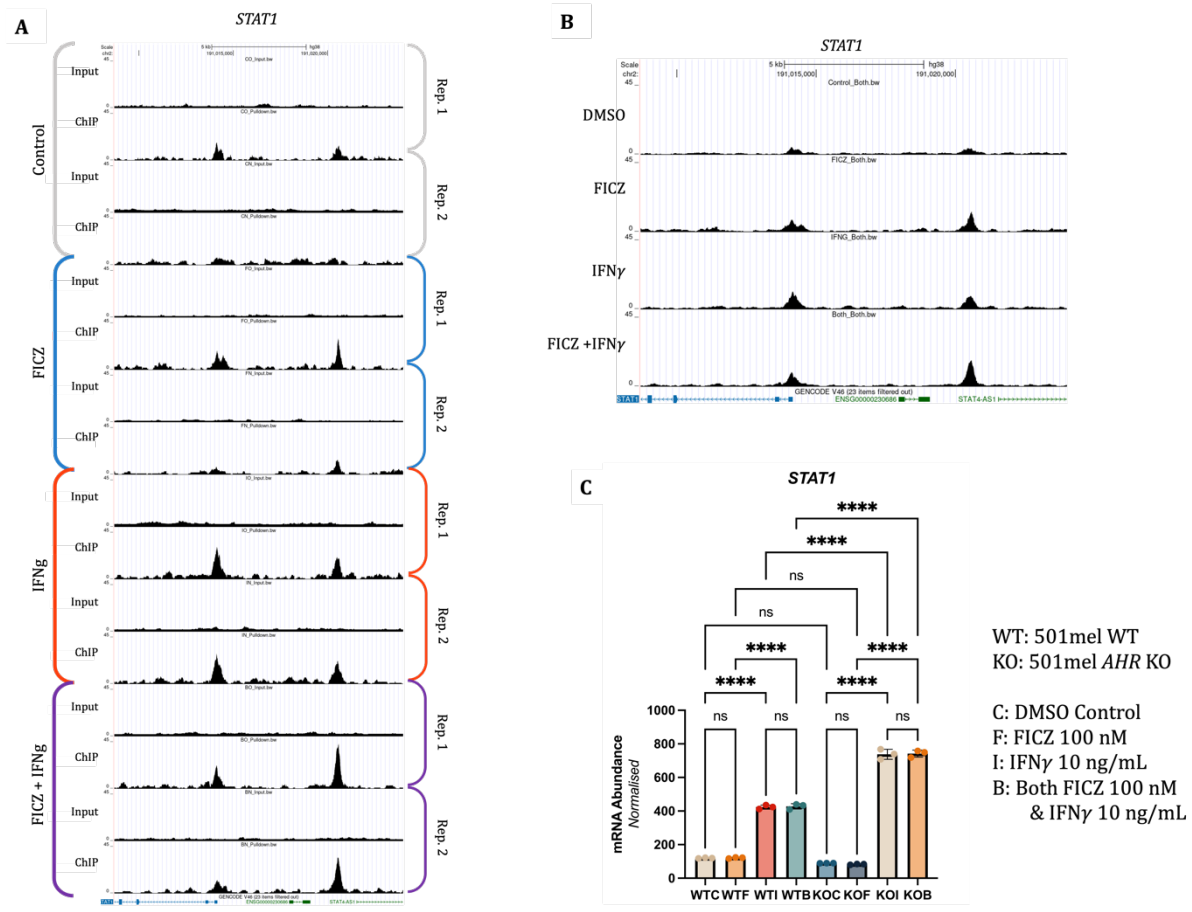

Figure 5.14. *STAT1* expression. Visualisation of the ChIP-Seq data in the UCSC genome browser examining each replicate and their corresponding input track (A) and visualisation of the peaks generated when generating peaks from the data averaged across both replicates (B). (C) *STAT1* in 501mel WT and 501mel *AHR* KO cell lines in response to 24-hours stimulation with FICZ 100 nM, IFNγ 10 ng/mL, neither, or both determined by RNA-Seq. Ad-hoc test: Ordinary One-way ANOVA, post-hoc test: Tukey-Kramer test for multiple comparisons which inherently corrects for multiple comparisons P > 0.05: ns, P < 0.05: *, P < 0.01: **, P < 0.001: ***, P < 0.0001: ****. Biological Repeats = 3.

These data also suggest the AhR may be modulating the expression of *STAT4-AS1* which may be driving a reduced accumulation of STAT4. STAT4 can induce expression of *IFNG*, which may provide an explanation for the observed dependency and changes

in the 501mel *AHR*$^{-/-}$ cell line. Under stimulation with endogenous ligands the AhR may be stimulating a limited expression of *STAT4-AS1,* reducing expression of STAT4 thereby limiting positive feedback loops in the expression of *IFNG* in response to IFNγ-treatment which is then alleviated by AhR-loss in the 501mel *AHR*$^{-/-}$ cells. This, however, is highly speculative, with no data for the expression of *STAT4* or *STAT4-AS1* in the RNA-Seq experiment and no further qRT-PCR having been performed for *STAT4-AS1* or Western Blot for STAT4. There's little further evidence that can be drawn on to support this hypothesis, thus it cannot be concluded from these data.

5.2.8. Gene Set Enrichment Analysis: AhR modulation of NF-κB

My hypothesised mechanism of action through which the AhR modulates IFNγ-signalling is through interactions with IRAK1 which impacts NF-κB activity (Fig. 3.16). This hypothesis depends on cytosolic AhR being an inhibitor of IRAK1, an activator of NF-κB via phosphorylation of IκK and TRAF6, and that stimulation of AhR with canonical agonists such as FICZ is sufficient to drive nuclear localisation of the AhR leading to de-inhibition of cytoplasmic IRAK1.

Treatment of 501mel^{WT} cells with FICZ drives enrichment of the NF-κB signalling pathway in the RNA-Seq data, with enrichment score of 0.36 ES[†††] (Fig. 5.15A). This shows that stimulation of the AhR with a canonical physiological ligand can upregulate expression of genes associated with NF-κB signaling. Furthermore, there's synergism between AhR-mediated activation of NF-κB and IFNγ-signalling, with co-

[†††] Normalised Enrichment Scores are only used when comparing between different gene sets as they are normalised to gene set size. When comparing enrichments of the same gene set, enrichment scores may be used.

treatment of 501mel^{WT} cells with FICZ and IFNγ causes enrichment of the TNF signalling via NF-κB hallmark compared to IFNγ only, with enrichment score of -0.48 ES (Fig. 5.15B). This demonstrates that enrichment of NF-κB signalling in 501mel cells treated with FICZ produces a synergistic effect with greater induction of IFNγ-signalling in response to IFNγ and FICZ and a greater induction of NF-κB in response to IFNγ and FICZ too. These effects are supportive of my hypothesis of the AhR acting as a modulator of both pathways, via regulation of NF-κB allowing both pathways to influencing activity of the other. If these effects of FICZ stimulation on NF-κB signalling are mediated through the AhR, then I would expect that treatment of 501mel *AHR*$^{-/-}$ cells with FICZ wouldn't produce enrichment of TNF signalling via NF-κB. I observe enrichment of TNF signalling via NF-κB in response in 501mel *AHR*$^{-/-}$ cells (0.37 ES) compared to FICZ-stimulated 501mel *AHR*$^{-/-}$ which have no enrichment (Fig. 5.15C). I did not expect to observe any enrichment of this pathway between these conditions, and due to no induction of canonical AhR target genes in response to FICZ in 501mel *AHR*$^{-/-}$, a potential explanation for this is that FICZ depresses TNF signaling to a limited degree independently of the AhR. When the AhR is intact, FICZ stimulates an AhR-dependent pathway that drives enrichment of the TNF signaling pathway. This demonstrates the upregulation of NF-κB signalling in 501mel in response to FICZ is mediated through the AhR, and that unstimulated AhR is a suppressor of NF-κB signalling, further supporting my proposed mechanism of action for the AhR in mediating IFNγ-signalling.

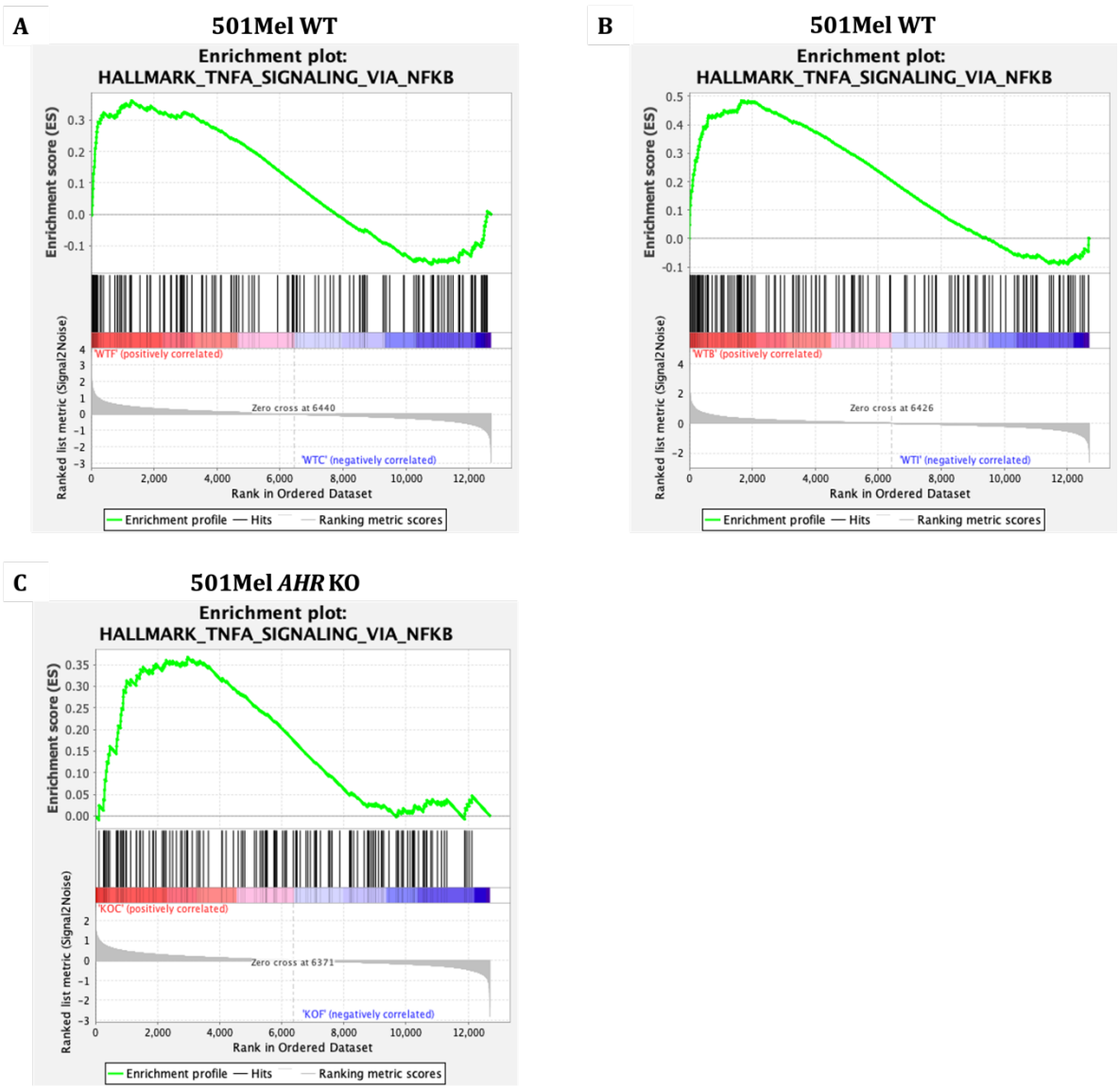

Figure 5.15. Enrichment of TNF signalling via NF-κB. GSEA of 501mel WT cells comparing enrichment of the TNF signalling via NF-κB between (A) 501mel WT unstimulated and FICZ 100 nM 24-hours treatment, (B) 501mel WT IFNγ 10 ng/mL 24-hours stimulation and IFNγ 10 ng/mL with FICZ 100 nM 24-hours treatment, and (C) 501mel *AHR* KO cells without stimulation and with FICZ 100 nM for 24-hours.

My proposed model of action for the AhR in IFNγ-stimulation would suggest that, as the AhR should be suppressing NF-κB signalling via IRAK1 suppression, that 501mel *AHR*$^{-/-}$ cells should've enriched NF-κB signalling compared to 501mel^{WT} cells. There's, however, enrichment of the TNF signalling via NF-κB pathway in 501mel^{WT} cells compared to 501mel *AHR*$^{-/-}$ cells, ES = 0.38 (Fig. 5.16A). Given that this is a hallmark pathway of TNF stimulation rather than of NF-κB activity specifically, I examined the

underlying gene list contributing to the TNF signalling via NF-κB pathway. The result revealed there are many genes of the TNF signalling via NF-κB GSEA hallmark whose proteins are involved in IFNγ-signalling still enriched in 501mel *AHR*$^{-/-}$ cells compared to 501mel^{WT}, including *IRF1* (Fig. 5.16B). Given the AhR positively regulates NF-κB signalling at the transcriptional level at some key NF-κB genes, I believe this is reflective of 501mel *AHR*$^{-/-}$ cells having a basal higher activity of NF-κB targeted to specific genes such as *IRF1*, but the overall presence of the AhR enhances the broad transcriptional activity of NF-κB but not at genes that influence IFNγ-signalling. Examination of this GSEA and no other analyses performed in this chapter is biased. It was performed because this was an unexpected result, whereas all other analyses gave anticipated results. This gene set is labelled "TNF signaling via NF-κB", whereas I'm interested in effects of non-canonical NF-κB stimulation therefore deviations from expect results were examined to attempt to understand why. However, given considerable limitations of GSEA with many genes in these gene lists not aligning with given titles, similar scrutiny should be given to each gene list used to ensure results are representative of their titles.

5.2.9. The AhR is a driver of a more plastic transcriptome

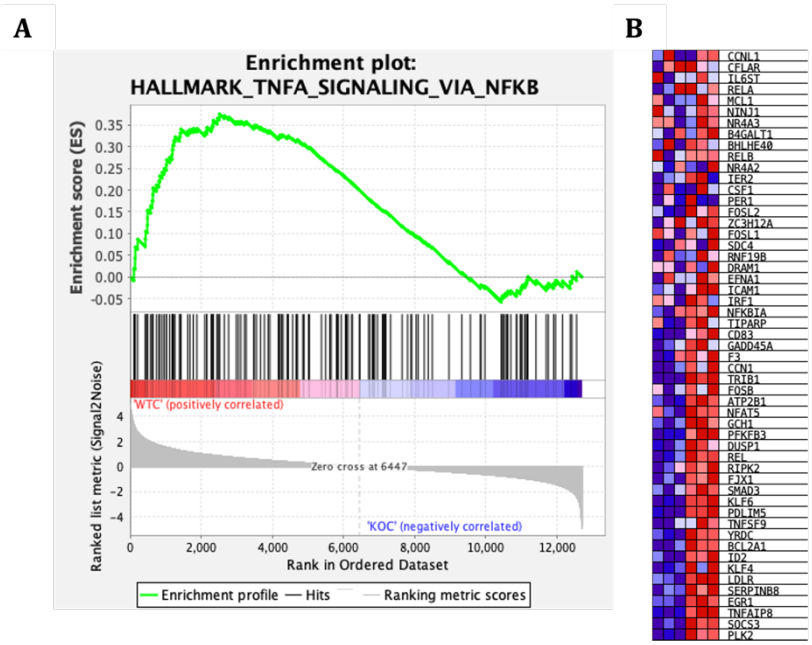

Figure 5.16. Enrichment of TNF signalling via NF-κB. (A) GSEA of DMSO-treated 501mel WT cells compared to DMSO-treated 501mel *AHR* KO cells for enrichment of the TNF signalling via NF-κB, with (B) the genes enriched in 501mel *AHR* KO cells over 501mel WT cells within the TNF signalling via NF-κB pathway hallmark.

My ChIP-Seq data demonstrated a probable antagonistic relationship between AhR activity and MITF activity in melanoma cells which is likely responsible for AhR-mediated acquisition of a more dedifferentiated, plastic, and invasive phenotype, summarised in Fig. 4.17. This hypothesis was developed primarily from ChIP-Seq data which demonstrates which genes are bound, with the potential for being regulated, rather than providing information about gene expression. Using my RNA-Seq data, however, I show that stimulation of 501mel^{WT} with FICZ causes enriched expression of genes associated with an epithelial to mesenchymal transition (Fig. 5.17A, 5.17B). 501mel cells treated with FICZ had enrichment score of magnitude 0.4 (Fig. 5.17B), which shows a relatively strong expression of this hallmark pathway in response to FICZ. Furthermore, I would expect more substantial enrichment of the EMT hallmark

pathway in 501mel^{WT} cells compared to 501mel *AHR*$^{-/-}$ cells if the AhR is antagonistic of MITF signalling. This is observed in greater contrast in expression of the genes involved in the EMT hallmark pathway when comparing the transcriptomes of 501mel^{WT} cells vs 501mel *AHR*$^{-/-}$ cells (Fig. 5.17C), compared to the response to FICZ in 501mel^{WT} cells (Fig. 5.17A). This is reflected in a greater enrichment score of 0.45, showing there's a greater EMT signature in 501mel^{WT} than in 501mel *AHR*$^{-/-}$ (Fig. 5.17D). These data demonstrate the AhR is responsible for mediating expression of a more dedifferentiated transcriptional program, with known major TFs responsible for expression of EMT genes being found in this gene set and found to be bound by the AhR and MITF (Fig. 4.16). These data align with my proposed mechanism of transcriptional antagonism of the AhR and MITF, where MITF promotes a differentiated melanocyte transcriptomic profile which is suppressed by the AhR.

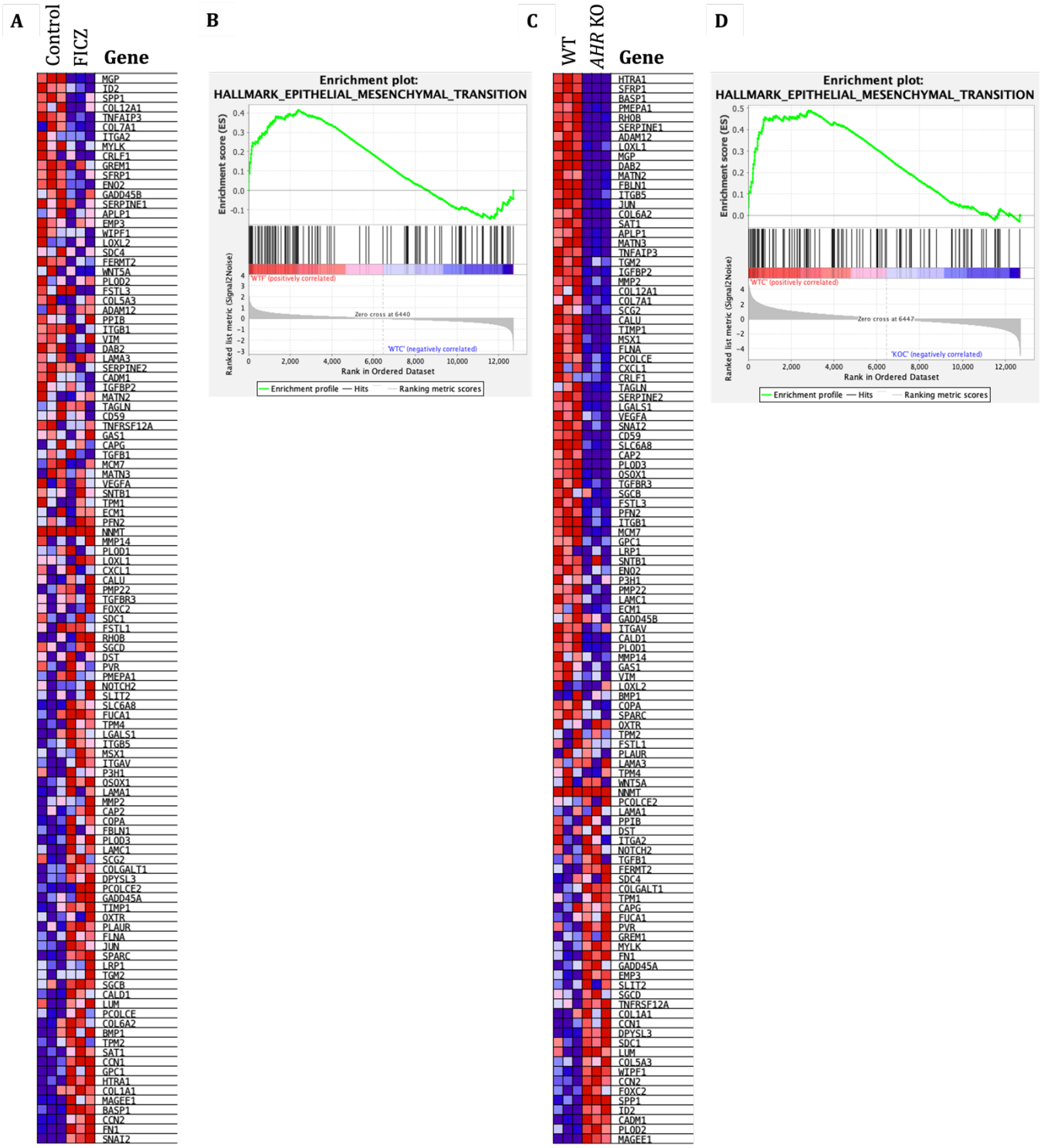

Figure 5.17. Enrichment of Hallmark Epithelial to Mesenchymal Transition. GSEA of (A & B) 501mel WT cells with and without 24-hours of FICZ 100 nM treatment and (C & D) 501mel WT and 501mel *AHR* KO cells DMSO control.

5.3. Discussion

In chapter 2, I demonstrated that for a select number of IFNγ-response genes, the unliganded-AhR may be an inhibitor of their expression in response to IFNγ-stimulation of 501mel cells. This led me to propose the AhR is an inhibitor of IFNγ-signalling. My RNA-Seq data has further supported this observation, with the expression of IFNγ-response genes being elevated in 501mel *AHR*$^{-/-}$ cells treated with IFNγ compared to 501mel^{WT} cells treated with IFNγ. I also demonstrated these effects are observed in IFNγ-responses broadly, rather than only in the panel of genes that I assessed the expression of using qRT PCR. Consequently, I do not believe the AhR-IDO1-Kynurenine axis, that is proposed to mediate the AhR's contribution to melanomagenesis, is reflective of the true mechanism through which the AhR is mediating enhanced *IDO1* expression or subsequent immunosuppressive mechanisms. However, as this study was performed in only a single clone of a single cell type, it's impossible to conclude whether this is a clonogenic effect or a finding that is relevant to melanoma as a whole.

I also demonstrated AhR-loss is likely causing STAT1-specific, not STAT3-specific, changes in gene expression in these cells. This is consistent with my earlier data which showed enhanced accumulation of phosphorylated STAT1 in 501mel *AHR*$^{-/-}$ cells and not STAT3. STAT1 signalling is an essential signalling pathway through which melanomas evade elimination by the immune system in mice (Zhou et al., 2022). Interactions between the AhR and IFNγ-signalling via STAT1 are of importance to understanding how the AhR contributes to immune tolerance in melanoma. My

results suggest that both tumours with highly transcriptionally active AhR or without functional AhR would be likely to have enhanced IFNγ-signalling and subsequent STAT1 activation in comparison to cells with wild-type AhR. This would suggest that a potential avenue for immunotherapeutic intervention in melanoma would be co-treatment with AhR inhibitors and anti-PD-L1 and/or anti-CTLA-4 treatments which could enhance responses to treatment in tumours expressing the AhR. Early *in vitro* studies have demonstrated proof of concept for the use of AhR inhibitors for enhanced immune responses in cancer immunotherapy (Kober et al., 2023), although the rationale for their use is still dependent of the AhR-IDO1-Kynurenine axis. Combination therapies of anti-IDO1 and anti-PD-L1 monoclonal antibodies have not proven more efficacious than only anti-PD-L1 therapies (Long et al., 2019; Van Den Eynde et al., 2020). I speculate that this is likely because elevated IDO1 activity in melanoma is indicative of enhanced STAT1 activity via IFNγ and, one of many pathways contributing to immunosuppression in melanoma, whereas AhR inhibitors could produce a broader anti-tolerogenic response in melanomas through inhibition of immunosuppressive IFNγ-STAT1 signalling given inhibited AhR suppresses IFNγ-responses whilst AhR-loss enhances it (Chapter 3). I would expect greater efficacy of small molecular inhibitors of the AhR in immunotherapeutic co-treatments than of IDO1 small molecule inhibitors, which have not been successful in the clinic.

There's, however, evidence presented herein the AhR modulates *STAT1* expression in a similar pattern to that of typical IFNγ-response genes (Fig. 5.14) (it is a canonical response gene), and there is enrichment of AhR peaks at the *STAT1* promoter from the AhR ChIP-Seq experiment performed in the 501mel cells in Chapter 4 (Fig. 5.14). Together, these data indicate that a potential mechanism through which the AhR is

affecting the IFNγ-response in these cells is through direct regulation of the *STAT1* gene. This, however, is hard to reconcile considering the results presented in Chapter 3 which indicated the AhR is likely mediating its effects on IFNγ-signaling through cytoplasmic interactions. These data, do, however, explain the enriched presence of STAT1 in 501mel cells beyond the increased accumulation of pSTAT1. One explanation for these effects, is the AhR is affecting IFNγ-signaling via STAT1 and STAT4, with the AhR binding at the upstream region of *STAT4-AS1* which may limit STAT4-mediated IFNγ-signalling pathways and enhance STAT1-mediated IFNγ-signaling pathways. Furthermore, the direct regulation of *STAT1* expression by the AhR in these cells, is not mutually exclusive with modulation of NF-κB signaling described in the discussion of Chapter 3.

My proposed model of activity through which the AhR mediates IFNγ-signalling is via cytoplasmic suppression of NF-κB signalling. I have demonstrated that stimulation of the AhR with FICZ drives enhanced expression of the hallmark TNF signalling via NF-κB pathway in 501mel^{WT} cells which agrees with my hypothesis. I did not, however, detect a significant difference in the enrichment of TNF signalling via NF-κB in 501mel^{WT} and *AHR*$^{-/-}$ cells treated with IFNγ. Equally, there is enrichment of TNF signalling via NF-κB pathway in 501mel^{WT} cells compared to 501mel *AHR*$^{-/-}$ cells, which is the opposite to what I would expect. However, analysis of the gene set list demonstrates that some NF-κB gene targets are enriched in 501mel *AHR*$^{-/-}$ cells compared to 501mel^{WT} cells. Amongst these are IFNγ-signalling pathway components including *IRF1*. Given that it is well-established the AhR is a mediator of NF-κB signalling, it is possible that there is a combinatorial effect where canonical AhR

stimulation enhances some transcriptional activities of the NF-κB machinery, but there are AhR-independent transcriptional activities of NF-κB which drives stimulation of IFNγ-signalling pathway components (Hiroi & Ohmori, 2005; Ohmori et al., 1997; Robinson et al., 2003). Consequences of this would be AhR-loss in cells would increase basal expression of some IFNγ-signalling components but would depress NF-κB and AhR co-mediated gene expression which is partially determined through AhR-RelB heterodimers (Vogel et al., 2007).

NF-κB signalling is pro-tumorigenic in melanoma and is often constitutively activated in melanoma (Madonna et al., 2012). Major oncogenic roles of NF-κB signalling in melanoma are promoting cell growth, resisting apoptosis, and mediating pro-tumorigenic inflammation (Madonna et al., 2012). One of the target genes of NF-κB is *CCND1*, which is a G_0 cyclin, expression of which promotes cell-cycle entry(Hinz et al., 1999). NF-κB also stimulates the expression of anti-apoptotic factors, most crucially Bcl-XL (C. Chen et al., 2000), which inhibits the oligomerisation of Bax after pro-apoptotic signalling (Lucianò et al., 2021). NF-κB also mediates the inflammatory response of cells in many biological contexts, but in cancer, it mediates its pro-inflammatory effects through expression of key cytokines, including TNF, IL-6, and IL-8 (Hoesel & Schmid, 2013). Together, these aspects of NF-κB biology highlight that its dysregulation by AhR is likely to have significant effects on cancer biology. My results indicate that, in melanomas with intact AhR, elevated AhR activity would potentially drive enhanced NF-κB activity and AhR-loss should further increase the canonical signalling of NF-κB. Given that NF-κB signalling is a key contributor to melanoma

development, this presents another avenue through which overstimulation of the AhR or AhR-loss may be responsible for enhanced tumorigenesis.

In Chapter 3, I described a potential novel function of the AhR as antagonistic of MITF transcriptional activity. From the ChIP-Seq data alone I was unable to determine the dynamics of AhR and MITF antagonism, but I did demonstrate they both bind to genes involved in cell differentiation. My RNA-Seq data demonstrates that stimulation of the AhR is sufficient to drive enhanced expression of hallmark EMT genes, but AhR-loss drives a greater suppression of the hallmark EMT pathway. Given that MITF is a suppressor of cellular dedifferentiation, these data reflect that without the AhR, expression of these genes is suppressed. This could be due to MITF binding no longer being antagonised. AhR activation may be leading to competition with MITF and enhanced EMT pathway component expression, suggesting that inhibition of the AhR should suppress expression of dedifferentiation genes. If these results are applicable beyond the 501mel cells used here, this may be important in the clinic, given that dedifferentiation and phenotypic plasticity are associated with poorer melanoma prognosis and immune evasion (Corre et al., 2018; Hossain & Eccles, 2023; Mengoni et al., 2020; Najem et al., 2022). To confirm whether the AhR is affecting MITF-mediated gene expression, RNA-Seq should be performed in cells alongside knocking-out *MITF,* to determine whether AhR-mediated effects on genes associated with MITF are dependent on MITF or if these observations of the AhR affecting MITF-related gene expression are independent of any potential mechanism of AhR-mediated antagonism of these genes. Further to this, these experiments must be performed in melanoma cell lines and primary melanocytes beyond the 501mel clones to

determine whether these effects are likely to be relevant to melanoma in general rather than just these cells.

If, however, these mechanisms are representative of the pathways occurring in melanoma cells, it would be of clinical importance. Speculation as the mechanisms underlying the data presented in the thesis reveals that AhR inhibitors could likely be efficacious in both suppressing STAT1 activation via IFNγ (See Chapter 3 for rationale) and tumour immune tolerance, but also suppressing expression of genes that contribute to melanoma dedifferentiation. Suppression of dedifferentiation in melanoma, would likely limit the rate of tumour progression in patients and prevent diffuse spread of melanoma metastases around the body, improving patient outcome. However, without further work to, improve the reliability of this work, demonstrate the causative mechanisms presented, and repeat these in a variety of melanoma models, it remains limited in its value to the field and its worth in exploring in the clinic.

6. Final Discussion

6.1. The AhR as an IFNγ-signaling regulator

The AhR is an oncogene in melanoma (Paris et al., 2022a; Walczak et al., 2020). Previous studies have demonstrated the AhR promotes tumour growth in melanoma through increased expression of *IDO1*, which in turn, depletes the TME of tryptophan which signals for T_{reg} cell fate adoption in tumours that in turn suppresses immune responses (Fallarino et al., 2006; Munn et al., 1999). The AhR is sufficient to drive immune tolerance in OSCC (Kenison et al., 2021), and the AhR is essential for IDO1-mediated immune suppression in cancer (D. Shi et al., 2022). However, *in vitro* studies have demonstrated that physiological agonists of the AhR aren't sufficient to drive robust *IDO1* induction (Vogel et al., 2008) which is responsible for AhR mediated-immune suppression *in vivo*. I have demonstrated the AhR is not likely a direct activator of *IDO1* expression in these 501mel cells and is rather a mediator of IFNγ-mediated stimulation of *IDO1* (Fig. 3.3). However, the reliability of the data presented in Chapter 3 and relevance of all data in this thesis to cells beyond the clones used limits the ability to conclude whether this is reflective of the biology of melanoma. With data from the CCLE and TCGA providing some confirmatory evidence, there can be some confidence in the relevance of this research to melanoma, and the mechanisms proposed are worth further exploration to determine whether they are, operating in melanomas in general or in specific phenotypic states.

In TCGA melanoma patient data, I found a positive correlation between AhR activity and IFNγ-response gene expression (Fig. 3.4) which I demonstrated was reproducible *in vitro* (Fig. 3.5). I determined the AhR was likely acting as a suppressor in its

unliganded state (Fig. 3.5), which led to the suggested role of the AhR as an inhibitor of IFNγ-signalling in the cytoplasm. One potential mechanism through which the AhR is mediating IFNγ-signaling in the cytoplasm that I did not explore here is the potential the AhR may bind RNA in the cytoplasm, mediating post-transcriptional regulation of gene expression, which I wouldn't have been able to detect throughout any of the experiment performed in this thesis. This should also be examined, through IP of the AhR and then RNA sequencing to determine the identity and quantity of any transcripts bound to it in the cytoplasm. I demonstrated that it was likely activation of STAT1, not STAT3 (Fig. 3.9) that was enhanced in 501mel *AHR*$^{-/-}$ cells in response to IFNγ compared to 501mel^{WT} cells. This is reflected in my RNA-Seq data, which demonstrates there's a STAT1-specific signature of gene expression in response to IFNγ-stimulation (Fig. 5.12). This effect, however, may be due to the AhR potentially binding to the *STAT1* locus and regulating *STAT1* expression directly (Fig. 5.14) . Using predominantly nuclear or cytoplasmic AhR expression vectors, I showed there was equivalent IFNγ-mediated stimulation of STAT1 in *AHR*$^{-/-}$ cells as there was in nuclear-AhR reconstituted *AHR*$^{-/-}$ cells (Fig. 3.12). This, however, raises uncertainty about the relevance of the AhR peaks associated with the *STAT1* locus, and demonstrates that this should be studied further. It is possible, there are contributions mediated by both transcriptomic regulation of *STAT1* and cytoplasmic regulation via interactions with the NF-κB pathway as described in Chapter 3. To understand these mechanisms further, there must be analysis of expression of STAT1 and STAT4 in response to AhR stimulation and status to confirm whether variations in *STAT4-AS1* and *STAT1* locus binding are contributing to the AhR-mediated effects on IFNγ-signaling. Furthermore, better characterisation of potential roles of the AhR

in affecting NF-κB signaling must be performed in these cells and beyond. While interactions of the AhR with NF-κB and NF-κB signaling in cancer (Ishihara et al., 2019; Kim et al., 2000; Madonna et al., 2012; Vogel et al., 2011; Xia et al., 2014) are well characterised, the potential of AhR-mediated perturbations in crosstalk with the IFNγ-pathway (Hiroi & Ohmori, 2005; Ohmori et al., 1997) provides new insight into potential mechanisms of AhR-mediated melanomagenesis. However, the limited scope and weaknesses of data presented in this thesis means that it's impossible to conclude these mechanisms exist in melanoma but are worth exploring further.

Furthermore, I demonstrated FICZ-stimulation of the AhR is sufficient to increase expression of hallmark TNF signalling via NF-κB pathway genes in 501mel cells (Fig. 5.13). I did not observe enrichment of the hallmark TNF signalling via NF-κB pathway in 501mel *AHR*$^{-/-}$ compared to 501mel^{WT} cells, which I did expect. However, I believe that this is indicative of the AhR performing multiple roles with respect to NF-κB signalling, which are distinct from TNF signalling (Hoesel & Schmid, 2013; Ishihara et al., 2019). My hypothesised model through which the AhR mediates IFNγ-signalling via NF-κB is through elevated basal expression of IFNγ-signalling components such as *IRF1*, not through enhanced TNF signalling. This model is supported through the elevated expression of *IRF1* in 501mel *AHR*$^{-/-}$ cells compared to 501mel^{WT} cells. However, without IFNγ, there's no difference between the expression of *IRF1* in 501mel^{WT} and *AHR*$^{-/-}$ cells (Fig. 3.8). There was also no confirmation that the binding of IRF1 in these cells or melanoma in general is greater in response to IFNγ in 501mel *AHR*$^{-/-}$. ChIP-seq experiments examining the binding of STAT1/IRF1 should be performed in these cells to determine if there are significant changes in their binding

in response to AhR modulation, which would be expected based on my data, whether it's due to AhR regulating *STAT1* expression directly (Fig. 5.14) and/or via NF-κB cross talk (Fig. 3.18, 3.19, 5.15) (Hiroi & Ohmori, 2005; Tian et al., 1999).

Irrespective of mechanism, these data support a new model through which the AhR contributes to immune suppression in the melanoma microenvironment, where the AhR is a mediator of IFNγ-signalling broadly, not just as an agonist of *IDO1* expression as previously described (Anzai et al., 2022; Campesato et al., 2020; Labadie et al., 2019). However, due to the limited breadth of models and systems used to perform experiments in this thesis, it's not possible to confirm whether this model is restricted in 501mel cells or melanoma more broadly. Should these conclusions prove applicable broadly to melanoma it highlights the potential of anti-AhR therapies as a for modulating melanoma immunotherapies. Previous clinical studies have demonstrated that combination therapies of IDO1 inhibitors with anti-PD-L1 therapies are no more efficacious than anti-PD-L1 therapies alone (Long et al., 2019). My data, however, suggests that IDO1 activity is only one component of the AhR mediated immunosuppression in the melanoma microenvironment, and targeting the AhR should suppresses STAT1 signalling which has been shown to be sufficient to drive immunosuppression in melanoma.

My RNA-Seq data, comparing the transcriptomes of unstimulated 501mel^{WT} and 501mel *AHR*$^{-/-}$ cells demonstrates the AhR is regulating expression of thousands of genes in its unliganded state. Given that I see limited binding of the AhR to DNA in the presence of only endogenous agonists, I believe that this could be a result of the AhR regulating the activity of many transcriptional regulators, driving other gene

expression networks. Part of this effect may be mediated through the role of the AhR as a substrate receptor for Cullin 4B E3 ubiquitin ligase complexes, where the AhR facilitates ubiquitination and degradation of TFs such as the Oestrogen receptor (Ohtake et al., 2009) and β-catenin (Kawajiri et al., 2009). Potential roles of ubiquitin-mediated degradation of key transcriptional regulators has not been examined herein but may be very relevant to the role of the AhR in 501mel cells and melanoma more widely.

6.2. An Environmental Sensor in Melanoma

Here I have discussed a potential role of the AhR in mediating melanomagenesis, however, this is not necessarily to be expected. The AhR is a highly evolutionarily conserved ligand-activated TF, involved in mediating detoxification responses (Dai et al., 2022; Williams et al., 2014). It's surprising to find the AhR being a key mediator of melanoma biology, partially through antagonism with the MITF-mediated transcriptome. MITF is an LDTF central to melanoma development, conferring melanocyte cell-fate on cells expressing MITF (Hemesath et al., 1994), with loss of MITF activity being a key contributor to melanoma cell dedifferentiation (Carreira et al., 2006).

Data presented in chapters 4 and 5 have alluded to a role of the AhR in driving melanoma cell dedifferentiation and metastases through antagonism of MITF-mediated transcription, which may contribute to the reason why the AhR is an oncogene in melanoma and not in other cancer types (Walczak et al., 2020). In my AhR ChIP-Seq experiment, I found enrichment of E-/M-box motifs flanking AhR

binding sites on the same face of the dsDNA helix (Fig. 4.14). These motifs are binding sites for MITF and other TFE family members; TFE3/TFEB/TFEC, it's worth exploring further the relationship of the AhR with these members beyond MITF. I used available MITF ChIP-Seq data in the 501mel and showed the AhR and MITF do bind to the same genes, and that this may be independent of ARNT, although to be confident of this the ChIP-Seq experiments needed to be better controlled to be certain the peaks observed are AhR-dependent (Fig. 4.16). This could be of interest, as the AhR forms transcriptionally active complexes beyond ARNT, and these sites could be a reflective of one such complex (Vogel et al., 2011). GSEA of the genes bound by the AhR and MITF revealed enrichment of these factors at genes involved in cellular differentiation (Fig. 4.16). I also demonstrated the AhR and MITF show anti-correlated activity and expression in *in vitro* data from transcriptomic data from melanoma cell lines, the Cancer Cell Line Encyclopaedia (Fig. 4.10, 4.13) and in *in vivo* data from TCGA (Fig. 4.14), which also aligned with increased AhR activity in more dedifferentiated cell phenotypes. Together, these data suggest the AhR could be antagonistic of MITF activity, promoting cellular dedifferentiation by limiting the activity of the cell LDTF MITF in melanocytes. Whether this role of the AhR as a mediator of cellar fate through antagonism with LDTFs beyond MITF in melanoma remains very unclear, with little consistency in patterns of AhR expression and LDTF expression in a small panel of cancer types (Fig. 4.14), however, there were significant correlations that indicate that this is perhaps worth further exploration.

I also demonstrated in my RNA-Seq experiment that AhR status and activity causes a greater expression of genes involved in the epithelial to mesenchymal transition pathway in these 501mel cells (Fig. 5.14). Given that it's known that loss of MITF

activity and expression drives dedifferentiation and transition towards more plastic phenotypes through genes involved in the hallmark EMT pathway (Goding & Arnheiter, 2019), it suggests that AhR activation produces a similar phenotype in 501mel cells as loss of MITF, but without further study of 501mel *MITF* KO cells it's not possible to confirm this. This correlation between AhR modulation and EMT pathway enrichment coupled with the ChIP Seq data presented allows for speculation of an AhR-MITF axis that mediates melanoma phenotype switching, which perhaps could be of interest in the clinic.

Should this speculated mechanism be representative of the biology of melanocytes, the AhR being a suppressor of MITF-mediated transcription, it presents an interesting biological mechanism for stress tolerance in cells. If the AhR is a canonical environmental toxin receptor, involved in the detection and metabolism of toxins in cells, then these data suggests that its activation temporarily permits the cell to become more plastic in its gene expression during the period of its activation. This enhanced transcriptional plasticity may enable cells to be more tolerant to the stressors and better poised to expressed toxin-metabolising genes, than if the cell was to remain entirely transcriptionally rigid. This mechanism, too, could allow for cell cycle entry, increasing melanocyte cell number that could enhance their capacity to protect against damage. This, however, is highly speculative.

If this mechanism is reflective of melanoma biology, where the AhR's contribution to dedifferentiation in melanoma is a consequence of over activation, where chronic AhR activation suppresses MITF activity leading to loss of phenotype of melanocytes through non-mutational means. This would also perhaps be an avenue through which

melanoma cell phenotype switches before and after metastasis. Primary tumours may have high abundance of AhR ligands: activating the AhR and suppressing MITF activity driving loss of melanocyte identity, and sites where melanoma cells metastasise to have limited abundance of AhR ligands facilitating restoration of MITF activity: switching back to a more differentiated, proliferative state.

To explore this fully, phenotypic changes associated with dedifferentiation and metastasis must be examined beyond the expression of certain genes and binding near their promoters. Cell mobility assays should be performed to demonstrate there is a difference in this in response to AhR status. There can also be more qualitative assessments on the cell shape, determining whether there's an AhR mediated dependency on this. Equally, introducing tumours into mouse models bearing either WT or deletion of the *AHR* gene would be invaluable to assessing both the effect of the AhR on invasion and metastases and the infiltration of the immune cells and the ability of the immune system to retard cancer growth. Similar studies have been performed in OSCC models and demonstrated the AhR is sufficient to drive significantly different responses of the immune system to cancer cells (Anzai et al., 2022; Kenison et al., 2021).

6.3. The AhR as a cell lineage specific oncogene

One major question remaining in determining the role of the AhR in cancer is the cell-type specific relationship, where the AhR is oncogenic in some tumours and tumour suppressive in others. A potential consequence of determining the relationship between MITF and the AhR is that it could allude to a pattern of AhR function, where

antagonism between the AhR and LDTFs could be the reason for some instances of tumour-specific pro-oncogenicity of the AhR.

If this relationship between the AhR and LDTFs is biologically relevant in cancers beyond melanoma, then the AhR should be implicated in the dedifferentiation of various cancer cell types. There's evidence of AhR agonists stimulating EMT-like transcriptional changes and a more plastic cell state in BrCa cell lines (Diry et al., 2006), a cancer where the AhR modulates tumorigenesis through interactions with the immune system (Vogel et al., 2011), paralleling what I have observed in 501mel cells. These effects of AhR agonists on BrCa cell lines were dependent on the cell lines relying on expression of the oestrogen receptor (Diry et al., 2006), which is expressed in limited organs including the uterus and ovaries. Interestingly, the AhR has been shown to be pro-oncogenic in both tumour types, also contributing to EMT and metastases in ovarian cancer (Therachiyil et al., 2022; Yoshizawa et al., 2009). Although expression of oestrogen receptor is not lineage-defining, as it is for MITF and melanocytes, it is a potential interactor of the AhR which may begin to account for some of the cell type-specific effects of whether the AhR is pro- or anti-tumorigenic.

6.4. Further Work

6.4.1. The AhR's role in inflammatory signalling in melanoma

My proposed mechanism through which the AhR mediates NF-κB signalling, and by extension IFNγ-signalling, is through cytoplasmic interactions with IRAK1, which I propose would inhibit IRAK1 activity. My proximity-tagged affinity-purified coupled mass spectrometry has demonstrated the AhR interacts with IRAK1 (Fig. 3.13), however, I have not demonstrated a direct effect of the AhR on IRAK1 activity. I have demonstrated there's increased expression of NF-κB target gene IRF1 in response to AhR stimulation and AhR-loss in 501mel cells, and FICZ-mediated stimulation of 501mel cells produces greater enrichment of TNF signalling via NF-κB pathways - reflective of greater NF-κB activity. The effect of the AhR on IFNγ-signalling may be mediated through interactions with NF-κB signalling as I have demonstrated that treatment of 501mel^{WT} cells with TNF and IFNγ produces the same magnitude of *IDO1* induction as IFNγ-stimulation in 501mel *AHR*$^{-/-}$ cells but this remains unclear considering binding of the AhR to the *STAT1* promoter and no elevated *IRAK1* in 501mel *AHR*$^{-/-}$ cells.

In vivo experiments to support my observations directly would be essential to proving validity of my findings in melanoma. I have used data from TCGA to demonstrate AhR activity is correlated with enhanced IFNγ-signalling in patient samples, but confirming AhR inhibitors *in vivo* could suppress IFNγ-signalling wouldn't only support my findings but also confirm whether combination therapies with AhR inhibitors would be worth pursuing in the clinic.

6.4.2. The AhR's role in melanoma dedifferentiation via MITF

To develop ideas put forward in this thesis, a MITF ChIP-Seq in 501mel^{WT} and 501mel *AHR*$^{-/-}$ cells would be very useful. I have only examined this relationship between the AhR and MITF from perturbations of AhR activity and status. Performing MITF ChIP-Seq in 501mel *AHR*$^{-/-}$ cells should show enhanced binding of MITF to cell fate and differentiation genes and a depression in expression of invasion and metastases genes. A reporter construct with an AhRE and M-box upstream of a GFP gene or luciferase gene would potentially be able to demonstrate the same effect. However, my evidence suggests there's not a direct competition of the AhR and MITF for binding, chromatin context of these promoters may be essential to the mechanism, with binding of the AhR causing redistribution of nucleosomes to occlude MITF binding sites. An MITF ChIP Seq in 501mel *AHR*$^{-/-}$ cells and 501mel^{WT} cells would better demonstrate the mechanism of antagonism between these two factors that I have described.

Equally, cell invasion assays would elucidate whether AhR agonists and inhibitors such as FICZ and CH223191, respectively, are sufficient to drive phenotypic changes *in vitro*. I would expect that treatment of 501mel^{WT} cells with FICZ would increase cell mobility and invasion, and 501mel *AHR*$^{-/-}$ cells would be less invasive than 501mel^{WT} cells. Together, these data would help to demonstrate the role of the AhR in mediating phenotypic changes of melanoma cells, further supporting the argument for introduction of AhR inhibitors as melanoma therapies.

6.4.3. The AhR and melanoma treatments

As referred to several times previously, these novel mechanisms through which the AhR is contributing to melanoma progression and development make the AhR a key target for clinical intervention in melanoma. Exploring efficacy of combination therapies of AhR inhibitors, including CH223191 alongside anti-PD-L1 and anti-CTLA-4 monoclonal antibody drugs currently available in mouse melanoma models, could be the pathway to discovering a novel targeted therapeutic approach to melanoma, with my data suggesting AhR inhibitors should both resensitize the immune system to the tumour and preventing acquisition of more dedifferentiated and invasive phenotypes characteristic of late-stage more lethal disease.

7. Bibliography

Aguirre-Ghiso, J. A., Estrada, Y., Liu, D., & Ossowski, L. (2003). ERK MAPK Activity as a Determinant of Tumor Growth and Dormancy; Regulation by p38 SAPK 1. *Cancer Research*, *63*, 1684–1695. http://aacrjournals.org/cancerres/article-pdf/63/7/1684/2513077/ch0703001684.pdf

Aksan, I., & Goding, C. R. (1998). Targeting the Microphthalmia Basic Helix-Loop-Helix–Leucine Zipper Transcription Factor to a Subset of E-Box Elements In Vitro and In Vivo. *Molecular and Cellular Biology*, *18*(12), 6930–6938. https://doi.org/10.1128/MCB.18.12.6930

Alcolea, M. P., & Jones, P. H. (2014). Lineage Analysis of Epidermal Stem Cells. *Cold Spring Harbor Perspectives in Medicine*, *4*(1). https://doi.org/10.1101/CSHPERSPECT.A015206

Ali, Z., Yousaf, N., & Larkin, J. (2013). Melanoma epidemiology, biology and prognosis. *EJC Supplements*, *11*(2), 81–91. https://doi.org/10.1016/J.EJCSUP.2013.07.012

Altevogt, P., Von Hoegen, P., Leidig, S., & Schirrmacher, V. (1985). Effects of Mutagens on the Immunogenicity of Murine Tumor Cells: Immunological and Biochemical Evidence for Altered Cell Surface Antigens. *CANCER RESEARCH*, *45*, 4270–4277. http://aacrjournals.org/cancerres/article-pdf/45/9/4270/2926678/cr0450094270.pdf

Anzai, H., Yoshimoto, S., Okamura, K., Hiraki, A., & Hashimoto, S. (2022). IDO1-mediated Trp-kynurenine-AhR signal activation induces stemness and tumor dormancy in oral squamous cell carcinomas. *Oral Science International*, *19*(1), 31–43. https://doi.org/10.1002/OSI2.1109

Aptekmann, A. A., Bulavka, D., Nadra, A. D., & Sánchez, I. E. (2022). Transcription factor specificity limits the number of DNA-binding motifs. *PLoS ONE*, *17*(1), e0263307. https://doi.org/10.1371/JOURNAL.PONE.0263307

Arozarena, I., & Wellbrock, C. (2019). Phenotype plasticity as enabler of melanoma progression and therapy resistance. *Nature Reviews Cancer*, *19*(7), 377–391. https://doi.org/10.1038/S41568-019-0154-4

Ascierto, P. A., Kirkwood, J. M., Grob, J. J., Simeone, E., Grimaldi, A. M., Maio, M., Palmieri, G., Testori, A., Marincola, F. M., & Mozzillo, N. (2012). The role of BRAF V600 mutation in melanoma. *Journal of Translational Medicine*, *10*(1), 85–94. https://doi.org/10.1186/1479-5876-10-85

Baban, B., Chandler, P. R., Sharma, M. D., Pihkala, J., Koni, P. A., Munn, D. H., & Mellor, A. L. (2009). IDO activates regulatory T cells and blocks their conversion into Th17-like T cells. *Journal of Immunology (Baltimore, Md. : 1950)*, *183*(4), 2475–2483. https://doi.org/10.4049/JIMMUNOL.0900986

Babraham Bioinformatics - FastQC A Quality Control tool for High Throughput Sequence Data. (n.d.). Retrieved January 11, 2024, from https://www.bioinformatics.babraham.ac.uk/projects/fastqc/

Baccarelli, A., Pesatori, A. C., Masten, S. A., Patterson, D. G., Needham, L. L., Mocarelli, P., Caporaso, N. E., Consonni, D., Grassman, J. A., Bertazzi, P. A., & Landi, M. T. (2004). Aryl-hydrocarbon receptor-dependent pathway and toxic effects of TCDD in humans: a population-based study in Seveso, Italy. *Toxicology Letters*, *149*(1–3), 287–293. https://doi.org/10.1016/J.TOXLET.2003.12.062

Badawy, A. A.-B. (2017). Kynurenine Pathway of Tryptophan Metabolism: Regulatory and Functional Aspects. *International Journal of Tryptophan Research*, *10*, 1–20.

https://www.ncbi.nlm.nih.gov/pmc/articles/PMC5398323/pdf/10.1177_1178646917691938.pdf
Bai, J., Gao, Z., Li, X., Dong, L., Han, W., & Nie, J. (2017). Regulation of PD-1/PD-L1 pathway and resistance to PD-1/PD-L1 blockade. *Oncotarget*, *8*(66), 110693–110707. https://doi.org/10.18632/ONCOTARGET.22690
Bailey, C. M., Morrison, J. A., & Kulesa, P. M. (2012). Melanoma revives an embryonic migration program to promote plasticity and invasion. *Pigment Cell and Melanoma Research*, *25*(5), 573–583. https://doi.org/10.1111/J.1755-148X.2012.01025.X
Bailey, T. L., Johnson, J., Grant, C. E., & Noble, W. S. (2015). The MEME Suite. *Nucleic Acids Research*, *43*(W1), W39–W49. https://doi.org/10.1093/NAR/GKV416
Baksh, K., & Weber, J. (2015). Immune checkpoint protein inhibition for cancer: preclinical justification for CTLA-4 and PD-1 blockade and new combinations. *Seminars in Oncology*, *42*(3), 363–377. https://doi.org/10.1053/J.SEMINONCOL.2015.02.015
Beischlag, T. V, Morales, J. L., Hollingshead, B. D., & Perdew, G. H. (2008). The Aryl Hydrocarbon Receptor Complex and the Control of Gene Expression. *Critical Reviews in Eukaryotic Gene Expression*, *18*(3), 207–250.
Benboubker, V., Boivin, F., Dalle, S., & Caramel, J. (2022). Cancer Cell Phenotype Plasticity as a Driver of Immune Escape in Melanoma. *Frontiers in Immunology*, *13*, 873116. https://doi.org/10.3389/FIMMU.2022.873116/BIBTEX
Benito-Martínez, S., Salavessa, L., Raposo, G., Marks, M. S., & Delevoye, C. (2021). Melanin Transfer and Fate within Keratinocytes in Human Skin Pigmentation. *Integrative and Comparative Biology*, *61*(4), 1546–1555. https://doi.org/10.1093/ICB/ICAB094
Berico, P., Cigrang, M., Davidson, G., Braun, C., Sandoz, J., Legras, S., Vokshi, B. H., Slovic, N., Peyresaubes, F., Mario, C., Robles, G., Egly, J.-M., Compe, E., Davidson, I., & Coin, F. (2021). CDK7 and MITF repress a transcription program involved in survival and drug tolerance in melanoma. *EMBO Reports*, *22*(e51683), 1–18. https://doi.org/10.15252/embr.202051683
Bertolotto, C., Abbe, P., Hemesath, T. J., Bille, K., Fisher, D. E., Ortonne, J. P., & Ballotti, R. (1998). Microphthalmia Gene Product as a Signal Transducer in cAMP-Induced Differentiation of Melanocytes. *Journal of Cell Biology*, *142*(3), 827–835. https://doi.org/10.1083/JCB.142.3.827
Blankenstein, T., Coulie, P. G., Gilboa, E., & Jaffee, E. M. (2012). The determinants of tumour immunogenicity. *Nature Reviews Cancer 2012 12:4*, *12*(4), 307–313. https://doi.org/10.1038/nrc3246
Bock, K. W., & Köhle, C. (2006). Ah receptor: Dioxin-mediated toxic responses as hints to deregulated physiologic functions. *Biochemical Pharmacology*, *72*(4), 393–404. https://doi.org/10.1016/J.BCP.2006.01.017
Borcoman, E., Marret, G., & Le Tourneau, C. (2021). Paradigm Change in First-Line Treatment of Recurrent and/or Metastatic Head and Neck Squamous Cell Carcinoma. *Cancers*, *13*(11), 2573–2587. https://doi.org/10.3390/CANCERS13112573
Boriack-Sjodin, P. A., Margarit, S. M., Bar-Sagi, D., & Kuriyan, J. (1998). The structural basis of the activation of Ras by Sos. *Nature 1998 394:6691*, *394*(6691), 337–343. https://doi.org/10.1038/28548
Børretzen, A., Gravdal, K., Haukaas, S. A., Mannelqvist, M., Beisland, C., Akslen, L. A., & Halvorsen, O. J. (2021). The epithelial–mesenchymal transition regulators Twist, Slug, and Snail are associated with aggressive tumour features and poor outcome in

prostate cancer patients. *The Journal of Pathology: Clinical Research*, *7*(3), 253–270. https://doi.org/10.1002/CJP2.202

Boukamp, P., Petrussevska, R. T., Breitkreutz, D., Hornung, J., Markham, A., & Fusenig, N. E. (1988). Normal Keratinization in a Spontaneously Immortalized Aneuploid Human Keratinocyte Cell Line. *Journal of Cell Biology*, *106*, 761–771. http://rupress.org/jcb/article-pdf/106/3/761/1461052/761.pdf

Boukamp, P., Popp, S., Altmeyer, S., Hülsen, A., Fasching, C., Cremer, T., & Fusenig, N. E. (1997). Sustained nontumorigenic phenotype correlates with a largely stable chromosome content during long-term culture of the human keratinocyte line HaCat. *Genes Chromosomes and Cancer*, *19*(4), 201–214. https://doi.org/https://doi.org/10.1002/(SICI)1098

Bradley, S. D., Chen, Z., Melendez, B., Talukder, A., Khalili, J. S., Rodriguez-Cruz, T., Liu, S., Whittington, M., Deng, W., Li, F., Bernatchez, C., Radvanyi, L. G., Davies, M. A., Hwu, P., & Lizée, G. (2015). BRAFV600E co-opts a conserved MHC class I internalization pathway to diminish antigen presentation and CD8+ T-cell recognition of melanoma. *Cancer Immunology Research*, *3*(6), 602–609. https://doi.org/10.1158/2326-6066.CIR-15-0030/470471/AM/BRAF-V600E-CO-OPTS-A-CONSERVED-MHC-CLASS-I

Brenner, M., & Hearing, V. J. (2008). The Protective Role of Melanin Against UV Damage in Human Skin†. *Photochemistry and Photobiology*, *84*(3), 539–549. https://doi.org/10.1111/J.1751-1097.2007.00226.X

Caldenhoven, E., Buitenhuis, M., Van Dijk, T. B., Raaijmakers, J. A. M., Lammers, J. W. J., Koenderman, L., & De Groot, R. P. (1999). Lineage-specific activation of STAT3 by interferon-γ in human neutrophils. *Journal of Leukocyte Biology*, *65*(3), 391–396. https://doi.org/10.1002/JLB.65.3.391

Campesato, L. F., Budhu, S., Tchaicha, J., Weng, C. H., Gigoux, M., Cohen, I. J., Redmond, D., Mangarin, L., Pourpe, S., Liu, C., Zappasodi, R., Zamarin, D., Cavanaugh, J., Castro, A. C., Manfredi, M. G., McGovern, K., Merghoub, T., & Wolchok, J. D. (2020). Blockade of the AHR restricts a Treg-macrophage suppressive axis induced by L-Kynurenine. *Nature Communications*, *11*(1), 1–11. https://doi.org/10.1038/s41467-020-17750-z

Carreira, S., Goodall, J., Aksan, I., La Rocca, S. A., Galibert, M. D., Denat, L., Larue, L., & Goding, C. R. (2005). Mitf cooperates with Rb1 and activates p21Cip1 expression to regulate cell cycle progression. *Nature*, *433*(7027), 764–769. https://doi.org/10.1038/nature03269

Carreira, S., Goodall, J., Denat, L., Rodriguez, M., Nuciforo, P., Hoek, K. S., Testori, A., Larue, L., & Goding, C. R. (2006). Mitf regulation of Dia1 controls melanoma proliferation and invasiveness. *Genes & Development*, *20*(24), 3426–3439. https://doi.org/10.1101/GAD.406406

Carvajal, R. D., Sacco, J. J., Jager, M. J., Eschelman, D. J., Olofsson Bagge, R., Harbour, J. W., Chieng, N. D., Patel, S. P., Joshua, A. M., & Piperno-Neumann, S. (2023). Advances in the clinical management of uveal melanoma. *Nature Reviews Clinical Oncology*, *20*(2), 99–115. https://doi.org/10.1038/s41571-022-00714-1

Cha, J.-H., Chan, L.-C., Li, C.-W., Hsu, J. L., & Hung, M.-C. (2019). Molecular Cell Review Mechanisms Controlling PD-L1 Expression in Cancer. *Molecular Cell*, *76*(3), 359–370. https://doi.org/10.1016/j.molcel.2019.09.030

Chaffer, C. L., Marjanovic, N. D., Lee, T., Bell, G., Kleer, C. G., Reinhardt, F., D'Alessio, A. C., Young, R. A., & Weinberg, R. A. (2013). Poised chromatin at the ZEB1 promoter enables breast cancer cell plasticity and enhances tumorigenicity. *Cell*, *154*(1), 61–74. https://doi.org/10.1016/J.CELL.2013.06.005

Chaffer, C. L., & Weinberg, R. A. (2011). A perspective on cancer cell metastasis. *Science*, *331*(6024), 1559–1564. https://doi.org/10.1126/SCIENCE.1203543/SUPPL_FILE/1559.MP3

Chang, J., & Chaudhuri, O. (2019). Beyond proteases: Basement membrane mechanics and cancer invasion. *The Journal of Cell Biology*, *218*(8), 2456–2469. https://doi.org/10.1083/JCB.201903066

Chapman, P. B., Hauschild, A., Robert, C., Haanen, J. B., Ascierto, P., Larkin, J., Dummer, R., Garbe, C., Testori, A., Maio, M., Hogg, D., Lorigan, P., Lebbe, C., Jouary, T., Schadendorf, D., Ribas, A., O'Day, S. J., Sosman, J. A., Kirkwood, J. M., … McArthur, G. A. (2011). Improved Survival with Vemurafenib in Melanoma with BRAF V600E Mutation. *New England Journal of Medicine*, *364*(26), 2507–2516. https://doi.org/10.1056/NEJMOA1103782/SUPPL_FILE/NEJMOA1103782_DISCLOSURES.PDF

Chauhan, J. S., Hölzel, M., Lambert, J. P., Buffa, F. M., & Goding, C. R. (2022). The MITF regulatory network in melanoma. *Pigment Cell & Melanoma Research*, *35*(5), 517. https://doi.org/10.1111/PCMR.13053

Chen, C., Edelstein, L. C., & Gélinas, C. (2000). The Rel/NF-κB Family Directly Activates Expression of the Apoptosis Inhibitor Bcl-xL. *Molecular and Cellular Biology*, *20*(8), 2687–2695. https://doi.org/10.1128/MCB.20.8.2687-2695.2000

Chen, C., Huang, Y., Li, Y., Mao, Y., & Xie, Y. (2007). Cytochrome P450 1A1 (CYP1A1) T3801C and A2455G polymorphisms in breast cancer risk: a meta-analysis. *Journal of Human Genetics 2007 52:5*, *52*(5), 423–435. https://doi.org/10.1007/s10038-007-0131-8

Chen, J. Y., Li, C. F., Kuo, C. C., Tsai, K. K., Hou, M. F., & Hung, W. C. (2014). Cancer/stroma interplay via cyclooxygenase-2 and indoleamine 2,3-dioxygenase promotes breast cancer progression. *Breast Cancer Research : BCR*, *16*(4), 410–424. https://doi.org/10.1186/S13058-014-0410-1

Chiang, S. P. H., Cabrera, R. M., & Segall, J. E. (2016). Tumor cell intravasation. *American Journal of Physiology - Cell Physiology*, *311*(1), C1–C14. https://doi.org/10.1152/AJPCELL.00238.2015

Cirenajwis, H., Lauss, M., Ekedahl, H., Torngren, T., Kvist, A., Saal, L. H., Olsson, H., Staaf, J., Carneiro, A., Ingvar, C., Harbst, K., Hayward, N. K., & Jonsson, G. (2017). NF1-mutated melanoma tumors harbor distinct clinical and biological characteristics. *Molecular Oncology*, *11*(4), 438–451. https://doi.org/10.1002/1878-0261.12050

Compe, E., & Egly, J. M. (2021). The Long Road to Understanding RNAPII Transcription Initiation and Related Syndromes. *Annual Reviews Biochemistry*, *90*, 193–219. https://doi.org/10.1146/ANNUREV-BIOCHEM-090220-112253

Cornel, A. M., Mimpen, I. L., & Nierkens, S. (2020). MHC Class I Downregulation in Cancer: Underlying Mechanisms and Potential Targets for Cancer Immunotherapy. *Cancers*, *12*(7), 1760–1791. https://doi.org/10.3390/CANCERS12071760

Corre, S., Tardif, N., Mouchet, N., Leclair, H. M., Boussemart, L., Gautron, A., Bachelot, L., Perrot, A., Soshilov, A., Rogiers, A., Rambow, F., Dumontet, E., Tarte, K., Bessede, A., Guillemin, G. J., Marine, J. C., Denison, M. S., Gilot, D., & Galibert, M. D. (2018). Sustained activation of the Aryl hydrocarbon Receptor transcription factor promotes resistance to BRAF-inhibitors in melanoma. *Nature Communications*, *9*(1), 1–13. https://doi.org/10.1038/s41467-018-06951-2

Cox, M. B., & Miller, C. A. (2004). Cooperation of Heat Shock Protein 90 and p23 in Aryl Hydrocarbon Receptor Signaling. *Cell Stress & Chaperones*, *9*(1), 4–20. https://about.jstor.org/terms

Croft, A., Tay, K. H., Boyd, S. C., Guo, S. T., Jiang, C. C., Lai, F., Tseng, H. Y., Jin, L., Rizos, H., Hersey, P., & Zhang, X. D. (2014). Oncogenic activation of MEK/ERK primes melanoma cells for adaptation to endoplasmic reticulum stress. *The Journal of Investigative Dermatology*, *134*(2), 488–497. https://doi.org/10.1038/JID.2013.325

Cui, C., Xu, C., Yang, W., Chi, Z., Sheng, X., Si, L., Xie, Y., Yu, J., Wang, S., Yu, R., Guo, J., & Kong, Y. (2021). Ratio of the interferon-γ signature to the immunosuppression signature predicts anti-PD-1 therapy response in melanoma. *NPJ Genomic Medicine*, *6*(1), 1–12. https://doi.org/10.1038/S41525-021-00169-W

Curtin, N. J. (2012). DNA repair dysregulation from cancer driver to therapeutic target. *Nature Reviews Cancer*, *12*(12), 801–817. https://doi.org/10.1038/nrc3399

Dai, S., Qu, L., Li, J., Zhang, Y., Jiang, L., Wei, H., Guo, M., Chen, X., & Chen, Y. (2022). Structural insight into the ligand binding mechanism of aryl hydrocarbon receptor. *Nature Communications*, *13*(1), 1–12. https://doi.org/10.1038/s41467-022-33858-w

Dai, W., & Gupta, S. L. (1990). Regulation of indoleamine 2,3-dioxygenase gene expression in human fibroblasts by interferon-gamma. Upstream control region discriminates between interferon-gamma and interferon-alpha. *Journal of Biological Chemistry*, *265*(32), 19871–19877. https://doi.org/10.1016/S0021-9258(17)45453-6

Danecek, P., Bonfield, J. K., Liddle, J., Marshall, J., Ohan, V., Pollard, M. O., Whitwham, A., Keane, T., McCarthy, S. A., & Davies, R. M. (2021). Twelve years of SAMtools and BCFtools. *GigaScience*, *10*(2), 1–4. https://doi.org/10.1093/GIGASCIENCE/GIAB008

David, R. M., Jones, H. S., Panter, G. H., Winter, M. J., Hutchinson, T. H., & Kevin Chipman, J. (2012). Interference with xenobiotic metabolic activity by the commonly used vehicle solvents dimethylsulfoxide and methanol in zebrafish (Danio rerio) larvae but not Daphnia magna. *Chemosphere*, *88*(8), 912–917. https://doi.org/10.1016/j.chemosphere.2012.03.018

Davies, H., Bignell, G. R., Cox, C., Stephens, P., Edkins, S., Clegg, S., Teague, J., Woffendin, H., Garnett, M. J., Bottomley, W., Davis, N., Dicks, E., Ewing, R., Floyd, Y., Gray, K., Hall, S., Hawes, R., Hughes, J., Kosmidou, V., … Futreal, P. A. (2002). Mutations of the BRAF gene in human cancer. *Nature*, *417*(6892), 949–954. https://doi.org/10.1038/nature00766

De Abrew, K. N., Kaminski, N. E., & Thomas, R. S. (2010). An integrated genomic analysis of aryl hydrocarbon receptor-mediated inhibition of B-cell differentiation. *Toxicological Sciences : An Official Journal of the Society of Toxicology*, *118*(2), 454–469. https://doi.org/10.1093/TOXSCI/KFQ265

Díaz-Díaz, C. J., Ronnekleiv-Kelly, S. M., Nukaya, M., Geiger, P. G., Balbo, S., Dator, R., Megna, B. W., Carney, P. R., Bradfield, C. A., & Kennedy, G. D. (2016). The Aryl Hydrocarbon Receptor is a Repressor of Inflammation-associated Colorectal Tumorigenesis in Mouse. *Annals of Surgery*, *264*(3), 429–435. https://doi.org/10.1097/SLA.0000000000001874

Diedrich, J. D., Cole, C. E., Pianko, M. J., Colacino, J. A., & Bernard, J. J. (2023). Non-Toxicological Role of Aryl Hydrocarbon Receptor in Obesity-Associated Multiple Myeloma Cell Growth and Survival. *Cancers*, *15*(21). https://doi.org/10.3390/CANCERS15215255

Dilshat, R., Fock, V., Kenny, C., Gerritsen, I., Lasseur, R. M. J., Travnickova, J., Eichhoff, O., Cerny, P., Möller, K., Sigurbjörnsdóttir, S., Kirty, K., Einarsdottir, B. Ó., Cheng, P. F., Levesque, M., Cornell, R. A., Patton, E. E., Larue, L., De Tayrac, M., Magnúsdóttir, E., … Steingrímsson, E. (2021). Mitf reprograms the extracellular matrix and focal adhesion in melanoma. *ELife*, *10*, 1–59. https://doi.org/10.7554/ELIFE.63093

Dimco, G., Knight, R. A., Latchman, D. S., & Stephanou, A. (2010). STAT1 interacts directly with cyclin D1/Cdk4 and mediates cell cycle arrest. *Cell Cycle*, *9*(23), 4638–4649. https://doi.org/10.4161/CC.9.23.13955

DiMeglio, P., Duarte, J. H., Ahlfors, H., Owens, N. D. L., Li, Y., Villanova, F., Tosi, I., Hirota, K., Nestle, F. O., Mrowietz, U., Gilchrist, M. J., & Stockinger, B. (2014). Activation of the Aryl Hydrocarbon Receptor Dampens the Severity of Inflammatory Skin Conditions. *Immunity*, *40*(6), 989. https://doi.org/10.1016/J.IMMUNI.2014.04.019

DiNatale, B. C., Murray, I. A., Schroeder, J. C., Flaveny, C. A., Lahoti, T. S., Laurenzana, E. M., Omiecinski, C. J., & Perdew, G. H. (2010). Kynurenic Acid Is a Potent Endogenous Aryl Hydrocarbon Receptor Ligand that Synergistically Induces Interleukin-6 in the Presence of Inflammatory Signaling. *Toxicological Sciences*, *115*(1), 89–97. https://doi.org/10.1093/TOXSCI/KFQ024

Diry, M., Tomkiewicz, C., Koehle, C., Coumoul, X., Bock, K. W., Barouki, R., & Transy, C. (2006). Activation of the dioxin/aryl hydrocarbon receptor (AhR) modulates cell plasticity through a JNK-dependent mechanism. *Oncogene 2006 25:40*, *25*(40), 5570–5574. https://doi.org/10.1038/sj.onc.1209553

Dobin, A., Davis, C. A., Schlesinger, F., Drenkow, J., Zaleski, C., Jha, S., Batut, P., Chaisson, M., & Gingeras, T. R. (2013). STAR: ultrafast universal RNA-seq aligner. *Bioinformatics*, *29*(1), 15–21. https://doi.org/10.1093/BIOINFORMATICS/BTS635

Dolwick, K. M., Schmidt, J. V, Carver, L. A., Swanson, H. I., & Bradfield, C. A. (1993). Cloning and expression of a human Ah receptor cDNA. *Molecular Pharmacology*, *44*(5), 911–917.

Drakoulis, N., Cascorbi, I., Brockmöller, J., Gross, C. R., & Roots, I. (1994). Polymorphisms in the human CYP1A1 gene as susceptibility factors for lung cancer: exon-7 mutation (4889 A to G), and a T to C mutation in the 3′-flanking region. *The Clinical Investigator*, *72*(3), 240–248. https://doi.org/10.1007/BF00189321/METRICS

Du, J., Miller, A. J., Widlund, H. R., Horstmann, M. A., Ramaswamy, S., & Fisher, D. E. (2003). MLANA/MART1 and SILV/PMEL17/GP100 Are Transcriptionally Regulated by MITF in Melanocytes and Melanoma. *The American Journal of Pathology*, *163*(1), 333–343. https://doi.org/10.1016/S0002-9440(10)63657-7

Du, J., Widlund, H. R., Horstmann, M. A., Ramaswamy, S., Ross, K., Huber, W. E., Nishimura, E. K., Golub, T. R., & Fisher, D. E. (2004). Critical role of CDK2 for melanoma growth linked to its melanocyte-specific transcriptional regulation by MITF. *Cancer Cell*, *6*(6), 565–576. https://doi.org/10.1016/j.ccr.2004.10.014

Eccles, M. R., He, S., Ahn, A., Slobbe, L. J., Jeffs, A. R., Yoon, H. S., & Baguley, B. C. (2013). MITF and PAX3 play distinct roles in melanoma cell migration; outline of a "genetic switch" theory involving MITF and PAX3 in proliferative and invasive phenotypes of melanoma. *Frontiers in Oncology*, *3*, 51476–51485. https://doi.org/10.3389/FONC.2013.00229/BIBTEX

Elson, D. J., & Kolluri, S. K. (2023). Tumor-Suppressive Functions of the Aryl Hydrocarbon Receptor (AhR) and AhR as a Therapeutic Target in Cancer. *Biology (Basel)*, *12*(4), 526–549. https://doi.org/10.3390/BIOLOGY12040526

Esser, C., Bargen, I., Weighardt, H., Haarmann-Stemmann, T., & Krutmann, J. (2013). Functions of the aryl hydrocarbon receptor in the skin. In *Seminars in Immunopathology* (Vol. 35, Issue 6, pp. 677–691). https://doi.org/10.1007/s00281-013-0394-4

Fallarino, F., Grohmann, U., Vacca, C., Bianchi, R., Orabona, C., Spreca, A., Fioretti, M. C., & Puccetti, P. (2002). T cell apoptosis by tryptophan catabolism. *Cell Death & Differentiation 2002 9:10*, *9*(10), 1069–1077. https://doi.org/10.1038/sj.cdd.4401073

Fallarino, F., Grohmann, U., You, S., McGrath, B. C., Cavener, D. R., Vacca, C., Orabona, C., Bianchi, R., Belladonna, M. L., Volpi, C., Santamaria, P., Fioretti, M. C., & Puccetti, P. (2006). The combined effects of tryptophan starvation and tryptophan catabolites down-regulate T cell receptor zeta-chain and induce a regulatory phenotype in naive T cells. *Journal of Immunology (Baltimore, Md. : 1950)*, *176*(11), 6752–6761. https://doi.org/10.4049/JIMMUNOL.176.11.6752

Fernandez-Salguero, P. M., Ward, J. M., Sundberg, J. P., & Gonzalez, F. J. (1997). Lesions of Aryl-hydrocarbon Receptor–deficient Mice. *Http://Dx.Doi.Org/10.1177/030098589703400609*, *34*(6), 605–614. https://doi.org/10.1177/030098589703400609

Fernández-Sánchez, A., Raneros, A. B., Palao, R. C., Sanz, A. B., Ortiz, A., Ortega, F., Suárez-Álvarez, B., & López-Larrea, C. (2013). DNA demethylation and histone H3K9 acetylation determine the active transcription of the NKG2D gene in human CD8+ T and NK cells. *Epigenetics*, *8*(1), 66–78. https://doi.org/10.4161/EPI.23115

Gabbert, H., Wagner, R., Moll, R., & Gerharz, C. D. (1985). Tumor dedifferentiation: An important step in tumor invasion. *Clinical & Experimental Metastasis*, *3*(4), 257–279. https://doi.org/10.1007/BF01585081/METRICS

Garcia-Lora, A., Algarra, I., & Garrido, F. (2003). MHC class I antigens, immune surveillance, and tumor immune escape. *Journal of Cellular Physiology*, *195*(3), 346–355. https://doi.org/10.1002/JCP.10290

García-Martínez, A., Gamboa-Loira, B., Tejero, M. E., Sierra-Santoyo, A., Cebrián, M. E., & López-Carrillo, L. (2017). CYP1A1, CYP1B1, GSTM1 and GSTT1 genetic variants and breast cancer risk in Mexican women. *Salud Publica de Mexico*, *59*(5), 540–547. https://doi.org/10.21149/8527

Garraway, L. A., Widlund, H. R., Rubin, M. A., Getz, G., Berger, A. J., Ramaswamy, S., Beroukhim, R., Milner, D. A., Granter, S. R., Du, J., Lee, C., Wagner, S. N., Li, C., Golub, T. R., Rimm, D. L., Meyerson, M. L., Fisher, D. E., & Sellers, W. R. (2005). Integrative genomic analyses identify MITF as a lineage survival oncogene amplified in malignant melanoma. *Nature*, *436*(7047), 117–122. https://doi.org/10.1038/NATURE03664

Gelboin, H. V. (1980). Benzo[alpha]pyrene metabolism, activation and carcinogenesis: role and regulation of mixed-function oxidases and related enzymes. *Physiological Reviews*, *60*(4), 1107–1166. https://doi.org/10.1152/PHYSREV.1980.60.4.1107

Genetics Glossary, Oncogene. (n.d.). Https://Www.Genome.Gov/Genetics-Glossary/Oncogene. Retrieved January 29, 2024, from https://www.genome.gov/genetics-glossary/Oncogene

Germain, R. N. (1994). MHC-dependent antigen processing and peptide presentation: providing ligands for T lymphocyte activation. *Cell*, *76*(2), 287–299. https://doi.org/10.1016/0092-8674(94)90336-0

Gialeli, C., Theocharis, A. D., & Karamanos, N. K. (2011). Roles of matrix metalloproteinases in cancer progression and their pharmacological targeting. *The FEBS Journal*, *278*(1), 16–27. https://doi.org/10.1111/J.1742-4658.2010.07919.X

Giuliano, S., Cheli, Y., Ohanna, M., Bonet, C., Beuret, L., Bille, K., Loubat, A., Hofman, V., Hofman, P., Ponzio, G., Bahadoran, P., Ballotti, R., & Bertolotto, C. (2010). Microphthalmia-associated transcription factor controls the DNA damage response and a lineage-specific senescence program in melanomas. *Cancer Research*, *70*(9), 3813–3822. https://doi.org/10.1158/0008-5472.CAN-09-2913/655681/P/MICROPHTHALMIA-ASSOCIATED-TRANSCRIPTION-FACTOR

Goding, C. R., & Arnheiter, H. (2019). MITF-the first 25 years. *Genes and Development*, *33*(15–16), 983–1007. https://doi.org/10.1101/gad.324657.119

Gottipati, S., Rao, N. L., & Fung-Leung, W. P. (2008). IRAK1: A critical signaling mediator of innate immunity. *Cellular Signalling*, *20*(2), 269–276. https://doi.org/10.1016/J.CELLSIG.2007.08.009

Gowthami, C., Kumar, P., Ravikumar, A., Joseph, L. D., & Rajendiran, S. (2014). Malignant Melanoma of the External Auditory Canal. *Journal of Clinical and Diagnostic Research : JCDR*, *8*(8), FD04–FD06. https://doi.org/10.7860/JCDR/2014/8841.4719

Greenlund, A. C., Morales, M. O., Vivlano, S. L., Yan, H., Krolewski, J., & Schrelber', R. D. (1995). Stat Recruitment by Tyrosine-Phosphorylated Cytokine Receptors: An Ordered Reversible Affinity-Driven Process. *Immunity*, *2*(6), 677–667.

Greenwald, R. J., Boussiotis, V. A., Lorsbach, R. B., Abbas, A. K., & Sharpe, A. H. (2001). CTLA-4 regulates induction of anergy in vivo. *Immunity*, *14*(2), 145–155. https://doi.org/10.1016/S1074-7613(01)00097-8

Grieshober, L., Graw, S., Barnett, M. J., Thornquist, M. D., Goodman, G. E., Chen, C., Koestler, D. C., Marsit, C. J., & Doherty, J. A. (2020). AHRR methylation in heavy smokers: Associations with smoking, lung cancer risk, and lung cancer mortality. *BMC Cancer*, *20*(1). https://doi.org/10.1186/s12885-020-07407-x

Gruszczyk, J., Grandvuillemin, L., Lai-Kee-Him, J., Paloni, M., Savva, C. G., Germain, P., Grimaldi, M., Boulahtouf, A., Kwong, H. S., Bous, J., Ancelin, A., Bechara, C., Barducci, A., Balaguer, P., & Bourguet, W. (2022). Cryo-EM structure of the agonist-bound Hsp90-XAP2-AHR cytosolic complex. *Nature Communications*, *13*(1), 1–13. https://doi.org/10.1038/s41467-022-34773-w

Guarino, M. (2010). Src signaling in cancer invasion. *Journal of Cellular Physiology*, *223*(1), 14–26. https://doi.org/10.1002/JCP.22011

Han, H., Safe, S., Jayaraman, A., & Chapkin, R. S. (2021). Diet-Host-Microbiota Interactions Shape Aryl Hydrocarbon Receptor Ligand Production to Modulate Intestinal Homeostasis. *Annual Review of Nutrition*, *41*, 455–478. https://doi.org/10.1146/ANNUREV-NUTR-043020-090050

Han, Y., Liu, D., & Li, L. (2020). PD-1/PD-L1 pathway: current researches in cancer. *American Journal of Cancer Research*, *10*(3), 727–742. /pmc/articles/PMC7136921/

Hanahan, D. (2022). Hallmarks of Cancer: New Dimensions. *Cancer Discovery*, *12*(1), 31–46. https://doi.org/10.1158/2159-8290.CD-21-1059

Hanahan, D., & Weinberg, R. A. (2000). The Hallmarks of Cancer. *Cell*, *100*(1), 57–70. https://doi.org/10.1016/S0092-8674(00)81683-9

Hanahan, D., & Weinberg, R. A. (2011). Hallmarks of cancer: the next generation. *Cell*, *144*(5), 646–674. https://doi.org/10.1016/J.CELL.2011.02.013

Hao, D., Wang, L., & Di, L. J. (2016). Distinct mutation accumulation rates among tissues determine the variation in cancer risk. *Scientific Reports*, *6*(19458), 1–5. https://doi.org/10.1038/SREP19458

Hargis, J. C., Schaefer, H. F., Houk, K. N., & Wheeler, S. E. (2010). Noncovalent interactions of a benzo[a]pyrene diol epoxide with DNA base pairs: Insight into the

formation of adducts of (+)-BaP DE-2 with DNA. *Journal of Physical Chemistry A*, *114*(4), 2038–2044. https://doi.org/10.1021/JP911376P/SUPPL_FILE/JP911376P_SI_001.PDF

Hartman, M. L., Talar, B., Noman, M. Z., Gajos-Michniewicz, A., Chouaib, S., & Czyz, M. (2014). Gene Expression Profiling Identifies Microphthalmia-Associated Transcription Factor (MITF) and Dickkopf-1 (DKK1) as Regulators of Microenvironment-Driven Alterations in Melanoma Phenotype. *PLoS ONE*, *9*(4), e95157–e95170. https://doi.org/10.1371/JOURNAL.PONE.0095157

Hassanain S, H. H., Young Chon, S., & Guptas, S. L. (1993). Differential regulation of human indoleamine 2,3-dioxygenase gene expression by interferons-gamma and -alpha. Analysis of the regulatory region of the gene and identification of an interferon-gamma-inducible DNA-binding factor. *THE JOURNAL OF BIOLOGICAL CHEMISTRY*, *268*(7), 182–191. https://doi.org/10.1016/S0021-9258(18)53504-3

Hayflick, L., & Moorhead, P. S. (1961). The serial cultivation of human diploid cell strains. *Experimental Cell Research*, *25*(3), 585–621. https://doi.org/10.1016/0014-4827(61)90192-6

Heinz, S., Benner, C., Spann, N., Bertolino, E., Lin, Y. C., Laslo, P., Cheng, J. X., Murre, C., Singh, H., & Glass, C. K. (2010). Simple Combinations of Lineage-Determining Transcription Factors Prime cis-Regulatory Elements Required for Macrophage and B Cell Identities. *Molecular Cell*, *38*(4), 576–589. https://doi.org/10.1016/j.molcel.2010.05.004

Hellemans, J., Mortier, G., De Paepe, A., Speleman, F., & Vandesompele, J. (2008). qBase relative quantification framework and software for management and automated analysis of real-time quantitative PCR data. *Genome Biology*, *8*(2), 1–14. https://doi.org/10.1186/GB-2007-8-2-R19/COMMENTS

Hemesath, T. J., Steingrímsson, E., McGill, G., Hansen, M. J., Vaught, J., Hodgkinson, C. A., Arnheiter, H., Copeland, N. G., Jenkins, N. A., & Fisher, D. E. (1994). microphthalmia, a critical factor in melanocyte development, defines a discrete transcription factor family. *Genes & Development*, *8*(22), 2770–2780. https://doi.org/10.1101/GAD.8.22.2770

Hewitt, E. W. (2003). The MHC class I antigen presentation pathway: strategies for viral immune evasion. *Immunology*, *110*(2), 163–169. https://doi.org/10.1046/J.1365-2567.2003.01738.X

Hinz, M., Krappmann, D., Eichten, A., Heder, A., Scheidereit, C., & Strauss, M. (1999). NF-κB Function in Growth Control: Regulation of Cyclin D1 Expression and G0/G1-to-S-Phase Transition. *Molecular and Cellular Biology*, *19*(4), 2690–2698. https://doi.org/10.1128/MCB.19.4.2690

Hirano, T., Ishihara, K., & Hibi, M. (2000). Roles of STAT3 in mediating the cell growth, differentiation and survival signals relayed through the IL-6 family of cytokine receptors. *Oncogene 2000 19:21*, *19*(21), 2548–2556. https://doi.org/10.1038/sj.onc.1203551

Hiroi, M., & Ohmori, Y. (2005). Transcriptional Synergism between NF-κB and STAT1. *Journal of Oral Biosciences*, *47*(3), 230–242. https://doi.org/10.1016/S1349-0079(05)80029-5

Hodi, F. S., Chesney, J., Pavlick, A. C., Robert, C., Grossmann, K. F., McDermott, D. F., Linette, G. P., Meyer, N., Giguere, J. K., Agarwala, S. S., Shaheen, M., Ernstoff, M. S., Minor, D. R., Salama, A. K., Taylor, M. H., Ott, P. A., Horak, C., Gagnier, P., Jiang, J., … Postow, M. A. (2016). Combined nivolumab and ipilimumab versus ipilimumab alone in patients with advanced melanoma: 2-year overall survival

outcomes in a multicentre, randomised, controlled, phase 2 trial. *The Lancet. Oncology*, *17*(11), 1558–1568. https://doi.org/10.1016/S1470-2045(16)30366-7

Hodi, F. S., Chiarion-Sileni, V., Gonzalez, R., Grob, J. J., Rutkowski, P., Cowey, C. L., Lao, C. D., Schadendorf, D., Wagstaff, J., Dummer, R., Ferrucci, P. F., Smylie, M., Hill, A., Hogg, D., Marquez-Rodas, I., Jiang, J., Rizzo, J., Larkin, J., & Wolchok, J. D. (2018). Nivolumab plus ipilimumab or nivolumab alone versus ipilimumab alone in advanced melanoma (CheckMate 067): 4-year outcomes of a multicentre, randomised, phase 3 trial. *The Lancet. Oncology*, *19*(11), 1480–1492. https://doi.org/10.1016/S1470-2045(18)30700-9

Hodi, F. S., O'Day, S. J., McDermott, D. F., Weber, R. W., Sosman, J. A., Haanen, J. B., Gonzalez, R., Robert, C., Schadendorf, D., Hassel, J. C., Akerley, W., van den Eertwegh, A. J. M., Lutzky, J., Lorigan, P., Vaubel, J. M., Linette, G. P., Hogg, D., Ottensmeier, C. H., Lebbé, C., … Urba, W. J. (2010). Improved Survival with Ipilimumab in Patients with Metastatic Melanoma. *New England Journal of Medicine*, *363*(8), 711–723. https://doi.org/10.1056/NEJMOA1003466/SUPPL_FILE/NEJMOA1003466_DISCLOSURES.PDF

Hodis, E., Watson, I. R., Kryukov, G. V., Arold, S. T., Imielinski, M., Theurillat, J. P., Nickerson, E., Auclair, D., Li, L., Place, C., Dicara, D., Ramos, A. H., Lawrence, M. S., Cibulskis, K., Sivachenko, A., Voet, D., Saksena, G., Stransky, N., Onofrio, R. C., … Chin, L. (2012). A landscape of driver mutations in melanoma. *Cell*, *150*(2), 251–263. https://doi.org/10.1016/J.CELL.2012.06.024

Hoek, K. S., Schlegel, N. C., Eichhoff, O. M., Widmer, D. S., Praetorius, C., Einarsson, S. O., Valgeirsdottir, S., Bergsteinsdottir, K., Schepsky, A., Dummer, R., & Steingrimsson, E. (2008). Novel MITF targets identified using a two-step DNA microarray strategy. *Pigment Cell & Melanoma Research*, *21*(6), 665–676. https://doi.org/10.1111/J.1755-148X.2008.00505.X

Hoesel, B., & Schmid, J. A. (2013). The complexity of NF-κB signaling in inflammation and cancer. *Molecular Cancer*, *12*(1), 1–15. https://doi.org/10.1186/1476-4598-12-86

Horvath, C. M. (2000). STAT proteins and transcriptional responses to extracellular signals. *Trends in Biochemical Sciences*, *25*(10), 496–502. https://doi.org/10.1016/S0968-0004(00)01624-8

Hossain, S. M., & Eccles, M. R. (2023). Phenotype Switching and the Melanoma Microenvironment; Impact on Immunotherapy and Drug Resistance. *International Journal of Molecular Sciences*, *24*(2), 1601–1620. https://doi.org/10.3390/IJMS24021601

Ikuta, T., Eguchi, H., Tachibana, T., Yoneda, Y., & Kawajiri, K. (1998). Nuclear localization and export signals of the human aryl hydrocarbon receptor. *Journal of Biological Chemistry*, *273*(5), 2895–2904. https://doi.org/10.1074/jbc.273.5.2895

Ikuta, T., Tachibana, T., Watanabe, J., Yoshida, M., Yoneda, Y., & Kawajiri, K. (2000). Nucleocytoplasmic Shuttling of the Aryl Hydrocarbon Receptor. *The Journal of Biochemistry*, *127*(3), 503–509. https://doi.org/10.1093/OXFORDJOURNALS.JBCHEM.A022633

Inukai, S., Hong Kock, K., & Bulyk, M. L. (2017). Transcription factor-DNA binding: beyond binding site motifs. *Current Opinions in Genetic Development*, *43*, 110–119. https://doi.org/10.1016/j.gde.2017.02.007

Ishihara, Y., Kado, S. Y., Bein, K. J., He, Y., Pouraryan, A. A., Urban, A., Haarmann-Stemmann, T., Sweeney, C., & Vogel, C. F. A. (2021). Aryl Hydrocarbon Receptor Signaling Synergizes with TLR/NF-κB-Signaling for Induction of IL-22 Through

Canonical and Non-Canonical AhR Pathways. *Frontiers in Toxicology*, *3*, 787360–787377. https://doi.org/10.3389/FTOX.2021.787360/BIBTEX

Ishihara, Y., Kado, S. Y., Hoeper, C., Harel, S., & Vogel, C. F. A. (2019). Role of NF-kB RelB in Aryl Hydrocarbon Receptor-Mediated Ligand Specific Effects. *International Journal of Molecular Sciences*, *20*(11), 2652–2662. https://doi.org/10.3390/IJMS20112652

Ishikawa, M., Sugino, S., Masuda, Y., Tarumoto, Y., Seto, Y., Taniyama, N., Wagai, F., Yamauchi, Y., Kojima, Y., Kiryu, H., Yusa, K., Eiraku, M., & Mochizuki, A. (2023). RENGE infers gene regulatory networks using time-series single-cell RNA-seq data with CRISPR perturbations. *Communications Biology*, *6*(1), 1–14. https://doi.org/10.1038/s42003-023-05594-4

Jacob, A., Hartz, A. M. S., Potin, S., Coumoul, X., Yousif, S., Scherrmann, J. M., Bauer, B., & Declèves, X. (2011). Aryl hydrocarbon receptor-dependent upregulation of Cyp1b1 by TCDD and diesel exhaust particles in rat brain microvessels. *Fluids and Barriers of the CNS*, *8*(1), 23–35. https://doi.org/10.1186/2045-8118-8-23

Jafri, M. A., Ansari, S. A., Alqahtani, M. H., & Shay, J. W. (2016). Roles of telomeres and telomerase in cancer, and advances in telomerase-targeted therapies. *Genome Medicine*, *8*(1), 1–18. https://doi.org/10.1186/S13073-016-0324-X

Jardim, D. L., Goodman, A., De Melo Gagliato, D., & Kurzrock, R. (2021). The Challenges of Tumor Mutational Burden as an Immunotherapy Biomarker. *Cancer Cell*, *39*(2), 154–173. https://doi.org/10.1016/j.ccell.2020.10.001

Jin, U. H., Karki, K., Cheng, Y., Michelhaugh, S. K., Mittal, S., & Safe, S. (2019). The aryl hydrocarbon receptor is a tumor suppressor–like gene in glioblastoma. *The Journal of Biological Chemistry*, *294*(29), 11342–11353. https://doi.org/10.1074/JBC.RA119.008882

Johannessen, C. M., Boehm, J. S., Kim, S. Y., Thomas, S. R., Wardwell, L., Johnson, L. A., Emery, C. M., Stransky, N., Cogdill, A. P., Barretina, J., Caponigro, G., Hieronymus, H., Murray, R. R., Salehi-Ashtiani, K., Hill, D. E., Vidal, M., Zhao, J. J., Yang, X., Alkan, O., … Garraway, L. A. (2010). COT drives resistance to RAF inhibition through MAP kinase pathway reactivation. *Nature*, *468*(7326), 968–972. https://doi.org/10.1038/NATURE09627

Jung, K. H., LoRusso, P., Burris, H., Gordon, M., Bang, Y. J., Hellmann, M. D., Cervantes, A., Ochoa de Olza, M., Marabelle, A., Stephen Hodi, F., Ahn, M. J., Emens, L. A., Barlesi, F., Hamid, O., Calvo, E., McDermott, D., Soliman, H., Rhee, I., Lin, R., … Lindsey Davis, S. (2019). Phase I study of the indoleamine 2,3-dioxygenase 1 (IDO1) inhibitor navoximod (GDC-0919) administered with PD-L1 inhibitor (atezolizumab) in advanced solid tumors. *Clinical Cancer Research*, *25*(11), 3220–3228. https://doi.org/10.1158/1078-0432.CCR-18-2740/74186/AM/PHASE-I-STUDY-OF-THE-INDOLEAMINE-2-3-DIOXYGENASE-1

Kado, S. Y., Bein, K., Castaneda, A. R., Pouraryan, A. A., Garrity, N., Ishihara, Y., Rossi, A., Haarmann-Stemmann, T., Sweeney, C. A., & Vogel, C. F. A. (2023). Regulation of IDO2 by the Aryl Hydrocarbon Receptor (AhR) in Breast Cancer. *Cells*, *12*(10), 1433. https://doi.org/10.3390/CELLS12101433

Kashyap, D., Garg, V. K., Sandberg, E. N., Goel, N., & Bishayee, A. (2021). Oncogenic and Tumor Suppressive Components of the Cell Cycle in Breast Cancer Progression and Prognosis. *Pharmaceutics*, *13*(4), 569–597. https://doi.org/10.3390/PHARMACEUTICS13040569

Kaunitz, G. J., Cottrell, T. R., Lilo, M., Muthappan, V., Esandrio, J., Berry, S., Xu, H., Ogurtsova, A., Anders, R. A., Fischer, A. H., Kraft, S., Gerstenblith, M. R.,

Thompson, C. L., Honda, K., Cuda, J. D., Eberhart, C. G., Handa, J. T., Lipson, E. J., & Taube, J. M. (2017). Melanoma subtypes demonstrate distinct PD-L1 expression profiles. *Laboratory Investigation*, *97*(9), 1063–1071. https://doi.org/10.1038/labinvest.2017.64

Kawajiri, K., Kobayashi, Y., Ohtake, F., Ikuta, T., Matsushima, Y., Mimura, J., Pettersson, S., Pollenz, R. S., Sakaki, T., Hirokawa, T., Akiyama, T., Kurosumi, M., Poellinger, L., Kato, S., & Fujii-Kuriyama, Y. (2009). Aryl hydrocarbon receptor suppresses intestinal carcinogenesis in Apc Min/+ mice with natural ligands. *Proceedings of the National Academy of Sciences of the United States of America*, *106*(32), 13481–13486. https://doi.org/10.1073/PNAS.0902132106/SUPPL_FILE/0902132106SI.PDF

Kawakami, A., & Fisher, D. E. (2017). The master role of microphthalmia-associated transcription factor in melanocyte and melanoma biology. *Laboratory Investigation*, *97*(6), 649–656. https://doi.org/10.1038/LABINVEST.2017.9

Kenison, J. E., Wang, Z., Yang, K., Snyder, M., Quintana, F. J., & Sherr, D. H. (2021). The aryl hydrocarbon receptor suppresses immunity to oral squamous cell carcinoma through immune checkpoint regulation. *Proceedings of the National Academy of Sciences of the United States of America*, *118*(19), e2012692118–e2102704. https://doi.org/10.1073/PNAS.2012692118/SUPPL_FILE/PNAS.2012692118.SAPP.PDF

Kent, W. J., Sugnet, C. W., Furey, T. S., Roskin, K. M., Pringle, T. H., Zahler, A. M., & Haussler, and D. (2002). The human genome browser at UCSC. *Genome Research*, *12*(6), 996–1006. https://doi.org/10.1101/GR.229102

Kim, D. W., Sovak, M. A., Zanieski, G., Nonet, G., Romieu-Mourez, R., Lau, A. W., Hafer, L. J., Yaswen, P., Stampfer, M., Rogers, A. E., Russo, J., & Sonenshein, G. E. (2000). Activation of NF-κB/Rel occurs early during neoplastic transformation of mammary cells. *Carcinogenesis*, *21*(5), 871–879. https://doi.org/10.1093/CARCIN/21.5.871

Kim, S. H., Henry, E. C., Kim, D. K., Kim, Y. H., Kum, J. S., Myoung, S. H., Lee, T. G., Kang, J. K., Gasiewicz, T. A., Sung, H. R., & Suh, P. G. (2006). Novel compound 2-methyl-2H-pyrazole-3-carboxylic acid (2-methyl-4-o-tolylazo-phenyl)-amide (CH-223191) prevents 2,3,7,8-TCDD-induced toxicity by antagonizing the aryl hydrocarbon receptor. *Molecular Pharmacology*, *69*(6), 1871–1878. https://doi.org/10.1124/MOL.105.021832

Kobayashi, A., Sogawa, K., & Fujii-Kuriyama, Y. (1996). Cooperative Interaction between AhR·Arnt and Sp1 for the Drug-inducible Expression of CYP1A1 Gene. *Journal of Biological Chemistry*, *271*(21), 12310–12316. https://doi.org/10.1074/JBC.271.21.12310

Kober, C., Roewe, J., Schmees, N., Roese, L., Roehn, U., Bader, B., Stoeckigt, D., Prinz, F., Gorjánácz, M., Roider, H. G., Olesch, C., Leder, G., Irlbacher, H., Lesche, R., Lefranc, J., Oezcan-Wahlbrink, M., Batra, A. S., Elmadany, N., Carretero, R., … Gutcher, I. (2023). Targeting the aryl hydrocarbon receptor (AhR) with BAY 2416964: a selective small molecule inhibitor for cancer immunotherapy. *Journal for Immunotherapy of Cancer*, *11*(11), e007495-e07508. https://doi.org/10.1136/JITC-2023-007495

Kontomanolis, E. N., Koutras, A., Syllaios, A., Schizas, D., Mastoraki, A., Garmpis, N., Diakosavvas, M., Angelou, K., Tsatsaris, G., Pagkalos, A., Ntounis, T., & Fasoulakis, Z. (2020). Role of Oncogenes and Tumor-suppressor Genes in Carcinogenesis: A Review. *Anticancer Research*, *40*(11), 6009–6015. https://doi.org/10.21873/ANTICANRES.14622

Korkalainen, M., Huumonen, K., Naarala, J., Viluksela, M., & Juutilainen, J. (2012). Dioxin Induces Genomic Instability in Mouse Embryonic Fibroblasts. *PLOS ONE*, *7*(5), e37895–e37903. https://doi.org/10.1371/JOURNAL.PONE.0037895

Krishnan, V., Porter, W., Santostefano, M., Wang, X., & Safe, S. (1995). Molecular mechanism of inhibition of estrogen-induced cathepsin D gene expression by 2,3,7,8-tetrachlorodibenzo-p-dioxin (TCDD) in MCF-7 cells. *Molecular and Cellular Biology*, *15*(12), 6710. https://doi.org/10.1128/MCB.15.12.6710

Kukurba, K. R., & Montgomery, S. B. (2015). RNA Sequencing and Analysis. *Cold Spring Harbor Protocols*, *11*, 951–969. https://doi.org/10.1101/PDB.TOP084970

Labadie, B. W., Bao, R., & Luke, J. J. (2019). Reimagining IDO pathway inhibition in cancer immunotherapy via downstream focus on the tryptophan–kynurenine–aryl hydrocarbon axis. *Clinical Cancer Research*, *25*(5), 1462–1471. https://doi.org/10.1158/1078-0432.CCR-18-2882

Lafleur, V. N., Halim, S., Choudhry, H., Ratcliffe, P. J., & Mole, D. R. (2023). Multi-level interaction between HIF and AHR transcriptional pathways in kidney carcinoma. *Life Science Alliance*, *6*(4). https://doi.org/10.26508/LSA.202201756

Lambert, J. P., Tucholska, M., Go, C., Knight, J. D. R., & Gingras, A. C. (2015). Proximity biotinylation and affinity purification are complementary approaches for the interactome mapping of chromatin-associated protein complexes. *Journal of Proteomics*, *118*, 81–94. https://doi.org/10.1016/J.JPROT.2014.09.011

Lambert, S. A., Jolma, A., Campitelli, L. F., Das, P. K., Yin, Y., Albu, M., Chen, X., Taipale, J., Hughes, T. R., & Weirauch, M. T. (2018). The Human Transcription Factors. *Cell*, *172*(4), 650–665. https://doi.org/10.1016/j.cell.2018.01.029

Le, L., Sirés-Campos, J., Raposo, G., Delevoye, C., & Marks, M. S. (2021). Melanosome Biogenesis in the Pigmentation of Mammalian Skin. *Integrative and Comparative Biology*, *61*(4), 1517–1545. https://doi.org/10.1093/ICB/ICAB078

Leclair, H. M., Tardif, N., Paris, A., & Galibert, M. (2020). Role of Flavonoids in the Prevention of AhR-Dependent Resistance During Treatment with BRAF Inhibitors. *International Journal of Molecular Sciences*, *21*, 5025–5046.

Lee, A., Kanuri, N., Zhang, Y., Sayuk, G. S., Li, E., & Ciorba, M. A. (2014). IDO1 and IDO2 Non-Synonymous Gene Variants: Correlation with Crohn's Disease Risk and Clinical Phenotype. *PLOS ONE*, *9*(12), e115848. https://doi.org/10.1371/JOURNAL.PONE.0115848

Lee, C. C., Yang, W. H., Li, C. H., Cheng, Y. W., Tsai, C. H., & Kang, J. J. (2016). Ligand independent aryl hydrocarbon receptor inhibits lung cancer cell invasion by degradation of Smad4. *Cancer Letters*, *376*(2), 211–217. https://doi.org/10.1016/J.CANLET.2016.03.052

Lee, E. Y. H. P., & Muller, W. J. (2010). Oncogenes and Tumor Suppressor Genes. *Cold Spring Harbor Perspectives in Biology*, *2*, a003236–a003254. https://doi.org/10.1101/CSHPERSPECT.A003236

Leicht, D. T., Balan, V., Kaplun, A., Singh-Gupta, V., Kaplun, L., Dobson, M., & Tzivion, G. (2007). Raf kinases: Function, regulation and role in human cancer. *Biochimica et Biophysica Acta (BBA) - Molecular Cell Research*, *1773*(8), 1196–1212. https://doi.org/10.1016/J.BBAMCR.2007.05.001

Lerdrup, M., Johansen, J. V., Agrawal-Singh, S., & Hansen, K. (2016). An interactive environment for agile analysis and visualization of ChIP-sequencing data. *Nature Structural & Molecular Biology*, *23*(4), 349–357. https://doi.org/10.1038/nsmb.3180

Leviyang, S. (2021). Interferon stimulated binding of ISRE is cell type specific and is predicted by homeostatic chromatin state. *Cytokine: X*, *3*, 100056–100066. https://doi.org/10.1016/J.CYTOX.2021.100056

Li, H., & Durbin, R. (2009). Fast and accurate short read alignment with Burrows-Wheeler transform. *Bioinformatics (Oxford, England)*, *25*(14), 1754–1760. https://doi.org/10.1093/BIOINFORMATICS/BTP324

Li, H., Luo, L., Wang, D., Duan, J., & Zhang, R. (2020). Lack of association between multiple polymorphisms in aryl hydrocarbon receptor (AhR) gene and cancer susceptibility. *Environmental Health and Preventative Medicine*, *25*(79). https://doi.org/10.1186/s12199-020-00907-z

Li, J., & Stanger, B. Z. (2020). How tumor cell dedifferentiation drives immune evasion and resistance to immunotherapy. *Cancer Research*, *80*(19), 4037–4041. https://doi.org/10.1158/0008-5472.CAN-20-1420/654544/AM/HOW-TUMOR-CELL-DEDIFFERENTIATION-DRIVES-IMMUNE

Li, M., Bolduc, A. R., Hoda, M. N., Gamble, D. N., Dolisca, S. B., Bolduc, A. K., Hoang, K., Ashley, C., McCall, D., Rojiani, A. M., Maria, B. L., Rixe, O., MacDonald, T. J., Heeger, P. S., Mellor, A. L., Munn, D. H., & Johnson, T. S. (2014). The indoleamine 2,3-dioxygenase pathway controls complement-dependent enhancement of chemo-radiation therapy against murine glioblastoma. *Journal for Immunotherapy of Cancer*, *2*(21), 1–13. https://doi.org/10.1186/2051-1426-2-21

Li, Q., Murphy, M., Ross, J., Sheehan, C., & Carlson, J. A. (2004). Skp2 and p27kip1 expression in melanocytic nevi and melanoma: an inverse relationship. *Journal of Cutaneous Pathology*, *31*(10), 633–642. https://doi.org/10.1111/J.0303-6987.2004.00243.X

Li, S., Pei, X., Zhang, W., Xie, H. Q., & Zhao, B. (2014). Functional Analysis of the Dioxin Response Elements (DREs) of the Murine CYP1A1 Gene Promoter: Beyond the Core DRE Sequence. *International Journal of Molecular Sciences*, *15*(4), 6475–6487. https://doi.org/10.3390/IJMS15046475

Li, Y., Gao, J., Kamran, M., Harmacek, L., Danhorn, T., Leach, S. M., O'Connor, B. P., Hagman, J. R., & Huang, H. (2021). GATA2 regulates mast cell identity and responsiveness to antigenic stimulation by promoting chromatin remodeling at super-enhancers. *Nature Communications 2021 12:1*, *12*(1), 1–17. https://doi.org/10.1038/s41467-020-20766-0

Li, Y., Innocentin, S., Withers, D. R., Roberts, N. A., Gallagher, A. R., Grigorieva, E. F., Wilhelm, C., & Veldhoen, M. (2011). Exogenous stimuli maintain intraepithelial lymphocytes via aryl hydrocarbon receptor activation. *Cell*, *147*(3), 629–640. https://doi.org/10.1016/J.CELL.2011.09.025

Lickwar, C. R., Mueller, F., Hanlon, S. E., McNally, J. G., & Lieb, J. D. (2012). Genome-wide protein–DNA binding dynamics suggest a molecular clutch for transcription factor function. *Nature 2012 484:7393*, *484*(7393), 251–255. https://doi.org/10.1038/nature10985

Lin, P. H., Lin, C. H., Huang, C. C., Chuang, M. C., & Lin, P. (2007). 2,3,7,8-Tetrachlorodibenzo-p-dioxin (TCDD) induces oxidative stress, DNA strand breaks, and poly(ADP-ribose) polymerase-1 activation in human breast carcinoma cell lines. *Toxicology Letters*, *172*(3), 146–158. https://doi.org/10.1016/J.TOXLET.2007.06.003

Lin, T., Wang, D., Chen, J., Zhang, Z., Zhao, Y., Wu, Z., & Wang, Y. (2021). IL-24 inhibits the malignancy of human glioblastoma cells via destabilization of Zeb1. *Biological Chemistry*, *402*(7), 839–848. https://doi.org/10.1515/HSZ-2020-0373

Liu, C., Cui, H., Gu, D., Zhang, M., Fang, Y., Chen, S., Tang, M., Zhang, B., & Chen, H. (2017). Genetic polymorphisms and lung cancer risk: Evidence from meta-analyses and genome-wide association studies. *Lung Cancer (Amsterdam, Netherlands)*, *113*, 18–29. https://doi.org/10.1016/J.LUNGCAN.2017.08.026

Liu, Y., Chen, Y., Sha, R., Li, Y., Xu, T., Hu, X., Xu, L., Xie, Q., & Zhao, B. (2021). A new insight into the role of aryl hydrocarbon receptor (AhR) in the migration of glioblastoma by AhR-IL24 axis regulation. *Environment International*, *154*, 106658–106671. https://doi.org/10.1016/J.ENVINT.2021.106658

Liu, Y., Liang, X., Dong, W., Fang, Y., Lu, J., & Zhang, T. (2018). The Kyn–AhR Pathway Upregulates PD-1 to Promote Tumor Immune Escape. *Cancer Discovery*, *8*(5), 480–494. https://doi.org/10.1158/2159-8290.cd-rw2018-048

Liu, Y., Liang, X., Yin, X., Lv, J., Tang, K., Ma, J., Ji, T., Zhang, H., Dong, W., Jin, X., Chen, D., Li, Y., Zhang, S., Xie, H. Q., Zhao, B., Zhao, T., Lu, J., Hu, Z. W., Cao, X., … Huang, B. (2017). Blockade of IDO-kynurenine-AhR metabolic circuitry abrogates IFN-γ-induced immunologic dormancy of tumor-repopulating cells. *Nature Communications*, *15207*, 1–15. https://doi.org/10.1038/NCOMMS15207

Liu, Z., Geboes, K., Hellings, P., Maerten, P., Heremans, H., Vandenberghe, P., Boon, L., van Kooten, P., Rutgeerts, P., & Ceuppens, J. L. (2001). B7 Interactions with CD28 and CTLA-4 Control Tolerance or Induction of Mucosal Inflammation in Chronic Experimental Colitis. *The Journal of Immunology*, *167*(3), 1830–1838. https://doi.org/10.4049/JIMMUNOL.167.3.1830

Liu, Z., Wu, X., Zhang, F., Han, L., Bao, G., He, X., & Xu, Z. (2013). AhR expression is increased in hepatocellular carcinoma. *Journal of Molecular Histology*, *44*(4), 455–461. https://doi.org/10.1007/s10735-013-9495-6

Loercher, A. E., Tank, E. M. H., Delston, R. B., & Harbour, J. W. (2005). MITF links differentiation with cell cycle arrest in melanocytes by transcriptional activation of INK4A. *The Journal of Cell Biology*, *168*(1), 35–40. https://doi.org/10.1083/JCB.200410115

Loertscher, J. A., Sattler, C. A., & Allen-Hoffmann, B. L. (2001). 2,3,7,8-Tetrachlorodibenzo-p-dioxin alters the differentiation pattern of human keratinocytes in organotypic culture. *Toxicology and Applied Pharmacology*, *175*(2), 121–129. https://doi.org/10.1006/TAAP.2001.9202

Long, G. V., Dummer, R., Hamid, O., Gajewski, T. F., Caglevic, C., Dalle, S., Arance, A., Carlino, M. S., Grob, J. J., Kim, T. M., Demidov, L., Robert, C., Larkin, J., Anderson, J. R., Maleski, J., Jones, M., Diede, S. J., & Mitchell, T. C. (2019). Epacadostat plus pembrolizumab versus placebo plus pembrolizumab in patients with unresectable or metastatic melanoma (ECHO-301/KEYNOTE-252): a phase 3, randomised, double-blind study. *The Lancet Oncology*, *20*(8), 1083–1097. https://doi.org/10.1016/S1470-2045(19)30274-8

Louphrasitthiphol, P., Ledaki, I., Chauhan, J., Falletta, P., Siddaway, R., Buffa, F. M., Mole, D. R., Soga, T., & Goding, C. R. (2019). MITF controls the TCA cycle to modulate the melanoma hypoxia response. *Pigment Cell and Melanoma Research*, *32*(6), 792–808. https://doi.org/10.1111/PCMR.12802/SUPPINFO

Louphrasitthiphol, P., Siddaway, R., Loffreda, A., Pogenberg, V., Friedrichsen, H., Schepsky, A., Zeng, Z., Lu, M., Strub, T., Freter, R., Lisle, R., Suer, E., Thomas, B., Schuster-Böckler, B., Filippakopoulos, P., Middleton, M., Lu, X., Patton, E. E., Davidson, I., … Goding, C. R. (2020). Tuning Transcription Factor Availability through Acetylation-Mediated Genomic Redistribution. *Molecular Cell*, *79*(3), 472–487. https://doi.org/10.1016/J.MOLCEL.2020.05.025

Lu, W., Zhang, H., Niu, Y., Wu, Y., Sun, W., Li, H., Kong, J., Ding, K., Shen, H. M., Wu, H., Xia, D., & Wu, Y. (2017). Long non-coding RNA linc00673 regulated non-small cell lung cancer proliferation, migration, invasion and epithelial mesenchymal transition by sponging miR-150-5p. *Molecular Cancer*, *16*(1), 1–14. https://doi.org/10.1186/S12943-017-0685-9/FIGURES/7

Lucianò, A. M., Pérez-Oliva, A. B., Mulero, V., & Bufalo, D. Del. (2021). Bcl-xL: A Focus on Melanoma Pathobiology. *International Journal of Molecular Sciences*, *22*(5), 1–17. https://doi.org/10.3390/IJMS22052777

Ludwig, A., Rehberg, S., & Wegner, M. (2004). Melanocyte-specific expression of dopachrome tautomerase is dependent on synergistic gene activation by the Sox10 and Mitf transcription factors. *FEBS Letters*, *556*(1–3), 236–244. https://doi.org/10.1016/S0014-5793(03)01446-7

Ly, M., Rentas, S., Vujovic, A., Wong, N., Moreira, S., Xu, J., Holzapfel, N., Bhatia, S., Tran, D., Minden, M. D., Draper, J. S., & Hope, K. J. (2019). Diminished AhR signaling drives human acute myeloid leukemia stem cell maintenance. *Cancer Research*, *79*(22), 5799–5811. https://doi.org/10.1158/0008-5472.CAN-19-0274/653836/AM/DIMINISHED-AHR-SIGNALING-DRIVES-HUMAN-ACUTE

Madonna, G., Ullman, C. D., Gentilcore, G., Palmieri, G., & Ascierto, P. A. (2012). NF-κB as potential target in the treatment of melanoma. *Journal of Translational Medicine*, *10*(1), 1–8. https://doi.org/10.1186/1479-5876-10-53/FIGURES/1

Maio, M., Lewis, K., Demidov, L., Mandalà, M., Bondarenko, I., Ascierto, P. A., Herbert, C., Mackiewicz, A., Rutkowski, P., Guminski, A., Goodman, G. R., Simmons, B., Ye, C., Yan, Y., Schadendorf, D., Cinat, G., Fein, L. E., Brown, M., Haydon, A., … Whitman, E. (2018). Adjuvant vemurafenib in resected, BRAFV600 mutation-positive melanoma (BRIM8): a randomised, double-blind, placebo-controlled, multicentre, phase 3 trial. *The Lancet Oncology*, *19*(4), 510–520. https://doi.org/10.1016/S1470-2045(18)30106-2

Malik, S., & Roeder, R. G. (2023). Regulation of the RNA polymerase II pre-initiation complex by its associated coactivators. *Nature Reviews Genetics*, *24*(11), 767–782. https://doi.org/10.1038/s41576-023-00630-9

Martin, M. (2011). Cutadapt removes adapter sequences from high-throughput sequencing reads. *EMBnet.Journal*, *17*(1), 10–12. https://doi.org/10.14806/EJ.17.1.200

Masteller, E. L., Chuang, E., Mullen, A. C., Reiner, S. L., & Thompson, C. B. (2000). Structural Analysis of CTLA-4 Function In Vivo. *The Journal of Immunology*, *164*(10), 5319–5327. https://doi.org/10.4049/JIMMUNOL.164.10.5319

Matsumoto, Y., Marusawa, H., Kinoshita, K., Endo, Y., Kou, T., Morisawa, T., Azuma, T., Okazaki, I. M., Honjo, T., & Chiba, T. (2007). Helicobacter pylori infection triggers aberrant expression of activation-induced cytidine deaminase in gastric epithelium. *Nature Medicine*, *13*(4), 470–476. https://doi.org/10.1038/nm1566

Matsunawa, M., Amano, Y., Endo, K., Uno, S., Sakaki, T., Yamada, S., & Makishima, M. (2009). The Aryl Hydrocarbon Receptor Activator Benzo[a]pyrene Enhances Vitamin D3 Catabolism in Macrophages. *Toxicological Sciences*, *109*(1), 50–58. https://doi.org/10.1093/TOXSCI/KFP044

McGill, G. G., Horstmann, M., Widlund, H. R., Du, J., Motyckova, G., Nishimura, E. K., Lin, Y. L., Ramaswamy, S., Avery, W., Ding, H. F., Jordan, S. A., Jackson, I. J., Korsmeyer, S. J., Golub, T. R., & Fisher, D. E. (2002). Bcl2 regulation by the melanocyte master regulator Mitf modulates lineage survival and melanoma cell viability. *Cell*, *109*(6), 707–718. https://doi.org/10.1016/S0092-8674(02)00762-6

Melanoma skin cancer incidence statistics | Cancer Research UK. (n.d.). Retrieved December 13, 2023, from https://www.cancerresearchuk.org/health-professional/cancer-statistics/statistics-by-cancer-type/melanoma-skin-cancer/incidence

Melanoma skin cancer survival statistics | Cancer Research UK. (n.d.). Retrieved January 4, 2024, from https://www.cancerresearchuk.org/health-professional/cancer-statistics/statistics-by-cancer-type/melanoma-skin-cancer/survival

Meng, F. D., Ma, P., Sui, C. G., Tian, X., & Jiang, Y. H. (2015). Association between cytochrome P450 1A1 (CYP1A1) gene polymorphisms and the risk of renal cell carcinoma: a meta-analysis. *Scientific Reports 2015 5:1*, *5*(1), 1–6. https://doi.org/10.1038/srep08108

Meng, X., Du, G., Ye, L., Sun, S., Liu, Q., Wang, H., Wang, W., Wu, Z., & Tian, J. (2017). Combinatorial antitumor effects of indoleamine 2,3-dioxygenase inhibitor NLG919 and paclitaxel in a murine B16-F10 melanoma model. *International Journal of Immunopathology and Pharmacology*, *30*(3), 215–226. https://doi.org/10.1177/0394632017714696

Mengoni, M., Braun, A. D., Gaffal, E., & Tüting, T. (2020). The aryl hydrocarbon receptor promotes inflammation-induced dedifferentiation and systemic metastatic spread of melanoma cells. *International Journal of Cancer*, *147*(10), 2902–2913. https://doi.org/10.1002/IJC.33252

Merches, K., Schiavi, A., Weighardt, H., Steinwachs, S., Teichweyde, N., Förster, I., Hochrath, K., Schumak, B., Ventura, N., Petzsch, P., Köhrer, K., & Esser, C. (2020). AHR Signaling Dampens Inflammatory Signature in Neonatal Skin γδ T Cells. *International Journal of Molecular Sciences*, *21*(6), 2249–2270. https://doi.org/10.3390/IJMS21062249

Mimura, J., Ema, M., Sogawa, K., & Fujii-Kuriyama, Y. (1999). Identification of a novel mechanism of regulation of Ah (dioxin) receptor function. *Genes & Development*, *13*(1), 20–25. https://doi.org/10.1101/GAD.13.1.20

Mimura, J., Yamashita, K., Nakamura, K., Morita, M., Takagi, T. N., Nakao, K., Ema, M., Sogawa, K., Yasuda, M., Katsuki, M., & Fujii-Kuriyama, Y. (1997). Loss of teratogenic response to 2,3,7,8-tetrachlorodibenzo-p-dioxin (TCDD) in mice lacking the Ah (dioxin) receptor. *Genes to Cells*, *2*(10), 645–654. https://doi.org/10.1046/J.1365-2443.1997.1490345.X

Missinato, M. A., Murphy, S., Lynott, M., Yu, M. S., Kervadec, A., Chang, Y. L., Kannan, S., Loreti, M., Lee, C., Amatya, P., Tanaka, H., Huang, C. T., Puri, P. L., Kwon, C., Adams, P. D., Qian, L., Sacco, A., Andersen, P., & Colas, A. R. (2023). Conserved transcription factors promote cell fate stability and restrict reprogramming potential in differentiated cells. *Nature Communications*, *14*(1), 1–17. https://doi.org/10.1038/s41467-023-37256-8

Mitchell, T. C., Hamid, O., Smith, D. C., Bauer, T. M., Wasser, J. S., Olszanski, A. J., Luke, J. J., Balmanoukian, A. S., Schmidt, E. V., Zhao, Y., Gong, X., Maleski, J., Leopold, L., & Gajewski, T. F. (2018). Epacadostat Plus Pembrolizumab in Patients With Advanced Solid Tumors: Phase I Results From a Multicenter, Open-Label Phase I/II Trial (ECHO-202/KEYNOTE-037). *Journal of Clinical Oncology : Official Journal of the American Society of Clinical Oncology*, *36*(32), 3223–3230. https://doi.org/10.1200/JCO.2018.78.9602

Moghadam, A. R., Mehramiz, M., Entezari, M., Aboutalebi, H., Kohansal, F., Dadjoo, P., Fiuji, H., Nasiri, M., Aledavood, S. A., Anvari, K., Simab, S. A., Khorrami, M. S., Moradi, A., Hassanian, S. M., Ferns, G. A., Sales, S. S., & Avan, A. (2018). A genetic polymorphism in the CYP1B1 gene in patients with squamous cell carcinoma of the esophagus: an Iranian Mashhad cohort study recruited over 10 years. *Pharmacogenomics*, *19*(6), 539–546. https://doi.org/10.2217/PGS-2018-0197

Mollaoglu, G., Jones, A., Wait, S. J., Mukhopadhyay, A., Jeong, S., Arya, R., Camolotto, S. A., Mosbruger, T. L., Stubben, C. J., Conley, C. J., Bhutkar, A., Vahrenkamp, J.

M., Berrett, K. C., Cessna, M. H., Lane, T. E., Witt, B. L., Salama, M. E., Gertz, J., Jones, K. B., … Oliver, T. G. (2018). The Lineage-Defining Transcription Factors SOX2 and NKX2-1 Determine Lung Cancer Cell Fate and Shape the Tumor Immune Microenvironment. *Immunity*, *49*(4), 764-779.e9. https://doi.org/10.1016/J.IMMUNI.2018.09.020

Mort, R. L., Jackson, I. J., & Elizabeth Patton, E. (2015a). The melanocyte lineage in development and disease. *Development*, *142*(4), 620–632. https://doi.org/10.1242/DEV.106567

Mort, R. L., Jackson, I. J., & Elizabeth Patton, E. (2015b). The melanocyte lineage in development and disease. *Development (Cambridge, England)*, *142*(4), 620. https://doi.org/10.1242/DEV.106567

Moura-Alves, P., Puyskens, A., Stinn, A., Klemm, M., Guhlich-Bornhof, U., Dorhoi, A., Furkert, J., Kreuchwig, A., Protze, J., Lozza, L., Pei, G., Saikali, P., Perdomo, C., Mollenkopf, H. J., Hurwitz, R., Kirschhoefer, F., Brenner-Weiss, G., Weiner, J., Oschkinat, H., … Kaufmann, S. H. E. (2019). Host monitoring of quorum sensing during Pseudomonas aeruginosa infection. *Science*, *366*(6472), 1–10. https://doi.org/10.1126/SCIENCE.AAW1629/SUPPL_FILE/AAW1629_MOURA-ALVES_SM.PDF

Müller, M., Briscoe, J., Laxton, C., Guschin, D., Ziemiecki, A., Silvennoinen, O., Harpur, A. G., Barbieri, G., Witthuhn, B. A., Schindler, C., Pellegrini, S., Wilks, A. F., Ihle, J. N., Stark, G. R., & Kerr, L. M. (1993). The protein tyrosine kinase JAK1 complements defects in interferon-α/β and -γ signal transduction. *Nature 1993 366:6451*, *366*(6451), 129–135. https://doi.org/10.1038/366129a0

Mumphrey, M. B., Hosseini, N., Raghavan, M., Parolia, A., Geng, J., Zou, W., Chinnaiyan, A., & Cieslik, M. (2023). Distinct mutational processes shape selection of MHC class I and class II mutations across primary and metastatic tumors . *Cell Reports*, *42*(8), 112965–112985. https://doi.org/10.1016/j.celrep.2023.112965

Munn, D. H., Shafizadeh, E., Attwood, J. T., Bondarev, I., Pashine, A., & Mellor, A. L. (1999). Inhibition of T cell proliferation by macrophage tryptophan catabolism. *Journal of Experimental Medicine*, *189*(9), 1363–1372. https://doi.org/10.1084/jem.189.9.1363

Munn, D. H., Sharma, M. D., Baban, B., Harding, H. P., Zhang, Y., Ron, D., & Mellor, A. L. (2005). GCN2 kinase in T cells mediates proliferative arrest and anergy induction in response to indoleamine 2,3-dioxygenase. *Immunity*, *22*(5), 633–642. https://doi.org/10.1016/J.IMMUNI.2005.03.013

Muñoz-Couselo, E., Adelantado, E. Z., Ortiz, C., García, J. S., & Perez-Garcia, J. (2017). NRAS-mutant melanoma: current challenges and future prospect. *OncoTargets and Therapy*, *10*, 3941–3947. https://doi.org/10.2147/OTT.S117121

Mutz-Rabl, C. G., Koelblinger, P., & Koch, L. (2023). Immunotherapy for metastatic melanoma—from little benefit to first-line treatment. *Memo - Magazine of European Medical Oncology*, *16*(2), 108–112. https://doi.org/10.1007/S12254-023-00881-6/FIGURES/1

Nacarino-Palma, A., Rejano-Gordillo, C. M., González-Rico, F. J., Ordiales-Talavero, A., Román, Á. C., Cuadrado, M., Bustelo, X. R., Merino, J. M., & Fernández-Salguero, P. M. (2021). Loss of Aryl Hydrocarbon Receptor Favors K-RasG12D-Driven Non-Small Cell Lung Cancer. *Cancers*, *13*(16), 2351–2363. https://doi.org/10.3390/CANCERS13164071

Naik, P. P. (2021). Cutaneous Malignant Melanoma: A Review of Early Diagnosis and Management. *World Journal of Oncology*, *12*(1), 7–19. https://doi.org/10.14740/WJON1349

Najem, A., Soumoy, L., Sabbah, M., Krayem, M., Awada, A., Journe, F., & Ghanem, G. E. (2022). Understanding Molecular Mechanisms of Phenotype Switching and Crosstalk with TME to Reveal New Vulnerabilities of Melanoma. *Cells*, *11*(7), 1157–1189. https://doi.org/10.3390/CELLS11071157

Nakano, H., Nakajima, A., Sakon-Komazawa, S., Piao, J. H., Xue, X., & Okumura, K. (2005). Reactive oxygen species mediate crosstalk between NF-κB and JNK. *Cell Death & Differentiation 2006 13:5*, *13*(5), 730–737. https://doi.org/10.1038/sj.cdd.4401830

Napolioni, V., Pariano, M., Borghi, M., Oikonomou, V., Galosi, C., De Luca, A., Stincardini, C., Vacca, C., Renga, G., Lucidi, V., Colombo, C., Fiscarelli, E., Lass-Flörl, C., Carotti, A., D'Amico, L., Majo, F., Russo, M. C., Ellemunter, H., Spolzino, A., … Costantini, C. (2019). Genetic polymorphisms affecting IDO1 or IDO2 activity differently associate with aspergillosis in humans. *Frontiers in Immunology*, *10*(MAY), 454610. https://doi.org/10.3389/FIMMU.2019.00890/BIBTEX

Nazarian, R., Shi, H., Wang, Q., Kong, X., Koya, R. C., Lee, H., Chen, Z., Lee, M. K., Attar, N., Sazegar, H., Chodon, T., Nelson, S. F., McArthur, G., Sosman, J. A., Ribas, A., & Lo, R. S. (2010). Melanomas acquire resistance to B-RAF(V600E) inhibition by RTK or N-RAS upregulation. *Nature*, *468*(7326), 973–977. https://doi.org/10.1038/NATURE09626

Nebert, D. W. (2017). Aryl hydrocarbon receptor (AHR): "pioneer member" of the basic-helix/loop/helix per-Arnt-sim (bHLH/PAS) family of "sensors" of foreign and endogenous signals. *Progress in Lipid Research*, *67*, 38–57. https://doi.org/10.1016/J.PLIPRES.2017.06.001

Nebert, D. W., Dalton, T. P., Okey, A. B., & Gonzalez, F. J. (2004). Role of aryl hydrocarbon receptor-mediated induction of the CYP1 enzymes in environmental toxicity and cancer. *The Journal of Biological Chemistry*, *279*(23), 23847–23850. https://doi.org/10.1074/JBC.R400004200

Nothdurft, S., Thumser-Henner, C., Breitenbücher, F., Okimoto, R. A., Dorsch, M., Opitz, C. A., Sadik, A., Esser, C., Hölzel, M., Asthana, S., Forster, J., Beisser, D., Kalmbach, S., Grüner, B. M., Bivona, T. G., Schramm, A., & Schuler, M. (2020). Functional screening identifies aryl hydrocarbon receptor as suppressor of lung cancer metastasis. *Oncogenesis*, *9*(102), 1–12. https://doi.org/10.1038/S41389-020-00286-8

Ohanna, M., Giuliano, S., Bonet, C., Imbert, V., Hofman, V., Zangari, J., Bille, K., Robert, C., Bressac-de Paillerets, B., Hofman, P., Rocchi, S., Peyron, J. F., Lacour, J. P., Ballotti, R., & Bertolotto, C. (2011). Senescent cells develop a PARP-1 and nuclear factor-κB-associated secretome (PNAS). *Genes & Development*, *25*(12), 1245–1261. https://doi.org/10.1101/GAD.625811

Ohmori, Y., Schreiber, R. D., & Hamilton, T. A. (1997). Synergy between interferon-gamma and tumor necrosis factor-alpha in transcriptional activation is mediated by cooperation between signal transducer and activator of transcription 1 and nuclear factor kappaB. *The Journal of Biological Chemistry*, *272*(23), 14899–14907. https://doi.org/10.1074/JBC.272.23.14899

Ohtake, F., Fujii-Kuriyama, Y., & Kato, S. (2009). AhR acts as an E3 ubiquitin ligase to modulate steroid receptor functions. *Biochemical Pharmacology*, *77*(4), 474–484. https://doi.org/10.1016/j.bcp.2008.08.034

Opitz, C. A., Litzenburger, U. M., Sahm, F., Ott, M., Tritschler, I., Trump, S., Schumacher, T., Jestaedt, L., Schrenk, D., Weller, M., Jugold, M., Guillemin, G. J., Miller, C. L., Lutz, C., Radlwimmer, B., Lehmann, I., Von Deimling, A., Wick, W.,

& Platten, M. (2011). An endogenous tumour-promoting ligand of the human aryl hydrocarbon receptor. *Nature*, *478*(7368), 197–203. https://doi.org/10.1038/nature10491

Ortiz, M. A., Mikhailova, T., Li, X., Porter, B. A., Bah, A., & Kotula, L. (2021). Src family kinases, adaptor proteins and the actin cytoskeleton in epithelial-to-mesenchymal transition. *Cell Communication and Signaling*, *19*(1), 1–19. https://doi.org/10.1186/S12964-021-00750-X

Øvrevik, J., Låg, M., Lecureur, V., Gilot, D., Lagadic-Gossmann, D., Refsnes, M., Schwarze, P. E., Skuland, T., Becher, R., & Holme, J. A. (2014). AhR and Arnt differentially regulate NF-κB signaling and chemokine responses in human bronchial epithelial cells. *Cell Communication and Signaling*, *12*(48), 1–17. https://doi.org/10.1186/S12964-014-0048-8

Pansoy, A., Ahmed, S., Valen, E., Sandelin, A., & Matthews, J. (2010). 3-methylcholanthrene induces differential recruitment of aryl hydrocarbon receptor to human promoters. *Toxicological Sciences : An Official Journal of the Society of Toxicology*, *117*(1), 90–100. https://doi.org/10.1093/TOXSCI/KFQ096

Pappas, B., Yang, Y., Wang, Y., Kim, K., Chung, H. J., Cheung, M., Ngo, K., Shinn, A., & Chan, W. K. (2018). p23 protects the human aryl hydrocarbon receptor from degradation via a heat shock protein 90-independent mechanism. *Biochemical Pharmacology*, *152*, 34–44. https://doi.org/10.1016/J.BCP.2018.03.015

Paris, A., Tardif, N., Baietti, F. M., Berra, C., Leclair, H. M., Leucci, E., Galibert, M., & Corre, S. (2022a). The AhR-SRC axis as a therapeutic vulnerability in BRAFi - resistant melanoma . *EMBO Molecular Medicine*, *14*(12), e15677–e15696. https://doi.org/10.15252/EMMM.202215677/SUPPL_FILE/EMMM202215677-SUP-0010-SDATAFIG5.ZIP

Paris, A., Tardif, N., Baietti, F. M., Berra, C., Leclair, H. M., Leucci, E., Galibert, M., & Corre, S. (2022b). The AhR-SRC axis as a therapeutic vulnerability in BRAFi-resistant melanoma. *EMBO Molecular Medicine*, *14*(12). https://doi.org/10.15252/EMMM.202215677

Paris, A., Tardif, N., Galibert, M. D., & Corre, S. (2021a). AhR and Cancer: From Gene Profiling to Targeted Therapy. *International Journal of Molecular Sciences 2021, Vol. 22, Page 752*, *22*(2), 752. https://doi.org/10.3390/IJMS22020752

Paris, A., Tardif, N., Galibert, M. D., & Corre, S. (2021b). AhR and Cancer: From Gene Profiling to Targeted Therapy. *International Journal of Molecular Sciences*, *22*(2), 1–22. https://doi.org/10.3390/IJMS22020752

Passarelli, A., Mannavola, F., Stucci, L. S., Tucci, M., & Silvestris, F. (2017). Immune system and melanoma biology: a balance between immunosurveillance and immune escape. *Oncotarget*, *8*(62), 106132–106142. https://doi.org/10.18632/ONCOTARGET.22190

Patel, A. B., Shaikh, S., Jain, K. R., Desai, C., & Madamwar, D. (2020). Polycyclic Aromatic Hydrocarbons: Sources, Toxicity, and Remediation Approaches. In *Frontiers in Microbiology* (Vol. 11). Frontiers Media S.A. https://doi.org/10.3389/fmicb.2020.562813

Patsoukis, N., Brown, J., Petkova, V., Liu, F., Li, L., & Boussiotis, V. A. (2012). Selective effects of PD-1 on Akt and ras pathways regulate molecular components of the cell cycle and inhibit T cell proliferation. *Science Signaling*, *5*(230), ra46–ra60. https://doi.org/10.1126/SCISIGNAL.2002796/SUPPL_FILE/5_RA46_SM.PDF

Patsoukis, N., Duke-Cohan, J. S., Chaudhri, A., Aksoylar, H. I., Wang, Q., Council, A., Berg, A., Freeman, G. J., & Boussiotis, V. A. (2020). Interaction of SHP-2 SH2

domains with PD-1 ITSM induces PD-1 dimerization and SHP-2 activation. *Communications Biology*, *3*(1), 1–13. https://doi.org/10.1038/s42003-020-0845-0

Pelaz, S. G., & Tabernero, A. (2022). Src: coordinating metabolism in cancer. *Oncogene*, *41*(45), 4917–4928. https://doi.org/10.1038/s41388-022-02487-4

Phane Cauchi, S., Stü Cker, I., Cé Né E B, S., Kremers, P., Beaune, P., & Massaad-Massade, L. (2003). Structure and polymorphisms of human aryl hydrocarbon receptor repressor (AhRR) gene in a French population: relationship with CYP1A1 inducibility and lung cancer. *Pharmacogenetics*, *13*, 339–347. https://doi.org/10.1097/01.fpc.0000054093.48725.79

Pozniak, J., Pedri, D., Landeloos, E., Van Herck, Y., Antoranz, A., Vanwynsberghe, L., Nowosad, A., Roda, N., Makhzami, S., Bervoets, G., Maciel, L. F., Pulido-Vicuña, C. A., Pollaris, L., Seurinck, R., Zhao, F., Flem-Karlsen, K., Damsky, W., Chen, L., Karagianni, D., … Marine, J. C. (2024). A TCF4-dependent gene regulatory network confers resistance to immunotherapy in melanoma. *Cell*, *187*(1), 166-183.e25. https://doi.org/10.1016/J.CELL.2023.11.037/ATTACHMENT/3929E7FB-6040-4435-882B-B7D0148F5F07/MMC6.XLSX

Pozzi, V., Campagna, R., Sartini, D., & Emanuelli, M. (2023). Enzymes Dysregulation in Cancer: From Diagnosis to Therapeutical Approaches. *International Journal of Molecular Sciences*, *24*(18), 13815–13818. https://doi.org/10.3390/IJMS241813815

Pylayeva-Gupta, Y., Grabocka, E., & Bar-Sagi, D. (2011). RAS oncogenes: weaving a tumorigenic web. *Nature Reviews Cancer 2011 11:11*, *11*(11), 761–774. https://doi.org/10.1038/nrc3106

Qian, J., Wang, C., Wang, B., Yang, J., Wang, Y., Luo, F., Xu, J., Zhao, C., Liu, R., & Chu, Y. (2018). The IFN-γ/PD-L1 axis between T cells and tumor microenvironment: Hints for glioma anti-PD-1/PD-L1 therapy. *Journal of Neuroinflammation*, *15*(1), 1–13. https://doi.org/10.1186/S12974-018-1330-2/FIGURES/7

Rabbie, R., Ferguson, P., Molina-Aguilar, C., Adams, D. J., & Robles-Espinoza, C. D. (2019). Melanoma subtypes: genomic profiles, prognostic molecular markers and therapeutic possibilities. *The Journal of Pathology*, *247*(5), 539–551. https://doi.org/10.1002/PATH.5213

Racioppi, C., Coppola, U., Christiaen, L., & Ristoratore, F. (2019). Transcriptional regulation of Rab32/38, a specific marker of pigment cell formation in Ciona robusta. *Developmental Biology*, *448*(2), 111–118. https://doi.org/10.1016/J.YDBIO.2018.11.013

Rannug, A., & Rannug, U. (2018). The tryptophan derivative 6-formylindolo[3,2-b]carbazole, FICZ, a dynamic mediator of endogenous aryl hydrocarbon receptor signaling, balances cell growth and differentiation. *Critical Reviews in Toxicology*, *48*(7), 555–574. https://doi.org/10.1080/10408444.2018.1493086

Rannug, A., Rannug, U., Rosenkranzll, H. S., Winqvist, L., Westerholmii, R., Agurellg, E., & Grafstromg, A.-K. (1987). Certain Photooxidized Derivatives of Tryptophan Bind with Very High Affinity to the Ah Receptor and Are Likely to be Endogenous Signal Substances*. *Journal of Biological Chemistry*, *262*(32), 15422–15427. https://doi.org/10.1016/S0021-9258(18)47743-5

Rettino, A., & Clarke, N. M. (2013). Genome-wide Identification of IRF1 Binding Sites Reveals Extensive Occupancy at Cell Death Associated Genes. *Journal of Carcinogenesis & Mutagenesis*, *Spec Iss Apoptosis*, S6-009. https://doi.org/10.4172/2157-2518.S6-009

Rico-Leo, E. M., Lorenzo-Martín, L. F., Román, Á. C., Bustelo, X. R., Merino, J. M., & Fernández-Salguero, P. M. (2021). Aryl hydrocarbon receptor controls skin

homeostasis, regeneration, and hair follicle cycling by adjusting epidermal stem cell function. *STEM CELLS*, *39*(12), 1733–1750. https://doi.org/10.1002/STEM.3443

Rimkus, T. K., Carpenter, R. L., Qasem, S., Chan, M., & Lo, H. W. (2016). Targeting the Sonic Hedgehog Signaling Pathway: Review of Smoothened and GLI Inhibitors. *Cancers*, *8*(2), 1–23. https://doi.org/10.3390/CANCERS8020022

Robinson, C. M., Shirey, K. A., & Carlin, J. M. (2003). Synergistic Transcriptional Activation of Indoleamine Dioxygenase by IFN-γ and Tumor Necrosis Factor-α. *Journal of Interferon & Cytokine Research*, *23*(8), 413–421. https://doi.org/10.1089/107999003322277829

Robinson, M. D., McCarthy, D. J., & Smyth, G. K. (2010). edgeR: a Bioconductor package for differential expression analysis of digital gene expression data. *Bioinformatics (Oxford, England)*, *26*(1), 139–140. https://doi.org/10.1093/BIOINFORMATICS/BTP616

Robinson, N. J., & Schiemann, W. P. (2022). Telomerase in Cancer: Function, Regulation, and Clinical Translation. *Cancers*, *14*(808), 1–22. https://doi.org/10.3390/CANCERS14030808

Rohs, R., Jin, X., West, S. M., Joshi, R., Honig, B., & Mann, R. S. (2010). Origins of specificity in protein-DNA recognition. *Annual Review of Biochemistry*, *79*, 233–269. https://doi.org/10.1146/ANNUREV-BIOCHEM-060408-091030

Rotte, A. (2019). Combination of CTLA-4 and PD-1 blockers for treatment of cancer. *Journal of Experimental & Clinical Cancer Research 2019 38:1*, *38*(1), 1–12. https://doi.org/10.1186/S13046-019-1259-Z

Rubin, D. C., Shaker, A., & Levin, M. S. (2012). Chronic intestinal inflammation: Inflammatory bowel disease and colitis-associated colon cancer. *Frontiers in Immunology*, *3*(107), 1–10. https://doi.org/10.3389/FIMMU.2012.00107/BIBTEX

Rudd, C. E., Taylor, A., & Schneider, H. (2009). CD28 and CTLA-4 coreceptor expression and signal transduction. *Immunological Reviews*, *229*(1), 12–26. https://doi.org/10.1111/J.1600-065X.2009.00770.X

Rudyak, S. G., Usakin, L. A., Tverye, E. A., Robertson, E. D., & Panteleyev, A. A. (2023). Aryl hydrocarbon receptor is regulated via multiple mechanisms in human keratinocytes. *Toxicology Letters*, *382*, 58–65. https://doi.org/10.1016/J.TOXLET.2023.05.007

Saatcioglus, F., Perry, D. J., Pasco, D. S., & Fagant, J. B. (1990). Aryl hydrocarbon (Ah) receptor DNA-binding activity. Sequence specificity and Zn2+ requirement. *The Journal of Biological Chemistry*, *265*(16), 9251–9258.

Saksouk, N., Simboeck, E., & Déjardin, J. (2015). Constitutive heterochromatin formation and transcription in mammals. *Epigenetics and Chromatin*, *8*(1), 1–17. https://doi.org/10.1186/1756-8935-8-3/FIGURES/4

Sakurai, S., Shimizu, T., & Ohto, U. (2017). The crystal structure of the AhRR-ARNT heterodimer reveals the structural basis of the repression of AhR-mediated transcription. *The Journal of Biological Chemistry*, *292*(43), 17609–17616. https://doi.org/10.1074/JBC.M117.812974

Sample, A., & He, Y. Y. (2018). Mechanisms and prevention of UV-induced melanoma. *Photodermatology, Photoimmunology & Photomedicine*, *34*(1), 13–24. https://doi.org/10.1111/PHPP.12329

Sarasin, A. (2003). An overview of the mechanisms of mutagenesis and carcinogenesis. *Mutation Research/Reviews in Mutation Research*, *544*(2–3), 99–106. https://doi.org/10.1016/J.MRREV.2003.06.024

Sari, G., & Rock, K. L. (2023). Tumor immune evasion through loss of MHC class-I antigen presentation. *Current Opinion in Immunology*, *83*, 102329–102336. https://doi.org/10.1016/J.COI.2023.102329

Sarić, N., Selby, M., Ramaswamy, V., Kool, M., Stockinger, B., Hogstrand, C., Williamson, D., Marino, S., Taylor, M. D., Clifford, S. C., & Basson, M. A. (2020). The AHR pathway represses TGFβ-SMAD3 signalling and has a potent tumour suppressive role in SHH medulloblastoma. *Scientific Reports*, *10*(148), 1–16. https://doi.org/10.1038/S41598-019-56876-Z

Sawrycki, P., Domagalski, K., Cechowska, M., Gasior, M., Jarkiewicz-Tretyn, J., & Tretyn, A. (2018). Relationship between CYP1B1 polymorphisms (c.142C > G, c.355G > T, c.1294C > G) and lung cancer risk in Polish smokers. *Future Oncology (London, England)*, *14*(16), 1569–1577. https://doi.org/10.2217/FON-2017-0719

Schulte, K. W., Green, E., Wilz, A., Platten, M., & Daumke, O. (2017). Structural Basis for Aryl Hydrocarbon Receptor-Mediated Gene Activation. *Structure*, *25*(7), 1025-1033.e3. https://doi.org/10.1016/j.str.2017.05.008

Schulthess, P., Löffler, A., Vetter, S., Kreft, L., Schwarz, M., Braeuning, A., & Blüthgen, N. (2015). Signal integration by the CYP1A1 promoter — a quantitative study. *Nucleic Acids Research*, *43*(11), 5318. https://doi.org/10.1093/NAR/GKV423

Sciullo, E. M., Dong, B., Vogel, C. F. A., & Matsumura, F. (2009). Characterization of the pattern of the nongenomic signaling pathway through which TCDD-induces early inflammatory responses in U937 human macrophages. *Chemosphere*, *74*(11), 1531–1537. https://doi.org/10.1016/J.CHEMOSPHERE.2008.11.010

Seok, S. H., Ma, Z. X., Feltenberger, J. B., Chen, H., Chen, H., Scarlett, C., Lin, Z., Satyshur, K. A., Cortopassi, M., Jefcoate, C. R., Ge, Y., Tang, W., Bradfield, C. A., & Xing, Y. (2018). Trace derivatives of kynurenine potently activate the aryl hydrocarbon receptor (AHR). *The Journal of Biological Chemistry*, *293*(6), 1994–2005. https://doi.org/10.1074/JBC.RA117.000631

Sérée, E., Villard, P.-H., Pascussi, J.-M., Pineau, T., Maurel, P., Nguyen, Q. B., Fallone, F., Martin, P.-M., Champion, S., Lacarelle, B., Savouret, J.-F., & Barra, Y. (2004). Evidence for a New Human CYP1A1 Regulation Pathway Involving PPAR-and 2 PPRE Sites. *Gastroenterology*, *127*, 1436–1445. https://doi.org/10.1053/j.gastro.2004.08.023

Sergi, M. C., Filoni, E., Triggiano, G., Cazzato, G., Internò, V., Porta, C., & Tucci, M. (2023). Mucosal Melanoma: Epidemiology, Clinical Features, and Treatment. *Current Oncology Reports*, *25*(11), 1247–1258. https://doi.org/10.1007/S11912-023-01453-X/TABLES/1

Shah, K., Maradana, M. R., Joaquina Delàs, M., Metidji, A., Graelmann, F., Llorian, M., Chakravarty, P., Li, Y., Tolaini, M., Shapiro, M., Kelly, G., Cheshire, C., Bhurta, D., Bharate, S. B., & Stockinger, B. (2022). Cell-intrinsic Aryl Hydrocarbon Receptor signalling is required for the resolution of injury-induced colonic stem cells. *Nature Communications*, *13*(1), 1827–1843. https://doi.org/10.1038/S41467-022-29098-7

Sharpe, A. H., & Pauken, K. E. (2017). The diverse functions of the PD1 inhibitory pathway. *Nature Reviews Immunology 2017 18:3*, *18*(3), 153–167. https://doi.org/10.1038/nri.2017.108

Shehin, S. E., Stephenson, R. O., & Greenlee, W. F. (2000). Transcriptional Regulation of the Human CYP1B1 Gene . *Journal of Biological Chemistry*, *275*, 6770–6776. https://doi.org/10.1074/jbc.275.10.6770

Sheppard, K. A., Fitz, L. J., Lee, J. M., Benander, C., George, J. A., Wooters, J., Qiu, Y., Jussif, J. M., Carter, L. L., Wood, C. R., & Chaudhary, D. (2004). PD-1 inhibits T-cell receptor induced phosphorylation of the ZAP70/CD3ζ signalosome and

downstream signaling to PKCθ. *FEBS Letters*, *574*(1–3), 37–41. https://doi.org/10.1016/j.febslet.2004.07.083
Sherr, C. J. (2004). Principles of Tumor Suppression. *Cell*, *116*(2), 235–246. https://doi.org/10.1016/S0092-8674(03)01075-4
Shi, D., Wu, X., Jian, Y., Wang, J., Huang, C., Mo, S., Li, Y., Li, F., Zhang, C., Zhang, D., Zhang, H., Huang, H., Chen, X., Wang, Y. A., Lin, C., Liu, G., Song, L., & Liao, W. (2022). USP14 promotes tryptophan metabolism and immune suppression by stabilizing IDO1 in colorectal cancer. *Nature Communications*, *13*(1), 1–18. https://doi.org/10.1038/s41467-022-33285-x
Shi, J., Chen, C., Ju, R., Wang, Q., Li, J., Guo, L., Ye, C., & Zhang, D. (2019). *Carboxyamidotriazole combined with IDO1- Kyn-AhR pathway inhibitors profoundly enhances cancer immunotherapy*. *7*, 1–14.
Shimada, T., & Fujii-Kuriyama, Y. (2004). Metabolic activation of polycyclic aromatic hydrocarbons to carcinogens by cytochromes P450 1A1 and1B1. *Cancer Science*, *95*(1), 1–6. https://doi.org/10.1111/J.1349-7006.2004.TB03162.X
Shimada, T., Inoue, K., Suzuki, Y., Kawai, T., Azuma, E., Nakajima, T., Shindo, M., Kurose, K., Sugie, A., Yamagishi, Y., Fujii-Kuriyama, Y., & Hashimoto, M. (2002). Arylhydrocarbon receptor-dependent induction of liver and lung cytochromes P450 1A1, 1A2, and 1B1 by polycyclic aromatic hydrocarbons and polychlorinated biphenyls in genetically engineered C57BL/6J mice. *Carcinogenesis*, *23*(7), 1199–1207. https://doi.org/10.1093/carcin/23.7.1199
Smith, A. K., Simon, J. S., Gustafson, E. L., Noviello, S., Cubells, J. F., Epstein, M. P., Devlin, D. J., Qiu, P., Albrecht, J. K., Brass, C. A., Sulkowski, M. S., McHutchinson, J. G., & Miller, A. H. (2011). Association of a polymorphism in the indoleamine- 2,3-dioxygenase gene and interferon-α-induced depression in patients with chronic hepatitis C. *Molecular Psychiatry 2012 17:8*, *17*(8), 781–789. https://doi.org/10.1038/mp.2011.67
Smits, J. P. H., Ederveen, T. H. A., Rikken, G., van den Brink, N. J. M., van Vlijmen-Willems, I. M. J. J., Boekhorst, J., Kamsteeg, M., Schalkwijk, J., van Hijum, S. A. F. T., Zeeuwen, P. L. J. M., & van den Bogaard, E. H. (2020). Targeting the Cutaneous Microbiota in Atopic Dermatitis by Coal Tar via AHR-Dependent Induction of Antimicrobial Peptides. *The Journal of Investigative Dermatology*, *140*(2), 415-424.e10. https://doi.org/10.1016/J.JID.2019.06.142
Sojka, D. K., Huang, Y. H., & Fowell, D. J. (2008). Mechanisms of regulatory T-cell suppression – a diverse arsenal for a moving target. *Immunology*, *124*(1), 13–22. https://doi.org/10.1111/J.1365-2567.2008.02813.X
Son, H., & Moon, A. (2010). Epithelial-mesenchymal transition and cell invasion. *Toxicological Research*, *26*(4), 245–252. https://doi.org/10.5487/TR.2010.26.4.245/METRICS
Soudet, J., Jolivet, P., & Teixeira, M. T. (2014). Elucidation of the DNA End-Replication Problem in Saccharomyces cerevisiae. *Molecular Cell*, *53*(6), 954–964. https://doi.org/10.1016/j.molcel.2014.02.030
Strilic, B., & Offermanns, S. (2017). Intravascular Survival and Extravasation of Tumor Cells. *Cancer Cell*, *32*(3), 282–293. https://doi.org/10.1016/J.CCELL.2017.07.001
Subramanian, A., Tamayo, P., Mootha, V. K., Mukherjee, S., Ebert, B. L., Gillette, M. A., Paulovich, A., Pomeroy, S. L., Golub, T. R., Lander, E. S., & Mesirov, J. P. (2005). Gene set enrichment analysis: A knowledge-based approach for interpreting genome-wide expression profiles. *Proceedings of the National Academy of Sciences of the United States of America*, *102*(43), 15545–15550. https://doi.org/10.1073/PNAS.0506580102/SUPPL_FILE/06580FIG7.JPG

Sun, K. L., Liu, W., Gao, X. M., Yang, M., & Chang, J. M. (2021). A Study of Normal Epidermal Melanocyte Distribution. *International Journal of Dermatology and Venereology*, *4*(1), 32–35. https://doi.org/10.1097/JD9.0000000000000125

Sun, L. (2021). Recent advances in the development of AHR antagonists in immuno-oncology. *RSC Medicinal Chemistry*, *12*(6), 902. https://doi.org/10.1039/D1MD00015B

Survival | Melanoma skin cancer | Cancer Research UK. (n.d.). Retrieved January 4, 2024, from https://www.cancerresearchuk.org/about-cancer/melanoma/survival

Sutter, C. H., Bodreddigari, S., Campion, C., Wible, R. S., & Sutter, T. R. (2011). 2,3,7,8-Tetrachlorodibenzo-p-dioxin increases the expression of genes in the human epidermal differentiation complex and accelerates epidermal barrier formation. *Toxicological Sciences : An Official Journal of the Society of Toxicology*, *124*(1), 128–137. https://doi.org/10.1093/TOXSCI/KFR205

Takagi, S., Tojo, H., Tomita, S., Sano, S., Itami, S., Hara, M., Inoue, S., Horie, K., Kondoh, G., Hosokawa, K., Gonzalez, F. J., & Takeda, J. (2003). Alteration of the 4-sphingenine scaffolds of ceramides in keratinocyte-specific Arnt-deficient mice affects skin barrier function. *The Journal of Clinical Investigation*, *112*(9), 1372–1382. https://doi.org/10.1172/JCI18513

Tan, Q., Cai, J., Peng, J., Hu, C., Wu, C. C., & Liu, H. (2022). VEGF-B targeting by aryl hydrocarbon receptor mediates the migration and invasion of choriocarcinoma stem-like cells. *Cancer Cell International*, *22*(1), 221. https://doi.org/10.1186/S12935-022-02641-8

Tan, Y., Wang, Z., Xu, M., Li, B., Huang, Z., Qin, S., Nice, E. C., Tang, J., & Huang, C. (2023). Oral squamous cell carcinomas: state of the field and emerging directions. *International Journal of Oral Science*, *15*(1), 1–23. https://doi.org/10.1038/s41368-023-00249-w

Tarhini, A., Lo, E., & Minor, D. R. (2010). Releasing the Brake on the Immune System: Ipilimumab in Melanoma and Other Tumors. *Cancer Biotherapy & Radiopharmaceuticals*, *25*(6), 601–613. https://doi.org/10.1089/CBR.2010.0865

Tauchi, M., Hida, A., Negishi, T., Katsuoka, F., Noda, S., Mimura, J., Hosoya, T., Yanaka, A., Aburatani, H., Fujii-Kuriyama, Y., Motohashi, H., & Yamamoto, M. (2005). Constitutive Expression of Aryl Hydrocarbon Receptor in Keratinocytes Causes Inflammatory Skin Lesions. *Molecular and Cellular Biology*, *25*(21), 9360–9368. https://doi.org/10.1128/mcb.25.21.9360-9368.2005

Tawbi, H. A., Forsyth, P. A., Algazi, A., Hamid, O., Hodi, F. S., Moschos, S. J., Khushalani, N. I., Lewis, K., Lao, C. D., Postow, M. A., Atkins, M. B., Ernstoff, M. S., Reardon, D. A., Puzanov, I., Kudchadkar, R. R., Thomas, R. P., Tarhini, A., Pavlick, A. C., Jiang, J., … Margolin, K. (2018). Combined Nivolumab and Ipilimumab in Melanoma Metastatic to the Brain. *The New England Journal of Medicine*, *379*(8), 722–730. https://doi.org/10.1056/NEJMOA1805453

TCGA study of genetic drivers of melanoma - NCI. (n.d.). Retrieved January 30, 2024, from https://www.cancer.gov/news-events/press-releases/2015/tcga-cutaneous-melanoma-mutated-genes

Teino, I., Matvere, A., Pook, M., Varik, I., Pajusaar, L., Uudeküll, K., Vaher, H., Trei, A., Kristjuhan, A., Org, T., & Maimets, T. (2020). Impact of AHR Ligand TCDD on Human Embryonic Stem Cells and Early Differentiation. *International Journal of Molecular Sciences*, *21*(23), 1–24. https://doi.org/10.3390/IJMS21239052

Terry, S., Savagner, P., Ortiz-Cuaran, S., Mahjoubi, L., Saintigny, P., Thiery, J. P., & Chouaib, S. (2017). New insights into the role of EMT in tumor immune escape. *Molecular Oncology*, *11*(7), 824–846. https://doi.org/10.1002/1878-0261.12093

The Process and Costs of Drug Development (2022) | FTLOScience. (n.d.). Retrieved January 29, 2024, from https://ftloscience.com/process-costs-drug-development/

Therachiyil, L., Krishnankutty, R., Ahmad, F., Mateo, J. M., Uddin, S., & Korashy, H. M. (2022). Aryl Hydrocarbon Receptor Promotes Cell Growth, Stemness Like Characteristics, and Metastasis in Human Ovarian Cancer via Activation of PI3K/Akt, β-Catenin, and Epithelial to Mesenchymal Transition Pathways. *International Journal of Molecular Science*, *23*(12), 6395–6406. https://doi.org/10.3390/ijms23126395

Tian, Y., Ke, S., Denison, M. S., Rabson, A. B., & Gallo, M. A. (1999). Ah receptor and NF-κB interactions, a potential mechanism for dioxin toxicity. *Journal of Biological Chemistry*, *274*(1), 510–515. https://doi.org/10.1074/jbc.274.1.510

Tie, Y., Tang, F., Wei, Y. quan, & Wei, X. wei. (2022). Immunosuppressive cells in cancer: mechanisms and potential therapeutic targets. *Journal of Hematology & Oncology*, *15*(1), 1–33. https://doi.org/10.1186/S13045-022-01282-8

Török, N., Maszlag-Török, R., Molnár, K., Szolnoki, Z., Somogyvári, F., Boda, K., Tanaka, M., Klivényi, P., & Vécsei, L. (2022). Single Nucleotide Polymorphisms of Indoleamine 2,3-Dioxygenase 1 Influenced the Age Onset of Parkinson's Disease. *Frontiers in Bioscience - Landmark*, *27*(9), 265. https://doi.org/10.31083/J.FBL2709265/7994362CEDC44F0B77A44D2597994469.PDF

Tsai, C. H., Li, C. H., Cheng, Y. W., Lee, C. C., Liao, P. L., Lin, C. H., Huang, S. H., & Kang, J. J. (2017). The inhibition of lung cancer cell migration by AhR-regulated autophagy. *Scientific Reports*, *7*, 1–14. https://doi.org/10.1038/SREP41927

Tsoi, J., Robert, L., Paraiso, K., Galvan, C., Sheu, K. M., Lay, J., Wong, D. J. L., Atefi, M., Shirazi, R., Wang, X., Braas, D., Grasso, C. S., Palaskas, N., Ribas, A., & Graeber, T. G. (2018). Multi-stage Differentiation Defines Melanoma Subtypes with Differential Vulnerability to Drug-Induced Iron-Dependent Oxidative Stress. *Cancer Cell*, *33*(5), 890-904.e5. https://doi.org/10.1016/J.CCELL.2018.03.017

Tsuboi, Y., Yamada, H., Munetsuna, E., Fujii, R., Yamazaki, M., Yoshitaka, A., Mizuno, G., Hattori, Y., Ishikawa, H., Ohashi, K., Hashimoto, S., Hamajima, N., & Suzuki, K. (2022). Increased risk of cancer mortality by smoking-induced aryl hydrocarbon receptor repression DNA hypo methylation in Japanese population: A long-term cohort study. *Cancer Epidemiology*, *78*, 1–7. https://doi.org/https://doi.org/10.1016/j.canep.2022.102162

Tsuchiya, Y., Nakajima, M., Takagi, S., Katoh, M., Zheng, W., Jefcoate, C. R., & Yokoi, T. (2006). Binding of steroidogenic factor-1 to the regulatory region might not be critical for transcriptional regulation of the human CYP1B1 gene. *Journal of Biochemistry*, *139*(3), 527–534. https://doi.org/10.1093/JB/MVJ055

Tsuchiya, Y., Nakajima, M., & Yokoi, T. (2003). Critical enhancer region to which AhR/ARNT and Sp1 bind in the human CYP1B1 gene. *Journal of Biochemistry*, *133*(5), 583–592. https://doi.org/10.1093/JB/MVG075

Tsuji, G., Hashimoto-Hachiya, A., Kiyomatsu-Oda, M., Takemura, M., Ohno, F., Ito, T., Morino-Koga, S., Mitoma, C., Nakahara, T., Uchi, H., & Furue, M. (2017). Aryl hydrocarbon receptor activation restores filaggrin expression via OVOL1 in atopic dermatitis. *Cell Death & Disease 2017 8:7*, *8*(7), e2931–e2931. https://doi.org/10.1038/cddis.2017.322

Tsuji, N., Fukuda, K., Nagata, Y., Okada, H., Haga, A., Hatakeyama, S., Yoshida, S., Okamoto, T., Hosaka, M., Sekine, K., Ohtaka, K., Yamamoto, S., Otaka, M., Grave, E., & Itoh, H. (2014). The activation mechanism of the aryl hydrocarbon receptor

(AhR) by molecular chaperone HSP90. *FEBS Open Bio*, *4*(1), 796–803. https://doi.org/10.1016/J.FOB.2014.09.003

Tucci, M., Passarelli, A., Mannavola, F., Felici, C., Stucci, L. S., Cives, M., & Silvestris, F. (2019). Immune System Evasion as Hallmark of Melanoma Progression: The Role of Dendritic Cells. *Frontiers in Oncology*, *9*, 1148–1162. https://doi.org/10.3389/FONC.2019.01148

TUMOR CELL MORPHOLOGY - Comparative Oncology - NCBI Bookshelf. (n.d.). Retrieved January 29, 2024, from https://www.ncbi.nlm.nih.gov/books/NBK9553/

Uberoi, A., Bartow-McKenney, C., Zheng, Q., Flowers, L., Campbell, A., Knight, S. A. B., Chan, N., Wei, M., Lovins, V., Bugayev, J., Horwinski, J., Bradley, C., Meyer, J., Crumrine, D., Sutter, C. H., Elias, P., Mauldin, E., Sutter, T. R., & Grice, E. A. (2021). Commensal microbiota regulates skin barrier function and repair via signaling through the aryl hydrocarbon receptor. *Cell Host & Microbe*, *29*(8), 1235-1248.e8. https://doi.org/10.1016/J.CHOM.2021.05.011

Urban, J. D., Budinsky, R. A., & Rowlands, J. C. (2011). Single nucleotide polymorphisms in the human Aryl Hydrocarbon Receptor Nuclear Translocator (ARNT) Gene. *Drug Metabolism and Pharmacokinetics*, *26*(6), 637–645. https://doi.org/10.2133/dmpk.DMPK-11-SC-031

Vaklavas, C., Blume, S. W., & Grizzle, W. E. (2017). Translational dysregulation in cancer: Molecular insights and potential clinical applications in biomarker development. *Frontiers in Oncology*, *7*(26), 259194–259210. https://doi.org/10.3389/FONC.2017.00158/BIBTEX

van Arensbergen, J., van Steensel, B., & Bussemaker, H. J. (2014). In search of the determinants of enhancer–promoter interaction specificity. *Trends in Cell Biology*, *24*(11), 695–702. https://doi.org/10.1016/J.TCB.2014.07.004

Van Den Eynde, B. J., Van Baren, N., & Baurain, J. F. (2020). Is There a Clinical Future for IDO1 Inhibitors After the Failure of Epacadostat in Melanoma? *Annual Review of Cancer Biology*, *4*, 241–256. https://doi.org/10.1146/ANNUREV-CANCERBIO-030419-033635

Van Der Merwe, P. A., Bodian, D. L., Daenke, S., Linsley, P., & Davis, S. J. (1997). CD80 (B7-1) binds both CD28 and CTLA-4 with a low affinity and very fast kinetics. *The Journal of Experimental Medicine*, *185*(3), 393–403. https://doi.org/10.1084/JEM.185.3.393

Van der Walde, A., Bellasea, S. L., Kendra, K. L., Khushalani, N. I., Campbell, K. M., Scumpia, P. O., Kuklinski, L. F., Collichio, F., Sosman, J. A., Ikeguchi, A., Victor, A. I., Truong, T. G., Chmielowski, B., Portnoy, D. C., Chen, Y., Margolin, K., Bane, C., Dasanu, C. A., Johnson, D. B., … Ribas, A. (2023). Ipilimumab with or without nivolumab in PD-1 or PD-L1 blockade refractory metastatic melanoma: a randomized phase 2 trial. *Nature Medicine*, *29*(9), 2278–2285. https://doi.org/10.1038/s41591-023-02498-y

Vandesompele, J., De Preter, K., Pattyn, F., Poppe, B., Van Roy, N., De Paepe, A., & Speleman, F. (2002). Accurate normalization of real-time quantitative RT-PCR data by geometric averaging of multiple internal control genes. *Genome Biology*, *3*(7), 1–12. https://doi.org/10.1186/GB-2002-3-7-RESEARCH0034/COMMENTS

Vermeulen, K., Van Bockstaele, D. R., & Berneman, Z. N. (2003). The cell cycle: a review of regulation, deregulation and therapeutic targets in cancer. *Cell Proliferation*, *36*(3), 131–149. https://doi.org/10.1046/J.1365-2184.2003.00266.X

Villanueva, J., Vultur, A., Lee, J. T., Somasundaram, R., Fukunaga-Kalabis, M., Cipolla, A. K., Wubbenhorst, B., Xu, X., Gimotty, P. A., Kee, D., Santiago-Walker, A. E., Letrero, R., D'Andrea, K., Pushparajan, A., Hayden, J. E., Brown, K. D., Laquerre,

S., McArthur, G. A., Sosman, J. A., … Herlyn, M. (2010). Acquired resistance to BRAF inhibitors mediated by a RAF kinase switch in melanoma can be overcome by cotargeting MEK and IGF-1R/PI3K. *Cancer Cell*, *18*(6), 683–695. https://doi.org/10.1016/J.CCR.2010.11.023

Villard, P. H., Barlesif, F., Armand, M., Dao, T. M. A., Pascussi, J. M., Fouchier, F., Champion, S., Dufour, C., Giniès, C., Khalil, A., Amiot, M. J., Barra, Y., & Seree, E. (2011). CYP1A1 Induction in the Colon by Serum: Involvement of the PPARα Pathway and Evidence for a New Specific Human PPREα Site. *PLOS ONE*, *6*(1), e14629. https://doi.org/10.1371/JOURNAL.PONE.0014629

Vlaar, J. M., Borgman, A., Kalkhoven, E., Westland, D., Besselink, N., Shale, C., Faltas, B. M., Priestley, P., Kuijk, E., & Cuppen, E. (2022). Recurrent exon-deleting activating mutations in AHR act as drivers of urinary tract cancer. *Scientific Reports 2022 12:1*, *12*(1), 1–12. https://doi.org/10.1038/s41598-022-14256-0

Vogel, C. F. A., Goth, S. R., Dong, B., Pessah, I. N., & Matsumura, F. (2008). Aryl hydrocarbon receptor signaling mediates expression of indoleamine 2,3-dioxygenase. *Biochemical and Biophysical Research Communications*, *375*(3), 331–335. https://doi.org/10.1016/J.BBRC.2008.07.156

Vogel, C. F. A., & Haarmann-Stemmann, T. (2017). The aryl hydrocarbon receptor repressor – More than a simple feedback inhibitor of AhR signaling: Clues for its role in inflammation and cancer. *Current Opinion in Toxicology*, *2*, 109–119. https://doi.org/10.1016/J.COTOX.2017.02.004

Vogel, C. F. A., Li, W., Wu, D., Miller, J. K., Sweeney, C., Lazennec, G., Fujisawa, Y., & Matsumura, F. (2011). Interaction of aryl hydrocarbon receptor and NF-κB subunit RelB in breast cancer is associated with interleukin-8 overexpression. *Archives of Biochemistry and Biophysics*, *512*(1), 78–86. https://doi.org/10.1016/J.ABB.2011.05.011

Vogel, C. F. A., Sciullo, E., Li, W., Wong, P., Lazennec, G., & Matsumura, F. (2007). RelB, a new partner of aryl hydrocarbon receptor-mediated transcription. *Molecular Endocrinology*, *21*(12), 2941–2955. https://doi.org/10.1210/ME.2007-0211

Vu, H. N., Dilshat, R., Fock, V., & Steingrímsson, E. (2021). User guide to MiT-TFE isoforms and post-translational modifications. *Pigment Cell & Melanoma Research*, *34*(1), 13–27. https://doi.org/10.1111/PCMR.12922

Walczak, K., Langner, E., Makuch-Kocka, A., Szelest, M., Szalast, K., Marciniak, S., & Plech, T. (2020). Effect of tryptophan-derived ahr ligands, kynurenine, kynurenic acid and ficz, on proliferation, cell cycle regulation and cell death of melanoma cells—in vitro studies. *International Journal of Molecular Sciences*, *21*(21), 1–20. https://doi.org/10.3390/ijms21217946

Wang, A., Al-Kuhlani, M., Johnston, S. C., Ojcius, D. M., Chou, J., & Dean, D. (2013). Transcription factor complex AP-1 mediates inflammation initiated by Chlamydia pneumoniae infection. *Cellular Microbiology*, *15*(5), 779–794. https://doi.org/10.1111/CMI.12071

Wang, Q., Li, M., Wu, T., Zhan, L., Li, L., Chen, M., Xie, W., Xie, Z., Hu, E., Xu, S., & Yu, G. (2022). Exploring Epigenomic Datasets by ChIPseeker. *Current Protocols*, *2*(10), 585–612. https://doi.org/10.1002/CPZ1.585

Wang, X. B., Zheng, C. Y., Giscombe, R., & Lefvert, A. K. (2001). Regulation of Surface and Intracellular Expression of CTLA-4 on Human Peripheral T Cells. *Scandinavian Journal of Immunology*, *54*(5), 453–458. https://doi.org/10.1046/J.1365-3083.2001.00985.X

Wang, Y., Liu, J., Ying, X., Lin, P. C., & Zhou, B. P. (2016). Twist-mediated Epithelial-mesenchymal Transition Promotes Breast Tumor Cell Invasion via Inhibition of Hippo Pathway. *Scientific Reports*, *6*(1), 1–10. https://doi.org/10.1038/srep24606

Wang, Y., Shi, J., Chai, K., Ying, X., & Zhou, B. (2014). The Role of Snail in EMT and Tumorigenesis. *Current Cancer Drug Targets*, *13*(9), 963–972. https://doi.org/10.2174/15680096113136660102

Wei, Y. D., Helleberg, H., Rannug, U., & Rannug, A. (1998). Rapid and transient induction of CYP1A1 gene expression in human cells by the tryptophan photoproduct 6-formylindolo[3,2-b]carbazole. *Chemico-Biological Interactions*, *110*(1–2), 39–55. https://doi.org/10.1016/S0009-2797(97)00111-7

Wels, C., Joshi, S., Koefinger, P., Bergler, H., & Schaider, H. (2011). Transcriptional activation of ZEB1 by Slug leads to cooperative regulation of the epithelial-mesenchymal transition-like phenotype in melanoma. *The Journal of Investigative Dermatology*, *131*(9), 1877–1885. https://doi.org/10.1038/JID.2011.142

Williams, E. G., Mouchiroud, L., Frochaux, M., Pandey, A., Andreux, P. A., Deplancke, B., & Auwerx, J. (2014). An Evolutionarily Conserved Role for the Aryl Hydrocarbon Receptor in the Regulation of Movement. *PLoS Genetics*, *10*(9), e1004673–e1004682. https://doi.org/10.1371/JOURNAL.PGEN.1004673

Wincent, E., Amini, N., Luecke, S., Glatt, H., Bergman, J., Crescenzi, C., Rannug, A., & Rannug, U. (2009). The suggested physiologic aryl hydrocarbon receptor activator and cytochrome P4501 substrate 6-formylindolo[3,2-b]carbazole is present in humans. *Journal of Biological Chemistry*, *284*(5), 2690–2696. https://doi.org/10.1074/jbc.M808321200

Wincent, E., Bengtsson, J., Bardbori, A. M., Alsberg, T., Luecke, S., Rannug, U., & Rannug, A. (2012). Inhibition of cytochrome P4501-dependent clearance of the endogenous agonist FICZ as a mechanism for activation of the aryl hydrocarbon receptor. *Proceedings of the National Academy of Sciences of the United States of America*, *109*(12), 4479–4484. https://doi.org/10.1073/PNAS.1118467109/-/DCSUPPLEMENTAL/PNAS.201118467SI.PDF

Witwicki, R. M., Ekram, M. B., Qiu, X., Janiszewska, M., Shu, S., Kwon, M., Trinh, A., Frias, E., Ramadan, N., Hoffman, G., Yu, K., Xie, Y., McAllister, G., McDonald, R., Golji, J., Schlabach, M., deWeck, A., Keen, N., Chan, H. M., … Polyak, K. (2018). TRPS1 Is a Lineage-Specific Transcriptional Dependency in Breast Cancer. *Cell Reports*, *25*(5), 1255-1267.e5. https://doi.org/10.1016/J.CELREP.2018.10.023/ATTACHMENT/9AD396BC-0D03-4F94-A24B-E87A2B99A026/MMC6.PDF

Wolchok, J. D., Chiarion-Sileni, V., Gonzalez, R., Rutkowski, P., Grob, J.-J., Cowey, C. L., Lao, C. D., Wagstaff, J., Schadendorf, D., Ferrucci, P. F., Smylie, M., Dummer, R., Hill, A., Hogg, D., Haanen, J., Carlino, M. S., Bechter, O., Maio, M., Marquez-Rodas, I., … Larkin, J. (2017). Overall Survival with Combined Nivolumab and Ipilimumab in Advanced Melanoma. *The New England Journal of Medicine*, *377*(14), 1345–1356. https://doi.org/10.1056/NEJMOA1709684

Wolf, Y., Bartok, O., Swanton, C., Ruppin, E., & Samuels Correspondence, Y. (2019). UVB-Induced Tumor Heterogeneity Diminishes Immune Response in Melanoma. *Cell*, *179*, 219–235. https://doi.org/10.1016/j.cell.2019.08.032

Wu, P. Y., Chuang, P. Y., Chang, G. D., Chan, Y. Y., Tsai, T. C., Wang, B. J., Lin, K. H., Hsu, W. M., Liao, Y. F., & Lee, H. (2019). Novel Endogenous Ligands of Aryl Hydrocarbon Receptor Mediate Neural Development and Differentiation of Neuroblastoma. *ACS Chemical Neuroscience*, *10*(9), 4031–4042. https://doi.org/10.1021/ACSCHEMNEURO.9B00273

Wu, Y., Niu, Y., Leng, J., Xu, J., Chen, H., Li, H., Wang, L., Hu, J., Xia, D., & Wu, Y. (2020). Benzo(a)pyrene regulated A549 cell migration, invasion and epithelial-mesenchymal transition by up-regulating long non-coding RNA linc00673. *Toxicology Letters*, *320*, 37–45. https://doi.org/10.1016/J.TOXLET.2019.11.024

Xia, Y., Shen, S., & Verma, I. M. (2014). NF-κB, an active player in human cancers. *Cancer Immunology Research*, *2*(9), 823–830. https://doi.org/10.1158/2326-6066.CIR-14-0112

Xie, G., Peng, Z., & Raufman, J. P. (2012). Src-mediated aryl hydrocarbon and epidermal growth factor receptor cross talk stimulates colon cancer cell proliferation. *American Journal of Physiology - Gastrointestinal and Liver Physiology*, *302*(9), G1006–G1015. https://doi.org/10.1152/AJPGI.00427.2011

Xie, N., Shen, G., Gao, W., Huang, Z., Huang, C., & Fu, L. (2023). Neoantigens: promising targets for cancer therapy. *Signal Transduction and Targeted Therapy*, *8*(1), 1–38. https://doi.org/10.1038/s41392-022-01270-x

Xie, X., Jiang, J., Ye, W., Chen, R., Deng, Y., & Wen, J. (2018). Sp1, instead of AhR, regulates the basal transcription of porcine CYP1A1 at the proximal promoter. *Frontiers in Pharmacology*, *9*(AUG). https://doi.org/10.3389/FPHAR.2018.00927/FULL

Ye, M., Zhang, Y., Gao, H., Xu, Y., Jing, P., Wu, J., Zhang, X., Xiong, J., Dong, C., Yao, L., & Zhang, J. (2018). Activation of the Aryl Hydrocarbon Receptor Leads to Resistance to EGFR TKIs in Non-Small Cell Lung Cancer by Activating Src-mediated Bypass Signaling. *Clinical Cancer Research*, *24*(5), 1227–1239. https://doi.org/10.1158/1078-0432.CCR-17-0396

Ye, W., Chen, R., Chen, X., Huang, B., Lin, R., Xie, X., Chen, J., Jiang, J., Deng, Y., & Wen, J. (2019a). AhR regulates the expression of human cytochrome P450 1A1 (CYP1A1) by recruiting Sp1. *The FEBS Journal*, *286*(21), 4215–4231. https://doi.org/10.1111/FEBS.14956

Ye, W., Chen, R., Chen, X., Huang, B., Lin, R., Xie, X., Chen, J., Jiang, J., Deng, Y., & Wen, J. (2019b). AhR regulates the expression of human cytochrome P450 1A1 (CYP1A1) by recruiting Sp1. *The FEBS Journal*, *286*(21), 4215–4231. https://doi.org/10.1111/FEBS.14956

Yokobori, T., Suzuki, S., Tanaka, N., Inose, T., Sohda, M., Sano, A., Sakai, M., Nakajima, M., Miyazaki, T., Kato, H., & Kuwano, H. (2013). MiR-150 is associated with poor prognosis in esophageal squamous cell carcinoma via targeting the EMT inducer ZEB1. *Cancer Science*, *104*(1), 48–54. https://doi.org/10.1111/CAS.12030

Yoshizawa, K., Brix, A. E., Sells, D. M., Jokinen, M. P., Wyde, M., Orzech, D. P., Kissling, G. E., Walker, N. J., & Nyska, A. (2009). Reproductive lesions in female Harlan Sprague-Dawley rats following two-year oral treatment with dioxin and dioxin-like compounds. *Toxicologic Pathology*, *37*(7), 921–937. https://doi.org/10.1177/0192623309351721

Yu, G., Wang, L. G., & He, Q. Y. (2015). ChIPseeker: an R/Bioconductor package for ChIP peak annotation, comparison and visualization. *Bioinformatics (Oxford, England)*, *31*(14), 2382–2383. https://doi.org/10.1093/BIOINFORMATICS/BTV145

Zandi, R., Larsen, A. B., Andersen, P., Stockhausen, M. T., & Poulsen, H. S. (2007). Mechanisms for oncogenic activation of the epidermal growth factor receptor. *Cellular Signalling*, *19*(10), 2013–2023. https://doi.org/10.1016/J.CELLSIG.2007.06.023

Zavyalova, M. V., Denisov, E. V., Tashireva, L. A., Savelieva, O. E., Kaigorodova, E. V., Krakhmal, N. V., & Perelmuter, V. M. (2019). Intravasation as a Key Step in Cancer

Metastasis. *Biochemistry (Moscow)*, *84*(7), 762–772. https://doi.org/10.1134/S0006297919070071/METRICS

Zhang, P., Sun, Y., & Ma, L. (2015). ZEB1: at the crossroads of epithelial-mesenchymal transition, metastasis and therapy resistance. *Cell Cycle (Georgetown, Tex.)*, *14*(4), 481–487. https://doi.org/10.1080/15384101.2015.1006048

Zhang, X., Liu, X., Zhou, W., Du, Q., Yang, M., Ding, Y., & Hu, R. (2021). Blockade of IDO-Kynurenine-AhR Axis Ameliorated Colitis-Associated Colon Cancer via Inhibiting Immune Tolerance. *Cellular and Molecular Gastroenterology and Hepatology*, *12*(4), 1179–1199. https://doi.org/10.1016/J.JCMGH.2021.05.018

Zhang, Y., Liu, T., Meyer, C. A., Eeckhoute, J., Johnson, D. S., Bernstein, B. E., Nussbaum, C., Myers, R. M., Brown, M., Li, W., & Shirley, X. S. (2008). Model-based analysis of ChIP-Seq (MACS). *Genome Biology*, *9*(9), 1–9. https://doi.org/10.1186/GB-2008-9-9-R137/FIGURES/3

Zhao, B., DeGroot, D. E., Hayashi, A., He, G., & Denison, M. S. (2010). CH223191 Is a Ligand-Selective Antagonist of the Ah (Dioxin) Receptor. *Toxicological Sciences*, *117*(2), 393–403. https://doi.org/10.1093/TOXSCI/KFQ217

Zhou, B., Basu, J., Kazmi, H. R., Chitrala, K. N., Mo, X., Preston-Alp, S., Cai, K. Q., Kappes, D., & Zaidi, M. R. (2022). Interferon-gamma signaling promotes melanoma progression and metastasis. *Oncogene*, *42*(5), 351–363. https://doi.org/10.1038/s41388-022-02561-x

Zhu, W., Liu, H., Wang, X., Lu, J., Zhang, H., Wang, S., & Yang, W. (2019). Associations of CYP1 polymorphisms with risk of prostate cancer: an updated meta-analysis. *Bioscience Reports*, *39*(3). https://doi.org/10.1042/BSR20181876

Zudaire, E., Cuesta, N., Murty, V., Woodson, K., Adams, L., Gonzalez, N., Martínez, A., Narayan, G., Kirsch, I., Franklin, W., Hirsch, F., Birrer, M., & Cuttitta, F. (2008). The aryl hydrocarbon receptor repressor is a putative tumor suppressor gene in multiple human cancers. *Journal of Clinical Investigation*, *118*(2), 640–650. https://doi.org/10.1172/JCI30024

8. Appendices

8.1. Mass Spectrometry – All data

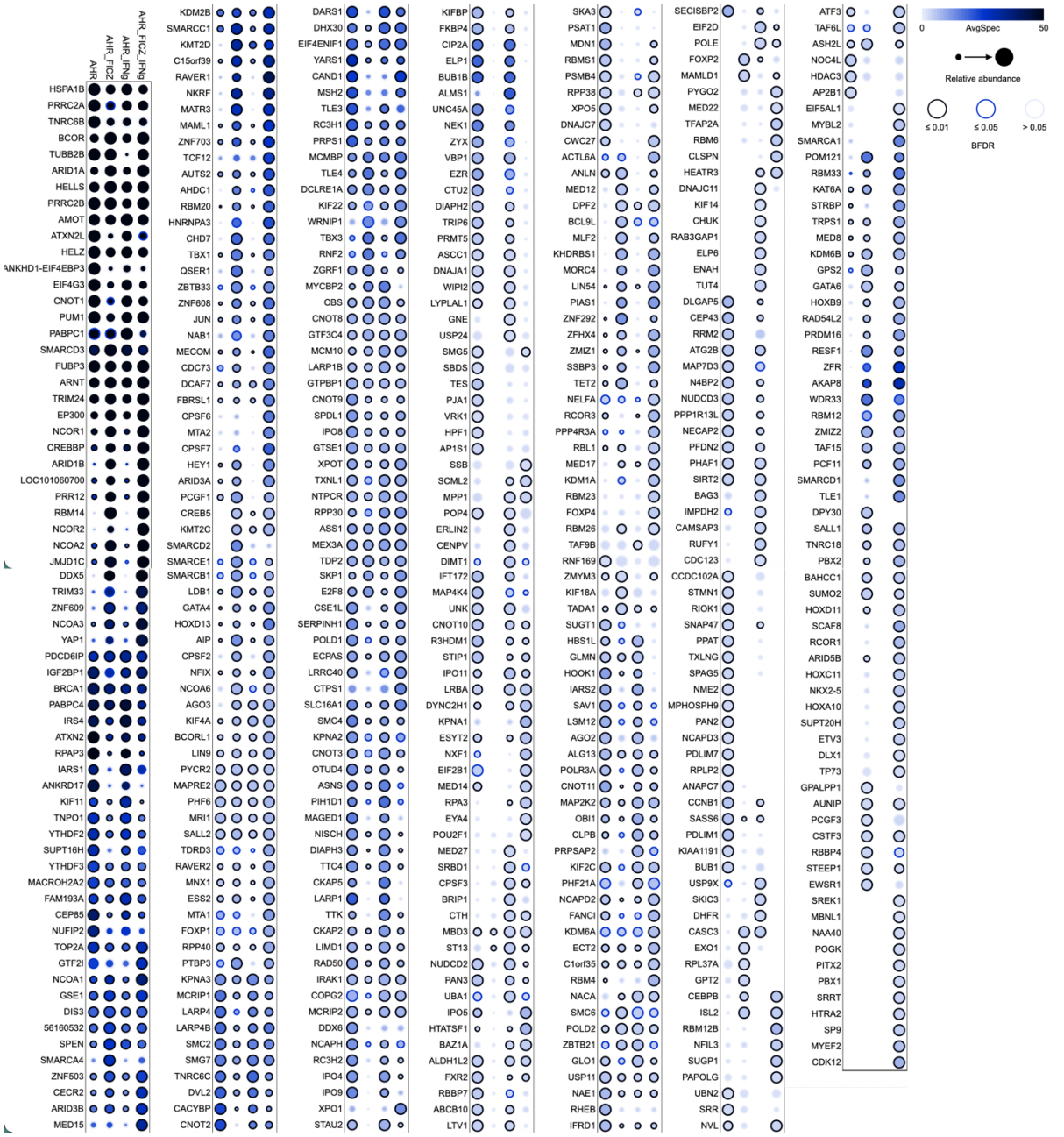

8.2. Comparison of distribution of peaks across AhR ChIP-Seq conditions

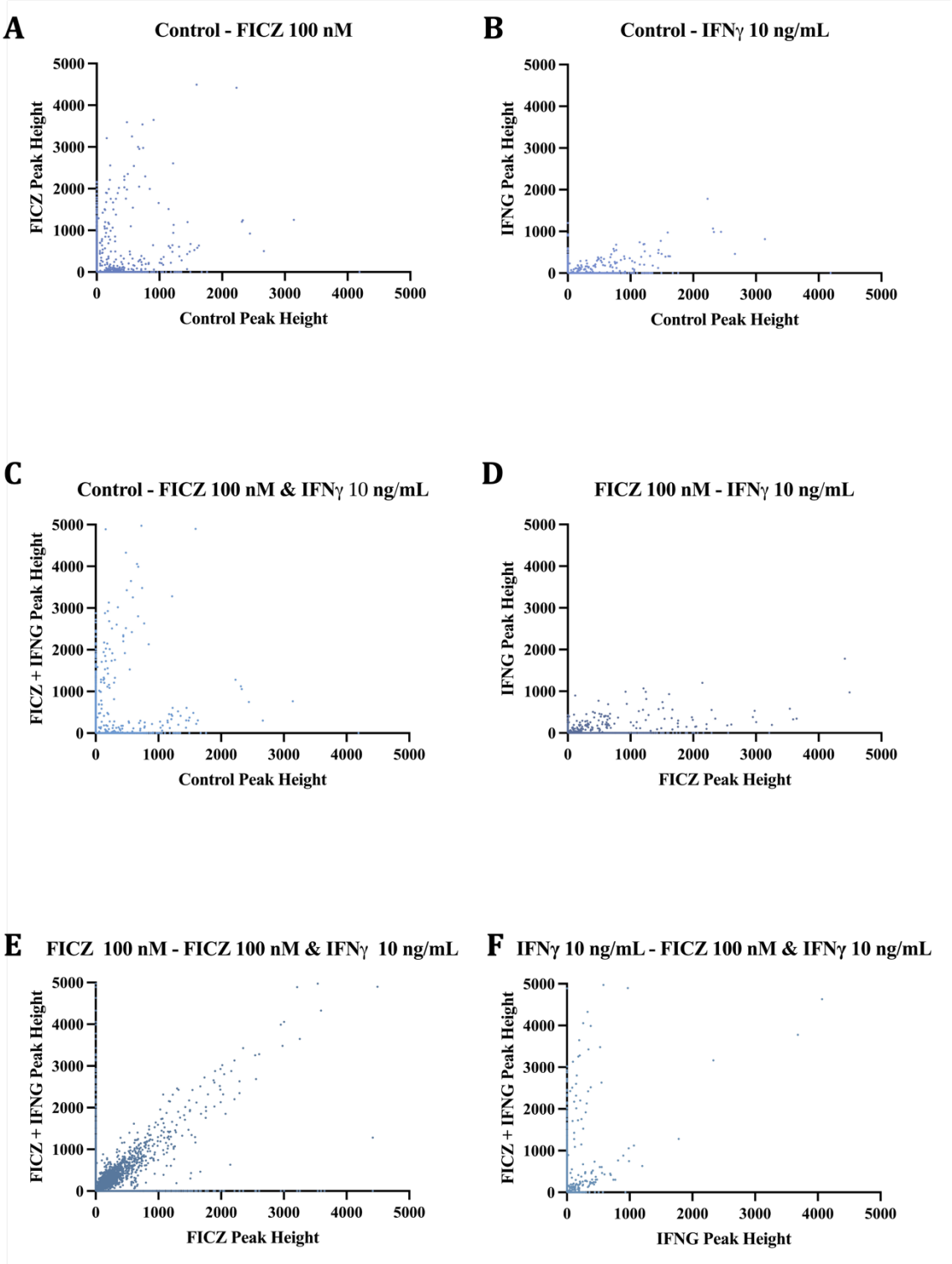

8.3. QPCT gene induction is dependent on the AhR

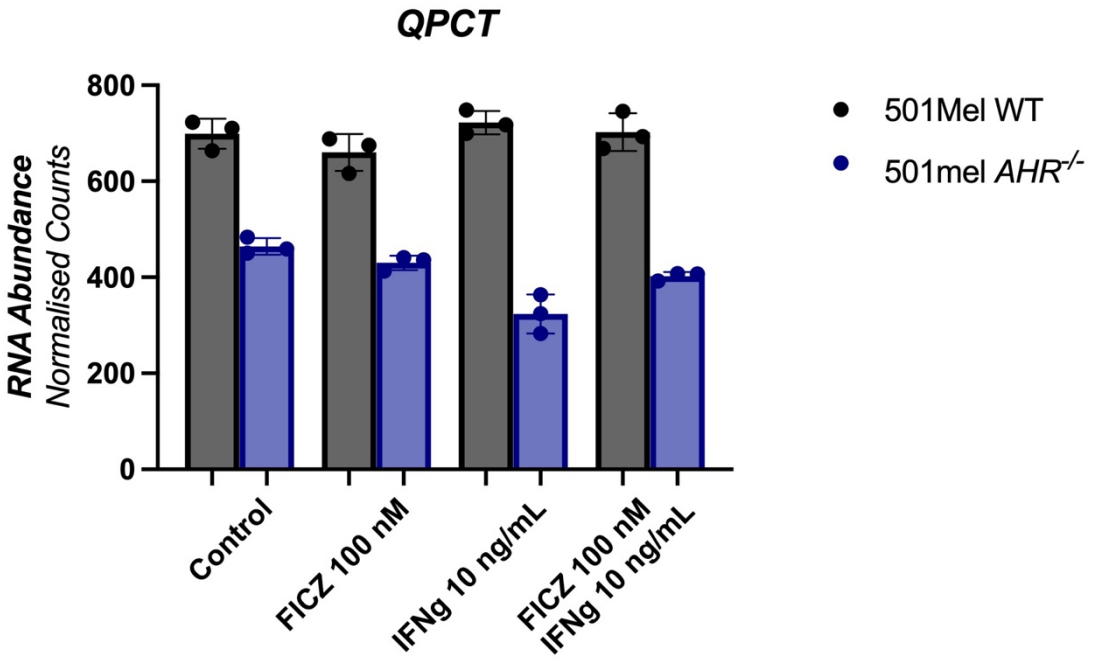

Expression of QPCT as determined from RNA-Seq data collected from 501mel^{WT} and 501mel *AHR* KO cells after 24-hours of treatment with FICZ 100 nM, IFNγ 10 ng/mL, both or neither.

8.4. RNA-Seq determined expression of genes bearing MITF and AhR Binding sites

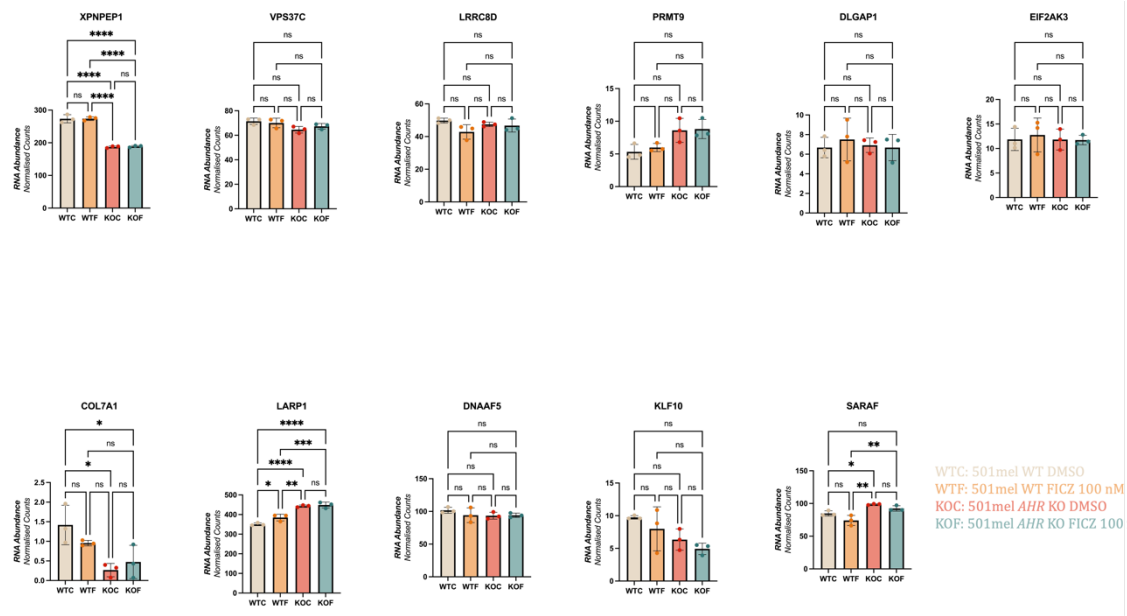

Data from the RNA-Seq experiment presented in Chapter 5. Statistical analysis: one-way ANOVA followed by Tukey-Kramer for comparison between means, which intrinsically accounts for multiple comparisons. $P > 0.05$: ns, $P < 0.05$: *, $P < 0.01$: **, $P < 0.001$: ***, $P < 0.0001$: ****.

8.5. MITF binding to MITF motifs identified in AhR ChIP-Seq

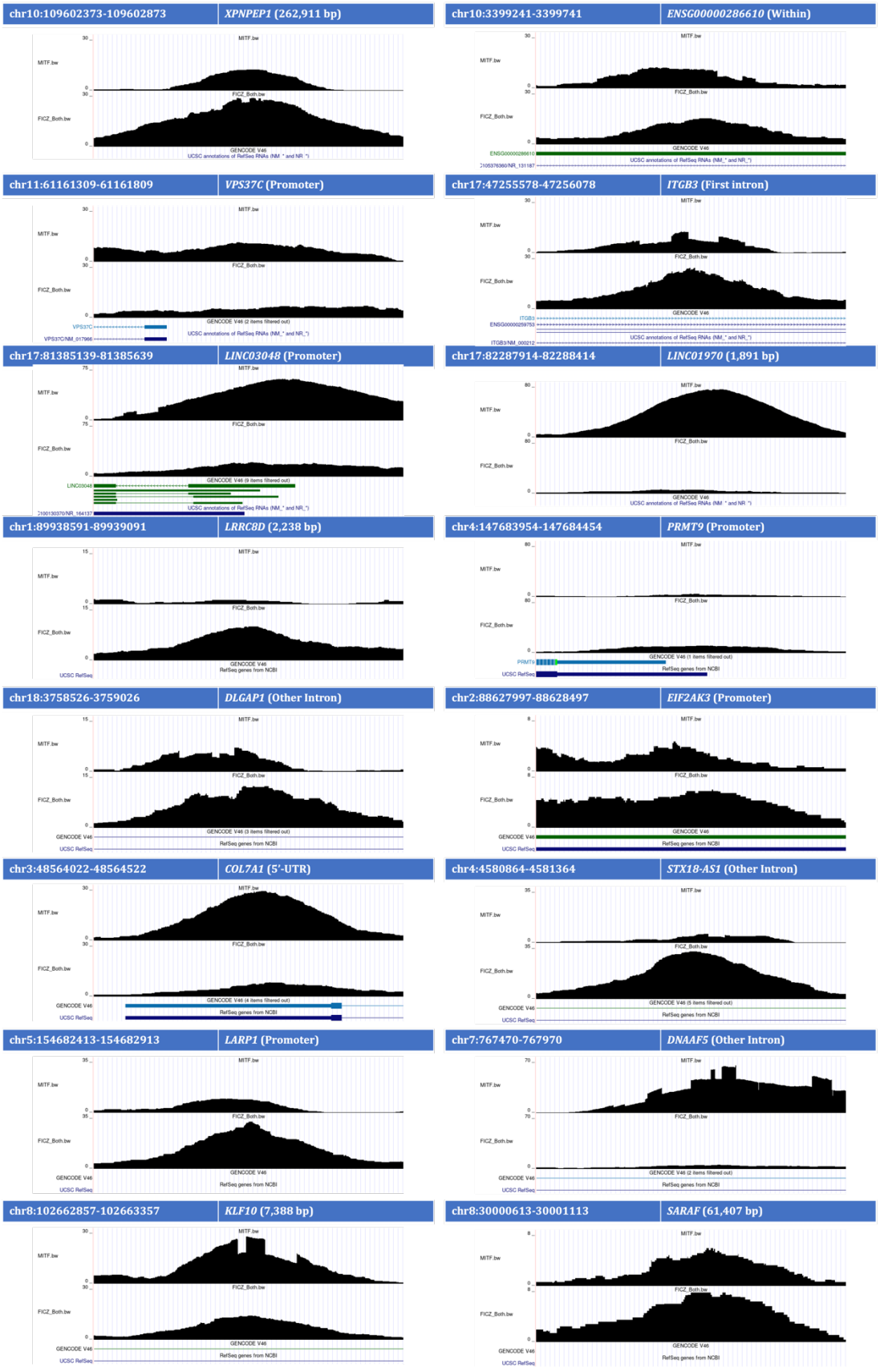

8.6. Gene Ontology analysis of MITF and AhR (FE > 2)

GO biological process complete	Homo sapiens - REFLIST (20592)	upload_1 (2661)	upload_1 (expected)	upload_1 (over/under)	Fold-Enrichment	upload_1 (raw P-value)	upload_1 (FDR)
Notch signaling involved in heart development (GO:0061314)	11	8	1.42	+	5.63	6.85E-04	2.29E-02
regulation of vascular associated smooth muscle cell differentiation (GO:1905063)	14	9	1.81	+	4.97	6.04E-04	2.05E-02
cell surface receptor signaling pathway involved in heart development (GO:0061311)	24	11	3.1	+	3.55	1.31E-03	3.98E-02
cardiac epithelial to mesenchymal transition (GO:0060317)	27	12	3.49	+	3.44	9.90E-04	3.14E-02
developmental pigmentation (GO:0048066)	43	19	5.56	+	3.42	3.98E-05	2.07E-03
positive regulation of heart growth (GO:0060421)	32	14	4.14	+	3.39	4.36E-04	1.55E-02
negative regulation of stem cell differentiation (GO:2000737)	28	12	3.62	+	3.32	1.27E-03	3.87E-02
pigment granule organization (GO:0048753)	39	16	5.04	+	3.17	3.10E-04	1.17E-02
positive regulation of viral genome replication (GO:0045070)	32	13	4.14	+	3.14	1.19E-03	3.69E-02
semaphorin-plexin signaling pathway (GO:0071526)	43	17	5.56	+	3.06	2.88E-04	1.09E-02
melanosome organization (GO:0032438)	38	15	4.91	+	3.05	6.53E-04	2.19E-02
ER-nucleus signaling pathway (GO:0006984)	33	13	4.26	+	3.05	1.49E-03	4.38E-02
pigment cell differentiation (GO:0050931)	33	13	4.26	+	3.05	1.49E-03	4.37E-02
platelet-derived growth factor receptor signaling pathway (GO:0048008)	36	14	4.65	+	3.01	1.10E-03	3.44E-02
positive regulation of telomere maintenance via telomere lengthening (GO:1904358)	37	14	4.78	+	2.93	1.36E-03	4.07E-02
actin filament bundle organization (GO:0061572)	61	23	7.88	+	2.92	4.80E-05	2.46E-03
regulation of cardiac muscle cell proliferation (GO:0060043)	38	14	4.91	+	2.85	1.66E-03	4.80E-02
regulation of heart growth (GO:0060420)	60	22	7.75	+	2.84	1.43E-04	6.26E-03
actin filament bundle assembly (GO:0051017)	58	21	7.5	+	2.8	2.26E-04	9.05E-03
cellular pigmentation (GO:0033059)	61	22	7.88	+	2.79	1.59E-04	6.77E-03
pigmentation (GO:0043473)	106	38	13.7	+	2.77	5.72E-07	4.88E-05
positive regulation of substrate adhesion-dependent cell spreading (GO:1900026)	45	16	5.82	+	2.75	1.68E-03	4.85E-02
positive regulation of viral process (GO:0048524)	65	23	8.4	+	2.74	1.27E-04	5.78E-03
regulation of cell-substrate junction organization (GO:0150116)	69	24	8.92	+	2.69	1.05E-04	4.89E-03
regulation of focal adhesion assembly (GO:0051893)	64	22	8.27	+	2.66	2.34E-04	9.33E-03
regulation of cell-substrate junction assembly (GO:0090109)	64	22	8.27	+	2.66	2.34E-04	9.31E-03
regulation of substrate adhesion-dependent cell spreading (GO:1900024)	62	21	8.01	+	2.62	3.76E-04	1.37E-02
regulation of miRNA transcription (GO:1902893)	71	24	9.17	+	2.62	1.43E-04	6.25E-03
regulation of cardiac muscle tissue growth (GO:0055021)	54	18	6.98	+	2.58	1.16E-03	3.61E-02
tissue regeneration (GO:0042246)	61	20	7.88	+	2.54	6.96E-04	2.32E-02
positive regulation of cell-matrix adhesion (GO:0001954)	58	19	7.5	+	2.54	9.62E-04	3.07E-02
regulation of cell-matrix adhesion (GO:0001952)	123	40	15.89	+	2.52	2.67E-06	1.98E-04
negative regulation of mRNA metabolic process (GO:1903312)	96	31	12.41	+	2.5	3.48E-05	1.84E-03
negative regulation of mRNA catabolic process (GO:1902373)	72	23	9.3	+	2.47	4.83E-04	1.69E-02
dendrite morphogenesis (GO:0048813)	63	20	8.14	+	2.46	1.38E-03	4.12E-02
regulation of stem cell differentiation (GO:2000736)	79	25	10.21	+	2.45	2.74E-04	1.06E-02
negative regulation of RNA catabolic process (GO:1902369)	84	26	10.85	+	2.4	2.54E-04	9.88E-03
positive regulation of DNA biosynthetic process (GO:2000573)	75	23	9.69	+	2.37	6.64E-04	2.22E-02
regulation of miRNA metabolic process (GO:2000628)	82	25	10.6	+	2.36	6.05E-04	2.05E-02
RNA stabilization (GO:0043489)	69	21	8.92	+	2.36	1.28E-03	3.89E-02
positive regulation of DNA repair (GO:0045739)	128	38	16.54	+	2.3	2.39E-05	1.34E-03
circadian regulation of gene expression (GO:0032922)	71	21	9.17	+	2.29	1.60E-03	4.64E-02
stem cell development (GO:0048864)	85	25	10.98	+	2.28	7.42E-04	2.44E-02
neutral lipid metabolic process (GO:0006638)	99	29	12.79	+	2.27	3.79E-04	1.38E-02
epithelial to mesenchymal transition (GO:0001837)	82	24	10.6	+	2.26	1.03E-03	3.25E-02
maintenance of protein location (GO:0045185)	97	28	12.53	+	2.23	5.57E-04	1.92E-02
regulation of cell-substrate adhesion (GO:0010810)	219	63	28.3	+	2.23	1.48E-07	1.41E-05
positive regulation of protein localization to nucleus (GO:1900182)	94	27	12.15	+	2.22	7.79E-04	2.54E-02
cellular response to insulin stimulus (GO:0032869)	150	43	19.38	+	2.22	1.85E-05	1.08E-03
acylglycerol metabolic process (GO:0006639)	98	28	12.66	+	2.21	5.89E-04	2.01E-02
dendrite development (GO:0016358)	112	32	14.47	+	2.21	1.93E-04	7.91E-03
roof of mouth development (GO:0060021)	92	26	11.89	+	2.19	1.14E-03	3.55E-02
positive regulation of double-strand break repair (GO:2000781)	85	24	10.98	+	2.18	1.36E-03	4.08E-02
mesenchymal cell differentiation (GO:0048762)	171	48	22.1	+	2.17	8.74E-06	5.47E-04
regulation of postsynapse organization (GO:0099175)	101	28	13.05	+	2.15	7.40E-04	2.44E-02
regulation of protein localization to nucleus (GO:1900180)	148	41	19.13	+	2.14	4.71E-05	2.43E-03
protein dephosphorylation (GO:0006470)	168	46	21.71	+	2.12	2.07E-05	1.18E-03
cholesterol metabolic process (GO:0008203)	121	33	15.64	+	2.11	3.22E-04	1.19E-02
regulation of endothelial cell migration (GO:0010594)	169	46	21.84	+	2.11	3.24E-05	1.74E-03
positive regulation of cell-substrate adhesion (GO:0010811)	129	35	16.67	+	2.1	2.84E-04	1.08E-02
cardiocyte differentiation (GO:0035051)	118	32	15.25	+	2.1	4.38E-04	1.56E-02
positive regulation of endothelial cell migration (GO:0010595)	107	29	13.83	+	2.1	9.73E-04	3.10E-02
regulation of mitochondrion organization (GO:0010821)	155	42	20.03	+	2.1	6.50E-05	3.14E-03
peptidyl-lysine acetylation (GO:0018394)	96	26	12.41	+	2.1	1.51E-03	4.41E-02
regulation of muscle cell differentiation (GO:0051147)	138	37	17.83	+	2.07	1.89E-04	7.81E-03
regulation of nucleocytoplasmic transport (GO:0046822)	113	30	14.6	+	2.05	8.76E-04	2.82E-02
negative regulation of protein kinase activity (GO:0006469)	200	53	25.84	+	2.05	1.47E-05	8.69E-04
regulation of epithelial cell migration (GO:0010632)	229	60	29.59	+	2.03	4.08E-06	2.77E-04
regulation of DNA replication (GO:0006275)	130	34	16.8	+	2.02	5.06E-04	1.76E-02
regulation of circadian rhythm (GO:0042752)	115	30	14.86	+	2.02	1.43E-03	4.24E-02
stem cell differentiation (GO:0048863)	182	47	23.52	+	2	6.17E-05	3.02E-03